STEADY STATE INDUCTIVE INFLUENCE OF HIGH VOLTAGE TRANSMISSION LINES

A thesis presented for the degree of
Doctor of Philosophy in Electrical and Electronic Engineering
at the University of Canterbury, Christchurch, New Zealand.

by

Gordon Cameron

August 1993

ABSTRACT

Harmonic current flows within High Voltage transmission lines induce voltages in neighbouring metallic conductors be they fences, pipelines, other transmission lines or telecommunications cables. These voltages may endanger organisms which come into contact with the conductors or impair the operation of electrical systems connected to them. Under steady state operating conditions the induced voltages are seldom of sufficient magnitude to be hazardous, however they are on occasions severe enough to impair telecommunications services. With the increasing use of non-linear loads within the power system, harmonic current flows and hence the incidence of telecommunication interference can be expected to rise.

Many potential interference problems may be avoided by the coordination of telecommunication and electricity transmission systems. The most cost effective time to engineer solutions to interference problems is during the design of the system. A need exists therefore for methods which accurately quantify the ability of High Voltage transmission lines to cause interference.

This thesis is concerned with methods, both experimental and analytical, for determining the *Inductive Influence* or ability of a transmission line to cause interference. Existing models for the mutual impedance of conductors in the presence of the earth are reviewed. Numerical studies of the factors effecting the inductive influence of single and three phase transmission lines are reported. Measures for reducing the inductive influence through the use of alternative transmission line geometries and continuously grounded earth wires are investigated. New measures for quantifying the inductive influence are proposed, which are superior to existing measures due to the inclusion of the effect of frequency, earth resistivity, current sequence and transmission line geometry on the inductive influence. Comparisons are made between a digital computer model of the New Zealand inter-island HVDC link, and measured currents using a non-invasive crossed loop antenna system. The accuracy of the new methods is confirmed, as is the need for sensitive equipment when undertaking such investigations.

ACKNOWLEDGEMENTS

During the course of my research and the writing of this thesis there have been many people who have provided me with assistance and support for which I am very grateful. I would especially like to thank my supervisor, Dr. P.S. Bodger for his advice, assistance, and patience during the course of my study.

I would also like to thank Professor J. Arrillaga for his guidance and technical assistance during the investigation on the HVDC link.

The Telecom Corporation of New Zealand Limited (formerly the New Zealand Post Office) provided me with financial support, for which I am grateful.

I am also grateful to Electricorp for the opportunity and the resources they provided which enabled me to undertake the study on the HVDC link.

Special thanks goes to my fellow students, academic staff, family and friends for their patience, interest and support. I would especially like to thank Dr Neville Watson and Lesley Paton for their support, generosity and encouragement.

CONTENTS

LIST OF FIGURES

LIST OF TABLES

LIST OF SYMBOLS

V	volt, S.I. unit of potential difference
A	ampere, S.I. unit of electric current
s	second, S.I. unit of time
F	farad, S.I. unit of capacitance
H	henry, S.I. unit of inductance
Ω	ohm, S.I. unit of resistance
Hz	hertz, S.I. unit of frequency
m	metre, S.I. unit of length
rad	radian, unit of plane angle
V	voltage phasor quantity
I	current phasor quantity
Z	impedance
Y	admittance
x,y,z	cartesian ordinates
V_{induced}	voltage in the induced conductor (V)
Z_{common}	impedance of the common conduction path (Ω)
I_{inducing}	current in inducing conductor (A)
j	the pure imaginary ($\sqrt{-1}$)
ω	angular frequency (rad.s^{-1})
V_{inducing}	voltage of the inducing conductor (V)
C_{mutual}	mutual capacitance between conductors (F)
C_{self}	self capacitance of the conductor (F)
$\vec{E}$	electric field vector (V.m^{-1})
Z_{mutual}	mutual impedance between conductors (Ω)
$\vec{H}$	magnetic field intensity (A.m^{-1})
$V_{\text{send-a}}$	sending voltage on conductor a (V)
$V_{\text{send-b}}$	sending voltage on conductor b (V)
V_{sending}	net sending end voltage (V)
$V_{\text{induced-a}}$	noise voltage induced on conductor a (V)
$V_{\text{induced-b}}$	noise voltage induced on conductor b (V)
$V_{\text{long-a}}$	longitudinal voltage on conductor a (V)
$V_{\text{long-b}}$	longitudinal voltage on conductor b (V)
$V_{\text{transverse}}$	transverse voltage at the telephone (V)

CHAPTER 1

INTRODUCTION

1.1 General

High voltage transmission lines are designed to convey electrical energy from power stations to load centres. The energy is carried by the electromagnetic field which propagates along the transmission line. Unfortunately the field is not confined to the immediate vicinity of the wires. This can result in undesirable side effects.

High intensity electromagnetic fields can induce significant voltages and currents in neighbouring conductors, be they fence lines, pipelines, telecommunication cables or other transmission lines. The induced signals may impair the operation of electrical systems connected to the conductors or endanger organisms which come in contact with them. If the problem is severe then protection measures such as the installation of ground electrodes and sectionalisation of the conductor may be required. As the capacity of transmission lines is increased and land utilisation pressures force utilities to share rights of way, inductive co-ordination problems of this type will increase.

Low intensity electromagnetic fields can impair the operation of electrical communication systems due to the low power of the desired signal. The effect of this inductive interference may range from a mild annoyance to the subscriber to engulfing the desired signal thereby disabling the system. With the increased use of electronic switching devices in the electrical distribution system, the magnitude of unwanted harmonic currents on transmission lines is likely to increase. Consequently increased levels of steady state noise on local subscriber lines can be expected. However, with improved isolation, the use of low susceptibility communications equipment and filters in the electrical distribution system, inductive interference problems can often be rectified.

In recent years concerns have been expressed about the effect of electromagnetic fields on biological material. There is now little doubt that it is influenced by magnetic fields, but the extent of these effects has yet to be determined. Of particular concern to the public is the effect of the fields induced by high voltage transmission lines crossing residential areas. Protection measures may be required in the future if it is determined that the electromagnetic field from transmission lines has a detrimental effect on humans.

Due to increased levels of interfering signals within power systems and increased concern about the fields these signals induce, it is likely that new operational procedures and design rules for power transmission systems will be required.

1.2 Thesis Aims

The Telecom Corporation of New Zealand Limited, sponsors of this research, defined the aims of this project to be:

1. The development of models which accurately predict the steady state inductive influence of UHV and HV transmission lines

2. The use of these models to :

   - Investigate preferred transmission line operating configurations
   - Investigate cost effective methods of limiting steady state harmonic current flows within the power system

3. The verification of model accuracy by comparison with field measurements.

A thorough study of these topics is beyond the scope of this project. In this thesis the steady state inductive influence of transmission lines or the ability that a transmission line has to cause interference, is considered. The mechanisms that cause disturbing currents to flow in transmission lines and methods for reducing these currents are not considered.

1.3 Chapter Summary

In Chapter 2 existing methods for determining the interference induced in buried telecommunication cables are described. A simplified sequential procedure for determining the resultant interference using computer simulations or a combination of modelling and experimental measurements is presented. The advantages, disadvantages and difficulties associated with simulating and measuring system state are discussed. Chapter 2 therefore satisfies the first aim of this project.

Chapter 2 also states which methods are employed to generate the results presented in this thesis thereby indicating how this work contributes to the study of inductive coordination. Details of the computer models and experimental techniques are contained in Chapters 3, 4, 5, 6, 8 and 9.

Accurate models of the fields induced by a transmission line above the earth are required to predict the inductive influence of transmission lines. Chapter 3 contains a review of existing models, the assumptions made during their derivation, implementation details and their applications in the course of this research project.

A measure for quantifying the inductive influence of transmission lines is presented in Chapter 4. This measure is then used to determine the accuracy of existing inductive coupling models.

An interpretation of the physical mechanisms affecting the inductive influence of single conductor earth return transmission lines is also reported in Chapter 4. A family of simple models which approximate the current distribution induced within the earth are described. These models are well suited for educational purposes and are used in Chapter 5 to explain the observed inductive influence phenomena associated with multiconductor transmission lines. New inductive influence measures based upon these models are presented in Chapter 7.

Chapters 4 and 5 summarise the gross dependencies of the inductive field induced by single and multiconductor lines on: line geometry, frequency, earth resistivity and the sequence of current flow.

The second aim is satisfied by Chapters 6 and 7, in which two methods for the reduction of the inductive influence of transmission lines are presented. Chapter 6 considers the effect of alternative transmission line geometries and continuously grounded shield wires on the inductive influence. The shielding effectiveness of various conductor types and the shield wire power losses are studied. Chapter 7 proposes the use of new inductive influence measures based upon the models derived in Chapter 4. The use of inductive influence measures in Harmonic Limitation Legislation which accurately reflect the ability of a transmission line to cause interference may improve the protection provided by such legislation and reduce the cost of compliance.

Verification of the computer models, the third aim of this project, is the subject of Chapters 8 and 9. These chapters describe the work undertaken by the author to assess the inductive influence of the New Zealand High Voltage Direct Current Transmission Link. Chapter 8 contains details of the multiconductor transmission line models used to predict the disturbing current profile along the link. Although much of this work involves the use of standard models and analysis techniques, special algorithms have been developed to improve the efficiency of solution. The experimental techniques, results and a comparison with computer simulations are reported in Chapter 9.

The thesis closes in Chapter 10 with a summary of the main conclusions and contributions made during this project.

1.4 Project Philosophy

From the organisation of this thesis, it appears that the project proceeded in a simple and direct manner designed to satisfy the project aims. In fact the research progressed in a more complicated manner to achieve the requirement of originality set by the University.

At the initiation of this project the author was confident that existing computer models of transmission lines provided reasonable estimates of the fields that exist in reality. Therefore emphasis was placed on satisfying the second aim by attempting to develop original methods for reducing the inductive influence of transmission lines.

To achieve this goal the standard engineering philosophy of determining system behaviour then developing methods to exploit it, was employed.

Two philosophies exist for determining system behaviour. The first method, or *Mechanistic* approach, requires the decomposition of the system into its component parts. Once the behaviour of each component is understood, the rules describing them may be combined to determine the behaviour of the entire system. This method is mechanistic in the sense that the response of the whole is constructed from that of its constituents and the process of decomposition and reconstruction is clearly defined and logical. A consequence of the mechanistic nature of this process is that a result is assured. Unfortunately as the relationships between components are bilateral, the resultant description of the system behaviour may be complicated, masking the dominant system behaviour with component details. In such cases approximations must frequently be made to aid comprehension which introduces error into the analysis.

The second approach, known as the *Experimental* method, requires the observation of numerous controlled experiments and the formulation of rules to explain the results. Such an approach is difficult as it requires the ability to order information, compare it with existing rules and specify new rules and experiments. This approach is not assured of success as the system behaviour may not be able to be described or approximated by simple rules. The rules obtained may never describe the system response in detail, although the dominant effects are generally determined early in the analysis. An advantage of this approach is that the researcher becomes very familiar with the system response, which is invaluable when devising ways to exploit system behaviour.

The factors affecting the inductive influence of multiconductor transmission line are difficult to understand due to the complexity of the interactions between the conductors and the earth. Although a mechanistic approach may be used to construct the response of a multiconductor line from that of a single conductor above the earth, it provides little insight into the dominant system characteristics. The reason for this is the complexity of existing mathematical models of a conductor above the earth (Chapter 3). Rigorous mathematical descriptions of this system yield integral equations which can only be evaluated numerically, obscuring the system behaviour. The use of approximate models,

such as the Complex Penetration Model, tends to hinder comprehension rather than aid it through the introduction of the mathematical artifice of complex dimensions. The experimental approach, although not assured of success, offers a more direct path to understanding the inductive influence of multiconductor lines and has therefore been used in this project.

It is impractical to conduct sufficient experiments on actual transmission lines to determine the system characteristics, hence numerical experiments on computer models were performed. The results of these experiments, designed to determine the sensitivity of the inductive influence to line geometry, frequency, earth resistivity and current flow variations, are reported in Chapters 4 and 5. The use of shielding conductors and alternative line geometries as a means of reducing the inductive influence were then considered (Chapter 6).

Attempts were then made to explain the experimental observations, resulting in the development of the earth return models presented in Chapter 4. In this thesis the models are reported before the work from which they originated as this simplifies the explanations for the observed multiconductor inductive influence effects. The models were also used to derive new measures of the inductive influence, described in Chapter 7, which may be used to specify and police harmonic limitation levels.

The other project aims have been achieved in a simple, direct manner. Chapter 2 contains a review of existing modelling techniques thereby satisfying the first aim, while Chapters 8 and 9 describe a study of the inductive influence of the New Zealand High Voltage Direct Current Transmission system designed to confirm the validity of the computer models.

1.5 Publications Associated with this Research Project

The following papers have been published during the course of this research project.

[Cameron *et al.* 1989]
Cameron, G., Arrillaga, J., Gleadow, J. and McKenzie, N. "Estimation of Equivalent Disturbing Currents in the Cook Strait HVDC Transmission System,", In *Symposium of Specialists in Electric Operational and Expansion Planning*, Sao Paulo - Brazil, August.

[Cameron and Bodger 1990]
Cameron, G.R. and Bodger, P.S. "Physical Interpretation of Inductive Interference of Power Systems on Communications Circuits,", In *Proceedings of Annual Conference*, Wellington, New Zealand, February 12-17, pp. 241–252.

[Cameron *et al.* 1990]
Cameron, G.R., Acha, E. and Arrillaga, J. "An Efficient Algorithm for the Calculation of Harmonic Interference from Long Transmission Lines," *Journal of Electrical and Electronics Engineering, Australia*, Vol. 10, No. 2, June, pp. 73–82.

[Cameron and Bodger 1991a]
Cameron, G.R. and Bodger, P.S. "Physical Interpretation of Inductive Interference of Power Systems on Communications Circuits," *International Journal of Electrical Power and Energy Systems*, Vol. 13, No. 3, June, pp. 153–159.

[Cameron and Bodger 1991b]
Cameron, G.R. and Bodger, P.S. "New Measures for Assessing the Inductive Influence of Multiconductor Transmission Lines," *Proceedings of the Institution of Electrical Engineers, Part C*, Vol. 138, No. 4, July, pp. 358–364.

CHAPTER 2

AN OVERVIEW OF INDUCTIVE CO-ORDINATION STUDIES

2.1 Introduction

Since the introduction of electricity distribution systems there have been problems of interference to communication services (Klewe, 1958, chapter 1). This interference results from unwanted coupling between the systems due to their close physical spacing. As these systems are designed to service the same geographical areas and are frequently forced to share the same right of way, it is not always possible to provide the desired separation between the networks and therefore some coupling must be tolerated.

Interference may also occur due to current flow in high voltage transmission lines (Syman and Hore, 1981). These lines do not generally share right of ways with communication cables, however due to the presence of larger currents in these lines interference can occur to communication services in the regions they traverse.

To minimise the resultant interference to communication services attention must be paid to the location, design, construction, operation and maintenance of the communication and power systems. Procedures which address these issues, known collectively as inductive co-ordination measures (IEEE, 1984), are the principal means of preventing inductive interference to communication services.

Depending on the severity and extent of the interference, the most economical solution to inductive influence problems may be :

- to reduce the inductive influence of the transmission line,
- to decrease the coupling between the systems,
- to lower the susceptibility of the communications network to interference,
- a combination of these measures.

As the best time to plan these protection measures is during the design of the networks, there is a need for accurate analysis techniques to quantify the severity of interference to telecommunication services due to current flow in transmission lines.

In this chapter a procedure for determining the noise voltage in a telecommunications circuit due to current flow in an adjacent power system is described. To evaluate the interfering voltage it is necessary to determine the voltages and currents in both the power and communication systems and the electromagnetic fields linking the systems. Therefore the procedure for determining the resultant noise voltage must incorporate algorithms for power system analysis, electromagnetic field calculation in the presence of the earth and communication system analysis. The simplifying assumptions upon which the procedure is based and algorithms suitable for inclusion in the procedure are the subject of the following subsections. This discussion has been written to demonstrate how existing algorithms may be combined to satisfy the first aim of this project, that of developing a model which accurately predicts the inductive influence of transmission lines. It has also been written to indicate how the work reported in this thesis

contributes to the study of the problem of predicting induced noise voltages in communication systems, and to discuss in general terms the simplifying assumptions upon which the algorithms used during this research project are based. Detailed descriptions of the techniques used are contained in latter chapters.

The chapter opens in Section 2.2 with a discussion of how algorithms for power system analysis, electromagnetic field calculation and communication system analysis may be combined in a sequential procedure for predicting induced noise voltages.

Methods for determining the state of a power system are discussed in Section 2.3. Direct measurement techniques and simulation methods are presented and the algorithmic approach employed in this project is discussed.

The mechanisms of coupling between power and telecommunication systems is the subject of Section 2.4.

Section 2.5 discusses the problems associated with modelling communication systems and describes the simplified approach used in the course of this project for assessing the interfering ability of a transmission line.

The chapter closes in Section 2.6 with a summary of the algorithms used during this research project and the assumptions upon which they are based.

2.2 Decoupling Power and Telecommunication System Studies

To determine the resultant interference to a telecommunication system due to current flow in a power transmission line, it is strictly necessary to simultaneously solve for the state of both systems as the coupling between them is bilateral. Both the power and telecommunication systems contribute to the electromagnetic field in their environment and are in turn influenced by it. As a consequence the voltages and currents in these systems are not independent, but are coupled via the electromagnetic field, as shown in Figure 2.1.

However, due to the physical separation between the power and communications systems, the currents and charges induced in the communications systems do not usually affect the currents and charges in the power system, and the energy coupled from one system to another is generally small in relation to that remaining within the system. The coupling is therefore considered to be *weak* (Olsen and Jaffa, 1984). Although the coupling is weak the large difference between the signal energies within each system (see Figure 2.1) means that power system signals weakly coupled into a communications system may still engulf the desired signal. Communication signals have an insignificant effect on power system operation however. Therefore as a first approximation the energy flow or coupling may be considered to be unilateral, from the power system to the communications network as shown in Figure 2.2.

Although Figure 2.2 indicates the effective coupling between the power and telecommunication systems from a noise interference perspective, it does not show the true relationship between the systems and the fields about them. Both systems contribute to, perturb, and are in turn influenced by the electromagnetic field. The presence of a communications cable will result in a significant distortion of the electromagnetic field induced by the line in the vicinity of the cable, from that which existed before the cable was installed. However it is unlikely to distort the field greatly in the vicinity of the power line under normal operating conditions. As a consequence the currents and charges on transmission lines are not usually disturbed by the presence of a cable.

There are two ways in which a telecommunications cable may alter the electromagnetic field, by distorting either the electric component and/or the magnetic component of the field (the electric and magnetic field effects are related by Maxwell's equations,

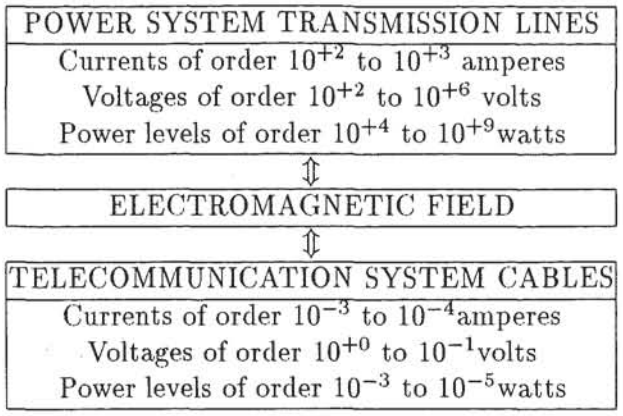

Figure 2.1. Electromagnetic Relationship between Power Lines and Communication Cables

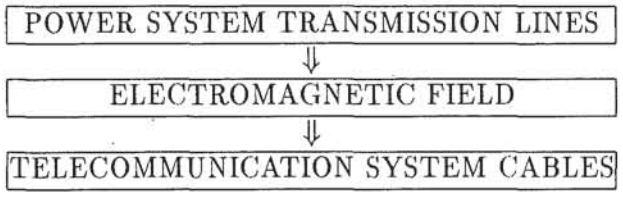

Figure 2.2. Unilateral Coupling Approximation

however at low frequencies the effects may be considered separately Section 2.4). A telecommunications cable, due to the high conductivity of the wire inside it, will significantly distort the electric field in its immediate vicinity. The magnetic field will only be distorted if currents comparable in magnitude to those in the transmission line are induced to flow in them.

Regardless of whether the power system is effected of not, it should be noted that electromagnetic field at the cable site will be perturbed by the presence of the cable. Therefore the electromotive force causing interference to the cable is not equal to that which existed at the site of the cable prior to the installation of the cable.

When the coupling between the power system and communication systems is weak, the power system may be solved independently by ignoring the effect of the telecommunication network. Once the state of the power system has been determined, the electromagnetic field induced by the transmission line at the site and in the presence of the cable can be calculated. The resultant interference to communication services can be derived from this. Thus the simultaneous solution of the systems may be reduced to the sequential solution of each network shown in Figure 2.3, resulting in a considerable saving of computational effort.

The weak coupling assumption is generally valid for steady state noise induction studies, however it may not be valid for fault studies or coupling to aerial conductors. Steady state noise currents induced in buried telecommunication cables are generally small as power and telecommunication companies endeavour to separate the systems as much as possible. Therefore the magnetic field and transmission line current are not significantly affected. Also, buried cables do not influence the electric field above ground at harmonic interference frequencies as the surface of the earth is effectively a zero potential plane, and hence the capacitance of the transmission line is unchanged.

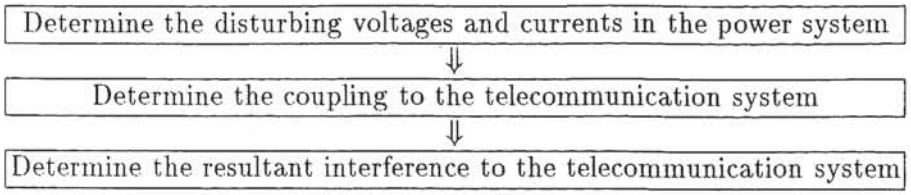

Figure 2.3. Procedure for Determining the Induced Noise Voltages

Consequently the weak coupling assumption is valid for steady state noise induction to buried cables. The assumption may not be valid for fault studies as earth potential rise or dielectric breakdown can result in strong coupling. As a consequence large currents can be induced in telecommunication cable sheaths or in the cables themselves, affecting the voltage and current distribution on the transmission line. Aerial telecommunication conductors may also experience strong coupling by virtue of their proximity to the transmission line, affecting the charge distribution on the line. In such cases the power and telecommunication system studies can not be decoupled.

Buried polyethylene sheathed cable is the dominant media used for subscriber reticulation in the New Zealand telecommunication system. Consequently under normal operating conditions the weak coupling assumption is valid. During this research project it has been assumed that the coupling between the systems is weak, and therefore the power and communication systems are solved independently using the sequential procedure shown in Figure 2.3.

2.3 Power System State Determination

To determine the noise voltages induced in a telecommunication system it is first necessary to determine the interfering voltages and currents in the power system. Two approaches exist for determining the state of a power system. Either the voltages and currents can be measured directly or the power system can be simulated. In this section measurement and simulation methods for determining the state of a power system are discussed.

2.3.1 Measurement of Power System State

The best way to determine the state of the power system is to measure it. However performing measurements on a power system is not a simple task due to the dynamic nature and complexity of the network, the range of frequencies that must be considered, the difficulty of conducting experiments on high power systems and the volume of data that must be processed.

A power system is never in a truly steady state as loading and generation vary continuously. As a consequence, the system frequency and waveform distortion change continuously. Therefore the spectra of the power system signals is not constant and multiple measurements made at different locations in the system must be taken in synchronism. Also, as human beings are diurnal, overall system loading and generation change greatly throughout the day. Consequently it is necessary to take measurements at a variety of times throughout the day as the system damping changes.

To determine the state of the entire power system it is necessary to measure the voltage or current on all phases at all busbars for all frequencies of interest. The power

system may be significantly unbalanced at high frequencies (Densem *et al.*, 1984) necessitating the measurement of the parameters on all phases. Due to the large electrical dimensions of power systems at high frequencies, many observations must be made to ensure that no resonant effects in the system are missed. Also as a resonance could occur at any frequency, measurements must be taken over a wide range of frequencies.

One of the major difficulties associated with performing measurements on a power system is obtaining suitable transducers and instrumentation. Existing transducers are designed to work at the fundamental frequency only and often have an unsuitable frequency response (Arrillaga *et al.*, 1985, chapter 7). Multichannel spectrum analysers are required to process the signals on all phases simultaneously. While digital instruments based on the Fast Fourier Transformation algorithm are suitable for this task (Arrillaga *et al.*, 1985, chapter 6), such instruments are expensive precluding their widespread use.

Assuming that it is practical to measure the state of the power system, the problem of storing and analysing the data still remains. These tasks are difficult to perform due to the high volume of data involved. In practise it is necessary to perform data reduction by time averaging or the use of transformations to extract only the data of interest prior to storage. However, care must be taken to ensure that important trends are not masked during the reduction process. Time averaging conceals the distribution of the variable of interest, which is necessary to determine the probability distribution of the resultant inductive interference. Other compression techniques involve the use of transformations to express the interfering ability of the power system by a single number. The most commonly used transformation of this type is the *Equivalent Disturbing Current* (CCITT, 1989a), which is defined as the 800 Hz current that will result in the same annoyance to a subscriber as the full spectrum of currents that actually exist on the line. Instruments known as *Psophometers* have been developed to calculate the equivalent disturbing current directly from the distorted power system waveforms. However the equivalent disturbing current may not provide a realistic appraisal of the interfering ability of the power system as it is calculated from the zero sequence current on the transmission line. The contribution from other sequences and the influence of conductor geometry and earth resistivity on the interfering ability are ignored.

Given the present lack of suitable transducers in the power system, the high cost of instrumentation, the enormity of the task of conducting simultaneous measurements and the difficulty of processing the information; it is not practical to perform continuous real time monitoring of the spectra of an entire power system at present. Modern measurements are generally limited to the investigation of localised signal levels and studies of small systems using simplified data processing techniques based upon the Equivalent Disturbing Current measure.

2.3.2 Simulation of Power System State

An alternative to performing measurements on a power system is to simulate it. The principal advantages of simulation over direct measurement are that simulation studies can be quicker, easier and cheaper to perform, and that the system can be modified to investigate future configurations.

Although simulator studies are easier to perform than experimental investigations, the problem of processing and interpreting the data still remains. A great many simulations must be performed to investigate all operating conditions and the results combined to determine the quantities of interest. Consequently great care must be taken during a simulation study to define the parameters of interest and the data processing methods used, to avoid masking features of interest and wasting resources.

In the past, special purpose analogue computers have been used for power system

studies. These devices represent system components by scaled down models. The main disadvantage of analogue simulators is the large number of components required to represent the system in detail and hence the high cost of the simulator. Digital computers have now largely supplanted analogue simulators due to their low cost, high speed and greater flexibility. Mathematical models are used to represent system components in digital studies, therefore the system component models are not constrained to be physically realisable, as in the case of analogue simulation, and large numbers of components can be represented at low cost.

The accuracy of all simulator studies is limited by the accuracy of the models used to represent the components and the validity of the data inserted into the models. Measurements of system parameters are required for insertion in the models and therefore the overall simulation accuracy is limited by the accuracy of these measurements. It is not always practical to represent every system component in a simulator study. Consequently system reduction and approximation methods must be used to derive equivalent circuits representing parts of the power system (Watson and Arrillaga, 1987).

It is not the intention of this thesis to provide a detailed discussion of all methods for predicting the state of a power system. However the discussion that follows has been provided to indicate to the reader the difficulties involved when simulating a power system, with particular reference to those algorithms in use at present.

There are two general classes of simulation used for interference studies. These may be classified as *Time domain* or *Frequency domain* studies and may be performed on either analogue or digital simulators.

2.3.2.1 Time Domain Simulation

A time domain simulation is a simulation in which the power system time waveform is calculated. The resultant spectra is then determined by performing a Fourier transformation of the time waveform. Time domain simulations are particularly useful for simulating systems containing time dependent elements such as high voltage direct current convertors (Arrillaga *et al.*, 1987).

The main disadvantages of time domain simulations are the difficulty of selecting suitable initial conditions, the time required for the simulator to attain a meaningful solution, and the difficulty of representing the frequency dependence of the system (Watson and Arrillaga, 1987). If improper initial conditions are used then a long simulation must be performed before the waveform reaches a steady state. The time constants of power system components vary enormously, therefore long duration studies with small time steps are required to determine the steady state waveform. Consequently time domain simulations tend to be inefficient.

2.3.2.2 Frequency Domain Simulation

Frequency domain simulations are based upon the assumption that the power system is in a periodic steady state, with a period equal to that of the supply. The power system will then contain frequency components equal to that of the supply frequency and possibly its harmonics. Harmonics are generated by non-linear elements in the power system. If the non-linearities are time invariant and under periodic excitation then the output will contain only harmonics of the excitation period. In practice a power system is never in a truly periodic steady state as loading and generation are time variant. However the rate at which these quantities vary is low in general, therefore as a first approximation the power system may be considered to be in a periodic steady state. This assumption simplifies the analysis of the system as the network state can be represented by a discrete set of harmonic voltage or current phasors at each busbar in

the system, rather than considering a continuous spectrum of time dependent voltages and currents.

Many frequency domain simulation techniques exist for determining the harmonic distortion in a power system. In the following sub-sections *Harmonic Penetration*, *Harmonic Power Flow*, and the *Harmonic Space Representation* are considered.

2.3.2.2.1 Harmonic Penetration

Harmonic penetration studies assume that the system can be represented by a linear passive network, with the harmonic sources represented as fixed injections (Arrillaga *et al.*, 1985, chapter 9). The network can then be expressed at each harmonic frequency as a linear system of equations relating the current injections and voltages at all nodes. Each system of equations is solved independently and the results combined to yield the distorted voltage and current waveforms throughout the system.

Harmonic penetration studies are best suited to the study of the propagation of harmonic signals within linear sub-systems, such as on transmission lines, as non-linear components can only be represented by fixed injections. However it is possible to study the interaction of non-linear elements with the power system using an iterative scheme which includes the harmonic penetration algorithm. The procedure is known as the *Iterative Harmonic Analysis* (IHA) algorithm (Arrillaga *et al.*, 1987), and proceeds as follows :

1. Initialise the harmonic current injection vector representing the non-linear harmonic source. The fundamental current injection into the network is calculated from Power-Flow data. All other harmonic injections are set to zero.

2. Using the Harmonic Penetration algorithm, determine the voltage waveform at the busbar to which the non-linearity is connected when the harmonic current vector is injected into the power system.

3. Apply the voltage waveform due to the current injections to the non-linear device and determine the resulting current waveform from knowledge of the type of non-linearity.

4. Update the harmonic current injection vector by performing a Fourier Transformation of the current waveform.

5. If the harmonic current injection vector has converged then go to step 6, otherwise repeat from step 2.

6. Use the Harmonic Penetration algorithm and the converged vector of injection currents to determine the harmonic voltages throughout the entire network.

The IHA algorithm employs time domain analysis methods to determine the response of the non-linear device to the applied voltage and therefore any deterministic non-linearity can be analysed using this approach. It is more efficient than purely time domain studies however (Arrillaga *et al.*, 1987), as only the non-linearity is represented in the time domain. The IHA algorithm is strictly a frequency domain method as the system is constrained to be in a periodic steady state.

To date the IHA algorithm has been successfully applied to the problem of determining the harmonics produced by high voltage direct current convertor plant (Eggleston, 1985; Arrillaga *et al.*, 1987). However problems have been experienced due to non-convergence of the algorithm. The interpretation of the results in such cases is under study at present.

2.3.2.2.2 Harmonic Power Flow

Harmonic power flow is an extension of fundamental frequency power flow which includes harmonic voltage magnitudes and angles in the state vector. This formulation makes it possible to represent inter-harmonic coupling effects, enabling non-linear loads to be included in the power flow. Harmonic power flows are used to calculate busbar voltages, branch currents and total distortion volt-amperes in addition to real and reactive power flows at harmonic frequencies. Two schemes have been proposed for modifying the power flow algorithm to include harmonics.

In the first scheme the Newton-Raphson algorithm has been adapted to include harmonics (Xia and Heydt, 1982). The formulation employs harmonic current and apparent volt-ampere balance equations in addition to real and reactive power balance to formulate the Jacobian matrix. The mismatch vector contains active and reactive power mismatches and current mismatches at all harmonic frequencies. The vector of unknown variables (state vector) contains the harmonic voltage magnitudes and angles. Additional variables, specifying the internal state of the non-linear loads, are included in the system state vector. Models for DC convertors, gaseous discharge lamps, iron cored transformers, rotating machines and transmission lines have been included in the basic algorithm (Tamby and John, 1988). The principal disadvantages of this method are the large and complicated Jacobian matrix which results and the difficulty in selecting appropriate initial conditions (Lo and Goh, 1986). To simplify the Jacobian matrix an alternative method has been proposed in which state variables for the non-linear loads are omitted from the power-flow state vector. The current injections from the non-linear loads are assumed to be constant during the power-flow iteration (Lo and Goh, 1986). At the end of each power-flow iteration the state variables for the non-linear loads are updated and the new current injections determined. The entire process is repeated until convergence is reached.

A simpler algorithm has recently been developed which is based upon a combination of fundamental frequency power-flow and the iterative harmonic analysis algorithm (Tamby and John, 1988; Arrillaga and Callaghan, 1989). The algorithm utilises the distorted voltages at the non-linear busbars, and knowledge of the type of non-linearity to calculate the injected currents and powers. A power flow algorithm is then used to update the fundamental frequency voltages, and the system impedance matrices are used to update the harmonic voltages. The process is then repeated until the voltages converge. This procedure is more efficient than the modified Newton-Raphson algorithm as the harmonic equations can be considered separately and therefore the matrix equations are smaller.

2.3.2.2.3 Harmonic Space Representation

In the harmonic space representation, the system state is represented by a single vector of nodal voltage or current injection phasors containing data for all harmonics and all busbars in the system (Eggleston, 1985). Using nodal analysis methods, an admittance matrix relating the voltage and current vectors can be formed. The harmonic space representation may be viewed as the combination of the independent systems of equations for each harmonic of the harmonic penetration algorithm into a single matrix equation.

The harmonic space representation is necessary to model devices in which there is coupling between harmonics, and is therefore well suited to the task of representing non-linear elements. Some classes of non-linearity may be linearised around a base operating point and expressed as a Norton source in the harmonic space. To date models for synchronous generators (Semlyen *et al.*, 1985), AC/DC convertors (Mizuma

et al., 1985), and magnetic non-linearities (Semlyen *et al.*, 1987) have been expressed in the harmonic space. Linear elements are modelled as simple admittances with no coupling between harmonics. Thus an entire power system can be represented in the harmonic space and the non-linearities solved using a Newton-type iterative algorithm (Acha, 1988).

While the harmonic space representation is necessary to study effects due to inter-harmonic coupling, it is not an efficient method for studying the propagation of harmonic signals in power systems. The main reason for this inefficiency is that transmission systems consist mainly of linear passive elements, such as transmission lines. Therefore there will be little inter-harmonic coupling, the admittance matrix describing the system in harmonic space will be sparse and the resulting algorithm will be inefficient unless the sparsity can be exploited.

A modified representation in which the system is torn into linear and nonlinear subsystems and the networks solved alternately until convergence is reached would improve solution efficiency (Acha, 1988). Only the nonlinear subsystems would need to be represented in the full harmonic space. The linear subsystems could be represented by an admittance matrix for each frequency of interest.

2.3.2.3 Summary

The principal difficulty in determining the distorted waveforms throughout a power system is calculating the contribution due to the non-linear elements. It is for this reason alone that new power system analysis algorithms are being developed. Unfortunately these algorithms tend to be inefficient as the power system must either be simulated in the time domain or an iterative frequency domain algorithm must be used. Given the large size of modern power systems it seems likely that new algorithms in which the linear and non-linear parts of the power system are analysed alternately in an iterative scheme will be used, as has been proposed for the Harmonic Power Flow and Harmonic Space algorithms.

It is apparent from the discussion presented above that there is a great variety of power system analysis techniques. Many of these algorithms are still under development and therefore it is inappropriate at this time to select a particular algorithm for inclusion in the procedure for predicting the noise voltages induced in a telecommunication cable. It is likely that different analysis techniques will be required for different types of non-linearity and therefore the solution to the problem of determining distorted signals in a power system may well incorporate features of many algorithms currently under development.

2.3.3 Power System State Determination Methods Used during this Project

Inductive coupling to communication cables may occur along the entire length of a transmission line; it is not usually confined to the vicinity of the terminals. However existing measurement systems and simulation algorithms are designed to provide busbar information only. While it is possible to install additional transducers and create fictitious busbars to obtain the required information, such an approach is inefficient when the inductive influence profile along the line is required. A more efficient approach, which is the one used during this project, is to break the power system state determination into two stages. In the first stage the busbar conditions are determined, the disturbing signal profile along a transmission line is then derived from the terminal conditions in the second stage.

The emphasis during this research project has been placed on the development of a model for predicting the inductive influence of transmission lines. Sources of disturbing signals within the power system are not considered. Therefore power system modelling has been limited to the second stage, that of determining the disturbing voltage and current profiles from the terminal conditions. It has been assumed that the busbar state may be obtained using existing monitoring systems or simulation techniques.

To calculate the current and voltage profiles it is only necessary to model the transmission lines in detail, the rest of the system being represented by a fixed injection. Although transmission lines exhibit non-linear effects, such as corona discharges and magnetic saturation, they can be accurately modelled as linear networks (see Chapters 3 and 8). Each frequency of interest may then be considered independently. While the transmission line may be analysed at any frequency, it was assumed that the system was in a periodic steady state and therefore only harmonic frequencies were considered. Details of the transmission line models are contained in Chapters 3 and 8. Chapter 8 also describes the circuit analysis technique used, which exploits the simple linear topology of transmission lines to improve the efficiency of solution.

To satisfy the third aim of this project, that of verifying the model accuracy, it was necessary to perform measurements of the transmission line currents and compare these with the currents calculated using the model and measured busbar voltages. Details of the equipment used, experimental method, data processing techniques and a comparison of the results with computer simulations is presented in Chapter 9.

New measures of the inductive influence of transmission lines are described in Chapter 7. Although not directly related to the problem of determining power system state, they may replace the Equivalent Disturbing Current measure as an efficient means for expressing the interfering ability of power systems.

2.4 Power-Communication Coupling Determination

The second step of an inductive co-ordination study is the determination of the interfering fields in the vicinity of the telecommunication cable.

2.4.1 Mechanisms of Coupling

The electric and magnetic fields induced by a transmission line are related by Maxwell's equations. However as wave propagation along the line may be approximated by a Quasi-Transverse Electromagnetic (Quasi-TEM) wave if the losses within the earth are small (see Section 3.3.3 and (Perz and Raghuveer, 1974a; Perz and Raghuveer, 1974b)), quasi-static field approximations may be used. The transverse electric and magnetic fields are then considered to be identical in form to static fields that satisfy the boundary conditions (Ramo *et al.*, 1984, chapters 1 and 2). It is instructive to use the quasi-static field approximation when describing mechanisms of coupling as the electric and magnetic fields may be considered independently. The electric field can be calculated from the potential of the line, while the magnetic field may be determined from the current (Chapter 3). The coupling mechanisms may then be decoupled and classified as being either conductive, electric or magnetic in origin (Klewe, 1958, chapter 2), depending on whether the interference is due to a shared conduction path, the potential of the line or the alternating current.

Each of these coupling mechanisms, their contribution to telecommunication interference and the coupling mechanisms considered during this research project are discussed in the sections that follow. As the mechanisms are described from a quasi-static view point it should be emphasised that these descriptions are a simplification of

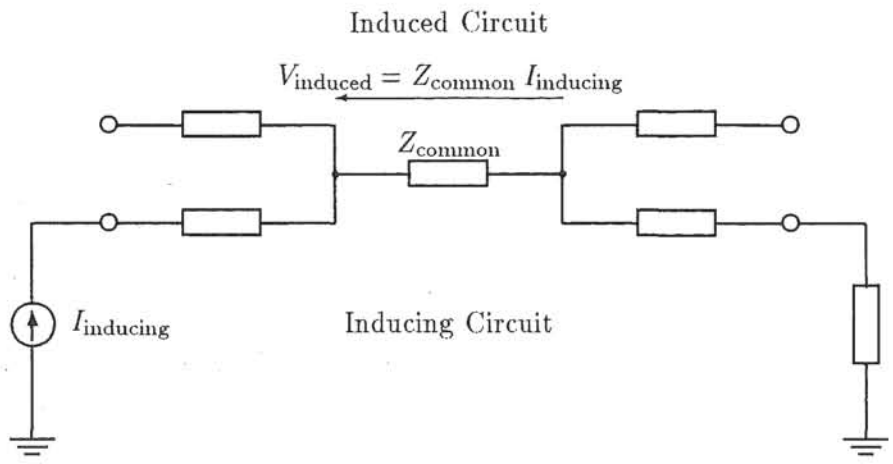

Where

$V_{induced}$ = voltage in the induced circuit (V)
Z_{common} = impedance of the common conduction path (Ω)
$I_{inducing}$ = current in inducing circuit (A)

Figure 2.4. Mechanism of Conductive Coupling

the actual situation. In reality the earth is lossy, therefore the electromagnetic field is distorted and differs from that determined using static concepts (see Chapter 3). The induced voltages are also dependent on circuit loading as the interfering signal has a finite source impedance. However in the descriptions that follow circuit loading effects have been neglected for clarity.

2.4.1.1 Conductive Coupling

Interference occurs due to conductive coupling when two circuits share the same conduction path as shown in Figure 2.4. A change in the current in one circuit will then induce a change in potential in the second circuit. Modern telecommunication systems do not usually share conductors with power circuits, except in the special case of telecommunication earthing systems which are usually directly bonded to power system electrodes or coupled via the earth. However during fault conditions on the power system direct contact with communication cables, dielectric breakdown or earth potential rise can result in conductive coupling. Conductive coupling does not produce significant noise voltages in well designed and maintained telecommunication systems under normal operating conditions.

2.4.1.2 Electric Coupling

A high voltage transmission line generates an electric field in the vicinity of the conductors which can interfere with other electrical systems. The field may induce an alternating voltage and current in neighbouring conductors, as indicated in Figure 2.5. As the induced current is proportional to the rate of change of conductor potential this effect is modelled by a mutual capacitance as shown in Figure 2.5.

The electric field induced by a transmission line is usually most intense in the immediate vicinity of the conductors, therefore coupling via the electric field may be minimised by maximising the spacing between cables and transmission lines. The

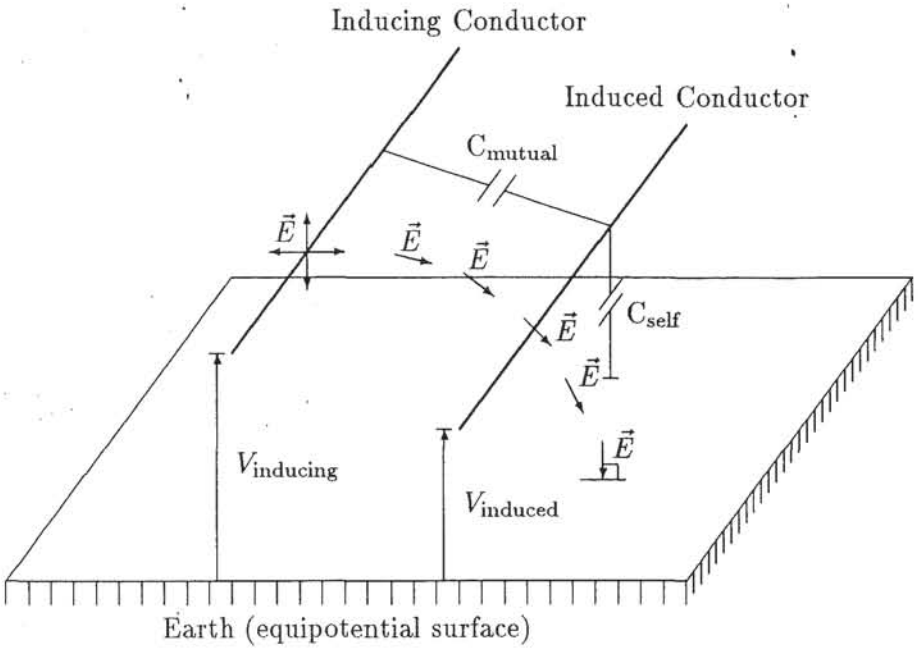

$$V_{induced} = V_{inducing} \frac{\frac{1}{\jmath\omega C_{self}}}{\frac{1}{\jmath\omega C_{mutual}} + \frac{1}{\jmath\omega C_{self}}}$$

$$= V_{inducing} \frac{C_{mutual}}{C_{self} + C_{mutual}}$$

Where

$\jmath$	= the pure imaginary ($\sqrt{-1}$)
ω	= angular frequency (rad.s^{-1})
$V_{inducing}$	= voltage of the inducing conductor (V)
C_{mutual}	= mutual capacitance between conductors (F)
C_{self}	= self capacitance of the conductor to earth (F)
$\vec{E}$	= electric field vector (V.m^{-1})

Figure 2.5. Mechanism of Electric Field Coupling

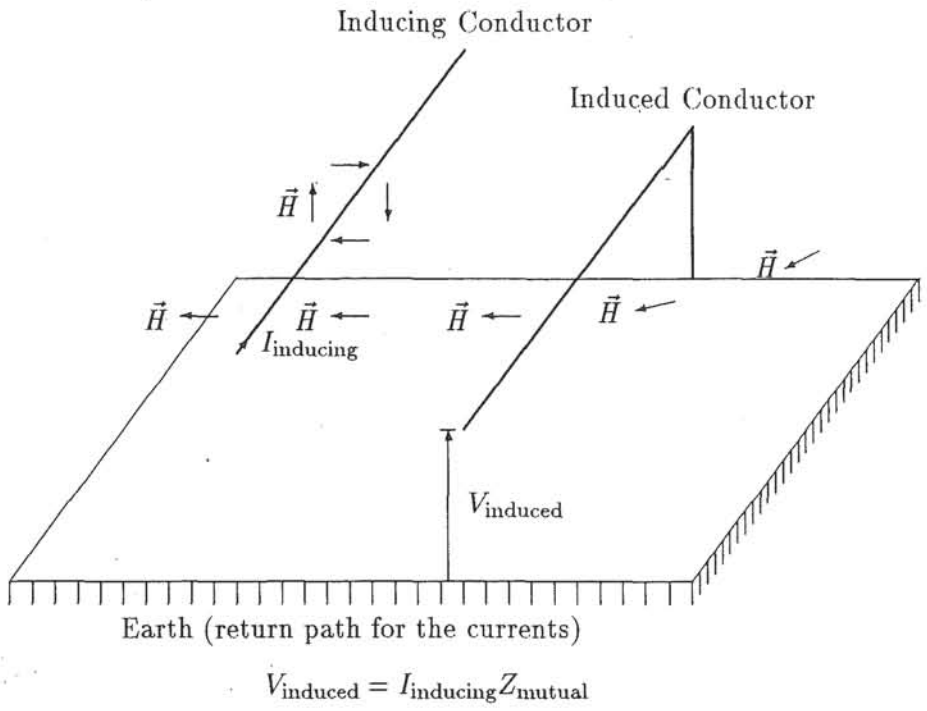

$$V_{\text{induced}} = I_{\text{inducing}} Z_{\text{mutual}}$$

Where

Z_{mutual} = mutual impedance between conductors (Ω)
$\vec{H}$ = magnetic field intensity (A.m^{-1})

Figure 2.6. Mechanism of Magnetic Field Coupling

intensity of the electric field is also proportional to the conductor voltage, therefore interference may be reduced by limiting interfering voltage levels on transmission lines. Earthing the induced conductor via a low impedance ($\ll \frac{1}{j\omega C_{\text{mutual}}}$) at one or more points reduces the interfering voltage, however interference currents will then flow along the conductor to ground which may or may not be desirable.

An alternative method for protecting communication cables is to shield them by surrounding the cable with a grounded conductor. The conductivity of the earth is sufficiently high for it to act as an electric field shield. Therefore electric field coupling to buried telecommunication cables is insignificant.

2.4.1.3 Magnetic Coupling

Current flow in a transmission line generates a magnetic field which may induce unwanted signals in neighbouring electrical systems as shown in Figure 2.6. If the flux links a telecommunication circuit then a voltage will be induced in that circuit which is proportional to the rate of change of flux. Magnetic coupling is modelled as a mutual impedance between the systems. Intuitively one would expect the mutual impedance to be purely inductive as the induced voltage is proportional to the rate of change of current, however the currents within the earth are not in phase with those in the conductors resulting in a resistive component of the mutual impedance.

The magnetic field generated by a transmission line is generally largest in the immediate vicinity of the conductors. Therefore magnetic coupling may be minimised by

insuring that there are large spacings between communication and power lines. The flux induced by a conductor is also directly proportional to the current producing it, therefore interference can be reduced by minimising the disturbing currents on the line.

An alternative method for reducing the flux in the vicinity of the cable is to install a shielding conductor near the cable or on the transmission line. Unfortunately, the resistivity of the earth is too high to act as an effective shield, and therefore buried telecommunication cables are susceptible to magnetic induction.

2.4.1.4 Dominant Power-Communication Coupling Mechanism

In a well designed telecommunication system in which the dominant form of subscriber reticulation is buried cable, such as the Telecom New Zealand system, the principal mechanism of power-communication coupling is by means of the magnetic field induced by the line. Therefore magnetic coupling is the only mechanism of power-communication coupling considered during this research project.

Electric field coupling must be considered when studying coupling to aerial telecommunication cables, while conductive coupling should be considered during fault studies. Both of these topics are beyond the scope of this project however.

2.4.2 Measurement of the Magnetic Coupling Fields

Direct measurement of the fields induced by a transmission line is the best way to assess the interfering ability. However measurements of the average inductive influence of a line are difficult to perform.

The problems faced by an experimenter conducting measurements of the electromagnetic field are similar to those faced when measuring the transmission line currents and voltages (Section 2.3.1). Due to the wide variation of the fields with distance along the line and time, it is necessary to conduct many measurements to obtain a true average. Also instrumentation suitable for performing these measurements is expensive and difficult to obtain. Care must be taken to ensure that the readings are not disturbed by other electromagnetic sources or irregularities in the local environment. Suitable assessment methods must be used to quantify the interfering ability of the line to ensure that important trends are not masked.

Despite these difficulties measurements of the inductive influence are regularly performed by telecommunication authorities (Syman and Hore, 1981). A simplified procedure is normally used, in which the psophometrically weighted noise voltage induced in a test cable laid near the line is measured. This method has the advantage that it directly measures the resultant equivalent disturbing voltage induced in a cable at that particular position, however the results are highly dependent on the cable position and construction. Consequently such measurements may not provide an accurate measure of the disturbing ability of the line.

2.4.3 Calculation of the Magnetic Coupling Fields

Given the high cost of performing experiments and the low cost of digital computers, it is frequently more economic to calculate the electromagnetic fields than to measure them. However the calculated fields will only be as accurate as the mathematical model of the transmission line above the earth.

A transmission line located above the earth is a difficult system to model due to the irregular structure of the earth, the non-linear behaviour of the materials and the geometry of a transmission line. The actual situation can not be represented exactly, however due to the great engineering importance of wave propagation along conductors

above the earth, considerable effort has been expended on developing mathematical models of idealised systems. Sophisticated models are now available, however they employ significant simplifications which may effect the accuracy of predictions.

The resultant inductive coupling determined using these models can not be expressed as a simple explicit relationship in many cases. Rigorous models of the fields around a transmission line require the evaluation of oscillatory integrals over an infinite range (Wait, 1972; Wedepohl and Efthymiadis, 1978). These integrals can not be solved symbolically in general, masking many of the properties of the coupling field by the complexity of the mathematics. However with the development of high speed computers and improved numerical methods, it is now practical to investigate the mechanism of inductive coupling through the numerical evaluation of the inductive field.

The accuracy of the field predictions made using these models is limited not only by the assumptions made during the derivation, but also by the validity of the data inserted into the models. Given the wide variation of the electrical characteristics of the earth with position and time, it is necessary to measure the parameters at the point of interest when comparing field measurements and computer predictions.

2.4.4 Magnetic Coupling Determination Methods Used in this Project

Both experimental and computational methods have been used during this research program to determine the magnetic coupling to buried telecommunication cables. However the majority of the results presented in this thesis were obtained from computer simulations, with the experimental results being used to establish the validity of the models.

As the simulation results can only be as accurate as the mathematical models used, particular care has been given during this project to the selection of suitable models. Many models were used during this project, as no single model can satisfy the requirements of high accuracy, simple mathematical form, clear physical interpretation and high computational efficiency. A summary of existing single conductor inductive coupling models, the simplifying assumptions made during their derivation, computer implementation and relative merits is presented in Chapter 3.

Measures for quantifying the inductive influence are discussed in Chapter 4. A comparison of the accuracy of existing models is also given.

Dissatisfaction with the complicated form of existing models led to the development of a family of models by the author that approximate the current distribution in the ground. Details of the derivation of the models are presented in Chapter 4. The simplest model of the family, known as the *Vertical Inducing Loop* model, is well suited to the task of predicting the inductive influence of multiconductor transmission lines without recourse to complicated mathematics.

The application of existing models to the task of determining the inductive influence of unshielded multiconductor lines is summarised in Chapter 5. It is demonstrated that simplified expressions based upon the Vertical Inducing Loop model accurately predict the inductive influence phenomena.

Chapter 6 extends the summary of the inductive influence of multiconductor lines to include the case of transmission lines with continuously grounded conductors. Two methods of reducing the inductive coupling from transmission lines are considered in this chapter: by lowering the internal impedance of the shielding conductor and changing the transmission line geometry.

Field measuring experiments have been performed during the course of this research to provide non-invasive sensing of the line currents and to confirm the accuracy of the coupling models used. Loop antennae were used to determine the line currents, and a

test cable method was used to confirm the validity of the power-communication coupling models. Details of the equipment used, the procedures followed and the results of these experiments are reported in Chapter 9. A comparison of measured and predicted cable voltages is also presented in this chapter.

A new measure of the inductive influence of a transmission line, based upon the Vertical Inducing Loop model, is described in Chapter 7.

2.5 Determination of the Resultant Interference to a Telecommunication Circuit

Once the fields in the vicinity of the cable have been calculated, the resultant interference to telecommunication services may be determined. In this section the operation of telecommunication circuits, the mechanism by which induced noise voltages interfere with the desired signal, and interference assessment and cable modelling methods employed during this project are described.

2.5.1 Mechanisms of Noise Voltage Induction

Telecommunication signals are usually propagated as a transverse or metallic voltage (V_{sending}) between a pair of conductors as indicated in Figure 2.7. The longitudinal voltages ($V_{\text{long-a}}$ and $V_{\text{long-b}}$), which are the voltages with respect to ground, do not individually convey any information. The information is contained in the difference between the longitudinal voltages ($V_{\text{transverse}} = V_{\text{long-a}} - V_{\text{long-b}}$). Induction from power lines into telecommunication circuits increases the longitudinal voltages. Interference will result if the induced voltages ($V_{\text{induced-a}}$ and $V_{\text{induced-b}}$) do not effect identical changes in the longitudinal voltages.

It is not possible for two conductors to occupy exactly the same location, therefore there is always some difference between the voltages induced in each conductor ($V_{\text{induced-a}} \neq V_{\text{induced-b}}$). This direct induction effect may be minimised by transposing open aerial lines and twisting cable pairs so that each conductor occupies similar average positions and experiences similar average electromagnetic fields. So effective is this technique that direct transverse voltage induction is rarely a problem in the New Zealand telecommunications network at typical power-telecommunication cable separations. Direct induction may be significant in imperfectly twisted cables in very close proximity to transmission lines, such as those which arise from the joint use of poles (Orr *et al.*, 1983) .

The principal mechanism by which an interfering voltage is produced in a telecommunications cable is by means of a process known as *longitudinal to metallic conversion* (Parker, Jr., 1978). Equal induced voltages in the conductors ($V_{\text{induced-a}} = V_{\text{induced-b}}$) will generate a net transverse voltage if the electrical parameters of the conductors forming the telecommunication circuit differ. The most common causes of this unbalance are: unequal source and/or termination impedances ($Z_{\text{send-a}} \neq Z_{\text{send-b}}$); differing conductor series impedances ($Z_{\text{series-a}} \neq Z_{\text{series-b}}$); and different conductor shunt admittances to earth ($Y_{\text{shunt-a}} \neq Y_{\text{shunt-b}}$). These differences arise from: variation of conductor position within the cable; normal distribution of cable parameters and terminating equipment component values; and poor design or fault conditions (bad joints, leakage to earth due to the ingress of water *etc.*). Furthermore these unbalances are frequency and position dependent, and may be time variant.

Care is taken to ensure that the cable is well balanced by twisting the conductors, and by moving the location of the twisted pairs around within the cable so that localised

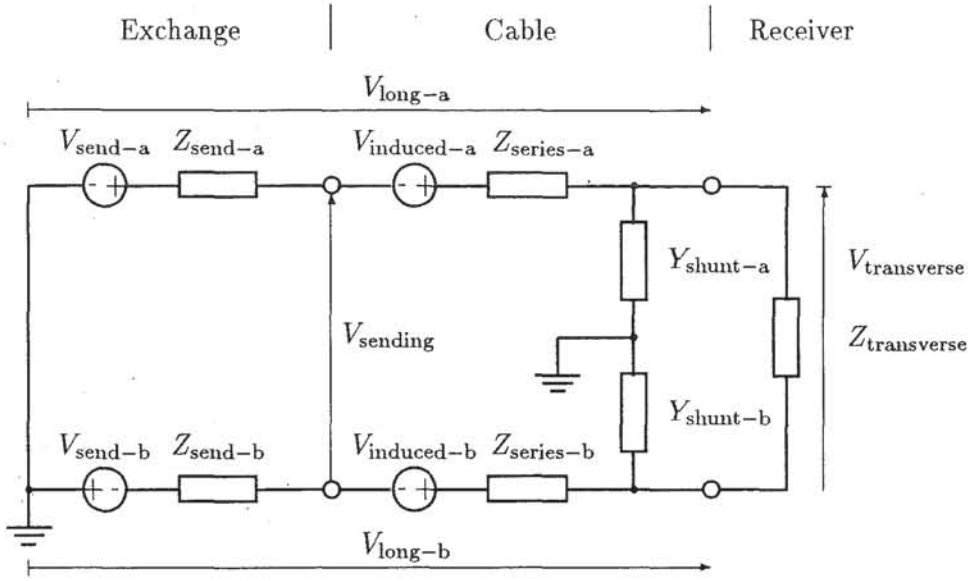

Where

V_{send-a} = sending voltage on conductor a (V)
V_{send-b} = sending voltage on conductor b (V)
$V_{sending}$ = net sending end voltage (V)
$V_{induced-a}$ = noise voltage induced on conductor a (V)
$V_{induced-b}$ = noise voltage induced on conductor b (V)
V_{long-a} = longitudinal voltage on conductor a (V)
V_{long-b} = longitudinal voltage on conductor b (V)
$V_{transverse}$ = transverse voltage at the receiver (V)
V_{common} = common mode (ground) voltage (V)
$= \frac{V_{long-a}+V_{long-b}}{2}$
$Y_{shunt-a}$ = shunt admittance of conductor a (S)
$Y_{shunt-b}$ = shunt admittance of conductor b (S)
Z_{send-a} = sending end source impedance on conductor a (Ω)
Z_{send-b} = sending end source impedance on conductor b (Ω)
$Z_{series-a}$ = series impedance of conductor a (Ω)
$Z_{series-b}$ = series impedance of conductor b (Ω)
$Z_{transverse}$ = transverse impedance of the receiver (Ω)

Figure 2.7. Telecommunication Signal Propagation

imbalances are averaged out. However over any finite length of cable there are localised imbalances which give rise to transverse noise voltages.

The balance of telecommunication cables is the ratio of the common (ground) mode voltage to the resultant transverse voltage, as defined in (2.1) It is of the order of 60 dB for well maintained plant (cable with no faulty pairs). This represents a 99.9% noise voltage rejection capability, as only 0.1% of the common mode voltage manifests itself as a transverse noise voltage.

$$\text{Telecommunication circuit balance (decibels, dB)} = 20 \log \left(\frac{V_{\text{common}}}{V_{\text{transverse}}} \right) \qquad (2.1)$$

This high level of performance can only be maintained if the balance of the terminal equipment exceeds that of the cable. The balance of electronic telephone exchanges is of the order of 50 dB. Improvements in the rejection capability of circuits with low equipment balance can be made by reducing the magnitude of the common mode voltage applied to the equipment and hence the transverse voltage that results, through the use of noise chokes and/or drainage coils.

2.5.2 Quantifying Telecommunications Interference

. A measure of the severity of interference to telecommunications services should accurately quantify the degradation as perceived by the end user. Whether an induced noise voltage results in unacceptable interference or not, is dependent on:

- characteristics of the cable (propagation constant, loss and balance),
- the characteristics of the equipment attached to the cable (balance, sensitivity to high levels of in-band noise, out-of-band noise and common mode noise),
- type of service (telephone, facsimile, modem, ISDN),
- the characteristics of the noise source (single frequency or broadband, constant or time variant),
- user expectations with regard to the quality of the service.

A wide range of services are now provided over copper telecommunications cables. These services often utilise the available bandwidth in different ways, and have differing sensitivities to noise (Orr *et al.*, 1983). Telephony uses a 300 - 3,400 Hz bandwidth according to the sensitivity of the human ear. Facsimiles and modems utilise the same bandwidth but have a flatter frequency response and are sensitive to interference at the carrier frequencies. Integrated Services Digital Network (ISDN) signals are broadband, and are centred on 40,000 Hz.

Many services can operate in the presence of noise through the use of adaptive algorithms. Telephone users speak louder and use repetition. Electronic systems may negotiate baud rates and employ error detection and correction or retransmission to rectify errors due to noise. Although adaptive systems may still function in the presence of noise, a penalty is incurred in the form of reduced through-put and hence higher cost for the telecommunications user.

Digital services without correction (voice services on ISDN) often exhibit a non-linear sensitivity to interference. No noise is experienced by the user until the interference is sufficient to cause bit errors. Each error results in an audible click whose volume is dependent on the bit that is corrupted, but is independent of the amplitude of the

interfering voltage level. The frequency of bit errors increases with interfering voltage level however. These digital systems offer better performance than corresponding analogue systems as long as no bit errors occur. Once the bit error threshold is exceeded a digital system may be more objectional from a users point of view than an analogue system experiencing the same interfering voltage.

The ability of telecommunications equipment to reject noise is a function of the design and implementation of the device. Many modern telecommunications devices are mains powered. This may introduce an earth connection to the device which can compromise the balance of the equipment and subject the line interface circuitry to the common mode noise in addition to the transverse noise voltage. The author has experienced problems where high levels of common mode out-of-band noise resulted in the generation of audible transverse noise due to overloading of the line interface electronics.

End users also have widely different expectations of the quality of service. What constitutes severe interference for one user may be acceptable for another.

As a consequence it is not possible to define a single measure which accurately quantifies the severity of interference, as perceived by users, for all services that may be provided over a given copper cable pair. Ultimately it is the user's opinion which determines whether a system is performing satisfactorily or not. Nevertheless quantitative measures of interference are required to identify and prioritise interference problems.

The International Telegraph and Telephone Consultative Committee (CCITT) of the International Telecommunication Union (ITU) has defined the following transverse noise voltage limit for telephony circuits :

> Where administrations commonly use psophometric weighting for noise measurements, the psophometric e.m.f. of the noise produced by magnetic and/or electrostatic induction from all power lines affecting the lines and trunks joining a subscriber's station to its international exchange should not exceed 1 millivolt. This value is measured at the "line" terminals of the subscriber's set. (CCITT, 1989b, Chapter 6, Page 53)

> The psophometric e.m.f. at the end of a telephone line is twice the psophometric voltage measured across a non-inductive resistance of 600 ohms, terminating the line at the place of measurement, if necessary via an impedance matching transformer, when the other end of the line is terminated with an impedance equal to the characteristic impedance of the line. (CCITT, 1989a, Chapter 4, Page 133)

The high penetration and high performance standards required of digital transmission technology in the Telecom New Zealand trunk network has effectively eliminated power system interference on the circuits between exchanges. As a consequence Telecom New Zealand's objective noise target is 1 millivolt of psophometric e.m.f. on the circuit between the customer and his local exchange.

Further work is required to define appropriate limits for other services. Limits for digital systems are likely to be based upon performance standards, such as the percentage of error free seconds in a specified period and/or the bit error rate (CCITT, 1989b).

Telecommunication interference measures are dependent on telecommunication system parameters, and therefore are unsuitable for quantifying the interfering ability of transmission lines. Common mode voltage on a particular cable pair is however a useful indicator of the time dependency of inductive influence. The magnitude of the common mode noise is dependent on cable length, location relative to transmission line, common mode impedances of the terminal equipment and parameters of the earth in addition to those of the transmission line. Therefore it is not an absolute measure of

interfering ability, unless it can be normalised. Normalisation is only possible where: detailed and accurate data on the physical environment is available; the environment is simple so that it can be accurately represented by mathematical models; and there is only one source of interference or the type of interference can be uniquely identified. In the author's experience normalisation is an expensive and inaccurate process at voice frequencies. Measures for accurately quantifying inductive influence are discussed in Section 4.2 and Chapter 7.

In the sections that follow the advantages and disadvantages of measuring and calculating common mode and transverse noise voltages in communications circuits are discussed, with particular emphasis on the methodology used by the author.

2.5.3 Measurement of Induced Noise Voltages

Measurement of the transverse and common mode noise voltages in the Telecom New Zealand network is accomplished with the aid of two devices. The first device, an *Automatic Line Termination*, provides a quiet balanced termination at the exchange for test calls originated from the circuit under test. The second instrument, a Psophometer, is used at the customers premises. It terminates the user end of the circuit, filters the noise (Psophometric or flat weighting) and calculates the resultant rms voltage.

Although the equipment involved is relatively inexpensive, such measurements are expensive to perform as a technician must visit the customers premises. Inexpensive estimates of the transverse noise voltage can be obtained from automatic test equipment at the exchange. Such measurements are not strictly valid as the voltage is measured at the exchange end of the circuit, the users end of the circuit is not terminated correctly and the exchange interface circuitry (which may be contributing to poor circuit balance) is bypassed during the test.

Should the transverse noise voltage prove to be excessive, then a common mode noise measurement is made to determine whether it is due to excessive interference and/or poor circuit balance. If the common mode noise exceeds 86 dBrnp then the circuit may be considered to be experiencing excessive interference. Telephone service may not meet the CCITT objective noise target of 26 dBrnp on a well maintained circuit (balance of 60 dB or better) when the common mode voltage exceeds 86 dBrnp. The high common mode voltage may be due to poor cable placement *etc.* , and therefore is not necessaryily an indicator of excessive emmission from the source. Telephone circuit balance may be estimated from the noise measurements using (2.1). If it is less than 60 dB then either the balance is poor or the circuit is experiencing direct transverse induction. Poor circuit balance can be confirmed using a direct reading instrument complying with IEEE, 1985.

If there is excessive common mode noise on the circuit it may be necessary to perform more detailed studies to identify the source, extent and severity of the interference (Robinson, 1966; Syman and Hore, 1981). Spectral analysis of the noise may be performed in synchronism with equivalent measurements on the power system (Section 2.3.1) to identify the source. Continuous monitoring of both the suspected source and noise in the telecommunications system is often required to establish whether there is a correlation between the events. Such detailed studies are expensive to perform and can only be justified in exceptional cases.

2.5.4 Calculation of Induced Noise Voltages

Given the huge variety of equipment, the complexity of the communication system, and the lack of data about the localised imbalances of particular circuits, it is not

practical to model a circuit in detail. Instead a simplified approach based on the concept of telecommunication circuit balance is used.

Balance figures provide a simple means to estimate the resultant transverse noise voltage in a telecommunication circuit. From estimates of the axial electric field at the site of the cable, the cables propagation characteristics and terminating impedances, the common mode voltage induced in the cable can be calculated. The resultant transverse noise voltage can be estimated from this figure using a "typical" balance figure for that type of cable to determine if satisfactory service can be provided.

2.5.5 Noise Voltage Determination Methods Used in this Project

Telecommunication system studies reported in this thesis have been limited to the measurement and simulation of the longitudinal voltage induced in a cable laid on the surface of the earth. The objective of this work was to establish the validity of the power-telecommunication coupling models, rather than to test the accuracy of the telecommunication system models. Details of the coupling models used are contained in Chapters 3, 4 and 8, while the results of this work are reported in Chapter 9.

2.6 Summary

This chapter satisfies the first aim of the project by describing a procedure for determining the resultant noise induced in a telecommunication circuit due to interference from neighbouring power system transmission lines. The procedure is based upon the weak coupling assumption which enables the power system, electromagnetic coupling and communication system studies to be decoupled. A survey of simulation and measurement methods for determining the state of power systems, coupling to cables and the resultant noise voltage in telecommunication circuits has been presented.

A complete algorithm for the determination of the resultant noise voltage in a telecommunication circuit has not been implemented during this project. The emphasis in this project has been placed on the mechanism of coupling between power system transmission lines and telecommunication cables, rather than on the generation of disturbing currents within the power system or the conversion of longitudinal electric fields to transverse noise voltages within a communication cable. However it is intended that the methods employed in this project be combined with algorithms for power system and communication system analysis according to the procedure described in this chapter.

As the weak coupling approximation has been used to decouple the power and telecommunication system studies from the coupling studies, the conclusions drawn in this thesis can only be applied to cases for which the coupling is weak. In particular the conclusions may not be valid for steady state coupling to aerial conductors or coupling under fault conditions.

To interface the algorithms used during this project to existing power system simulation and measurement methods, it has been necessary to develop an algorithm to determine the current profile along a transmission line from it's terminal conditions. It is assumed that the power system is in a periodic steady state and that the transmission line may be approximated by a linear network. The transmission system is then analysed at each harmonic frequency using an efficient harmonic penetration type algorithm which exploits the linear topology of transmission lines. Measurements have been conducted on a transmission line during this project to confirm the accuracy of the method.

The mechanisms of coupling between power and communication systems have been

discussed. Due to the widespread use of buried cable in the subscriber loop of New Zealand telecommunication system, magnetic field coupling is the only coupling mechanism that has been considered in detail in this project. The effect of the earth upon the fields induced by a transmission line is discussed in this thesis, and the validity of the models used is established by experiment.

Finally the difficulties associated with measuring and modelling noise within a telecommunications system have been described.

CHAPTER 3

EARTH-RETURN TRANSMISSION LINE MODELLING

3.1 Introduction

Detailed knowledge of the electromagnetic fields around aerial transmission lines is required to determine their electrical parameters and interaction with neighbouring systems.

The electromagnetic field around a multiconductor transmission line may be determined by superposition of the fields induced by each conductor if the conductor material, air and earth are electrically linear. Although these materials are non-linear, they only display significant non-linearities when subjected to intense electromagnetic fields (see Section 3.2). Under normal operating conditions they may be considered to be linear. Therefore during this project, which is concerned with steady state interference, the field induced by multiconductor lines has been determined by the superposition of single conductor earth return fields (see Chapters 5 and 8).

At present it is not possible to solve for the electromagnetic field around a single conductor suspended above the earth. However given the great technical importance of the problem, considerable effort has been expended on solving simplified problems in which the transmission line and earth are represented by simple, regular and electrically linear structures. As a consequence there now exist a wide variety of models employing a range of simplifying approximations. Unfortunately the rigorous models (those that make the lowest number of simplifications) tend to be mathematically complicated and computationally expensive to evaluate, and are therefore unsuitable for some applications.

A number of single conductor earth return line models have been employed during this project to satisfy the many and various modelling requirements. Accurate yet computationally efficient models were required for the numerical investigations of the fields induced by single and multiconductor lines (Chapters 4, 6 and 8) and for comparisons with measurements (Chapter 9). Mathematically simple models were used for theoretical studies of the factors affecting the inductive influence of transmission lines (Chapter 4). As the majority of the results presented in this thesis have been obtained from computer simulations and theoretical investigations based upon these models, the validity of the conclusions stated in this thesis is limited by the accuracy of the models. Therefore particular care has been taken during this project to select appropriate models for each application.

A summary of single conductor line models is presented in this chapter with particular emphasis on the representation accuracy, derivation, implementation, applications and the physical interpretation of the models. This chapter has been written to describe existing models and their relative merits. As these models have been used extensively throughout this project, this chapter effectively summarises the fundamental approximations upon which the conclusions presented in this thesis are based. Physical interpretations of the models are included as background information for Chapter 4,

in which the factors affecting the inductive influence of single conductor earth return transmission lines are discussed. Chapter 4 also compares the numerical accuracy of the models used during this project, and summarises the sensitivity of the resultant inductive influence to frequency, earth resistivity and geometry variations.

The chapter opens in Section 3.2 with details of the assumptions commonly made when modelling a single conductor earth return transmission line.

A discussion on wave propagation along a single conductor line is presented in Section 3.3. The decomposition of the electromagnetic field into *Internal* and *External* components is also described. Only external field models, or models of the field outside the conductor are considered in this chapter. Models for determining the internal fields within the conductor are discussed in Chapter 8.

Section 3.4 contains a discussion on infinite and finite length transmission line modelling. The requirements of this project and the assumptions regarding the length of transmission lines used during this project are presented. Infinite and finite length transmission line models are the subject of Sections 3.5 and 3.6 respectively with particular emphasis on those models which have been used during this project.

The chapter closes in Section 3.7 with a summary of single conductor line models, their relative merits and applications.

3.2 Mathematical Representation of Transmission Lines

A transmission line above the earth is a particularly difficult system to model due to irregularities in the structure of the line, the conductor and the earth. In the sections that follow the difficulties associated with modelling transmission lines are discussed together with the approximations commonly made.

3.2.1 Transmission Line

Transmission lines are of finite length and generally vary in height and deviate from a straight path between their terminal busbars due to the nature of the terrain they traverse. The conductors of the line also sag between the support structures. It is not practical to model these irregularities in detail, and therefore simplifying assumptions must be made.

In reality all transmission lines are of finite length, however it is difficult to calculate the electromagnetic fields around a finite structure. As a consequence transmission line models are usually based upon the assumption that the line is infinitely long. Calculations based upon these models will only yield valid results for lines which are so long that they may be regarded as being infinite. The conditions which must be satisfied before a line may be represented by an infinite model are discussed in Section 3.4.

Finite length transmission line models have also been developed, however it is not practical to represent the terminal busbars and earthing system in detail in these models. The usual approximations that are made are that the circuit is completed by either radial current flows from the ends of the conductor, or by a vertical connection to a point electrode in the earth from which the current radiates. The distribution of current from the point electrode may be assumed to be a radial direct current distribution or an alternating current distribution (Section 3.6).

Unfortunately these approximations may not be realistic for high voltage transmission lines. High voltage transmission lines are terminated at substations, the earthing systems of these stations are frequently large in relation to the skin depth of the earth at

harmonic interference frequencies and are composed of metallic elements which further distort the current distribution.

The conductor in models proposed to date is assumed to be perfectly straight and parallel to the surface of a planar earth. The height of the conductor is set to be the average height of the actual conductor, and may be calculated from the maximum and minimum heights assuming the conductor hangs in a catenary curve. A significant error can result if the line crosses mountainous terrain or if the conductor sag is large, as the actual conductor length is then significantly greater than that of the model. Indeed Densem (1983) found it necessary to increase the length of a model of a transmission line which traversed a mountainous region to match the measured electrical characteristics.

The effect of the quasi-periodic intrusion of the supporting structures and the aperiodic intrusion of trees and buildings into the immediate vicinity of the conductors must also be considered. These structures distort the electric field, increasing the capacitive leakage current to ground, thereby changing the propagation characteristics of the line. Yang and Matsuura (1988) consider that these effects must be included when calculating the induced voltages on the de-energised halves of double circuit EHV and UHV lines. This can be achieved by reducing the height of the conductor above ground when calculating the capacitance matrix for the line.

The quasi-periodic intrusion of the supporting structures into the neighbourhood of the conductors could also affect wave propagation on the line. Discretely bonded earth wires on transmission lines can act like selective filters at frequencies for which the electrical distance between supports is a multiple of one half wavelength (Wedepohl and Wasley, 1965). It is plausible that the increase in localised capacitance to ground at each support could have a similar effect. However, such effects, if they are significant, need only be considered at frequencies for which the electrical distance between supports is greater than one quarter of a wavelength. For typical spans this corresponds to 250 kilohertz, and therefore this effect need not be considered when studying voice frequency interference to telecommunication systems.

In general the effect of the intrusion of structures on the line is ignored at present as the situation is too complicated to model in detail. Corrections for these effects may be introduced in the form of a scaling factor for the capacitance, or a reduction in the effective height of the conductor when calculating the shunt capacitance of the line. However, these modifications must be viewed as corrections to the models as they are not accounted for in the derivations.

3.2.2 Conductor

Modern aerial electricity transmission and distribution lines generally use steel reinforced aluminium conductors (ACSR). These conductors consist of concentric layers of spiral wound strands, with the layers wound in alternate directions. Steel strands are used in the centre, while the outer layers are aluminium.

The electrical characteristics of these conductors are dependent on the electromagnetic properties of the conductor materials, which are non-linear. The magnetic core of an ACSR conductor experiences a magnetising force due to current flow in the spiral strands. This results in hysteresis and eddy-current losses within the steel which are current dependent (Lewis and Tuttle, 1958). If the potential of the line is such that the electric field at the surface of the conductor exceeds 30 kilovolts per centimetre, or pollution is present on the conductor, corona discharges may occur. These discharges increase the effective conductor radius, changing the capacitance to ground and increasing line resistance due to hysteresis loop losses (Ovick and Kusic, 1984). However as these non-linear effects are generally insignificant under normal operating conditions, the conductors are usually represented by linear models.

The resistance and internal inductance of a conductor are frequency dependent due to the skin effect (Dwight, 1918). As the frequency is increased the surface current density rises while the internal current density decreases, producing a non-linear variation of internal conductor parameters with frequency. This effect can be accounted for using expressions derived by Dwight (1918) and is discussed in greater detail in Chapter 8.

Conductor resistance is also temperature dependent, being approximately linearly proportional to the absolute temperature. Significant changes of conductor parameters can occur due to seasonal temperature variations of thirty degrees kelvin or more. However in practice the parameters of a line are normally calculated at the typical operating temperature.

3.2.3 Earth

The major difficulty associated with the calculation of the electromagnetic field around a single conductor transmission line is in determining the effect of the earth on the field. Transmission lines induce currents within the body of the earth. These currents in turn contribute to the electromagnetic field, affecting the electrical characteristics of the line. However, as the current distribution is highly dependent on the electromagnetic properties of the earth, the electrical parameters of the line will also be dependent on these properties. Unfortunately, the earth is a large irregular inhomogeneous body which is electrically non-linear and whose properties vary greatly with position and time.

The surface of the earth below a transmission line is irregular and finite in extent. However, it is modelled as an infinite plane surface parallel to the conductor. The length of a transmission line is usually small in relation to the dimensions and curvature of the earth, therefore it is reasonable to model the earth with an infinite structure. Transmission lines generally follow easy paths such as along valley floors where surface irregularities are small in relation to the height of the line. Consequently the plane surface approximation is well based. In cases where the earth is inclined it may be necessary to incline the plane representing the earth, or equivalently adjust the height of the conductors to account for the imbalance that results (Yang and Matsuura, 1988).

Due to the mechanisms of erosion, sedimentation, leaching and volcanism the earth usually has a stratified structure. In models developed to date the earth is often approximated by a stratified structure of homogeneous layers. Such models usually provide better agreement with measured transmission line parameters than those models which approximate the earth by a single homogeneous layer (Sunde, 1949, chapter 4).

Under very intense electromagnetic fields the earth behaves in a non-linear fashion due to ionisation of the air between soil particles and saturation of magnetic minerals. However, the field strengths below a transmission line under normal operating conditions are such that these effects may be ignored allowing linear time-invariant models of the earth to be used.

The electrical characteristics of the earth are highly dependent on the minerals present in the soil or rock, moisture content and temperature (Vance, 1978). Very large variations in the parameters of the soil may be observed from one location to another and from one season to another. In particular the earth resistivity may vary from about 0.2 to 15000 Ω.m, the permittivity of soil from 5 to 15$\times$ the free space value and up to 80$\times$ for fresh or sea water, and the permeability from 1.0 up to 1.6$\times$ the free space value for high grade iron ore (Gill and MacDonald, 1967; Vance, 1978; MacDonald, 1988). Earth resistivity is the most important factor to model accurately as it has a significant effect on the current distribution within the ground and hence the electromagnetic field (Efthymiadis and Wedepohl, 1978). The permeability should also be modelled explicitly as it can have an important effect on the fields (Efthymiadis and

Wedepohl, 1978), although in practice it is unlikely to vary significantly from the free space value (Vance, 1978). Although the permittivity of the earth can vary greatly, it does not seem to significantly affect the electromagnetic fields (Efthymiadis and Wedepohl, 1978). All models developed to date represent the finite conductivity of the earth, whilst some allow permittivity and permeability values for the earth different from those of free space. Given the wide variation of the electrical parameters of the earth it is recommended that data for insertion in models be measured at the point of interest otherwise significant errors may result.

3.2.4 Decoupling the Internal and External Field Calculations

To calculate the electrical parameters of a high voltage transmission line, it is strictly necessary to simultaneously solve for the electromagnetic fields within the conductor, air and the earth as they are interrelated. Current flow within the conductor induces fields which perturb the current distribution within the earth and *vice versa* . As a consequence of this proximity effect the current distribution in the earth is concentrated in that part immediately below the line (Section 4.7.2), while that in the conductor has an angular dependence and angular currents flow (Pogorzelski and Chang, 1977). It is unrealistic to ignore the proximity effect of the conductor on the current distribution within the earth, however if the conductor radius to height ratio is small then the effect on the conductor may be neglected with little loss in accuracy (Pogorzelski and Chang, 1977). The conductor current is then considered to flow in the axial direction only and to be uniformly distributed around the circumference.

A cylindrical conductor carrying an angularly independent current may be replaced by an infinitely thin conductor carrying the same current. The external magnetic field from the filamentary conductor is identical to that of the actual conductor, while boundary conditions on the electric field, at the former surface of the conductor, may be imposed to ensure that the electric fields are identical. Thus when the influence of the proximity effect on the conductor current distribution is ignored, the calculation of the external fields may be simplified by the use of a filamentary current model for the conductor.

The calculation of the fields internal to the conductor is also simplified by this assumption. When the proximity effect is ignored the conductor current distribution is independent of external fields, therefore the internal field calculations can be decoupled from those for the external fields. However the decoupling is not bilateral. The internal electric field on the conductor surface is generally the dominant component of the external axial electric field in the immediate vicinity of the conductor (Olsen and Pankaskie, 1983).

When simplified transmission line models based upon Quasi-TEM propagation theory are used (see Section 3.3.3), the decoupling is complete as continuity of the field at the conductor surface is not required to solve for the external fields. This greatly simplifies the calculation of the external line parameters as a general conductor-independent solution can be formulated. However the internal component of the conductor impedance is significant at harmonic interference frequencies due to ohmic losses and the skin effect, and must be added to the external field component before the propagation constant can be calculated.

In the single conductor transmission line models discussed in this chapter the conductor is modelled as a filamentary current on the conductor axis. Only models for the determination of the external fields, associated electrical parameters and the propagation constant are considered here. Models for calculating the internal fields are presented in Chapter 8.

3.3 Wave Propagation along a Conductor above the Earth

An understanding of the external fields around a single conductor transmission line is required to appreciate the assumptions made in the derivation of the models discussed in this chapter. In this section a discussion of propagation on the single conductor transmission line shown in Figure 3.1 is presented.

An infinitely long cylindrical conductor of radius a_c is located at height y_c above the planar surface of the homogeneous earth. The conductor lies parallel to the $\hat{z}$ axis of the cartesian coordinate system and is located at $x = x_c$ and $y = y_c$, while the surface of the earth is located in the plane $y = 0$. The electrical parameters of the conductor, air and earth are $(\rho_c,\mu_c,\epsilon_c)$, $(\rho_a,\mu_a,\epsilon_a)$ and $(\rho_e,\mu_e,\epsilon_e)$ respectively.

Three cases are considered: lossless propagation, ρ_c and $\rho_e = 0$; lossy propagation, ρ_c and $\rho_e > 0$; and Quasi-TEM propagation, in which results based on lossless propagation are used to derive an approximation to the lossy fields. In all cases the air is assumed to be a perfect insulator (ρ_a infinite).

Mathematical details of the external electromagnetic field and the resultant circuit parameters of a lossless system are presented in this section for comparison with the lossy models described in Sections 3.5 and 3.6.

3.3.1 Lossless Propagation

As the resistivities of the conductor ρ_c and earth ρ_e are zero, no alternating electromagnetic fields can exist within these bodies and the field is confined to the air. The boundary conditions on the field at the conductor-air and air-earth interfaces are that the tangential electric field and normal magnetic field must be zero (Ramo *et al.*, 1984, chapter 3). As the conductor height is very much less than a wavelength at harmonic interference frequencies, the only field that can propagate along the line and satisfy the boundary conditions is a *Transverse Electromagnetic* (TEM) wave.

TEM waves have zero axial ($\hat{z}$) fields, and propagate without attenuation at the velocity of light in air. The time and z dependence of the time-harmonic field is described by $\exp(\jmath\omega t - \gamma z)$, which can be separated from the other spacial variables as shown in Equation (3.1).

$$f(x,y,z,t) = f(x,y)\exp(\jmath\omega t - \gamma z) \tag{3.1}$$

Where

$f(x,y,z,t)$ = component of the electromagnetic field at point (x,y,z) and time t
t = time (s)
γ = propagation constant (rad.m^{-1})
= $\pm\jmath\omega\sqrt{\mu_a\epsilon_a}$
+ for a wave propagating in the increasing z direction
− for a wave propagating in the decreasing z direction

Both forward and backward travelling waves may exist on the line. Reflections occur from the ends of lines that are not terminated by their characteristic impedance, generating backward travelling waves (Ramo *et al.*, 1984).

Both the electric and magnetic fields satisfy Laplace's equation in the transverse (z constant) planes, *i.e.* they have the same form as static fields which satisfy the boundary conditions (Ramo *et al.*, 1984, chapter 8). The electric and magnetic fields of a given travelling wave (forward or backward) are normal to each other, in phase and are related by the impedance of the air,

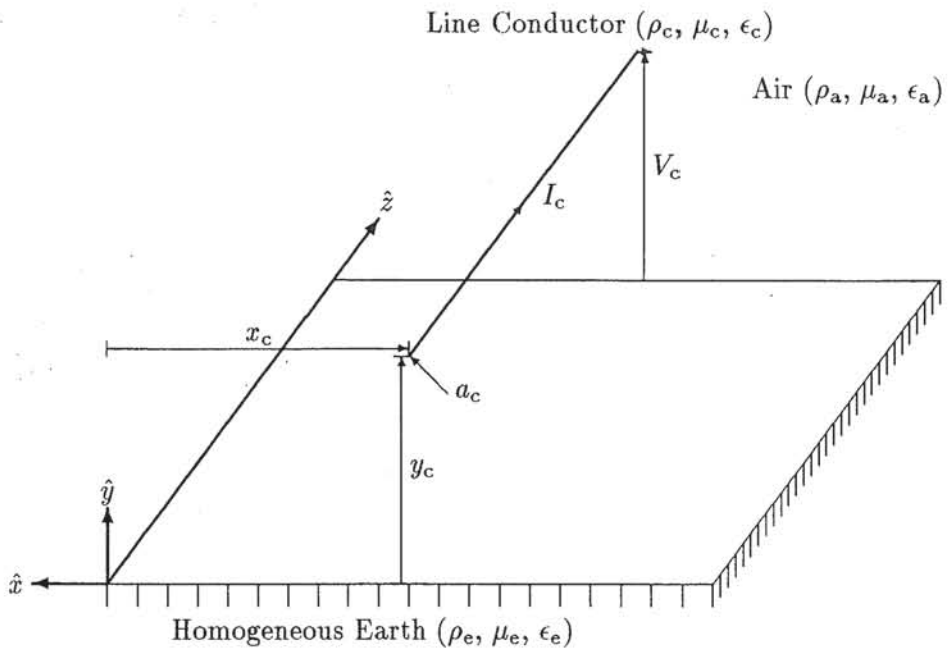

Where

I_c	=	transmission line conductor current (A)
V_c	=	transmission line conductor voltage, with respect to an infinitely remote earth connection (V)
y_c	=	y ordinate of the conductor (m)
x_c	=	x ordinate of the conductor (m)
a_c	=	radius of the conductor (m)
ρ_c, ρ_a, ρ_e	=	resistivity of the conductor, air and earth (Ω.m)
μ_c, μ_a, μ_e	=	permeability of the conductor, air and earth (H.m^{-1})
ϵ_c, ϵ_a, ϵ_e.	=	permittivity of the conductor, air and earth (F.m^{-1})

Figure 3.1. Idealised Single Conductor Transmission Line

$$E = \sqrt{\frac{\mu_a}{\epsilon_a}}\, H \tag{3.2}$$

Where

E = magnitude of electric field ($\mathrm{V.m^{-1}}$)
H = magnitude of magnetic field ($\mathrm{A.m^{-1}}$)

The boundary conditions at the surface of the ideal earth can be satisfied by replacing the earth with an image conductor as shown in Figure 3.2, provided that the voltage and current of the image are of equal magnitude and opposite sign to those of the conductor. Note that the reference plane in Figure 3.2 represents the former location of the air-earth interface, both conductors in this figure are located in air.

As the height of the transmission line is generally much greater than the conductor radius ($y_c \gg a_c$) the proximity effect may be ignored. The conductor and image may then be replaced by filamentary line charges when calculating the transverse electric field and by filamentary currents for magnetic field calculations. Superposition is then used to determine the resultant field from those induced by the filaments representing the conductor and image. Equations (3.3) to (3.8) describe the fields in the air, no fields exist within the conducting regions.

$$E_x(x,y,z,t) = \frac{Q_c(z,t)}{2\pi\epsilon_a}\left(\frac{(x-x_c)}{{r_c}^2} - \frac{(x-x_c)}{{r_i}^2}\right) \tag{3.3}$$

$$E_y(x,y,z,t) = \frac{Q_c(z,t)}{2\pi\epsilon_a}\left(\frac{(y-y_c)}{{r_c}^2} - \frac{(y+y_c)}{{r_i}^2}\right) \tag{3.4}$$

$$E_z(x,y,z,t) = 0 \tag{3.5}$$

$$H_x(x,y,z,t) = \frac{I_c(z,t)}{2\pi}\left(\frac{(y+y_c)}{{r_i}^2} - \frac{(y-y_c)}{{r_c}^2}\right) \tag{3.6}$$

$$H_y(x,y,z,t) = \frac{I_c(z,t)}{2\pi}\left(\frac{(x-x_c)}{{r_c}^2} - \frac{(x-x_c)}{{r_i}^2}\right) \tag{3.7}$$

$$H_z(x,y,z,t) = 0 \tag{3.8}$$

Where

$E_x(x,y,z,t)$ = $\hat{x}$ component of the electric field ($\mathrm{V.m^{-1}}$)
$E_y(x,y,z,t)$ = $\hat{y}$ component of the electric field ($\mathrm{V.m^{-1}}$)
$E_z(x,y,z,t)$ = $\hat{z}$ component of the electric field ($\mathrm{V.m^{-1}}$)
$H_x(x,y,z,t)$ = $\hat{x}$ component of the magnetic field ($\mathrm{A.m^{-1}}$)
$H_y(x,y,z,t)$ = $\hat{y}$ component of the magnetic field ($\mathrm{A.m^{-1}}$)
$H_z(x,y,z,t)$ = $\hat{z}$ component of the magnetic field ($\mathrm{A.m^{-1}}$)
$I_c(z,t)$ = conductor current (A)
= $I_c(z=0,t=0)\exp(\jmath\omega t - \gamma z)$
$Q_c(z,t)$ = charge per unit length on the line ($\mathrm{C.m^{-1}}$)
= $\sqrt{\mu_a\epsilon_a}I_c(z,t)$

The mutual impedance to a cable located at point (x,y) may be determined by calculating the time rate of change of flux linking the circuit formed by the cable and an infinitely remote reference point per unit current on the line. Using similar methods, the potential of the point (x,y), and hence the mutual capacitance and admittance, may be calculated. Equations (3.9) and (3.10) give the resultant expressions for the mutual admittance and impedance per unit length. These equations ignore the proximity effect of the cable and are therefore only valid when the conductor-cable separation is large compared to the radii of the conductor and the cable.

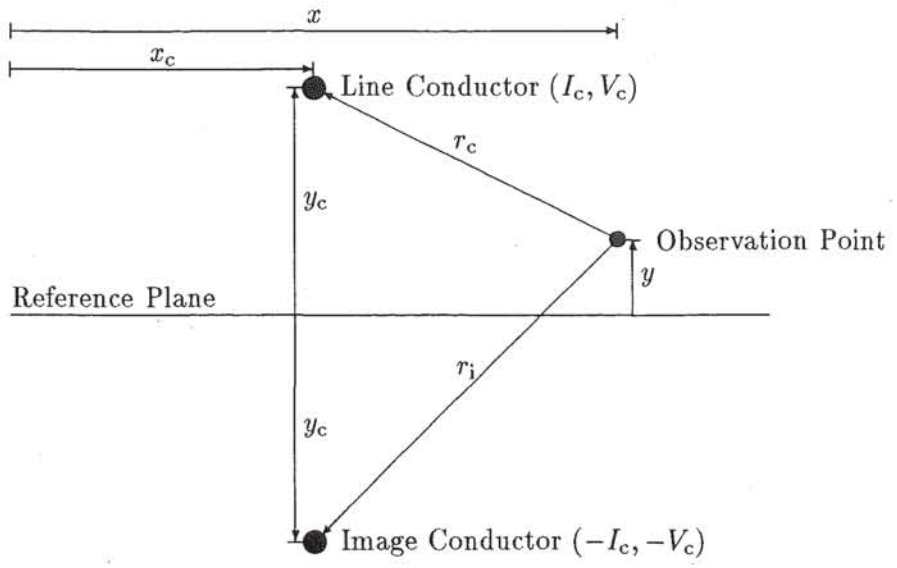

Where

y = y ordinate of the observation point (m)
x = x ordinate of the observation point (m)
r_c = radial separation between the observation point and the transmission line conductor (m)
$= \sqrt{(x - x_c)^2 + (y - y_c)^2}$
r_i = radial separation between the observation point and the image conductor (m)
$= \sqrt{(x - x_c)^2 + (y + y_c)^2}$

Figure 3.2. Replacing the Lossless Earth with an Image Conductor

$$Z_m = \frac{j\omega\mu_a}{2\pi} \ln \frac{r_i}{r_c} \tag{3.9}$$

$$Y_m = \frac{j2\pi\omega\epsilon_a}{\ln \frac{r_i}{r_c}} \tag{3.10}$$

Where

π = the ratio of circle circumference to diameter
ln = the natural logarithm
Z_m = mutual impedance per unit length ($\Omega.m^{-1}$)
Y_m = mutual admittance per unit length ($S.m^{-1}$)

The external self impedance and admittance of the transmission line is simply the relevant mutual parameter evaluated at a point on the conductor surface. Substituting the point $x = x_c$ and $y = y_c - a_c$ for the bottom of the conductor into these equations yields

$$Z_s = \frac{j\omega\mu_a}{2\pi} \ln \frac{2y_c - a_c}{a_c} \tag{3.11}$$

$$Y_s = \frac{j2\pi\omega\epsilon_a}{\ln\frac{2y_c - a_c}{a_c}} \tag{3.12}$$

Where

Z_s = external self impedance per unit length ($\Omega.m^{-1}$)
Y_s = self admittance per unit length ($S.m^{-1}$)

Different results will be obtained if another point on the surface of the conductor is selected as the conductor surface is not an equipotential surface because the proximity effect has not been modelled.

It must be emphasised that the product of the mutual impedance and the inducing current I_c does not yield the $\hat{z}$ component of the electric field, E_z. E_z is dependent on both the alternating magnetic and electric fields. The product $-Z_m I_c$ gives the magnetic component of E_z. In this lossless case the components of E_z due to the alternating magnetic and electric fields are of equal magnitude and opposite sign, resulting in a zero axial ($\hat{z}$) field.

The telegrapher's equations for this lossless case may be derived directly from Maxwell's equations (Ramo *et al.*, 1984, chapter 8). Therefore distributed circuit transmission line models and field analysis yield identical results. As a consequence the propagation constant and characteristic impedance of the wave may be calculated using the following distributed circuit relationships.

$$\gamma = \sqrt{Z_s Y_s} \tag{3.13}$$

$$Z_0 = \sqrt{\frac{Z_s}{Y_s}} \tag{3.14}$$

Where

Z_0 = characteristic impedance of the propagation mode ($\Omega.m^{-1}$)

In this lossless case the propagation constant reduces to that of a wave in air ($j\omega\sqrt{\mu_a\epsilon_a}$) presented earlier, which is independent of the geometry of the line. The characteristic impedance Z_0 is geometry dependent however.

3.3.2 Lossy Propagation

The situation is considerably more complicated when the conductor and earth are lossy (ρ_e and $\rho_c > 0$) as internal electromagnetic fields may exist. Indeed a finite electric field is required to force current to flow through the lossy media. Current flow is not constrained to the surface of the conducting regions as in the lossless case and is highly dependent on both the electrical characteristics of the media and frequency, due to the skin effect. Displacement currents flow within the lossy media resulting in increased losses which overwhelm the conduction current effects at high frequencies and in regions of great earth resistivity.

The boundary conditions on the surface of a lossy conductor subject to alternating fields are that the tangential components of the electric and magnetic fields be continuous at the interface. As an axial (E_z) electric field exists within the conductor and earth to force current to propagate along the transmission line, an axial field will also exist in the air. Consequently the field will not be a pure Transverse Electromagnetic wave, but may be considered to be the sum of *Transverse Electric* (TE) and *Transverse Magnetic* (TM) waves (Wedepohl and Efthymiadis, 1978).

The time and z dependence of the fields may still be described by equation (3.1) (Wait, 1972). A superposition of fields with dependences of this form can be shown to be a complete description of fields around a conductor above a lossy earth excited by a finite source (Kuester *et al.*, 1978). However the presence of fields within the resistive conductor and earth results in energy loss and therefore the fields are attenuated with distance (the propagation constant γ contains a real component) and no longer propagate at the velocity of light.

Both forward and backward travelling waves will exist on the line as power system transmission lines are unlikely to be terminated by their characteristic impedance. Furthermore the electric and magnetic fields are not related by (3.2) because of the earth losses and the fact that forward and backward waves are present (Olsen and Wong, 1992).

A single conductor transmission line above the earth may support multiple propagation modes which vary in number depending on the parameters of the earth, frequency and conductor height. These modes of propagation may be divided into two classes, continuous spectra of radiating modes and discrete propagating modes (Kuester *et al.*, 1978).

Continuous spectra radiation modes describe radiating fields which are the result of a integration over a semi-infinite spectrum of modes (an individual radiation mode has no meaning by itself) (Kuester *et al.*, 1978). These fields are not constrained to propagate along the axis of the conductor but radiate into the air, earth, or along the interface. Such fields are dependent on the properties of the air and earth and are not strongly affected by conductor geometry (Bridges *et al.*, 1988). The axial decay rate of the continuous spectra of radiating modes in air is proportional to $1/z$.

A usually finite number of discrete modes propagate on an aerial line. Each mode is characterised by a single propagation constant, which is not necessarily unique. Unlike the radiation fields which are bounded at infinity, the fields associated with discrete propagation modes decay exponentially in the axial direction and in the transverse plane with distance from the line (Kuester *et al.*, 1978).

A single conductor line above a homogeneous earth will in general have two discrete propagating modes: a *structure attached* or *transmission line* mode, and a *surface attached* or *fast wave* mode (Olsen *et al.*, 1978). The fields associated with the transmission line mode tend to penetrate the earth more than the fast wave mode, resulting in higher attenuation and a lower phase velocity.

The field around an aerial line contains contributions from all modes. However the contribution from each mode depends on the degree of excitation of the mode by the source, and the distance along the line. In the region very close to the source and at extremely large distances from the source the continuous radiation modes' contributions may be significant as they decay at a rate proportional to $1/z$, while the discrete modes decay exponentially. However where the structure's dimensions are small compared with the wavelength, as is the case for power system transmission lines, the discrete modes are considered to be dominant (Bridges *et al.*, 1988). Of the two discrete modes, only the transmission line mode needs to be considered at low frequencies on power lines as the relative excitation of the fast wave mode and the total line attenuation are small (Chang and Olsen, 1975; Bridges *et al.*, 1988). Therefore the fast wave mode will not dominate despite its lower rate of attenuation.

It seems that for normal earth parameters and transmission line heights, the transmission line mode is the only mode that needs to be considered at frequencies below a few megahertz (Dudley and Casey, 1989). This result is fortunate as traditional transmission line theory may be used to calculate the line currents and voltages. When all modes are significant transmission line theory can not be applied and the complete solu-

tion must be used. Care should be exercised when studying high frequency propagation effects on power lines using traditional transmission line theory however, especially in the vicinity of discontinuities, as it is possible that other modes are also significant.

The Exact mode equation may be cast into the form of a generalised transmission line equation containing terms representing the series impedance and shunt admittance per unit length (Wait, 1972; Bridges *et al.*, 1988). Unfortunately the per length parameters are integral functions of the propagation constant, and therefore can not be evaluated until the discrete propagation constant has been determined, and vary according to the mode of propagation.

A discussion on the derivation and solution of the Exact model for infinite length transmission lines is presented in Section 3.5.1.

Exact solutions are also possible for finite length transmission lines. In this case other modes may be significant given the short length of the line. Exact finite length models are discussed in Section 3.6.1.

3.3.3 Quasi-TEM Propagation

The most commonly used theory to describe propagation on aerial lines is *Quasi-TEM* propagation. This theory was originally derived by Carson (1926) and Pollaczek (1926). It predates the Exact theory but is considerably simpler and therefore easier and more efficient to implement.

The Quasi-TEM theory employs lossless field concepts to simplify the problem. It is assumed that the axial variation of the field is equal to the free space value, therefore the fields in the air are the solution of the two dimensional Laplace equation in the transverse plane rather than the three dimensional wave equation (Bridges and Shafai, 1989). As static fields satisfy the Laplace equation this theory is also known as the *Quasi-Static* or *constant current* approximation. This approximation is valid provided that the following conditions are satisfied (Degauque *et al.*, 1983; Olsen and Pankaskie, 1983):

- the conductor radius must be small in relation to the height (proximity effect can be ignored);
- the dimensions of the system must be small in relation to the wavelength (less than one twentieth of a wavelength);
- the wave number of the earth must be much greater than that of the air (generally true at low frequencies where displacement currents within the earth are insignificant in relation to conduction currents);
- the propagation constant of the wave must be much smaller than the wave number of the earth (true for conductors which are not in continuous contact with the earth).

Olsen *et al.* demonstrated that satisfaction of these conditions is sufficient to justify the validity of the Quasi-TEM model by deriving it from the Exact model by applying only these assumptions (Olsen and Pankaskie, 1983).

A single propagation constant is determined using this approach which will be close to the transmission line mode propagation constant determined using the Exact theory if the assumptions are valid. Therefore this method is subject to the same constraints as the Exact theory when only the transmission line mode is considered.

Experimental investigations have shown that the agreement between measured currents on a transmission line and Quasi-TEM theory is good, even when the displacement currents in the ground are comparable to the conduction currents (Degauque *et*

al., 1983). When the line is very lossy the assumption of a single exponential mode of propagation is not adequate, and additional modes must be included. However for the test system described by Degauque *et al.* (1983) this is only necessary when the attenuation exceeds 60 dB, which suggests that additional modes are not required to accurately model propagation on power system transmission lines.

The Quasi-TEM approximation greatly simplifies the calculation of the transmission line parameters as the Exact modal equation reduces to an explicit expression when the Quasi-TEM approximation is applied (Bridges *et al.*, 1988, equations (13) and (14)). Elements of the shunt admittance matrix reduce to their lossless earth values given by equations (3.12) and (3.10), while the series impedance matrix elements reduce to Carson's equation (equation (3.31)) augmented by the internal impedance of the conductors. Once the equivalent circuit parameters for the transmission line have been determined by assuming that the wave propagates at the free space velocity, a refined estimate of the propagation constant is obtained using equation (3.13). This differs from the Exact theory which states that the fields are dependant on the propagation mode and therefore the field and circuit parameters can not be determined until the propagation constant is known. The Quasi-TEM approach to determining the propagation may be viewed as one of iterative refinement, as an initial estimate of the propagation constant (free space value) is used to derive fields and hence the circuit constants. These are then used to give a refined estimate of the propagation constant (Wise, 1934).

A discussion on the historical development and implementation of Carson's infinite length Quasi-TEM model is presented in Section 3.5.2. Sections 3.5.3 and 3.5.4 describe the infinite Complex Penetration and Conductor Element models which are also based upon the Quasi-TEM wave propagation approximation. These models should only be applied to situations which satisfy the Quasi-TEM conditions stated above.

Finite length models have also been based upon the Quasi-Static field theory (Sections 3.6.2 and 3.6.3). These models assume that the displacement current flows are negligible, and hence that the conductor current is constant. This assumption is only valid for lines which are short in relation to the wavelength. Finite length Quasi-Static models can therefore only be applied to short lines which meet the Quasi-TEM requirements.

3.4 Modelling Finite and Infinite Length Transmission Lines

Earth return transmission line models are based upon the assumption that the line is either infinitely long or of finite length. The difference between these models is that the distortion of the field due to the end of the conductor, the vertical connection to earth and the perturbed current flow in the earth (the *End Effect*) is represented in finite models, while it is ignored in infinite models. This distortion influences both the electrical parameters of the line and the resultant coupling to neighbouring systems. In reality all lines are finite and therefore should ideally be represented by finite models. Unfortunately finite models tend to be more complicated and computationally expensive to evaluate, as a consequence infinite length models are often used in practice. In this section the conditions which must be satisfied before infinite length models can be applied are discussed. The requirement for both finite and infinite models during this project is summarised.

The increased complexity of finite length transmission line models results from the fact that fields around the line no longer have a simple exponential z dependence. As a consequence the parameters of the line are not uniform which results in inter-

mode coupling, complicating the calculation of propagation along the line. Furthermore mutual coupling calculations, which are performed by integration of the relevant field components over the length of the induced conductor, are more difficult to perform.

As the length of a finite line increases, the fields about the centre of the line tend towards the infinite result. If the line is electrically long then the fields over much of its length may be approximated by infinite fields (Kuester *et al.*, 1978). The self and mutual parameters of the line can then be approximated by the per unit length parameters for an infinite line. It must be noted that although the infinite field approximation may be accurate over much of the length of a finite line it is not valid to simply represent a finite conductor with an infinite parameter model as the End Effect can have a profound influence on both propagation along the conductor and coupling to neighbouring systems.

Circuit models based upon parameters derived from infinite length transmission line models may be used to approximate finite structures if they are augmented with terms which account for the End Effect. This is achieved in propagation studies by applying equivalent sources to the end of uniform circuit models, or by modelling the coupling between modes (Kuester *et al.*, 1978). Self and mutual impedance calculations must be augmented with terms which represent the impedance of the connections to earth and the coupling between these connections (Sunde, 1949, Chapter 4). It should be noted however that these augmented models are only approximate representations of the finite system as they do not fully include the effect of the non-exponential field variation along the line.

In the case of mutual coupling calculations to telecommunications systems, it is not usually necessary to augment the infinite model with the mutual coupling between the earthing points as telecommunications circuits are normally only earthed at one point which is isolated from the earthing systems of high voltage transmission lines for safety and noise immunity reasons.

The accuracy of an augmented infinite model is a function of the parameters of the inducing conductor and earth, and also the location and orientation of the induced conductor in mutual coupling calculations. As a consequence, it is difficult to make a general recommendation as to when augmented models may be applied. Semi-empirical guidelines have been derived for the case of Quasi-TEM propagation along finite conductors. The error incurred in self impedance calculations is small if the length of the inducing conductor is large in relation to the skin depth of the earth. Sunde (1949) studied the error in mutual impedance calculations and found that

> For a given allowable error in the mutual inductance, the distance ℓ that one wire has to extend beyond the ends of the other to be regarded as infinite is smaller the longer the shorter wire. When one of two parallel wires is of infinitesimal length, and great accuracy is required, as in determining the earth resistivity from mutual inductance measurements, the distance should be such that $\ell\sqrt{j\omega\mu_e(1/\rho_e + j\omega\epsilon_e)} > 2$.

This requirement is excessively stringent when the separation is small as in the immediate vicinity of the inducing conductor (separation much less than the skin depth) the direct field dominates. In this case the length ℓ need only be greater than the separation between the inducing and induced conductors for acceptable accuracy. In cases where high accuracy is required the author recommends that preliminary calculations be performed using both finite and augmented infinite models to determine whether the accuracy of the augmented models is adequate.

At an early stage of this project it was necessary to decide whether to use finite or augmented infinite length transmission line models. The main requirement of the

project was for a measure to quantify the inductive influence of hypothetical transmission lines and to investigate the relationships between the parameters of the line and earth, and the resultant inductive influence. To achieve these goals an inductive influence measure was required which would yield a single number for a given line type which accurately quantified the interfering ability of the line along its entire length, yet was substantially independent of the parameters of the induced system (Further details of the inductive influence measure are contained in Chapter 4). To achieve this using a finite length transmission line model it is necessary to combine the resultant inductive interference for a variety of line and induced conductor lengths and positions along the line into a single equivalent figure. If the line is long in relation to the skin depth, as is generally the case for high voltage transmission lines at harmonic frequencies, then this process is unnecessary as the per unit length mutual coupling obtained from an infinite model has the desired properties at a fraction of the computational effort. Augmented infinite length transmission lines models have been used almost exclusively throughout the course of this project to assess the inductive influence of transmission lines for reasons of simplicity and computational efficiency. A consequence of this decision however is that the conclusions presented in this thesis are only valid when the conditions stated in the previous paragraph are satisfied, and therefore should not be applied to inductive interference phenomena in the vicinity of the ends of a transmission line. Finite models have also been used during the course of this project for determining the characteristics of a one hundred metre length of cable used to measure the inductive influence of the NZ HVDC transmission system in Chapter 9. In this case the length of the cable was small in relation to the skin depth and therefore an infinite length model could not be applied.

3.5 Infinite Length Transmission Line Models

A summary of existing infinite length transmission line models is presented in the following sections with implementation details for those models which were employed during this project.

It should be noted that the parameters of an infinite line can also be calculated by integrating the field contributed by each electric and magnetic dipole (determined using a finite line model from Section 3.6), along the infinite line. However such an approach is computationally expensive.

3.5.1 Exact Model

The *Exact* model is so named because it completely and uniquely satisfies Maxwell's equations for the field around an infinitely long conductor parallel to a homogeneous earth. The only approximations in this analysis are the thin wire assumption and the simplified representation of the conductor and earth. A discussion of the fields around the transmission line and the modes of propagation that it can support has been presented in Section 3.3.2. In the sections that follow the derivation, implementation and physical interpretation of the model is discussed.

3.5.1.1 Derivation and Evolution

Wait (1972), and Wedepohl and Efthymiadis (1978) have independently derived expressions for the exact fields around an earth return transmission line. The resultant equations are equivalent (Olsen and Pankaskie, 1983), however Wait (1972) has expressed his result in a simpler form. The author has chosen to use simplified versions

of Wedepohl's equations during this project as detailed notes on the derivation and numerical implementation of the model are available, together with extensive numerical examples (Efthymiadis and Wedepohl, 1978).

Following the derivation of Wedepohl and Efthymiadis (1978), the electromagnetic field in the air and earth is assumed to be the sum of a complementary pair of Transverse Electric and Transverse Magnetic waves propagating exponentially along the line. To obtain a solution, continuity of the fields at the air-earth interface is applied. This yields integral equations for the electromagnetic field components in the air and earth in terms of the as yet unknown propagation constant, *i.e.* equations (3.15) and (3.16) for the axial component of the electric field.

For $y > 0$

$$E_z(x,y,z,t) = \frac{I_c(z,t)\lambda_a{}^2}{\pi m_a{}^2}\int_0^\infty \mathrm{f}(\alpha,\gamma)\exp\left[-k_a(y+y_c)\right]\cos\left[\alpha(x-x_c)\right]\,d\alpha + \frac{I_c(z,t)\lambda_a{}^2}{2\pi m_a{}^2}\left[\mathrm{K}_0(\jmath\lambda_a r_c) - \mathrm{K}_0(\jmath\lambda_a r_i)\right] \tag{3.15}$$

For $y \leq 0$

$$E_z(x,y,z,t) = \frac{I_c(z,t)\lambda_a{}^2}{\pi m_a{}^2}\int_0^\infty \mathrm{f}(\alpha,\gamma)\exp(k_e y - k_a y_c)\cos\left[\alpha(x-x_c)\right]\,d\alpha \tag{3.16}$$

Where

$\mathrm{K}_0(u)$ = modified Bessel function of the second kind of order 0 of the complex argument u

$$\mathrm{f}(\alpha,\gamma) = \left[k_a + \frac{k_e\lambda_a{}^2 m_e{}^2}{\lambda_e{}^2 m_a{}^2} + \frac{\jmath(\alpha\gamma)^2(\lambda_a{}^2-\lambda_e{}^2)^2}{\omega\lambda_e{}^2 m_a{}^2(k_a\lambda_e{}^2\mu_a + k_e\lambda_a{}^2\mu_e)}\right]^{-1}$$

$$m_a = \sqrt{\frac{1}{\rho_a} + \jmath\omega\epsilon_a}$$

$$m_e = \sqrt{\frac{1}{\rho_e} + \jmath\omega\epsilon_e}$$

$$\lambda_a = \sqrt{\gamma^2 - \jmath\omega\mu_a m_a{}^2}$$

$$\lambda_e = \sqrt{\gamma^2 - \jmath\omega\mu_e m_e{}^2}$$

$$k_a = \sqrt{\alpha^2 - \lambda_a{}^2}$$

$$k_e = \sqrt{\alpha^2 - \lambda_e{}^2}$$

When the permeability of the air and earth are equal ($\mu_e = \mu_a$)

$$\mathrm{f}(\alpha,\gamma) = \frac{m_a{}^2}{\lambda_a{}^2}\left(\frac{\gamma^2}{m_a{}^2 k_e + m_e{}^2 k_a} - \frac{\jmath\omega\mu_a}{k_a + k_e}\right) \tag{3.17}$$

and the equations reduce to Wait's result.

Valid propagation constants are determined by requiring continuity of the axial component of the electric field at one point on the conductor surface, $E_z^s = E_z(x = x_c, y = y_c - a_c)$. The external field must equal that within the conductor due to its internal impedance. Wedepohl and Efthymiadis (1978) assume that the conductor is ideal and therefore require that the surface field be zero, but lossy conductors may be represented by requiring that the field be finite. A solution for the propagation constant is found by calculating the surface field from the conductor parameters (see Chapter 8)

and then using an iterative algorithm to vary the propagation constant until equation (3.15) matches this value.

The Exact model has been extended to include multiconductor transmission lines (Wedepohl and Efthymiadis, 1978) and layered media (Kuester *et al.*, 1981). Multiconductor line models are constructed by superimposing the fields induced by each conductor. Conductors are modelled as filamentary currents in the Exact model, consequently proximity effects are not represented. Therefore this method should only be applied to lines for which the conductor radii are small compared to the free space wavelength, the height of the conductors and the inter-conductor spacings (Bridges *et al.*, 1988).

On a multiconductor line of n conductors there will in general be n transmission line modes of propagation (there may also be additional discrete fast wave propagation modes and continuous spectra radiation modes). In addition to the propagation constant of each discrete transmission line mode, there is an associated modal current distribution on the conductors which together with the propagation constant satisfies the E_z field boundary condition on all conductor surfaces simultaneously.

In an electrically linear multiconductor system the E_z field at a conductor surface E_z^s is the sum of the fields due to each conductor in the line. As the E_z field induced by a conductor is a linear function of the current, the n simultaneous boundary conditions can be expressed as matrix equation (3.18) (Wedepohl and Efthymiadis, 1978).

$$\left[\boldsymbol{E}_{z,u}^{s,ext}\right](\boldsymbol{I}_c) = (\boldsymbol{E}_z^s) \tag{3.18}$$

Where

$\left[\boldsymbol{E}_{z,u}^{s,ext}\right]$ = $(n \times n)$ matrix of external axial surface electric fields per unit current

$(\boldsymbol{I}_c)$ = $(n \times 1)$ vector of conductor currents

$(\boldsymbol{E}_z^s)$ = $(n \times 1)$ vector of axial electric fields on the conductor surfaces

$E_{z,u}^{s,ext}[i,j] \in \left[\boldsymbol{E}_{z,u}^{s,ext}\right]$
= external axial electric field that exists at the position of the surface of conductor i, in the absence of all conductors apart from j, per unit current in conductor j, calculated using equation (3.15) ($\mathrm{V.m^{-1}.A^{-1}}$

$I_c[i] \in (\boldsymbol{I}_c)$
= current in conductor i (A)

$E_z^s[i] \in (\boldsymbol{E}_z^s)$
= total axial electric field on the surface of conductor i ($\mathrm{V.m^{-1}}$)
= 0 for lossless conductors ($\rho_c = 0$)
$\neq$ 0 for lossy conductors ($\rho_c > 0$)

As the internal fields are linear functions of the conductor current, they may also be expressed as the product of an axial electric field matrix per unit current and the conductor currents as shown below.

$$\left[\boldsymbol{E}_{z,u}^{s,int}\right](\boldsymbol{I}_c) = (\boldsymbol{E}_z^s) \tag{3.19}$$

Where

$\left[\boldsymbol{E}_{z,u}^{s,int}\right]$ = $(n \times n)$ diagonal matrix of internal axial surface electric fields per unit current ($\mathrm{V.m^{-1}.A^{-1}}$)

$E_{z,u}^{s,int}[i,j] \in \left[\boldsymbol{E}_{z,u}^{s,int}\right]$
= axial electric field that exists on the surface of a conductor due to internal current flow for $i = j$. Models for determining this field are described in Chapter 8 ($\mathrm{V.m^{-1}.A^{-1}}$)
= 0 for $i \neq j$

Subtracting equation (3.18) from (3.19) yields,

$$[\boldsymbol{E}_{\mathrm{t}}](\boldsymbol{I}_{\mathrm{c}}) = (0) \tag{3.20}$$

Where

$[\boldsymbol{E}_{\mathrm{t}}] = \left[\boldsymbol{E}_{z,u}^{s,int}\right] - \left[\boldsymbol{E}_{z,u}^{s,ext}\right]$ (V.m^{-1}.A^{-1})
(0) = zero vector

The resultant equation, for either lossless or lossy conductors, is a general eigenvalue equation. Solution of this problem is difficult as each element of $[\boldsymbol{E}_{\mathrm{t}}]$ is an integral equation of the unknown propagation constant. Valid propagation constants are found by forcing the determinant of $[\boldsymbol{E}_{\mathrm{t}}]$ to zero using an iterative algorithm. Once the propagation constant of a mode has been calculated the corresponding current vector $(\boldsymbol{I}_{\mathrm{c}})$ may be found by arbitrarily specifying the current in one conductor and solving equation (3.20) for the others.

Equation (3.20) can be rewritten as a generalised transmission line equation for the discrete propagation modes when the permeability of the air and earth are equal (Wait, 1972; Bridges *et al.*, 1988).

$$[\boldsymbol{Z}_{\mathrm{p}}] - \gamma^2[\boldsymbol{Y}_{\mathrm{p}}]^{-1} = [0] \tag{3.21}$$

Where

$[\boldsymbol{Z}_{\mathrm{p}}]$ = $(n \times n)$ primitive series impedance matrix
$[\boldsymbol{Y}_{\mathrm{p}}]$ = $(n \times n)$ primitive shunt admittance matrix
$[0]$ = $(n \times n)$ zero matrix

The elements of $[\boldsymbol{Z}_{\mathrm{p}}]$ and $[\boldsymbol{Y}_{\mathrm{p}}]^{-1}$ are defined by the following integral equations of the propagation constant (Wait, 1972).

$$\begin{aligned}
Z_{\mathrm{p}}[i,j] = \quad & Z_{\mathrm{int}}[i,j] \\
& + \frac{\jmath\omega\mu_{\mathrm{a}}}{2\pi}\mathrm{K}_0\left(\jmath\lambda_{\mathrm{a}}\sqrt{(x-x_i)^2+(y-y_i)^2}\right) \\
& - \frac{\jmath\omega\mu_{\mathrm{a}}}{2\pi}\mathrm{K}_0\left(\jmath\lambda_{\mathrm{a}}\sqrt{(x-x_i)^2+(y+y_i)^2}\right) \\
& + \frac{\jmath\omega\mu_{\mathrm{a}}}{\pi}\int_0^\infty \frac{\exp[-k_{\mathrm{a}}(y+y_i)]}{k_{\mathrm{a}}+k_{\mathrm{e}}}\cos[\alpha(x-x_i)]\,d\alpha
\end{aligned} \tag{3.22}$$

$$\begin{aligned}
{Y_{\mathrm{p}}}^{-1}[i,j] = \quad & \frac{1}{2\pi {m_{\mathrm{a}}}^2}\mathrm{K}_0\left(\jmath\lambda_{\mathrm{a}}\sqrt{(x-x_i)^2+(y-y_i)^2}\right) \\
& - \frac{1}{2\pi {m_{\mathrm{a}}}^2}\mathrm{K}_0\left(\jmath\lambda_{\mathrm{a}}\sqrt{(x-x_i)^2+(y+y_i)^2}\right) \\
& + \frac{1}{\pi}\int_0^\infty \frac{\exp[-k_{\mathrm{a}}(y+y_i)]}{{m_{\mathrm{a}}}^2 k_{\mathrm{e}} + {m_{\mathrm{e}}}^2 k_{\mathrm{a}}}\cos[\alpha(x-x_i)]\,d\alpha
\end{aligned} \tag{3.23}$$

Where

$Z_{\mathrm{p}}[i,j] \in [\boldsymbol{Z}_{\mathrm{p}}]$ (Ω.m^{-1})
Z_{int} = $(n \times n)$ diagonal matrix of internal self impedances of the conductors (Ω.m^{-1})
$Z_{\mathrm{int}}[i,j] \in [\boldsymbol{Z}_{\mathrm{int}}]$ (Ω.m^{-1})
${Y_{\mathrm{p}}}^{-1}[i,j] \in [\boldsymbol{Y}_{\mathrm{p}}]^{-1}$ (S.m^{-1})

(x,y) = co-ordinates of the point at which the field is evaluated (m)
= $(x_i,y_i - a_i)$, For $i = j$
= (x_j,y_j), For $i \neq j$
(x_i,y_i) = co-ordinates of the centre of the inducing conductor i (m)
(x_j,y_j) = co-ordinates of the centre of the induced conductor j (m)

The circuit parameters obtained are only valid when the aerial line supports the mode of propagation corresponding to the propagation constant inserted into equations (3.22) and (3.23). Other modes will have different propagation constants in general, and therefore different modal field distributions and conductor parameters.

As the proximity effect has been ignored during the derivation of this model, different values will be obtained for $Z_p[i,j]$ and $Y_p[i,j]$ depending on the particular point (x,y) on the induced conductor's surface at which the field is evaluated. When calculating mutual parameters ($i \neq j$) the field is usually calculated at the centre of the induced conductor to provide a reasonable estimate of the average value over the surface. Self parameters must be evaluated at the surface of the inducing conductor as the primary wave due to the filament representing the conductor is infinite at the centre (Wedepohl and Efthymiadis, 1978). The field is therefore evaluated at the point $(x_i, y_i - a_i)$ one radius below the centre.

As the media are isotropic the matrices are symmetric and therefore only those elements on or above the leading diagonal need to be evaluated.

The circuit parameters of each mode of propagation on a transmission line may be calculated directly using a method proposed by Wedepohl and Efthymiadis (1978). This method does not require that the air and earth permeabilities be equal, and therefore is more general than the previous method derived by Wait (1972).

The first step of this procedure is to determine the characteristic impedance (Z_0) for the given mode of propagation. Z_0 is defined as the instantaneous ratio of voltage to current at a fixed point when the mode of interest is the only wave propagating along the line (Ramo *et al.*, 1984). Once the propagation constant γ and the conductor current distribution ($\boldsymbol{I}_c$) have been calculated by solving equation (3.20), the modal field distribution around the transmission line can be evaluated. The characteristic impedance is determined by integrating the $\hat{y}$ component of the electric field (E_y) from $-\infty$ to a point on the surface of a conductor, then dividing by the conductor current as shown in equation (3.24).

$$Z_0 = \int_{-\infty}^{y_i - a_i} E_y \, dy \; / \; I_c[i] \tag{3.24}$$

Where

E_y = $\hat{y}$ component of the electric field due to the current distribution ($\boldsymbol{I}_c$) travelling along the line with propagation constant γ

In practice the integration need only be performed to a finite depth, where the contribution of the remaining E_y field is negligible (Wedepohl and Efthymiadis, 1978).

The modal series impedance and shunt admittance are calculated using equations (3.25) and (3.26), and the entire process repeated to obtain the parameters for all propagation modes.

$$Z_{\text{modal}} = \gamma Z_0 \tag{3.25}$$

$$Y_{\text{modal}} = \frac{\gamma}{Z_0} \tag{3.26}$$

Where

Z_{modal} = modal series impedance ($\Omega.\text{m}^{-1}$)
Y_{modal} = modal shunt admittance (S.m^{-1})

3.5.1.2 Implementation

During this project algebraically simplified versions of the multiconductor equations of Wedepohl and Efthymiadis (1978), extended to include lossy conductors, were implemented. A program was developed to calculate: modal propagation constants; electric and magnetic fields, scalar potential and magnetic vector potential both above and below ground; transmission line parameters.

The calculation of these quantities requires the evaluation of integrals of oscillatory functions over infinite ranges which can not be performed analytically in general (*e.g.* equations (3.15) and (3.16)). Automatic integration algorithms (de Boor, 1971; Piessens *et al.*, 1983) have been used during this project to evaluate these integrals numerically. By integrating between integrand zeros with adaptive error control based upon knowledge of the function, partitioning the integral at points of difficulty and extrapolating the integrals over each cycle of the integrand, the integrals can be evaluated efficiently and reliably. Particular care was taken over the selection of the integrator tolerance and computer coding of the integrands to minimise error. Such precautions are necessary to prevent divergence of the iterative propagation constant algorithm due to integration noise.

Müller's method with deflation has been used during this project to calculate the propagation constants, with initial values selected around the lossless value. Convergence to the transmission line propagation mode was rapid and stable.

3.5.1.3 Physical Interpretation

The field in the air around a single conductor transmission line, as determined using the Exact model, may be considered to consist of three components (Wedepohl and Efthymiadis, 1978):

- a direct field from the conductor
- an image field, or reflection from the air-earth interface
- and a ground field which represents the effect of the lossy earth.

This can be clearly seen in Equation (3.15) for the axial electric field in the air, which can be decomposed into a function of r_c alone, a function of r_i alone and an integral. Unfortunately little insight can be gained into the physical mechanisms that produce the ground wave due to the complexity of the mathematics.

The conductor and image fields cancel exactly at the air-earth interface, therefore the field at the interface is dependent solely on the ground field. When the earth is lossless the ground field is zero and the field reduces to that of the conductor/image system described in Section 3.3.1.

3.5.2 Carson's Model

In 1926 Carson and Pollaczek independently derived equations for the fields induced in the air and earth by an aerial conductor, based upon the Quasi-TEM wave propagation approximation. Pollaczek also derived expressions for the fields induced within the air and earth by a buried conductor while Carson determined the propagation constant of an aerial line.

Although both Carson and Pollaczek used the Quasi-TEM approximation to derive expressions for the fields around transmission lines, their equations are not equivalent. Pollaczek's expression for the magnetic vector potential may be reduced to Carson's by making further mathematical approximations (Perz and Raghuveer, 1974b). The expressions for the axial electric field in the air differ as Pollaczek ignored all propagation effects while Carson included the contribution due to the axial variation of conductor potential.

Historically Carson's equation has been more widely used than Pollaczek's, therefore the following discussion has been based upon Carson's model.

3.5.2.1 Derivation and Evolution

Carson studied a simplified system based upon the idealised single conductor transmission line shown in Figure 3.1. He assumed that the permeability and permittivity of the homogeneous earth equalled those of the air ($\mu_e = \mu_a$ and $\epsilon_e = \epsilon_a$), and that the conductor was thin and supported a single exponential mode of propagation. Furthermore the modal propagation constant was assumed to be very small, so that the axial variation of the conductor and earth currents could be neglected during the calculation of the fields induced by these currents.

Carson's derivation proceeded as follows. The axial electric field E_z within the earth was expressed as a general solution of the wave equation. Carson assumed that the transverse components of the electric field (E_x and E_y) within the earth were negligible in comparison to E_z. Formulas for the transverse magnetic fields (H_x and H_y) in the earth were then written in terms of E_z alone. The magnetic fields (H_x and H_y) in the air were formulated as the sum of a general solution of the wave equation (similar to those for the fields within the earth) and a direct field from the conductor (assuming that it was infinitely thin and carried a uniform current). Axial (z) components of the displacement current in the air were neglected during this calculation. Continuity of H_x and H_y at the air-earth interface was applied to solve for the unknown weight functions in the general solutions for E_z, H_x and H_y below ground and H_x and H_y in the air. The resultant equation for E_z in the earth is given below.

$$E_z(x,y,z,t) = -\frac{j\omega\mu_a I_c(z,t)}{\pi}\int_0^\infty \frac{\exp\left[y\sqrt{\alpha^2+j\omega\mu_a/\rho_e}-\alpha y_c\right]}{\alpha+\sqrt{\alpha^2+j\omega\mu_a/\rho_e}}\cos\left[\alpha(x-x_c)\right]d\alpha \qquad (3.27)$$

The axial electric field in the air was calculated using the relationship that the field is proportional to the sum of the temporal variation of the magnetic vector potential and the spacial variation of the scalar electric potential. Using this identity, Carson derived a difference equation between the axial field E_z at a point in the air and a second point on the surface of the earth directly below it. The vector potential component of this equation was expressed in terms of the known magnetic field, while the scalar potential term reduced to the variation of the potential at the point in the air as the surface of the earth was assumed to be at zero potential. Rearranging this expression and inserting equation (3.27) evaluated at the surface yielded the following explicit equation for E_z in the air.

$$E_z(x,y,z,t) = -\frac{j\omega\mu_a I_c(z,t)}{\pi}\int_0^\infty \frac{\exp[-\alpha(y+y_c)]}{\alpha+\sqrt{\alpha^2+j\omega\mu_a/\rho_e}}\cos\left[\alpha(x-x_c)\right]d\alpha - \frac{j\omega\mu_a I_c(z,t)}{2\pi}\ln\left(\frac{r_i}{r_c}\right)$$

$$- \frac{\partial}{\partial z} V(x, y, z, t) \tag{3.28}$$

Where

$V(x, y, z, t)$ = scalar potential at point (x, y, z) and time t (V)

The propagation constant and characteristic impedance of the wave were calculated using distributed circuit transmission line theory. However before this theory could be applied it was necessary to calculate the series impedance and shunt admittance of the line per unit length. The series impedance (Z_s) was derived using the relationship that the external axial electric field (E_z) equals the product of the conductor current and internal impedance ($I_c Z_{int}$) at one point on the surface of the conductor ($x = x_c, y = y_c - a_c$). By rearranging this equality and comparing it with the relationship $I_c Z_s = -\frac{\partial}{\partial z} V_c$, Carson derived the following equation for Z_s.

$$\begin{aligned} Z_s = \quad & Z_{int} \\ & + \frac{j\omega\mu_a}{2\pi} \ln\left(\frac{2y_c - a_c}{a_c}\right) \\ & + \frac{j\omega\mu_a}{\pi} \int_0^\infty \frac{\exp[-\alpha(2y_c - a_c)]}{\alpha + \sqrt{\alpha^2 + j\omega\mu_a/\rho_e}} \, d\alpha \end{aligned} \tag{3.29}$$

The shunt admittance of the line was determined by assuming that the surface of the earth was the zero equipotential surface. This analysis yielded equation (3.12) for the shunt admittance.

Equations (3.13) and (3.14) were then used to calculate the propagation constant and characteristic impedance of the lossy line.

The same method may be used to solve for the modal propagation constants and characteristic impedances of multiconductor lines. In this case however the terms of the equation are square matrices $[\boldsymbol{Z}_p]$ and $[\boldsymbol{Y}_p]$ containing both self and mutual elements. Square root functions are not defined for general matrices however, and it is necessary to resort to eigenvalue analysis to solve the equations. This process is discussed in greater detail in Chapter 8.

All Quasi-TEM models share the same definition for the self and mutual admittance of the conductors (equations (3.12) and (3.10)). Therefore in this section and the following sections dealing with Quasi-TEM models the discussion has been restricted to the impedance formulas which vary between models.

The mutual impedance Z_m between an aerial line and a parallel aerial conductor is defined by Carson to be :

> the axial electric intensity at the axis of the second wire due to the varying magnetic field of unit current in the first wire and its accompaning distribution of ground current.

By convention the sign of the mutual impedance is opposite to that of the axial electric field. This relationship is expressed mathematically in the following equation, which holds for all Quasi-TEM models.

$$E_z(x, y, z, t) = -Z_m(x, y) I_c(z, t) - \frac{\partial}{\partial z} V(x, y, z, t) \tag{3.30}$$

Comparing this relationship with equation (3.28) yields the following equation for the mutual impedance.

$$Z_{\mathrm{m}}(x,y) = \frac{\jmath\omega\mu_{\mathrm{a}}}{2\pi}\ln\left(\frac{r_{\mathrm{i}}}{r_{\mathrm{c}}}\right) + \frac{\jmath\omega\mu_{\mathrm{a}}}{\pi}\int_0^{\infty}\frac{\exp[-\alpha(y+y_{\mathrm{c}})]}{\alpha+\sqrt{\alpha^2+\jmath\omega\mu_{\mathrm{a}}/\rho_{\mathrm{e}}}}\cos[\alpha(x-x_{\mathrm{c}})]\,d\alpha \qquad (3.31)$$

The first term of equation (3.31) is the mutual impedance in the presence of a perfectly conducting earth equation (3.9), while the second term is known as the Carson correction as it corrects for the effect of lossy earth.

Carson defined two real functions $P_{\mathrm{carson}}(R,\theta)$ and $Q_{\mathrm{carson}}(R,\theta)$ which represent the real and reactive parts of the complex correction integral respectively. Inserting these functions into equation (3.31) yields:

$$Z_{\mathrm{m}}(x,y) = \frac{\jmath\omega\mu_{\mathrm{a}}}{2\pi}\ln\left(\frac{r_{\mathrm{i}}}{r_{\mathrm{c}}}\right) + \frac{\omega\mu_{\mathrm{a}}}{\pi}\left(P_{\mathrm{carson}}(R,\theta)+\jmath Q_{\mathrm{carson}}(R,\theta)\right) \qquad (3.32)$$

Where

$P_{\mathrm{carson}}(R,\theta)$ = real Carson correction term
$Q_{\mathrm{carson}}(R,\theta)$ = imaginary Carson correction term
R = variable of Carson's infinite series which is the radial separation between the induced conductor and the image of the inducing conductor scaled by a factor of $\sqrt{2}$ times the skin depth of the earth
$= \sqrt{\dfrac{\omega\mu_{\mathrm{a}}}{\rho_{\mathrm{e}}}}\,r_{\mathrm{i}}$
θ = variable of Carson's infinite series which is equal to the angle between a vertical plane through the inducing conductor and the plane containing the inducing and induced conductors
$= \arctan\left(\dfrac{x-x_{\mathrm{c}}}{y+y_{\mathrm{c}}}\right)$

Where the following series is used to evaluate $P_{\mathrm{carson}}(R,\theta)$ and $Q_{\mathrm{carson}}(R,\theta)$.

$$\begin{aligned} P_{\mathrm{carson}}(R,\theta) &= \frac{\pi}{8} \\ &\quad - b_{\mathrm{carson}}(1)R^1\cos(1\theta) \\ &\quad + b_{\mathrm{carson}}(2)R^2\left[(c_{\mathrm{carson}}(2)-\ln(R))\cos(2\theta)+\theta\sin(2\theta)\right] \\ &\quad + b_{\mathrm{carson}}(3)R^3\cos(3\theta) \\ &\quad - d_{\mathrm{carson}}(4)R^4\cos(4\theta) \\ &\quad - b_{\mathrm{carson}}(5)R^5\cos(5\theta) \\ &\quad + b_{\mathrm{carson}}(6)R^6\left[(c_{\mathrm{carson}}(6)-\ln(R))\cos(6\theta)+\theta\sin(6\theta)\right] \\ &\quad + b_{\mathrm{carson}}(7)R^7\cos(7\theta) \\ &\quad - d_{\mathrm{carson}}(8)R^8\cos(8\theta) \\ &\quad + \ldots \qquad (3.33) \\ Q_{\mathrm{carson}}(R,\theta) &= \frac{1}{2}\left[\ln\left(\frac{2}{R}\right)-\mathrm{Euler}+\frac{1}{2}\right] \\ &\quad + b_{\mathrm{carson}}(1)R^1\cos(1\theta) \\ &\quad - d_{\mathrm{carson}}(2)R^2\cos(2\theta) \end{aligned}$$

$$
\begin{aligned}
&+ b_{\text{carson}}(3)R^3\cos(3\theta) \\
&- b_{\text{carson}}(4)R^4\left[(c_{\text{carson}}(4) - \ln(R))\cos(4\theta) + \theta\sin(4\theta)\right] \\
&+ b_{\text{carson}}(5)R^5\cos(5\theta) \\
&- d_{\text{carson}}(6)R^6\cos(6\theta) \\
&+ b_{\text{carson}}(7)R^7\cos(7\theta) \\
&- b_{\text{carson}}(8)R^8\left[(c_{\text{carson}}(8) - \ln(R))\cos(8\theta) + \theta\sin(8\theta)\right] \\
&+ \ldots
\end{aligned} \tag{3.34}
$$

Where

$$
\begin{aligned}
b_{\text{carson}}(n) &= \frac{\sqrt{2}}{6} && \text{For } n = 1 \\
&= \frac{1}{16} && \text{For } n = 2 \\
&= b_{\text{carson}}(n-2)\frac{\text{sign}(n)}{n(n+2)} && \text{For } n > 2 \\
c_{\text{carson}}(n) &= \ln(2) - \text{Euler} + \frac{5}{4} && \text{For } n = 2 \\
&= c_{\text{carson}}(n-2) + \frac{1}{n} + \frac{1}{n+2} && \text{For } n = 4,6,8,\ldots \\
d_{\text{carson}}(n) &= b_{\text{carson}}(n)\frac{\pi}{4} && \text{For } n = 2,4,6,\ldots \\
\text{Euler} &= \text{Euler's constant} \\
&= 0.577215664901532\ldots \\
\text{sign}(n) &= +1 && \text{For } n = 1,2,3,4,9,10,11,12,17,\ldots \\
&= \text{-}1 && \text{For } n = 5,6,7,8,13,14,15,16,21,\ldots
\end{aligned}
$$

Unfortunately the above series are slow to converge when $R > 5$ and therefore the following asymptotic series are generally used.

$$
\begin{aligned}
P_{\text{carson}}(R,\theta) = \frac{1}{\sqrt{2}}\Bigg[&\frac{\cos(\theta)}{R} - \frac{\sqrt{2}\cos(2\theta)}{R^2} + \frac{\cos(3\theta)}{R^3} \\
&+ \frac{3\cos(5\theta)}{R^5} - \frac{45\cos(7\theta)}{R^7} + \ldots\Bigg]
\end{aligned} \tag{3.35}
$$

$$
\begin{aligned}
Q_{\text{carson}}(R,\theta) = \frac{1}{\sqrt{2}}\Bigg[&\frac{\cos(\theta)}{R} - \frac{\cos(3\theta)}{R^3} \\
&+ \frac{3\cos(5\theta)}{R^5} - \frac{45\cos(7\theta)}{R^7} + \ldots\Bigg]
\end{aligned} \tag{3.36}
$$

The assumptions made during the derivation of Carson's equation are essentially those of the Quasi-TEM theory (Section 3.3.3) with the addition of a homogeneous earth with a permeability and permittivity equal to that of free space. As the permeability of the earth is typically unity (Vance, 1978) and the fields are not very sensitive to the permittivity of the earth, the major restrictions on the use of Carson's equation arise from the Quasi-TEM propagation assumption. Conditions under which this assumption is valid have been discussed in Section 3.3.3. In general Carson's equation is valid for low frequency studies where the conductor is not in close contact with the earth (Olsen and Pankaskie, 1983).

Numerous extensions have been made to Carson's model since 1926. The majority of these extensions were simply relaxations of the permeability, permittivity and homogeneity restrictions whilst others provided alternative derivations or mathematical simplifications to improve accuracy or computational speed.

Wise (1931) was the first to incorporate the effect of the permeability of the earth into Carson's model. It has been included in many Quasi-TEM models derived since (Mullineux and Reed, 1965; Wedepohl and Wasley, 1966; Nakagawa *et al.*, 1973; Perz and Raghuveer, 1974b; Nakagawa and Iwamoto, 1976).

Wise also included the effect of displacement currents in the earth on the mutual and self impedances (Wise, 1934) and the potential coefficients (Wise, 1948) for a unity permeability earth. It should be noted that the inclusion of displacement currents in a Quasi-TEM model does not make it equivalent to the Exact model as only axial displacement currents are considered, the wave is still assumed to propagate without attenuation when calculating the fields. Quasi-TEM models which incorporate both the permittivity and permeability of the earth have also been developed (Wedepohl and Wasley, 1966; Nakagawa *et al.*, 1973; Perz and Raghuveer, 1974b; Nakagawa and Iwamoto, 1976).

To improve the accuracy of calculated impedances many researchers developed models in which the earth was represented by a stratified structure. Two layer models were developed by Evans (1930), Sunde (1949), Wedepohl and Wasley (1966) and Nakagawa *et al.* (1973). Sunde (1949) also developed a multi-layer model while Wedepohl and Wasley (1966) described how their technique could be used to derive more complicated models. Nakagawa *et al.* (1973) derived a three layer model for the earth and later extended it to a multi-layer model (Nakagawa and Iwamoto, 1976).

Of all the stratified models Nakagawa's multi-layer model is potentially the most accurate as it can approximate complicated earth structures in detail and it includes the effect of the permeability and permittivity of the earth (Nakagawa and Iwamoto, 1976). Nakagawa's equation can be reduced to the two layer model derived by Wedepohl *et al.*, Wise's homogeneous earth model with displacement currents and Carson's equation. The equations for this model are given below.

$$Z_{\mathrm{m}}(x,y) = \frac{\jmath\omega\mu_{\mathrm{a}}}{2\pi}\left[\ln\left(\frac{r_{\mathrm{i}}}{r_{\mathrm{c}}}\right) + J_{\mathrm{naka}}(x,y)\right] \tag{3.37}$$

Where

$$\begin{aligned}
J_{\mathrm{naka}}(x,y) &= \text{Correction integral of Nakagawa's multi-layer mutual impedance model} \\
&= 2\int_0^{\infty} \frac{F_{\mathrm{naka}}(1) + G_{\mathrm{naka}}(1)}{(\alpha+\mu_{\mathrm{a}}b_{\mathrm{naka}}(1))F_{\mathrm{naka}}(1) + (\alpha-\mu_{\mathrm{a}}b_{\mathrm{naka}}(1))G_{\mathrm{naka}}(1)} \\
&\quad \times \exp\left[-(y+y_{\mathrm{c}})\alpha\right]\cos[\alpha(x-x_{\mathrm{c}})]\,\mathrm{d}\alpha \\
F_{\mathrm{naka}}(n) &= \left(b_{\mathrm{naka}}(n) + b_{\mathrm{naka}}(n+1)\right)F_{\mathrm{naka}}(n+1) \\
&\quad + \left(b_{\mathrm{naka}}(n) - b_{\mathrm{naka}}(n+1)\right)G_{\mathrm{naka}}(n+1) \\
&\quad \times \exp\left(2c_{\mathrm{naka}}(n+1)d_{\mathrm{naka}}(n)\right) \\
&\quad \text{For } 1 \le n \le m_{\mathrm{naka}} - 2 \\
&= b_{\mathrm{naka}}(m_{\mathrm{naka}}-1) + b_{\mathrm{naka}}(m_{\mathrm{naka}}) \\
&\quad \text{For } n = m_{\mathrm{naka}} - 1 \\
G_{\mathrm{naka}}(n) &= [\ \left(b_{\mathrm{naka}}(n) - b_{\mathrm{naka}}(n+1)\right)F_{\mathrm{naka}}(n+1) \\
&\quad + \left(b_{\mathrm{naka}}(n) + b_{\mathrm{naka}}(n+1)\right)G_{\mathrm{naka}}(n+1) \\
&\quad \times \exp\left(2c_{\mathrm{naka}}(n+1)d_{\mathrm{naka}}(n)\right) \\
&\quad]\ \times \exp\left(-2c_{\mathrm{naka}}(n)d_{\mathrm{naka}}(n)\right) \\
&\quad \text{For } 1 \le n \le m_{\mathrm{naka}} - 2 \\
&= \left(b_{\mathrm{naka}}(m_{\mathrm{naka}}-1) - b_{\mathrm{naka}}(m_{\mathrm{naka}})\right) \\
&\quad \times \exp\left(-2c_{\mathrm{naka}}(m_{\mathrm{naka}}-1)d_{\mathrm{naka}}(m_{\mathrm{naka}}-1)\right) \\
&\quad \text{For } n = m_{\mathrm{naka}} - 1 \\
b_{\mathrm{naka}}(n) &= \frac{c_{\mathrm{naka}}(n)}{\mu_{en}}
\end{aligned}$$

For $n = 1, 2, \ldots m_{\text{naka}}$

$c_{\text{naka}}(n) = \sqrt{\alpha^2 + k_a^2 - k_{en}^2}$

For $n = 1, 2, \ldots m_{\text{naka}}$

$d_{\text{naka}}(n)$ = distance between the air-earth interface and the interface between the n and $(n+1)$ layers of the earth (m)

m_{naka} = number of layers representing the earth. The layers are numbered from the top down.

k_{a} = wave number of the air

$$= \sqrt{-\jmath\omega\mu_{\text{a}}\left(\frac{1}{\rho_{\text{a}}} + \jmath\omega\epsilon_{\text{a}}\right)}$$

k_{en} = wave number of the n'th layer of the earth

$$= \sqrt{-\jmath\omega\mu_{en}\left(\frac{1}{\rho_{en}} + \jmath\omega\epsilon_{en}\right)}$$

For $n = 1, 2, \ldots m_{\text{naka}}$

μ_{en} = permeability of the n'th layer of the earth (H.m^{-1})

ϵ_{en} = permittivity of the n'th layer of the earth (F.m^{-1})

ρ_{en} = resistivity of the n'th layer of the earth ($\Omega.\text{m}^{-1}$)

The models discussed in this section give the mutual impedance between parallel wires which are also parallel to the surface of the earth. Krakowski (1967) derived a Quasi-TEM model for the mutual impedance between an infinitely long conductor and a finite conductor which are both parallel to the earth but not parallel to each other by integrating the component of Carson's mutual impedance along the axis of the finite conductor. This model is significant as in practice telecommunications circuits rarely parallel high voltage transmission lines. The case where the conductors are not parallel, either to themselves or to the earth has also been investigated by integrating the components of Carson's mutual impedance and admittance along the path of the conductor (Ametani and Aoki, 1989). This approach is not strictly valid however as Carson's equations are only valid for infinite length inducing conductors which are parallel to the earth.

The Quasi-TEM models although less complicated than the Exact model are not easy to evaluate as they require either the integration of oscillatory integrand functions over infinite intervals, or the sum of infinite oscillatory series (Carson, 1926; Pollaczek, 1926; Wise, 1931; Wise, 1934; Krakowski, 1967). To overcome this difficulty many researchers have developed approximate functions based upon truncation of the infinite series (Sunde, 1949; Dommel, 1985). Unfortunately these equations are frequently inaccurate over the wide range of parameters encountered during telecommunications interference studies.

Since the introduction of digital computers it has become practical to evaluate the integral equations numerically (Mullineux and Reed, 1965; Wedepohl and Wasley, 1966; Nakagawa *et al.*, 1973; Perz and Raghuveer, 1974b; Nakagawa and Iwamoto, 1976), providing accurate results for all parameter ranges. Nevertheless the numerical evaluation of integrals is computationally expensive especially when high accuracy is required.

In an effort to improve the accuracy and efficiency of the evaluation of Carson's equation for inductive interference studies, Tevan and Deri (1984) derived the following correction series which is added to the asymptotic series (equations (3.35) and (3.36)) when $\theta > \frac{\pi}{4}$ and $R > 5$.

$$Z_{\text{m}}(x, y) = \frac{\jmath\omega\mu_{\text{a}}}{2\pi} \ln\left(\frac{r_{\text{i}}}{r_{\text{c}}}\right) + \frac{\omega\mu_{\text{a}}}{\pi}\Big[$$

$$
\begin{aligned}
& P_{\text{carson}}(R,\theta) \\
+\ & \jmath Q_{\text{carson}}(R,\theta) \\
+\ & \frac{\sqrt{\pi}\exp(2s_{\text{tevan}})}{4\sqrt{s_{\text{tevan}}^3}}\left(1-\frac{3}{16s_{\text{tevan}}}-\frac{15}{512s_{\text{tevan}}^2}-\frac{105}{8192s_{\text{tevan}}^3}-\ldots\right)\Bigg] \qquad (3.38)
\end{aligned}
$$

Where

s_{tevan} = complex variable of Tevan and Deri's correction for Carson's asymptotic series.

$$= \frac{R}{2}\exp\left(\jmath\left(\frac{3}{4}\pi+\theta\right)\right)$$

Recently an accurate and efficient piece-wise curve fitting approximation to Carson's equation was developed for use in harmonic penetration studies (Daza, 1988; Cameron *et al.*, 1990). Although this model is not strictly a Quasi-TEM model it is included here as it has been fitted to Carson's equation and therefore is subject to the same limitations. The model is based upon the following simple approximations for $P_{\text{carson}}(R,\theta)$ and $Q_{\text{carson}}(R,\theta)$.

$$P_{\text{carson}}(R,\theta) = s_{\text{acha}} - t_{\text{acha}}R \qquad (3.39)$$

$$Q_{\text{carson}}(R,\theta) = u_{\text{acha}} - v_{\text{acha}}\ln(R) \qquad (3.40)$$

Where

$s_{\text{acha}}, t_{\text{acha}}, u_{\text{acha}}, v_{\text{acha}}$ = piece-wise curve fitted coefficients of Acha's model

The coefficients of equations (3.39) and (3.40) were evaluated for R over the range from 0.5 to 12 in steps of 0.5 (with an additional point at $R = 0.2$) and for θ from 0 to 90 degrees in steps of 15 degrees. To apply this model the user calculates R and θ and then selects the row in Table A.1 (Appendix A) with the closest R value to that calculated. Linear interpolation is then used between the two sets of coefficients in the row that bracket the calculated θ value to estimate the coefficients at that angle. Finally the interpolated coefficients are inserted into equations (3.39) and (3.40). The relative error of these formulas with respect to Carson's model is less than 3%. These formulas are faster to evaluate than either Carson's equation or the Complex Penetration model (Section 3.5.3) (Daza, 1988; Cameron *et al.*, 1990).

3.5.2.2 Implementation

Due to the conflicting requirements of high accuracy, the need to be able to model earth structures in detail, and high computational speed, a variety of Quasi-TEM models were implemented during this project.

The mutual impedance integrals of Carson (Equation (3.31)) and Nakagawa (Equation (3.37)) are similar in form to those of the Exact model and were evaluated numerically using the adaptive integration algorithms discussed in Section 3.5.1. In practice only Nakagawa's model was implemented as it reduces to Carson's integral for a single layer earth.

Carson's infinite series formulas (Equations (3.32), (3.33), (3.34)) were evaluated using a loop algorithm to sum terms of the series until convergence was detected, as suggested by Dommel (1974). Groups of four terms were evaluated until the magnitude of the last group fell below $10^{-14}\times$ the running total. Double precision arithmetic (sixteen significant digits) was used to minimise the round-off error that results from

summing oscillating series terms. A maximum of eighty eight terms could be summed, which was found to be sufficient to calculate the impedances to an accuracy in excess of five significant digits for $0 \leq R \leq 20$ and $0 \leq \theta \leq \frac{\pi}{2}$. The coefficients of the series were calculated in advance. Recursive definitions of the coefficients and trigonometric identities were utilised to improve the efficiency of the computation.

The asymptotic series ((3.35) and (3.36)) were evaluated by direct encoding of the series for terms up to and including $\frac{1}{R^7}$. Additional terms were not included as they reduce the accuracy of the results in general as the series are oscillatory and divergent. The truncated series were found to provide optimum accuracy over the range $0 \leq R \leq 20$ and $0 \leq \theta \leq \frac{\pi}{2}$. More accurate results can be obtained by including more terms when R is large as the point at which the series diverges increases with R however the author did not exploit this behaviour in his implementation.

To improve the accuracy of the asymptotic series the correction series derived by Tevan *et al.* (Equation (3.38)) was applied when $R > \frac{\pi}{4}$. This series is also divergent and was truncated after the first term as this provided optimum accuracy over the range $0 \leq R \leq 20$ and $0 \leq \theta \leq \frac{\pi}{2}$ when combined with the truncated asymptotic series.

Acha's curve fitting model (equations (3.39) and (3.40)) was implemented using a table look up and linear interpolation algorithm operating on the fixed coefficient tables.

3.5.2.3 Physical Interpretation

The Quasi-TEM (Equations (3.31) and (3.37)) and Exact models (Section 3.5.1) share the same physical interpretation. In both cases the fields can be decomposed into a direct component from the conductor, an image component due to reflection from the air-earth interface and a ground component due to current flow within the earth.

It is difficult to gain an understanding of the physical phenomena which give rise to the ground field from the correction integrals. However Acha's approximations to Carson's equations offers some insight as to what might be the dominant effect. Equation (3.39) suggests that for small perturbations of R the resistive component of the correction is approximately linearly proportional to R while the inductive correction is proportional to $\ln(R)$, where R is the radial separation between the inducing conductor and the image of the induced scaled by a factor of $\sqrt{2}$ times the skin depth of the earth. As the induction from a current filament varies as the logarithm of the radial separation, this approximation suggests that the inductive component of the correction may be approximated by an image which is a factor of $\sqrt{2}$ times the skin depth further away than the lossless image. It should be noted however that the coefficients of the approximation equations are not constants and therefore this interpretation is not strictly valid. This concept is discussed further in Chapter 4.

3.5.3 Complex Penetration Model

The Complex Penetration model (or Dubanton model) was developed by Ball *et al.* (Bannister, 1970) and Dubanton (Gary, 1976). Its name derives from the fact that the lossy earth is represented in this model by a perfectly conducting plane at a complex depth which is related to the skin depth or "depth of penetration" of current into the earth as shown in Figure 3.3. As this plane is perfectly conducting it can be replaced by an image conductor at a depth equal to the height of the inducing conductor above it (Figure 3.3). The mutual impedance is then given by (3.41) which is of the same form as the lossless mutual impedance formula (3.9) except that in this case the radial distance to the image is complex.

$$\begin{aligned} Z_{\mathrm{m}} &= \frac{j\omega\mu_{\mathrm{a}}}{2\pi} \ln \frac{r_{\mathrm{i}}}{r_{\mathrm{c}}} \\ &= \frac{j\omega\mu_{\mathrm{a}}}{2\pi} \ln \frac{\sqrt{(x-x_{\mathrm{c}})^2 + (y+y_{\mathrm{c}}+2\psi)^2}}{\sqrt{(x-x_{\mathrm{c}})^2 + (y-y_{\mathrm{c}})^2}} \end{aligned} \tag{3.41}$$

The power of the Complex Penetration model lies in the simple closed form expression for the mutual impedance and the geometric interpretation of this equation. This makes it possible to calculate earth return impedances on simple computing machines and to formulate explicit expressions for the inductive influence of multiconductor transmission lines using geometrical concepts (Semlyen and Shirmohammadi, 1982). It should be noted however that the complex image in this model is a computational convenience not a physical hypothesis (Semlyen, 1981; Bannister, 1986). A physical interpretation of this model is presented latter in this section.

3.5.3.1 Derivation and Evolution

The original derivations of the Complex Penetration model were not mathematically rigorous (Olsen and Pankaskie, 1983). Dubanton's derivation was based upon intuitive reasoning (Gary, 1976), while Ball *et al.* used plane wave analysis to determine the complex depth of penetration (Bannister, 1970). Wait and Spies (1969) were the first to derive the Complex Penetration model in a rigorous manner. They took as their starting point the integral equation for the axial electric field in space due to a conductor above a homogeous earth with the permeability of free space and arbitrary permittivity which they simplified by applying the Quasi-TEM propagation approximation. To see if the integral could be approximated by an expression of the form of (3.41) they expanded the integrand in terms of a series, the leading term of which reduced to (3.41) after integration when displacement currents in the earth are ignored. The range of applicability of this approximation (relative to the full Quasi-TEM model) was then established by determining the conditions under which the remaining terms of the integrand could be ignored.

Equation (3.41) was found to be valid when the Quasi-TEM propagation model is valid, and the observation point is greater than approximately four times the skin depth of the earth from the inducing conductor (Wait and Spies, 1969; Bannister, 1986). This is a particularly stringent requirement from a power system point of view as the skin depth at fifty Hertz with a one hundred ohmmetre earth is seven hundred and ten metres. Therefore in theory this model should not be applied to this case unless the observation point is further than two thousand eight hundred and forty metres from the line. However in the immediate vicinity of the line the direct field from the conductors dominates, and therefore the fact that the image component does not accurately represent the field component due to current flow within the earth is irrelevant for observation points within one half of a skin depth of the line (Bannister, 1968; Bannister, 1986). It is in the intermediate region between one half and four times the skin depth that the accuracy of this model is poor.

Numerous researchers have studied the error in equation (3.41) (Bannister, 1970; Gary, 1976; Deri *et al.*, 1981; Deri and Tevan, 1981; Semlyen, 1981; Metwally and Mahmoud, 1982; Semlyen and Shirmohammadi, 1982; Alvarado and Betancourt, 1983; Olsen and Pankaskie, 1983; Tevan and Deri, 1984; Dommel, 1985; Bannister, 1986). The conclusion of these investigations is that for power line self impedance calculations the maximum error is less than 3% while the maximum error for power line interference calculations does not exceed 16% (Tevan and Deri, 1984). Where the error is defined to be the ratio of the difference between the real or reactive component calculated using

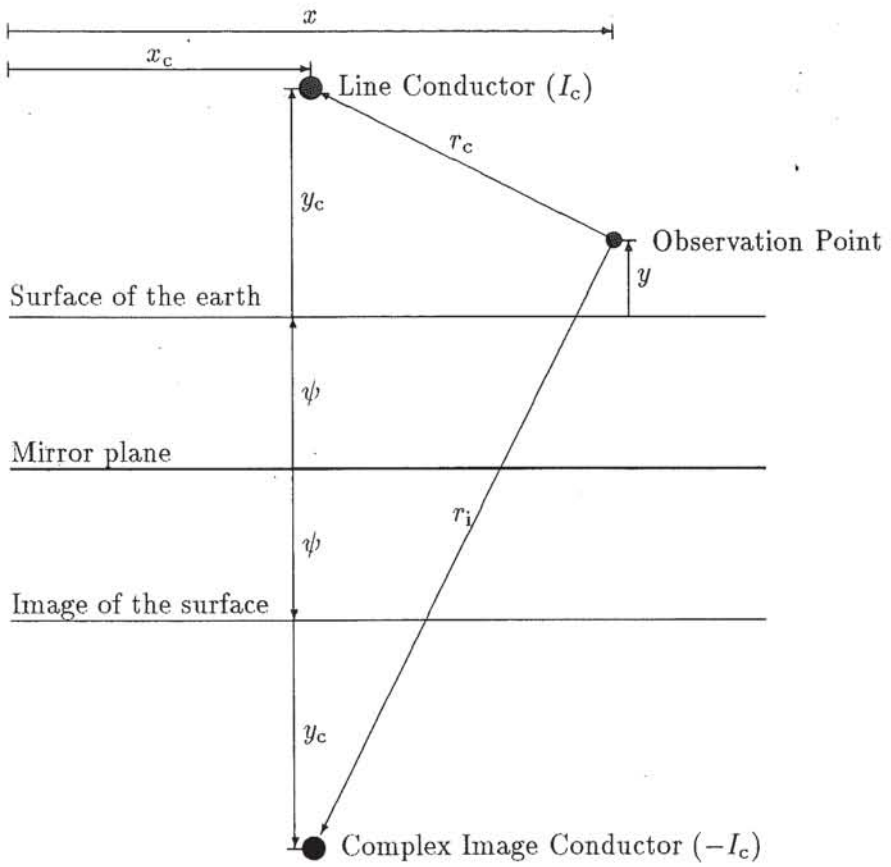

Where

ψ = complex depth of penetration
$= (1 - j)\frac{\delta}{2}$
δ = real depth of penetration (skin depth)
$= \sqrt{\frac{2\rho_e}{\omega\mu_e}}$
r_i = radial separation between the observation point and the complex image conductor (m)
$= \sqrt{(x - x_c)^2 + (y + y_c + 2\psi)^2}$

Figure 3.3. Replacing the Lossy Earth with a Complex Image Conductor

the complex penetration model and that of Carson's model, divided by the magnitude of the Carson impedance.

Many extensions to the complex penetration model have been proposed. These extensions may be divided into two groups, improvements in the accuracy of the image approximation and improvements in the way in which the earth is represented.

The simplest way to improve the accuracy of the complex image theory is to add more terms of the series derived by Wait and Spies (1969). A number of researchers have studied the improvement gained through the addition of the second term of this series (Metwally and Mahmoud, 1982; Alvarado and Betancourt, 1983; Olsen and Pankaskie, 1983). Alvarado and Betancourt (1983) found that the error is reduced to less than 2.5% for power system applications. Unfortunately the addition of the correction term complicates the geometrical interpretation of the model, as this term corresponds to a multipole image at the same depth as the single image of Figure 3.3 (Bannister, 1986).

Metwally and Mahmoud (1982) also studied a number of image forms that are more accurate than the truncated Wait and Spies series. These forms are combinations of discrete and continuous images. One of the forms proposed by Metwally *et al.* had a maximum error of less than 1%, but his error assessment technique differs from that used by Tevan and Deri (1984) and therefore can not be directly compared.

The effect of the permittivity of the earth was incorporated in the complex penetration model by Wait and Spies (1969), while Deri *et al.* (1981) added the permeability but excluded the permittivity dependence.

During the course of this project the author derived (3.42) which combines the permeability and permittivity dependence of the earth and the first correction term of the series derived by Wait and Spies (1969) into a single equation. This equation was derived by reducing Wedepohl's Exact model for differing air/earth permeabilities using the method developed by Wait and Spies (1969). It reduces to the forms given by Wait and Spies (1969) and Olsen and Pankaskie (1983), however it differs from the expression derived by Deri *et al.* (1981).

$$\begin{aligned} Z_{\mathrm{m}} = \quad & \jmath\frac{\omega\mu_{\mathrm{a}}}{2\pi}\ln\frac{\sqrt{(x-x_{\mathrm{c}})^2+(y+y_{\mathrm{c}}+2\mu_{\mathrm{e}}/(\mu_{\mathrm{a}}\zeta))^2}}{\sqrt{(x-x_{\mathrm{c}})^2+(y-y_{\mathrm{c}})^2}} \\ + \quad & \jmath\frac{\omega\mu_{\mathrm{a}}}{2\pi}\frac{2}{3\zeta^3}\frac{\mu_{\mathrm{e}}{}^3}{\mu_{\mathrm{a}}{}^3}\left(2-3\frac{\mu_{\mathrm{a}}{}^2}{\mu_{\mathrm{e}}{}^2}\right) \\ & \left(\frac{(y+y_{\mathrm{c}}+2\mu_{\mathrm{e}}/(\mu_{\mathrm{a}}\zeta))^3-3(x-x_{\mathrm{c}})^2(y+y_{\mathrm{c}}+2\mu_{\mathrm{e}}/(\mu_{\mathrm{a}}\zeta))}{\left((x-x_{\mathrm{c}})^2+(y+y_{\mathrm{c}}+2\mu_{\mathrm{e}}/(\mu_{\mathrm{a}}\zeta))^2\right)^3}\right) \end{aligned} \tag{3.42}$$

Where

$$\zeta = \sqrt{\jmath\omega\mu_{\mathrm{e}}\left(\frac{1}{\rho_{\mathrm{e}}}+\jmath\omega\epsilon_{\mathrm{e}}\right)}$$

The complex penetration model has also been extended to include stratified earth structures (Deri *et al.*, 1981; Mahmoud and Mohsen, 1985). Deri *et al.* (1981) developed a continuously stratified earth model. It has been found that the complex image methods only approximate one part of the full solution for the fields above a stratified earth structure (Mahmoud and Mohsen, 1985), regardless of the number and form of the image representation. In particular the component of the solution associated with the lowest subsurface and the waveguide modes that exist in a stratified earth are not included. The waveguide modes may be ignored when the displacement currents in the

earth are small in relation to the conduction current, which is normally the case at power system frequencies. If they are significant then they can be added to the solution obtained from this method (Mahmoud and Mohsen, 1985). It should also be noted that the accuracy of the stratified earth complex penetration model is poor unless the separation from the line is greater than four times the skin depth in each layer of the earth (Bannister, 1986).

3.5.3.2 Implementation

The simple closed form expressions for the mutual impedance according to the complex penetration model ((3.41) and (3.42)) were evaluated directly during the course of this project.

3.5.3.3 Physical Interpretation

The complex penetration model appears to offer a simple physical equivalent for the conductor earth system consisting of the conductor and a single image located in air as shown in Figure 3.3. Unfortunately complex dimensions have no physical meaning, and therefore in reality little physical insight into the mechanisms of induction can be gained from this.

Equation (3.41) may be rewritten as

$$\begin{aligned} Z_{\mathrm{m}} = & -\frac{\omega\mu_{\mathrm{a}}}{4\pi}\arctan\frac{-2\delta(y+y_{\mathrm{c}}+\delta)}{(x-x_{\mathrm{c}})^2+(y+y_{\mathrm{c}}+\delta)^2-\delta^2} \\ & + \jmath\frac{\omega\mu_{\mathrm{a}}}{4\pi}\ln\frac{\sqrt{(x-x_{\mathrm{c}}+\delta)^2+(y+y_{\mathrm{c}}+\delta)^2}}{\sqrt{(x-x_{\mathrm{c}})^2+(y-y_{\mathrm{c}})^2}} \\ & + \jmath\frac{\omega\mu_{\mathrm{a}}}{4\pi}\ln\frac{\sqrt{(x-x_{\mathrm{c}}-\delta)^2+(y+y_{\mathrm{c}}+\delta)^2}}{\sqrt{(x-x_{\mathrm{c}})^2+(y-y_{\mathrm{c}})^2}} \\ = & -\frac{\omega\mu_{\mathrm{a}}}{4\pi}\arctan\frac{-2\delta(y+y_{\mathrm{c}}+\delta)}{(x-x_{\mathrm{c}})^2+(y+y_{\mathrm{c}}+\delta)^2-\delta^2} \\ & + \jmath\frac{\omega\mu_{\mathrm{a}}}{4\pi}\ln\frac{r_{\mathrm{r1}}}{r_{\mathrm{c}}} \\ & + \jmath\frac{\omega\mu_{\mathrm{a}}}{4\pi}\ln\frac{r_{\mathrm{r2}}}{r_{\mathrm{c}}} \end{aligned} \tag{3.43}$$

The first term of (3.43) represents the mutual resistance and the subsequent terms the mutual inductance. This form does not provide any insight into the mechanism producing the resistive component; however the inductive component is equivalent to that from the three conductor system shown in Figure 3.4. The implication is that at large distances from the line (greater than four times the skin depth δ) the distribution of the current within the earth that is in phase with the conductor current is accurately approximated by the pair of filamentary current sources shown in Figure 3.4.

3.5.4 Conductor Element Model

Calculating the fields around a conductor above the earth is difficult due to the complexity of the problem of determining the current distribution within the earth. Solutions to this skin effect problem discussed thus far have been based upon Exact or approximate solutions of Maxwell's equations for semi-infinite earth structures. The Conductor Element method (Hartenstein *et al.*, 1972) described in this section utilises a different approach based upon a quantised physical approximation of the earth.

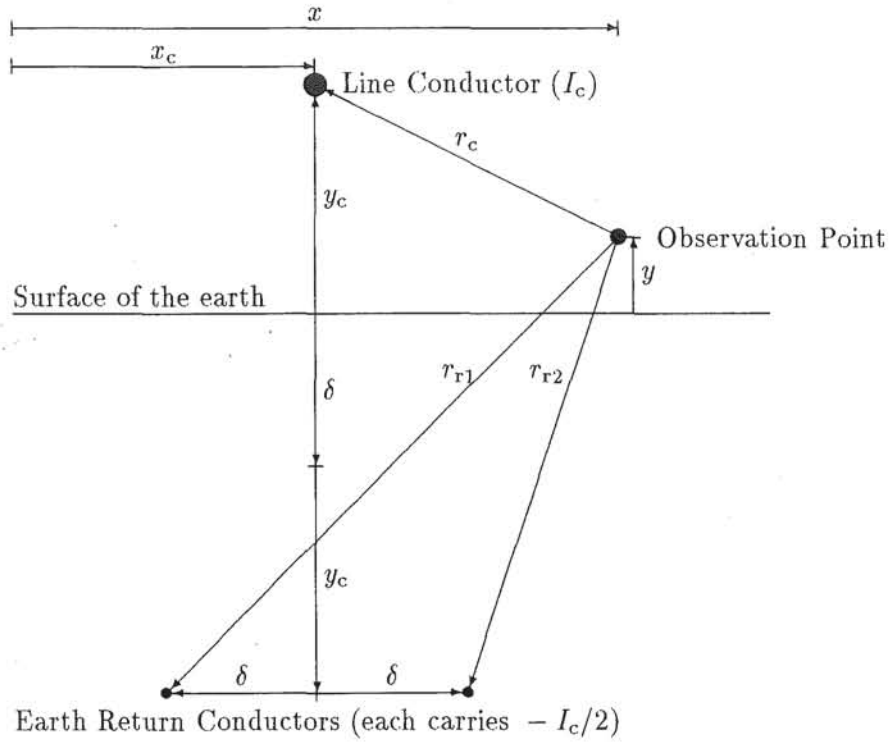

Where

r_{r1} = radial separation between the observation point and the first earth return conductor (m)
$= \sqrt{(x - x_c + \delta)^2 + (y + y_c + \delta)^2}$

r_{r2} = radial separation between the observation point and the second earth return conductor (m)
$= \sqrt{(x - x_c - \delta)^2 + (y + y_c + \delta)^2}$

Figure 3.4. Complex Penetration Equivalent Inductive Conductor System

3.5.4.1 Derivation and Evolution

In the conductor element method the infinite earth is modelled as a finite number of lossy conductors of finite dimensions. The self and mutual parameters of the conductor and the conductor elements representing the earth are calculated and formed into an impedance matrix relating the currents in the conductor and conductor elements to the resultant series voltage drops. At this stage the only known quantity is the conductor current. However it is known that the net current in the conductor elements must equal the conductor current, but flow in the opposite direction as they form the return path for the conductor. Using this relationship the unknown conductor element currents can be systematically eliminated from the system of equations until only the conductor current remains. The resulting sub-matrix relating conductor current to voltage is the desired series impedance for the conductors with earth return.

The technique is readily extended to multiconductor lines by including the other conductors in the matrix and reducing the system until only the conductors remain.

A number of assumptions are inherent in this analysis. Firstly it is assumed that the current along each conductor and conductor element is constant and does not leak off to neighbouring elements. Essentially this means that it is assumed that there is no transverse current flow during the derivation of the series impedance, which is the assumption upon which the Quasi-TEM theory is based. The range of validity of this model is therefore limited to that of Quasi-TEM theory.

It is also assumed that the earth can be accurately represented by a finite number of conductor elements. In theory as the number of conductor elements tends to infinity the result will tend to that of Carson's equation at the expense of greater computational effort. The computational effort can be minimised by careful selection of the number, size and shape of the conductor elements. This is discussed further in the implementation section.

A major advantage of the conductor element method is that different electrical parameters can be assigned to each conductor element, allowing inhomogeneous earth structures to be modelled.

3.5.4.2 Implementation

The conductor element method trades the complexity of solving the problem of the skin effect in the earth, for the problem of solving a system of conductor elements. Therefore no advantage is gained unless it is easier to solve for the conductor element parameters than those of the entire earth.

To simplify the calculation of the conductor element parameters Hartenstein *et al.* (1972) assumed that the current density in each element was uniform. This is a reasonable approximation for sufficiently small and well chosen regions of the earth. The parameters of the conductor elements could then be determined using low frequency formulas which ignore the skin effect. The self impedances of each element were calculated using formulas for equivalent area round conductors, while the mutual parameters were calculated for equivalent conductors at the centre of gravity of the conductor element.

The success of this method depends upon how well the system of conductor elements approximates regions of constant current density within the earth. The current density in the earth decreases with depth and separation from the transmission line. This effect was exploited when selecting the size and number of conductor elements. As the current density at large distances is small it may be ignored, reducing the problem to one of finite dimensions. Furthermore, the rate of decrease of current density reduces with increasing distance, therefore larger conductor elements may be used at large distances.

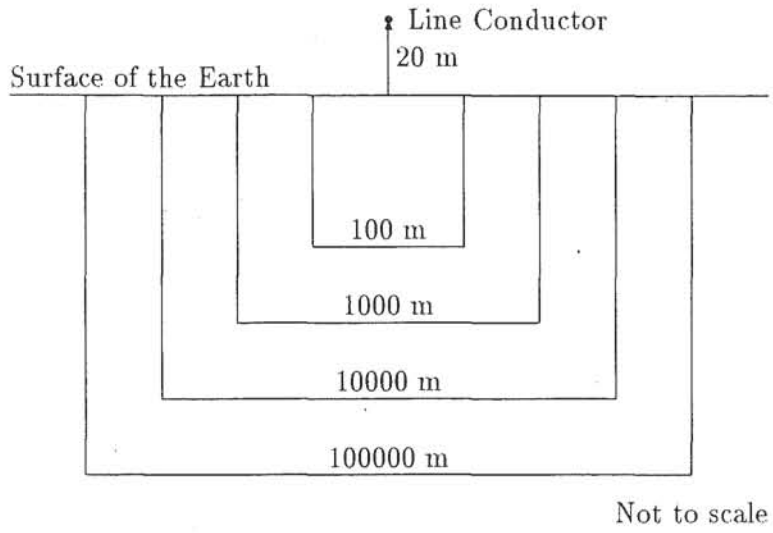

Figure 3.5. Earth Conductor Elements below a Single Conductor Line

Hartenstein *et al.* (1972) suggest using elements with exponentially increasing cross-sectional areas as shown in Figure 3.5. This minimises the computational burden which is proportional to the square of the number of conductor elements. The distribution of current within the earth is related to the skin depth of the earth (which is frequency and earth resistivity dependant) and the height of the conductor and in the case of multi-conductor lines the mode of propagation along the line. Therefore it is difficult in theory to select a conductor element system that will perform well over a wide range of conditions. Hartenstein *et al.* (1972) found that the maximum error in the sequence impedances for a two pole HVDC link that they studied was of the order of 9% over the frequency range from 10^{-3} to 10^{5} Hz, indicating that it is not necessary to model the earth current distribution in great detail.

Although the model has been developed for the calculation of the parameters of transmission lines, it could also be used for mutual impedance calculations. In this case the induced conductor would be included as an additional line conductor in the system of equations.

The author has not implemented this model and therefore can give no indication of the errors that are likely to result from the application of this model.

3.5.4.3 Physical Interpretation

The conductor element model is a physical model of the current distribution within the earth. The success of the model indicates that the earth can simply be regarded as a system of parallel lossy conductors inducing current in one another. Unfortunately the complexity of the interrelationships between the conductor elements obscures the overall phenomena.

A model based upon physical approximation of the current distribution in the earth was developed by the author during the course of this project. It differs from the

subconductor model in that it replaces the earth with a system of ideal filamentary currents, the current in each filament being determined from empirical formulas rather than the physical parameters of each region within the earth. This model is discussed further in Chapter 4.

3.5.5 Applications of Infinite Line Models during this Project

The applications of infinite length earth return transmission line models during this project were many and varied. They included

1. numerical and theoretical investigations of the factors affecting the steady state inductive influence of high voltage transmission lines,
2. calculation of transmission line parameters,
3. prediction of the shielding effectiveness of continuously grounded earth wires,
4. determination of harmonic current profiles along transmission lines from terminal busbar conditions,
5. estimation of transmission line currents from magnetic field measurements,
6. comparisons between measured and predicted inductive interference levels from transmission lines.

Furthermore the models were required to give accurate results with a minimum of computational effort, and yet have a simple mathematical form and physical interpretation. Clearly no single model can meet all of these requirements, therefore a number of models were used during this project.

Particular care was taken to ensure that appropriate models were chosen for each application. When selecting an infinite length transmission line model consideration must be given to the model representation accuracy, the form of the mathematical equations and the computational efficiency and accuracy of the model implementation.

Model representation accuracy is the accuracy with which a model can approximate a given physical environment. It is necessary for all models to make some simplifications regarding the structure of the earth (homogeneous or stratified with unity or arbitrary permeability and permittivity Section 3.2) and the mode of propagation along the line (Quasi-TEM or Exact). Accurate model representations are necessary for all applications, however detailed representations of the earth are essential for models which are to be matched with measured data.

The mathematical form of a model is important as it influences the computational efficiency, implementation accuracy, and suitability of a model for theoretical investigations. Existing models may be classified into one of three mathematical forms: integral equations over infinite intervals; infinite series summations, or explicit equation forms. Numerical methods are used to approximate infinite integral and infinite series forms, while explicit forms may be evaluated directly. Automatic adaptive algorithms were used to implement integral equation and infinite series model forms during this project, to maximise accuracy while minimising computational effort. Theoretical studies are greatly simplified if models with simple mathematical forms are used, as symbolic studies of the inductive influence of multiconductor transmission lines can then be undertaken.

Computational efficiency must also be considered when selecting models for repetitive or real-time studies.

Table 3.1 summarises the properties of the infinite length transmission line models used during this project. Qualitative comparisons are given rather then quantitative

measures as the model properties vary greatly with input parameters. Comparisons of model accuracy are not given in this table. An accuracy comparison is presented in Chapter 4 between infinite models when they are applied to the particular case of predicting the harmonic coupling between a single conductor earth return transmission line and a buried telecommunications cable. Physical interpretations of the models are not presented either, as they generally share the interpretation that the field can be decomposed into direct, image and correction components.

Model	Model representation	Mathematical form	Implementation
Exact	Exact propagation Homogeneous earth Arbitrary μ_e, ϵ_e High accuracy	E_z, Z_m: integral equations [a] γ: eigenvalue equation [c] Very high complexity	E_z, Z_m: numerical integration [b] γ: iterative algorithm [d] Very low efficiency
Carson Integral	Quasi-TEM propagation Homogeneous earth Free space μ_e, ϵ_e Medium accuracy	E_z, Z_m: integral equations [e] γ: eigenvalue equation Medium complexity	E_z, Z_m: numerical integration [2] γ: linear algebra [f] Low efficiency
Carson Series	Quasi-TEM propagation Homogeneous earth Free space μ_e, ϵ_e Medium accuracy	E_z, Z_m: infinite series [g] γ: eigenvalue equation Medium complexity	E_z, Z_m: series summation [h] γ: linear algebra [6] Medium efficiency
Nakagawa Integral	Quasi-TEM propagation Stratified earth Arbitrary μ_e, ϵ_e High accuracy	E_z, Z_m: integral equations [i] γ: eigenvalue equation High complexity	E_z, Z_m: numerical integration [2] γ: linear algebra [6] Low efficiency
Acha Curve Fitting	Quasi-TEM propagation Homogeneous earth Free space μ_e, ϵ_e Medium accuracy	E_z, Z_m: explicit equations [j] γ: eigenvalue equation Very low complexity	E_z, Z_m: direct evaluation [k] γ: linear algebra [6] Very high efficiency
Complex Penetration	Quasi-TEM propagation Homogeneous earth Free space μ_e, ϵ_e Low accuracy	E_z, Z_m: explicit equations [l] γ: eigenvalue equation Low complexity	E_z, Z_m: direct evaluation γ: linear algebra [6] High efficiency
Corrected Complex Penetration	Quasi-TEM propagation Homogeneous earth Arbitrary μ_e, ϵ_e Medium accuracy	E_z, Z_m: explicit equation [m] γ: eigenvalue equation Medium complexity	E_z, Z_m: direct evaluation γ: linear algebra [6] Medium efficiency

[a] Equations (3.15), (3.16), (3.22), (3.23) and (3.18)

[b] Automatic integration algorithms were used to evaluate the integral equations (de Boor, 1971; Piessens *et al.*, 1983)

[c] Equation (3.20) is a "general" eigenvalue equation as the elements of the equation are integral functions of the unknown eigenvalue.

[d] Müller's method with deflation was used to calculate the eignvalues by forcing the determinant of the eigenvalue equation to zero.

[e] Equations (3.27), (3.28), (3.29) and (3.31)

[f] EISPACK routines were used to calculate the eignvalues (Garbow *et al.*, 1977; Smith *et al.*, 1974).

[g] Equations (3.32), (3.33), (3.34), (3.35), (3.36) and (3.38)

[h] An adaptive algorithm was used to ensure that sufficient terms were summed to satisfy the requested accuracy requirement.

[i] Equation (3.37)

[j] Equations (3.39) and (3.40)

[k] The appropriate coefficients are selected from the look up table.

[l] Equation (3.41)

[m] Equation (3.42)

Table 3.1. Comparison of infinite transmission line models.

The majority of the results presented in this thesis were generated using Quasi-TEM models. The Exact model was implemented during this project to establish the accuracy of Quasi-TEM models at high frequencies. Of the Quasi-TEM models, Carson's series was the most frequently used model as it yielded accurate results with a minimum of computational effort. Carson's integral form was used to establish the accuracy of the series formulation and to generate reference data during the development of Acha's

curve fitting model (Section 3.5.2). Nakagawa's integral form was used during comparisons between measured and predicted interference voltages where the parameters of the earth were known. Acha's curve fitting model was used for the real-time and repetitive calculation of transmission line parameters, while the Complex Penetration model (with and without correction) was used as a rapid check on the validity of results from other models and for theoretical investigations of the factors effecting the inductive influence of high voltage transmission lines. The mathematical artifice of a complex image depth in the complex penetration model limited its usefulness as an educational aid for studying inductive influence phenomena, leading to the development of the filamentary models presented in Chapter 4.

3.6 Finite Length Transmission Line Models

The difference between finite and infinite length transmission line models is that the End Effect is represented in finite models but is ignored in infinite models. Finite models are therefore more complicated than comparable infinite length models.

In the following subsections finite length transmission line models are reviewed.

3.6.1 Sommerfeld's model

An "exact" solution for the fields about a transmission line can be calculated by integrating the contributions from infinitesimal current elements along the length of the line. To achieve this knowledge of the fields generated by current elements in the presence of the earth and the current distribution along the line are required. The only assumption in this analysis is that conductor diameter is small in relation to its height so that the thin wire approximation can be applied.

The fields generated by infinitesimal horizontal and vertical sources located above a dissipative region have been derived by Sommerfeld (1909). Unfortunately the resultant integral expressions can not be solved analytically and have a slow rate of convergence.

By combining the Sommerfeld integrals for horizontal and vertical sources it is theoretically possible to calculate the fields about any line. The resultant expression for the field at a given point is the integral along the length of the inducing line of the current element fields given by Sommerfeld integrals. To calculate mutual impedances between finite conductors it is necessary to integrate the field over the length of the induced conductor, resulting in a triple integration.

The current distribution along a finite length line can be calculated by requiring that the axial electric field along the surface of the conductor equal the internal field. This is the same condition that was used to determine propagation constant of the infinite Exact model. In this case however the condition is more difficult to satisfy as neither the field nor the current have a simple exponential variation and therefore the condition must be evaluated along the entire length of the conductor.

It is apparent from the above discussion that the "exact" finite transmission line model is both difficult and computationally expensive to evaluate. Considerable effort has been devoted to the development of approximate and efficient methods for evaluating Sommerfeld integrals (Miller *et al.*, 1972a; Miller *et al.*, 1972b; Faure *et al.*, 1979; Lindell and Alanen, 1984a)). Of particular note is the exact complex image interpretation of the Sommerfeld integrals (Lindell and Alanen, 1984a; Lindell and Alanen, 1984b; Lindell and Alanen, 1984c; Lindell *et al.*, 1986). This model yields accurate results from integrals which are easier to evaluate than Sommerfeld integrals.

Neither the Sommerfeld nor exact complex image models of finite length transmission lines were implemented during this project.

3.6.2 Foster's Model

One of the most difficult aspects of applying the "exact" Sommerfeld model to the calculation of fields around finite structures is the determination of the current flow along the conductor. At power system frequencies on short transmission lines it is reasonable to assume that the current along the line is uniform. This is the fundamental assumption upon which Foster's model is based.

3.6.2.1 Derivation and Evolution

In 1931 Foster derived a formula for the mutual impedance of two infinitely thin insulated wires lying on the surface of a homogeneous earth and grounded at their ends (Foster, 1931). The model was derived from Sommerfeld's result by assuming that the permeabilities of the air and earth equalled those of free space and that displacement currents were negligible. This amounts to an assumption of uniform current flow along the transmission line which is the Quasi-Static field approximation. As propagation effects are ignored the model is only valid for lines which are short in relation to a wavelength and are terminated by admittances which are high in relation to the shunt admittance of the line. The resultant formula for the mutual impedance was expressed as a double integral over the inducing and induced conductors of an integral function, and a low frequency infinite series based upon the Neumann integral over the two conductors. Foster's formula reduces to Campbell's direct current mutual impedance equation (Campbell, 1923) as the frequency tends to zero, and Carson's formula (Carson, 1926) as the length of the inducing conductor tends to infinity.

Riordan and Sunde (1933) derived an expression for the mutual impedance of finite conductors either lying on the surface or buried at the lower interface of a two layer earth. Simplified formulas were also derived for a number of limiting cases. Riordan and Sunde (1933) formula reduces to Foster's result for homogeneous earth.

Foster's model has also been extended to include finite length wires lying in horizontal planes above the surface of the earth and grounded by vertical wires at the ends (3.44) (Foster, 1933). This model is based upon the same assumptions as Foster's original model (Foster, 1931).

$$Z_{\text{mutual}} = \int\int \left[\frac{d^2 P_{\text{foster}}(r_{\text{foster}}, y_i, y_j)}{ds_j\, ds_i} + \cos(\phi) M_{\text{foster}}(r_{\text{foster}}, y_i, y_j) \right] ds_j\, ds_i \quad (3.44)$$

Where

$$\begin{aligned}
P_{\text{foster}}(r_{\text{foster}}, y_i, y_j) = & \\
& \frac{\rho_e}{2\pi r_{\text{foster}}} \\
+ & \frac{\jmath\omega\mu_a}{4\pi} \int_0^\infty \frac{y_i + y_j}{\alpha} \mathrm{J}_0(r_{\text{foster}}\alpha)\, d\alpha \\
- & \frac{\jmath\omega\mu_a}{4\pi} \int_0^\infty \frac{1 - \exp(-\alpha(y_i + y_j))}{\alpha^2} \left(\frac{\sqrt{\alpha^2 + \Gamma_e{}^2} - \alpha}{\sqrt{\alpha^2 + \Gamma_e{}^2} + \alpha} \right) \mathrm{J}_0(r_{\text{foster}}\alpha)\, d\alpha \\
- & \frac{\jmath\omega\mu_a}{4\pi} |y_i - y_j| \ln \frac{\sqrt{r_{\text{foster}}{}^2 + (y_i - y_j)^2} + |y_i - y_j|}{r_{\text{foster}}} \\
+ & \frac{\jmath\omega\mu_a}{4\pi} \left(\sqrt{r_{\text{foster}}{}^2 + (y_i - y_j)^2} - r_{\text{foster}} \right) \\
M_{\text{foster}}(r_{\text{foster}}, y_i, y_j) = &
\end{aligned}$$

$$\frac{\rho_e}{2\pi {r_{foster}}^3}\left(1-(1+\Gamma_e\, r_{foster})\exp(-\Gamma_e\, r_{foster})\right)$$

$$+\ \frac{j\omega\mu_a}{4\pi}\int_0^\infty (1-exp(-\alpha(y_i+y_j)))\frac{\sqrt{\alpha^2+{\Gamma_e}^2}-\alpha}{\sqrt{\alpha^2+{\Gamma_e}^2}+\alpha}\mathrm{J}_0(r_{foster}\alpha)\,d\alpha$$

$$-\ \frac{j\omega\mu_a}{4\pi}\left(\frac{1}{r_{foster}}-\frac{1}{\sqrt{{r_{foster}}^2+(y_i-y_j)^2}}\right)$$

$P_{foster}(r_{foster}, y_i, y_j)$ = sub-function of Fosters model
$M_{foster}(r_{foster}, y_i, y_j)$= sub-function of Fosters model
$\mathrm{J}_0(u)$ = Bessel function of the first kind of order 0
ds_i = incremental unit of length along the horizontal part of conductor i
ds_j = incremental unit of length along the horizontal part of conductor j
r_{foster} = horizontal distance between the elements ds_i and ds_j
ϕ = angular difference between the directions of the conductor elements ds_i and ds_j
Γ_e = propagation constant of a plane wave in the earth (ignoring displacement currents)
$= \sqrt{j\omega\mu_a/\rho_e}$

To evaluate this model it is necessary to perform the integrations over the horizontal parts of the inducing and induced conductors. It is not necessary to integrate over the vertical segments of the conductors as the effect of the vertical wires at the ends is included in the integrand function.

This model can also be expressed in the form of an infinite series involving the Neumann integral between the two lines at low frequencies, which can be reduced to Campbell's direct current formula (Campbell, 1923) and Carson's equation. Care must be exercised when using the truncated series forms as they diverge as the line length is increased (Rodgers and White, 1989).

The main disadvantage of Foster's model is that the formula is complicated and difficult to evaluate. It is not surprising therefore to learn that the main area of research on this model has been on the development of simplified or approximate formulas. Carter (1947) derived approximate formulas for the mutual impedance of finite parallel wires on the surface of the earth separated by large distances. These equations were later extended by Lacey (1952) to the case of angled wires at any separation, however the solution was expressed in terms of an integral function. Closed form formulas for parallel and angled wires starting at the same point based upon the truncated low frequency series were derived by Velazquez *et al.* (1983). These formulas were later extended to the case when one of the wires is above the earth (Sarmiento *et al.*, 1988).

3.6.2.2 Implementation

The method chosen to evaluate Foster's equation during this project was direct numerical integration of an algebraically simplified version of (3.44). This approach was used as it is valid and stable for a wider range of parameters than the truncated series formulas. Series approximations were used to calculate the Bessel integrand function to improve computational efficiency. An automatic integration algorithm employing cautious Romberg extrapolation (de Boor, 1971) was used to evaluate the integrals.

3.6.2.3 Physical Interpretation

The physical interpretation of Foster's model is similar to that of Carson's Equation. Foster's equation for the mutual impedance of finite wires above the earth can be decomposed into an ideal term which is the mutual impedance for wires above a lossless earth and a correction term to account for the finite resistivity of the earth (Foster, 1933). The correction term can be further subdivided into components representing the direct current mutual resistance of the grounding points and an additional correction component. Unfortunately little insight can be gained into the physical phenomena which give rise to the additional correction component due to the mathematical complexity of the model.

3.6.3 Complex Penetration Model

The finite complex penetration model (Rodgers and White, 1989) is an extension of the complex penetration concept for infinite length transmission lines (Section 3.5.3). In this model the earth is replaced by a perfectly conducting plane at a complex depth. As the plane is perfectly conducting it can it turn be replaced by an image of the finite inducing conductor. By evaluating the Neumann integral of the inducing conductor and its image an estimate of the mutual impedance between the finite inducing and induced conductors in the presence of the earth is obtained (Rodgers and White, 1989). The Neumann integral can be evaluated analytically for simple parallel conductor geometries, producing an explicit equation containing logarithmic terms of complex arguments (Rodgers and White, 1989, equations (7) and (11)).

There are a number of assumptions inherent in the derivation of this model. Firstly it is assumed that the return current flow is confined to the perfectly conducting plane at the complex depth. This is clearly not the case for finite length transmission lines as the current must enter the earth through point contacts on the surface at the ends of the lines. Furthermore the fields generated by the vertical connections to ground are ignored. As a consequence this model should only be applied when the height of the conductor is small in relation to it's length (Rodgers and White, 1989). Propagation effects are also ignored (Quasi-static approximation), therefore this model should only be applied to lines which are short in relation to the wavelength.

A comparison of this method and Foster's equation has shown that this model is valid, provided that the end effects due to the ground connection and vertical conductors can be ignored (Rodgers and White, 1989).

More recently an exact image solution has been derived for the case of finite dipole sources above homogeneous earth with complex permeability and permittivity values different from those of air (Lindell and Alanen, 1984a; Lindell and Alanen, 1984b; Lindell and Alanen, 1984c). It has been found that the image of a vertical magnetic dipole is a line source in complex space. This theory differs from the other image theories in that it is an exact theory (the Quasi-TEM propagation assumption is not employed during the derivation from Maxwell's equations) and it yields integral equations for the fields, unlike the other image theories which produce closed form equations. It should therefore be viewed as an alternative mathematical form of the exact model for the homogeneous earth case rather than a refinement of the complex penetration model.

The finite complex penetration model was not implemented during this project.

3.6.4 Applications of Finite Line Models during this Project

A finite length transmission line model was required during this project for determining the electrical characteristics of a cable used to measure the field induced by a

neighbouring transmission line.

However the application of the complete Sommerfeld model in this thesis was not warranted in the author's opinion as the dimensions of the system studied were extremely small (100m) in relation to the wavelength at harmonic interference frequencies. The Sommerfeld model is however ideally suited to the study of the unsolved problems of the effect of conductor sag and pylons on the fields around transmission lines, however such a study would be extremely expensive, if not impractical to perform at present, and was not considered during this project.

Direct numerical integration of Foster's equation was used to determine the characteristics of finite length cable transducer during this project.

3.7 Summary

Steady state harmonic interference studies of high voltage transmission lines require accurate models to determine the electromagnetic fields about the line, and hence current propagation along the line and coupling to neighbouring systems. Unfortunately it is impractical to model all aspects of a transmission line above the earth due to the complicated structure of the line and earth, and the non-linear nature of the media. It is therefore necessary to make simplifying approximations which may compromise the validity of the results.

A summary of the fundamental assumptions upon which the models presented in this chapter are based, is presented below.

- The media are linear, and therefore the properties of a multiconductor line can be determined from single conductor line models using superposition.

- Transmission lines are assumed to be perfectly straight and parallel to the earth. They may be either infinitely long or of a finite length. The effect of supporting structures is ignored, and all dimensions are small relative to the wavelength.

- Conductors are electrically linear and the proximity effect of earth current flows on the conductor current distribution is negligible, so that it may be replaced by a filamentary current. This allows the fields internal to the conductor to be calculated independently of the external fields. Furthermore those fields external to the conductor can be calculated independently of the internal fields if Quasi-TEM propagation is assumed.

- The earth can be represented by a semi-infinite body bounded by a plane surface. Furthermore the earth is either homogeneous, isotropic and linear; or it can be represented by stratified structure of homogeneous layers with these properties. The resistivity of the earth is explicitly modelled in all cases, however the permeability and permittivity may or may not be modelled.

- Wave propagation along the line may be considered to be lossless (True TEM), lossy (Exact) or Quasi-TEM (constant current). As significant losses occur within the earth, only Exact and Quasi-TEM models are appropriate for steady state harmonic interference studies. It is sufficient to consider only the transmission line mode of propagation at voice interference frequencies on aerial power system transmission lines.

- Quasi-TEM models are valid if:

    1. proximity effect can be ignored;

2. dimensions of the system (including the transmission line – telecommunication cable separation) are small in relation to the wavelength;
3. wave number of the earth is much greater than that of the air (conduction currents are larger than the displacement currents within the earth);
4. propagation constant of the wave must be much smaller than the wave number of the earth.

A summary of the models used during this project has also been presented. Emphasis has been placed on the derivation, implementation and physical interpretation of these models. The question of the suitability of these models for inductive coupling calculations is addressed in Chapter 4.

The majority of the results presented in this thesis were generated using Quasi-TEM infinite length transmission line models, as they are more efficient than the Exact model and they meet the requirements of this project. A consequence of this decision however is that the conclusions presented in this thesis are only valid for lines which meet the Quasi-TEM requirements listed above. The author considers that these requirements will be satisfied in the majority of situations that steady state inductive interference problems arise.

CHAPTER 4

SINGLE CONDUCTOR EARTH RETURN TRANSMISSION LINE EFFECTS

4.1 Introduction

An understanding of the physical phenomena which effect the steady state inductive influence of high voltage transmission lines is required to coordinate power and telecommunication systems. Unfortunately it is difficult to gain such an understanding from existing single conductor transmission line models due to the complexity of the mathematics and the lack of simple physical interpretations of these models (Chapter 3). The problem is compounded in the case of balanced sequence current flow in multiconductor lines as the fields interfere destructively. This results in rapid field variations with distance from the line which are difficult to predict without recourse to numerical evaluation.

The objective of this chapter is to develop an understanding of the factors affecting the steady state inductive influence of single conductor earth return transmission lines, from which the inductive influence phenomena of multiconductor high voltage transmission lines may be determined. This is achieved through observation of numerical experiments, discussion of the physical phenomena that give rise to these effects, and the development of a family of simple Quasi-TEM models based upon physical approximations of the current distribution in the earth. These new models have a simple mathematical form and physical interpretation that enables accurate predictions of the inductive influence to be made without resorting to numerical calculations.

Three issues must be addressed before the development of new models can commence. Firstly, a measure of the ability of a high voltage transmission line to cause interference to telecommunication services is required, to enable quantitative studies of the accuracy of mutual coupling models to be performed, and sensitivity studies of the factors affecting the inductive influence. This issue is addressed in Section 4.2. Secondly the domain of parameter values must be defined as model accuracy and sensitivity to environmental variables are functions of the range of input parameters. The parameter domains are defined in Section 4.3. Finally it is necessary to calculate the accuracy of existing models to determine their suitability for interference calculations. The results of this study are presented in Section 4.4.

Section 4.5 reports on the results of numerical studies to determine the factors effecting the inductive influence of single conductor earth return transmission lines.

A review of the physical interpretations of existing models is presented in Section 4.6.

By approximating the ground current distribution, a new family of single conductor earth return models is derived in Section 4.7. The simplest member of this family, the *Vertical Inducing Loop Model* is discussed in Section 4.8. This model provides insight into the effect of frequency, earth resistivity, and line geometry variations on the inductive influence. It is used in Chapters 5, 6 and 7 to assess the inductive influence

of high voltage transmission lines.

4.2 Quantifying the Inductive Influence of Transmission Lines

The best way to quantify the interfering ability of a transmission line is to determine the resultant disruption to neighbouring telecommunication services. Unfortunately the resultant interference is dependent not only on the interfering ability of the line, but also on the parameters of the earth, the location and susceptibility of the communications plant, the type of service, and user expectations with respect to grade of service (as discussed in Section 2.5.2). While measures based upon disruption to telecommunication services are the only true indicator as to whether a problem exists from the telecommunication users perspective, they do not indicate what the cause of the problem is and therefore who should be held responsible for rectifying it.

In the author's opinion measures for quantifying the interfering ability of high voltage transmission lines should be based upon the intensity of the electromagnetic field generated by the line. Such an approach would be consistent with the philosophy of shared responsibility upon which other electromagnetic compatibility regulations are based (Whitehouse, 1988). In this scenario electricity transmission and distribution companies would have a responsibility to ensure that their transmission lines did not generate excessive fields. Telecommunication companies would be responsible for ensuring that their systems were immune from interference when subjected to electromagnetic fields which are within the limits.

The advantages of limits based upon electromagnetic field intensity include:

- Higher degree of protection for telecommunications users. By limiting the intensity of the electromagnetic field, a ceiling is placed upon the maximum interference to telecommunication services. Existing limits are based upon containment of harmonic voltages at all power system voltage levels and harmonic currents in systems operating at 66 kV and above (NZECP 36, 1993). A consequence of the lack of current limits at lower system voltages is that there is effectively no limit on the magnitude of noise that these systems may induce in neighbouring telecommunication cables.

- Lower compliance costs. Transmission line geometry, earth wires, parameters of the earth and the presence of other structures can reduce the interference from transmission lines. The existing measures, by ignoring these effects, may be unnecessarily increasing the cost of compliance. It is difficult to accurately predict what influence these parameters will have on the inductive influence of a line due to the lack of accurate data on particular environments and suitable models. To fully exploit the advantages of field intensity based limits it would be necessary to measure the field to verify compliance.

- Compliance can be easily checked by any party as access to neither the power nor telecommunication systems is required. This is a significant advantage in the case of high voltage transmission lines as existing limits are based upon voltages and currents within the power system (NZECP 36, 1993) which are difficult to measure (Section 2.3.1).

- Limits for the protection of human beings from the potentially harmful effects of the electromagnetic fields generated by transmission lines, should they be introduced, are also likely to based upon the limitation of the field intensities rather

than voltages or currents within the power system. Cost savings may be made if electromagnetic compatibility limits for telecommunications systems and biological material are based on the same quantity.

The principal disadvantage of field intensity measures for the inductive influence of high voltage transmission lines arise from the fact that the electromagnetic field, and in particular the magnetic component of this field, is highly sensitive to the parameters of the environment. Balanced sequence current flow in a transmission line generates a destructive interference pattern. A consequence of this near complete field cancellation is that small parameter variations can produce significant changes in the resultant field (Olsen and Jaffa, 1984). Therefore detailed knowledge of the environment is required to accurately predict the field. This problem is compounded by the fact that the environmental parameters are often space and time dependent.

Typical parameter variations that might be encountered along a given transmission line include:

- Transmission line geometry and conductor type. These may vary along the line to accommodate local environmental conditions. For example longer insulator strings and greater conductor spacings on towers subject to salt spray or heavy pollution, and greater conductor height over cultivated and inhabited regions than in uncultivated or uninhabited regions (Dickens, 1965).

- Magnitude, frequency and sequence of transmission line currents. These vary with time according to the nature of the harmonic sources, power system loading and distance along the line due to propagation effects and changes in the structure of the line and earth.

- Structure and parameters of the earth. The parameters of the earth vary with position due to the non-homogeneous structure of the earth, and with time due to moisture content and temperature changes.

- Location and orientation of the telecommunications cables. In reality there will be numerous cable locations in both the air and/or earth at various separations and orientations which will be subjected to electromagnetic fields from a given transmission line.

The great dependency of the electromagnetic field on parameters which are variable and seldom accurately known is a considerable barrier to the application of field intensity measures to actual transmission lines. As the calculated field is only valid for the particular set of parameters for which it was evaluated, the field should be evaluated for all possible parameter combinations and then be combined into a single "equivalent" figure for the line. Such an approach is computationally very expensive and impractical, therefore alternative if less accurate ways must be found to assess the interfering ability of actual transmission lines. This issue is discussed further in Chapter 7.

Electromagnetic field measures are however, well suited to the requirements of this chapter. In this chapter the factors effecting the inductive influence of single conductor transmission lines are discussed. This is achieved through numerical experimentation on mathematical models. To study the sensitivity of the inductive influence to each parameter, perturbations were made about a base operating point. With careful planning, the number of required field evaluations was kept to a minimum, whilst benefiting from the full accuracy obtained from the use of the electromagnetic field intensity as a measure of the inductive influence. To do this however it was necessary to make some further simplifications regarding the mechanism of interference.

The longitudinal voltage induced in a telecommunications cable may be calculated by integrating the axial electric field around the loop formed by the cable and its associated earth return path. Unfortunately the presence of the cable perturbs the electromagnetic field. The severity of the perturbation is a function of conductor location, type and the impedance of any connections to earth. This dependency compounds the problem of assessing the inductive influence of a transmission line. A field measure is required which is independent of the cable parameters yet accurately quantifies the interfering ability of the line. It is not strictly valid to use fields calculated in the absence of the cable to assess the interfering ability, however under certain circumstances these fields yield results which are good approximations to the coupling due to the perturbed fields.

Consider the case of a cable located at (x_t, y_t) from $z = 0$ to $z = \ell$ above a lossless earth, grounded by vertical conductors at each end, lying parallel to a single conductor transmission line as shown in Figure 4.1. The transmission line supports a TEM mode of propagation (Section 3.3.3). Coupling to the cable may be considered to be a combination of electric and magnetic field coupling phenomena, which are proportional to transmission line voltage and current respectively (Section 2.4).

The open circuit induced voltage V_{induced} is the sum of the electric and magnetic field contributions around the loop formed by the induced conductor and the earth return path. Olsen and Jaffa (1984) employed circuit theory concepts and Faraday's Law to derive the following expression for V_{induced}.

$$V_{\text{induced}} = \frac{\jmath\omega\ell \mathrm{C}_{\text{mutual}} \mathrm{Z}_{\text{terminate}} V_{\text{inducing}}}{\jmath\omega\ell \mathrm{C}_{\text{mutual}} \mathrm{Z}_{\text{terminate}} + \jmath\omega\ell \mathrm{C}_{\text{self}} \mathrm{Z}_{\text{terminate}} + 1} - \jmath\omega\mu_{\text{a}} \int_s \vec{H}_{\text{p}} \cdot \vec{ds} \qquad (4.1)$$

Where

$\vec{H}_{\text{p}}$ = perturbed magnetic field (A.m^{-1})
s = surface of the loop formed by the cable and its earth return path

If it is assumed that little current flows in the induced conductor when it is open circuited, then as a first approximation it may be assumed that the magnetic field in the presence of the cable is equal to that when it was absent.

$$\vec{H}_{\text{p}} = \vec{H} \qquad (4.2)$$

Where

$\vec{H}$ = magnetic field in the absence of the cable (A.m^{-1})

Then from Faraday's Law the integral of the electric field around the loop must be the same both before and after the cable is installed, even though the electric field may be perturbed by the presence of the cable such that $\vec{E} \neq \vec{E}_{\text{p}}$ (Olsen and Jaffa, 1984).

$$\oint_c \vec{E}_{\text{p}} \cdot \vec{dc} = -\jmath\omega\mu_{\text{a}} \int_s \vec{H}_{\text{p}} \cdot \vec{ds} \approx -\jmath\omega\mu_{\text{a}} \int_s \vec{H} \cdot \vec{ds} = \oint_c \vec{E} \cdot \vec{dc} \qquad (4.3)$$

Where

$\vec{E}$ = electric field in the absence of the cable (V.m^{-1})
$\vec{E}_{\text{p}}$ = perturbed electric field (V.m^{-1})
c = contour of the loop formed by the cable and it's earth return path

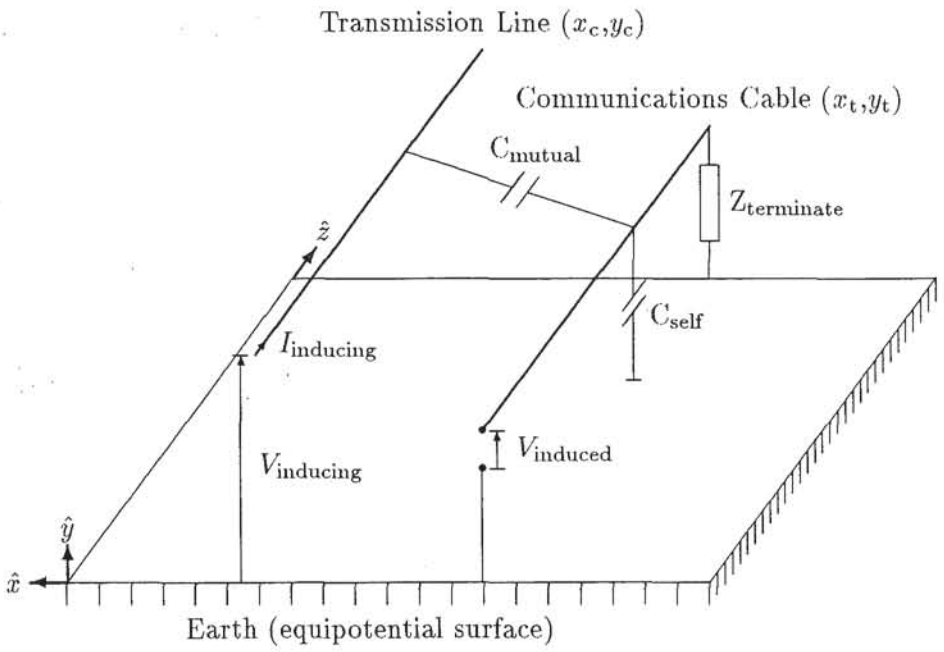

Where

$I_{inducing}$	=	current flowing along the transmission line (A)
$V_{inducing}$	=	voltage of the transmission line (V)
$V_{induced}$	=	induced voltage in the cable (V)
$Z_{terminate}$	=	cable terminating impedance (Ω)
C_{mutual}	=	mutual capacitance per unit length ($F.m^{-1}$)
Z_m	=	mutual impedance per unit length ($\Omega.m^{-1}$)
C_{self}	=	self capacitance per unit length ($F.m^{-1}$)
ℓ	=	length of the cable (m)
x_c, y_c	=	ordinates of the transmission line conductor (m)
x_t, y_t	=	ordinates of the telecommunications cable (m)

Figure 4.1. Electric and Magnetic Coupling Mechanisms

As a consequence the magnetic coupling to the cable can be calculated from the electromagnetic field in the absence of the cable.

The inductive coupling to the cable of Figure 4.1 will now be determined by integrating the unperturbed axial electric field around the loop formed by the cable and earth return path.

$$\begin{aligned}
&\oint_c \vec{E}_\mathrm{p} \cdot \vec{dc} \\
&\approx \oint_c \vec{E} \cdot \vec{dc} \\
&\approx \int_0^{y_\mathrm{t}} E_y|_{x=x_\mathrm{t},z=0}\, dy + \int_0^{\ell} E_z|_{x=x_\mathrm{t},y=y_\mathrm{t}}\, dz + \int_y^0 E_y|_{x=x_\mathrm{t},z=\ell}\, dy
\end{aligned} \tag{4.4}$$

The electric field through the mass of the earth being neglected as it is assumed to be lossless.

The transverse electric field may be described in terms of a scalar potential function $V(x, y, z, t)$, where the surface of the earth is the zero potential plane. The contributions from the first and third integrals are therefore $-V(x_\mathrm{t}, y_\mathrm{t}, 0, t)$ and $V(x_\mathrm{t}, y_\mathrm{t}, \ell, t)$ respectively.

The axial electric field is given by Equation (3.30), repeated below.

$$E_z(x, y, z, t) = -Z_\mathrm{m}(x, y) I_\mathrm{c}(z, t) - \frac{\partial}{\partial z} V(x, y, z, t) \tag{4.5}$$

Where

Z_m = mutual impedance per unit length ($\Omega.\mathrm{m}^{-1}$)

If the length of the cable ℓ, is small with respect to the wavelength, then

$$\begin{aligned}
\frac{\partial}{\partial z} V(x, y, z, t) &\approx \frac{V(x_\mathrm{t}, y_\mathrm{t}, \ell, t) - V(x_\mathrm{t}, y_\mathrm{t}, 0, t)}{\ell} \\
\int_0^{\ell} E_z\, dz &= -\ell Z_\mathrm{m}(x, y) I_\mathrm{c}(z, t) - (V(x_\mathrm{t}, y_\mathrm{t}, \ell, t) - V(x_\mathrm{t}, y_\mathrm{t}, 0, t))
\end{aligned}$$

Substituting these equalities into (4.4) yields

$$\begin{aligned}
&\oint_c \vec{E}_\mathrm{p} \cdot \vec{dc} \\
&= -V(x_\mathrm{t}, y_\mathrm{t}, 0, t) + V(x_\mathrm{t}, y_\mathrm{t}, \ell, t) \\
&\quad -\ell Z_\mathrm{m}(x_\mathrm{t}, y_\mathrm{t}) I_\mathrm{c}(z, t) - (V(x_\mathrm{t}, y_\mathrm{t}, \ell, t) - V(x_\mathrm{t}, y_\mathrm{t}, 0, t)) \\
&= -\ell Z_\mathrm{m}(x_\mathrm{t}, y_\mathrm{t}) I_\mathrm{c}(z, t)
\end{aligned} \tag{4.6}$$

The total induced voltage due to both electric and magnetic coupling mechanisms is then given by

$$V_\mathrm{induced} = \frac{\jmath\omega\ell \mathrm{C}_\mathrm{mutual} \mathrm{Z}_\mathrm{terminate} V_\mathrm{inducing}}{\jmath\omega\ell \mathrm{C}_\mathrm{mutual} \mathrm{Z}_\mathrm{terminate} + \jmath\omega\ell \mathrm{C}_\mathrm{self} \mathrm{Z}_\mathrm{terminate} + 1} - \ell Z_\mathrm{m}(x_\mathrm{t}, y_\mathrm{t}) I_\mathrm{c}(z, t) \tag{4.7}$$

Although this has been derived for the case of a highly conductive earth, it is also valid for a lossy earth if Z_m is calculated using one of the models presented in Chapter 3, the Quasi-TEM propagation assumption is valid and the cable length is small with respect to the wavelength (Olsen and Jaffa, 1984).

Electric field coupling, represented by the first term of equation (4.7) is only significant for cables which are above ground and are not earthed via a low impedance at one or more points, at power system harmonic frequencies. As the dominant form

of reticulation used in telecommunication systems within New Zealand is buried cable, the cable is effectively shielded from the electric field by the earth and therefore the first term of (4.7) may be neglected.

The severity of inductive interference may therefore be quantified using the product of the mutual impedance between a power line and the telecommunications cable, Z_m, and the power line current I_c. It must be emphasised that this product is the voltage magnetically induced in the loop formed by the cable, vertical connections to earth at each end and the earth return path. It includes the effect of the lossy earth. To evaluate this product it is only necessary to integrate $-Z_m I_c$ along the cable itself, it is **not** evaluated along the vertical connections to earth, or through the earth. Furthermore it is independent of the type and presence of the cable, yet accurately quantifies the inductive influence to cables that may be installed at that location.

The product $-Z_m I_c$ is known as the *Longitudinal Electric Field* (LEF) (Olsen and Jaffa, 1984).

Longitudinal Electric Field (LEF): The component of the time variant electric field induced by a transmission line, at the site of the telecommunications cable but in the absence of the cable, acting along the axis of the cable, that is explicitly related to the magnetic flux linking the circuit formed by the cable, vertical connections to earth and the earth return path.

During this project the magnitude of the LEF has been used to quantify the interfering ability of high voltage transmission lines.

The common mode and hence the transverse voltage within a cable may be estimated from this quantity by integrating the LEF along the length of the cable.

Note that the LEF is not the axial component of the electric field at the site of the cable, in the absence of the cable. The LEF is but one component of the unperturbed electric field, as can be seen from equation (4.5). The second component of the axial electric field, $-\frac{\partial}{\partial z}V(x,y,z,t)$, is significant in the immediate vicinity of the transmission line despite the very low rate of change in the axial direction, due to the high potentials that exist on transmission lines (Olsen and Pankaskie, 1983).

Ideally the measure used to assess the interfering ability of transmission lines should be independent of telecommunication cable location and orientation. To achieve this it would be necessary to combine the individual LEF values for all cable locations and orientations into a single figure by integrating over all space the product of the LEF and a probability density function for telecommunication cables. Such an approach, assuming a valid probability density function could be derived, would be computationally expensive.

In practice it is not necessary to consider all possible locations and orientations. The majority of the copper telecommunication circuits in New Zealand are provided on underground cables that are either directly buried or installed in duct lines. Therefore as a first approximation it may be assumed that LEF need only be calculated in the horizontal planes below ground in which the cables may lie.

To determine if it is necessary to calculate the LEF in all horizontal planes and for all possible cable orientations in these planes, and to support the statements made earlier regarding the dominant field components, consider the fields induced in the ground by the single conductor transmission line depicted in Figure 4.2. The resultant fields below ground are presented in Figure 4.3.

This example is representative of a case where a rural telecommunications cable lies very close to one pole of the Benmore Haywards High Voltage Direct Current transmission link between the North and South Islands of New Zealand (excluding the effect of the second pole and the earth wire, therefore it is a poor approximation of

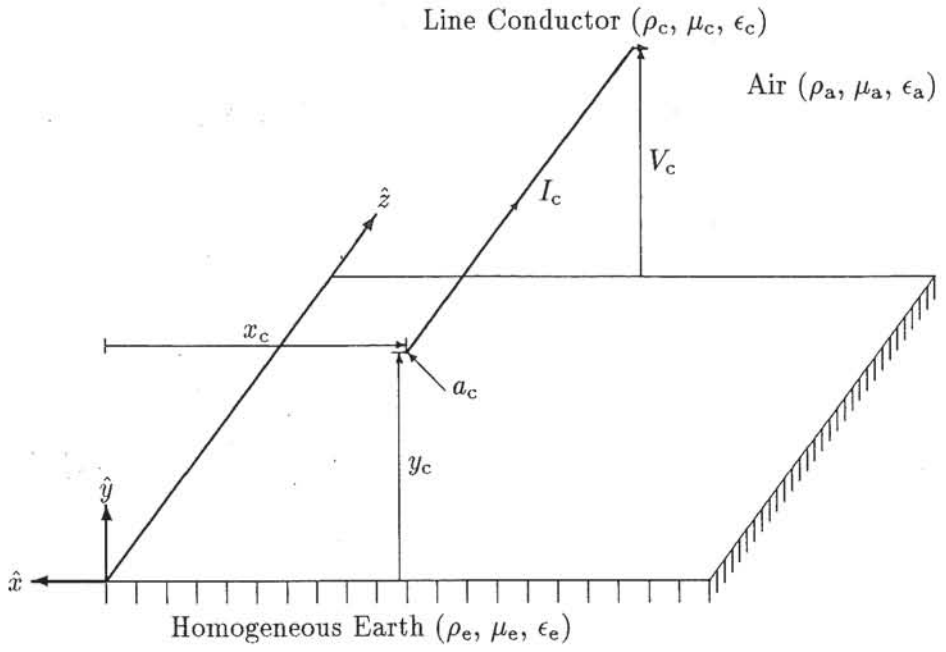

Where

I_c = transmission line conductor current = 9 A at 600 H_z
V_c = transmission line conductor voltage (V)
y_c = height of the conductor = 10 m
x_c = x ordinate of the conductor = 0 m
a_c = radius of the conductor = 0.0192 m
ρ_c = resistivity of the conductor material = $2.69e-8$ Ω.m
μ_c = permeability of the conductor material = $4\pi \times 10^{-7}$ H.m^{-1}
ϵ_c = permittivity of the conductor material = 8.854×10^{-12} F.m^{-1}
ρ_a = resistivity of the air = $1.0e+30$ Ω.m
μ_a = permeability of the air = $4\pi \times 10^{-7}$ H.m^{-1}
ϵ_a = permittivity of the air = 8.854×10^{-12} F.m^{-1}
ρ_e = resistivity of the earth = 400 Ω.m
μ_e = permeability of the earth = $4\pi \times 10^{-7}$ H.m^{-1}
ϵ_e = permittivity of the earth = 8.854×10^{-12} F.m^{-1}

Figure 4.2. Single Conductor Transmission Line Parameters

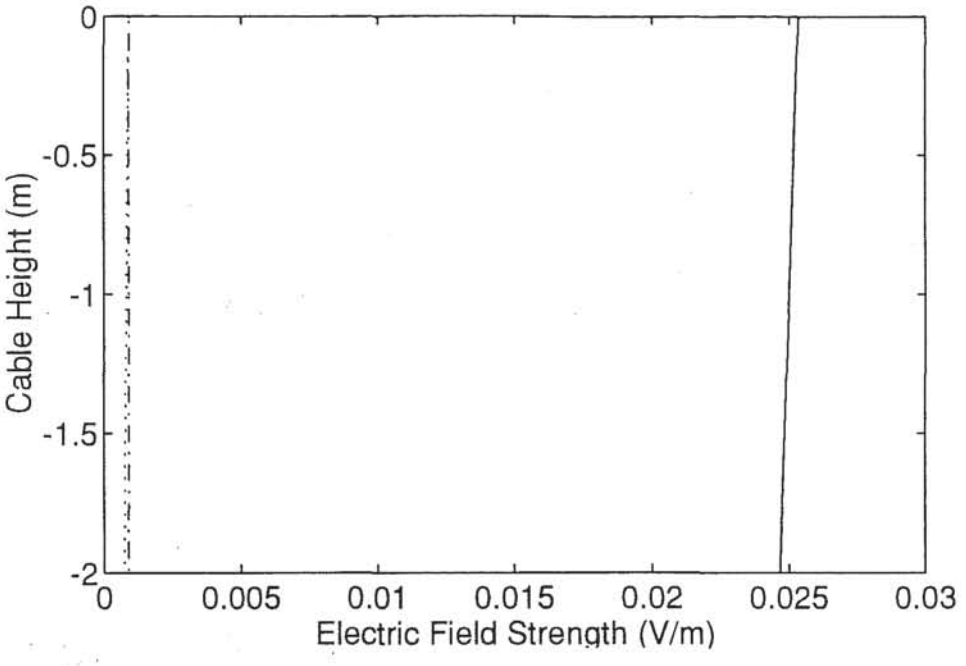

Figure 4.3. Magnitude of the Electric Field Induced in the Earth by the Single Conductor Line as a Function of Cable Height ($|E_x|$ dotted line, $|E_y|$ dot-dash line, $|E_z|$ dashed line and $|E_z^m|$ solid line obscuring $|E_z|$, negative cable heights indicate that the cable is underground.)

the actual situation, which is discussed in Chapters 8 and 9). The majority of the harmonic interference incidents investigated by the author have occured in rural areas in New Zealand, as telecommunication cables are longer than those in urban areas and hence are more susceptible to interference. Furthermore high voltage transmission lines, which are the major source of power line interference in New Zealand, rarely traverse urban areas.

Figure 4.3 is a plot of the absolute magnitude of E_x, E_y E_z and E_z^m induced within the earth by the single conductor transmission line of Figure 4.2, as a function of y for $x = 10$ m. The fields were calculated using the Exact model (Section 3.5.1) for the electromagnetic field around a conductor above the earth. The fields E_x, E_y and E_z include the contributions from both the electric and magnetic fields, and are calculated in the absence of the cable. E_z^m is the component of E_z that is explicitly related to magnetic flux linkage.

From this figure it can be seen that; E_z is the dominant component of the $\vec{E}$ field below ground; the dominant component of E_z is E_z^m which is due to magnetic flux linkages; the variation of E_z^m with cable depth is small over the range of depths at which cables are buried. The transverse components of the field (E_x and E_y) are only significant when the earth resistivity and/or frequency is very high. Under these conditions the surface of the earth can no longer be regarded as a zero potential surface for the "transverse electric" component of the electromagnetic field, and the Quasi-TEM wave propagation approximation is no longer valid (Olsen and Pankaskie, 1983). The condition that must be satisfied to guarantee that E_z is the dominant component of $\vec{E}$ below ground is that the wave number of the earth must be much greater (at least one order of magnitude) than that of the air. This is expressed mathematically in the following equation.

$$\sqrt{-j\omega\mu_e\left(\frac{1}{\rho_e}+j\omega\epsilon_e\right)} \gg \sqrt{-j\omega\mu_a\left(\frac{1}{\rho_a}+j\omega\epsilon_a\right)} \tag{4.8}$$

This condition will generally be satisfied over the range of parameters encountered during voice frequency telecommunication interference studies.

Two simplifications may be made as a consequence of this result. Firstly as E_z^m is dominant below ground, the predominant coupling mechanism is magnetic induction and therefore the worst case coupling to buried telecommunications cables will occur when they parallel the transmission line, which is the well known quasi-static result. Secondly as E_z^m is relatively insensitive to cable depth, it may be assumed that all telecommunication cables are located in the plane $y = -0.5$m with little loss of accuracy. This depth was chosen as it is the depth at which rural telecommunication cables are usually buried.

Despite these simplifications, it is still necessary to evaluate the LEF at a great many locations in the plane $y = -0.5$m to ensure that no interference phenomena are missed. The fields decay with distance from the line (Section 3.3.2), and therefore it is seldom necessary to evaluate the LEF for separations of more than a few kilometres, unless the telecommunications cable parallels the line for a long distance.

In summary, the measure used to quantify the interfering ability of single conductor transmission line models in this chapter is the Longitudinal Electric Field (LEF) in the earth at a depth of 0.5 m acting in the direction parallel to the transmission line. It is evaluated for all separations from directly underneath the line to the separation at which the field is sufficiently small that it may be neglected, on both sides of the line if it is asymmetric.

4.3 Domain of Parameter Values Considered during this Project

The accuracy with which a model predicts the LEF is a function of the values inserted into the model. It is therefore necessary to define the range of values that the parameters may take before models can be compared.

The emphasis during this project has been placed upon the modelling of systems that exist within New Zealand, with a view to gaining a better understanding of them, and the ways in which their inductive influence may be reduced. Therefore during this project care has been taken to select parameter ranges that reflect the conditions that occur within New Zealand, subject to the limitations of the models. A summary of the parameter ranges used is presented in the following subsections.

4.3.1 Transmission Line Geometry and Conductor Type Domains

A range of existing and hypothetical transmission line geometries, including single conductor lines (Section 4.5), single and double circuit three phase lines both with and without earth wires (Chapters 5 and 6) and an HVDC transmission line (Chapters 8 and 9) are considered. Details of these lines are presented as they are required. In all cases the lines are assumed to be infinitely long, perfectly straight, and the effect of supporting structures is ignored.

Transmission line conductor types have been restricted to those ACSR and steel wires that are either in use in New Zealand, or are commercially available.

4.3.2 Transmission Line Current Magnitude, Frequency and Sequence Domain

The transmission line currents have been defined to be one ampere per phase conductor of either positive, negative or zero sequence current for the purposes of comparing the interfering ability of different transmission lines (Chapters 5 and 6). Where comparisons with measurements of the inductive influence have been made, either the conductor currents from non-invasive measuring systems (Chapter 9), or calculated values from terminal busbar voltages (Chapter 8) have been used.

The range of frequencies that must be considered is determined by the sensitivity of the telecommunications plant. During this project it has been assumed that the telecommunications cable only supports the services of telephony, facsimile and modems, which represent the majority of the present applications within New Zealand. These services are based upon *Plain Old Telephone Service* (POTS) circuits which have a nominal bandwidth of 300 - 3,400 Hz, although in practice frequencies up to 4,000 Hz may be propagated. The author has experienced problems in telecommunication circuits due to high levels of power line induction from the fundamental frequency to the one hundredth harmonic. Therefore all harmonic orders from the fundamental to the hundredth inclusive (50 to 5,000 Hz), have been considered during this project.

4.3.3 Earth Structure and Parameter Domain

The limiting factor as far as the representation of the earth is concerned is that it must be a situation that can be represented in all models. Furthermore it is desirable to minimise the number of variables used in the models to represent the earth, as doing so greatly reduces the complexity of the task of understanding inductive influence phenomena. Therefore the earth has been represented as a semi-infinite homogeneous, time-invariant structure with permeability and permittivity equal to those of free space during the numerical studies of the inductive influence of transmission lines (Section 4.5 and Chapters 5 and 6).

In New Zealand, excluding seawater, the range of resistivities expected for the layer of earth from the surface to 100 m deep is 20 to 2000 Ω.m and is typically of the order of 200 Ω.m (MacDonald, 1988). The apparent resistivity at depths of the order of tens of kilometres is thought to be 1,500 - 15,000 Ω.m(Gill and MacDonald, 1967). The resistivity was therefore considered to vary over the range from 20 to 2000 Ω.m as at the high frequencies which cause the most interference to telecommunication users the skin depth of the earth and the lower resistivity of the upper layers will cause the majority of the current to flow in the upper layers. Hence the effective resistivity of the earth is that of the upper layers.

4.3.4 Telecommunications Cable Location Domain

As discussed in Section 4.2 the telecommunications cable is assumed to lie in the plane $y = -0.5$m, be parallel to the transmission line, but may be at any distance from the line.

4.4 Accuracy of Existing Inductive Coupling Models

In the following sections comparisons are made between the mutual impedances (and hence the Longitudinal Electric Field since LEF$= -I_c Z_m$), calculated using Quasi-TEM models and the Exact model to establish the suitability of Quasi-TEM models for predicting harmonic coupling from high voltage transmission lines to buried telecommu-

nications cables. Uncertainty existed regarding the accuracy of these models at high frequencies and earth resistivities due to the validity of the Quasi-TEM approximation. Furthermore the Quasi-TEM models implemented are only strictly valid for conductors above the ground, although it is reported that Carson's equation applies to:

> "two parallel, ground return conductors (usually taken as above the earth but will give good results for shallowly buried conductors also)" (Judkins and Nordell, 1974)

Finally all model implementations, apart from the Acha Series, employ adaptive algorithms which were designed to give accurate results with a minimum of computational effort. It was necessary to confirm that these model implementations did yield accurate results for coupling to buried cables over the range of parameters specified in Section 4.3.

Prior to comparing the Quasi-TEM models to the Exact model, it was necessary to verify the accuracy of the Exact model. Two independent implementations of the Exact model were developed during this project. Model accuracy was verified by comparison of the results of these implementations with one another, with equations (3.3) to (3.8) for lossless earth, with Quasi-TEM models for conditions under which the Quasi-TEM propagation assumption is valid, and with the results published by Efthymiadis and Wedepohl, 1978.

The mutual impedance between the single conductor transmission line of Figure 4.2 and a cable 0.5 m below the surface of the earth was calculated using the Exact and Quasi-TEM models. Cable separations from 0 to 10 times the skin depth δ of the earth were considered. Comparisons were made for all combinations of the frequencies of 50, 500 and 5,000 Hz, and earth resistivities of 20, 200 and 2,000 Ω.m. Percentage errors, defined below, were evaluated and plotted as a function of separation.

$$\varepsilon_r = \frac{R_{\text{Exact}} - R_{\text{Quasi-TEM}}}{|Z_{\text{Exact}}|} \times 100\%$$

$$\varepsilon_x = \frac{X_{\text{Exact}} - X_{\text{Quasi-TEM}}}{|Z_{\text{Exact}}|} \times 100\%$$

$$\varepsilon_m = \frac{|Z_{\text{Exact}}| - |Z_{\text{Quasi-TEM}}|}{|Z_{\text{Exact}}|} \times 100\%$$

Where

ε_m = percentage error of the magnitude of the mutual impedance
ε_r = percentage error of the real component of the mutual impedance
ε_x = percentage error of the imaginary component of the mutual impedance
R_{Exact} = real component of the mutual impedance calculated using the Exact model
$R_{\text{Quasi-TEM}}$ = real component of the mutual impedance calculated using the Quasi-TEM model
X_{Exact} = imaginary component of the mutual impedance calculated using the Exact model
$X_{\text{Quasi-TEM}}$ = imaginary component of the mutual impedance calculated using the Quasi-TEM model
Z_{Exact} = mutual impedance calculated using the Exact model
$Z_{\text{Quasi-TEM}}$ = mutual impedance calculated using the Quasi-TEM model

4.4.1 Carson/Nakagawa Integral

Plots of ε_r, ε_x and ε_m for the numerical integration implementation of Carson's equation ((3.31) and (3.37)), as a function of separation from the single conductor line in units of the skin depth of the earth, are presented in Figure 4.4. Peak percentage errors for each trace are tabulated in Table 4.1.

Frequency (Hz)	Earth Resistivity (Ω.m)	Extreme ε_r (%)	Extreme ε_x (%)	Extreme ε_m (%)
50	20	0.008	0.000	0.008
50	200	0.070	-0.003	0.070
50	2000	0.547	-0.013	0.547
500	20	0.059	0.002	0.059
500	200	0.501	-0.011	0.500
500	2000	3.474	-0.040	3.473
5000	20	0.363	0.023	0.358
5000	200	3.167	-0.020	3.154
5000	2000	16.849	0.142	16.847

Table 4.1. Extreme Relative Percentage Errors for the Carson Integral Model

The error of the real component ε_r, tends to increase with distance from the line, and with frequency and earth resistivity. It is under these conditions that the Quasi-TEM propagation model would be expected to become inaccurate, as displacement currents in the earth will no longer be small in relation to conduction currents, and the transverse electric field in the earth will become significant. Therefore in the author's opinion the observed increase in error is due to limitations of the Quasi-TEM propagation assumption rather than the implementation of the model.

The reactive component error ε_x, is low in relation to ε_r as at large separations where the Quasi-TEM propagation assumption error is significant, the resistive component of the mutual impedance is approximately an order of magnitude larger than the inductive component. Both components decay with increasing distance from the line. As a consequence ε_x is small and ε_m is approximately equal to ε_r.

As the peak relative error in both the real and reactive components of the mutual impedance is within 17% for the range of frequencies and earth resistivities considered during this project, the author considers that it is valid to use Carson's integral mutual impedance equation to calculate the coupling between high voltage transmission lines and buried telecommunications cables.

4.4.2 Carson Series

Comparison of the error in the mutual impedance calculated using the Carson series implementation (Figure 4.5 and Table 4.2), with the Carson integral implementation (Figure 4.4 and Table 4.1) reveals that the author's adaptive algorithm for the evaluation of the Carson series equations ((3.33) and (3.34)) yields results which are essentially identical to those of the Carson Integral implementation.

The author also implemented the asymptotic formulae, (3.35) and (3.36) with the correction series (3.38). However discontinuities resulted in the plots of mutual impedance as a function of separation at the changeover point between the standard and asymptotic series. This proved to be a significant problem when calculating the LEF from multiconductor transmission lines carrying balanced sequence currents as the changeover points for each conductor differed due to the different physical locations of each conductor. Furthermore as cancellation of the conductor fields was nearly

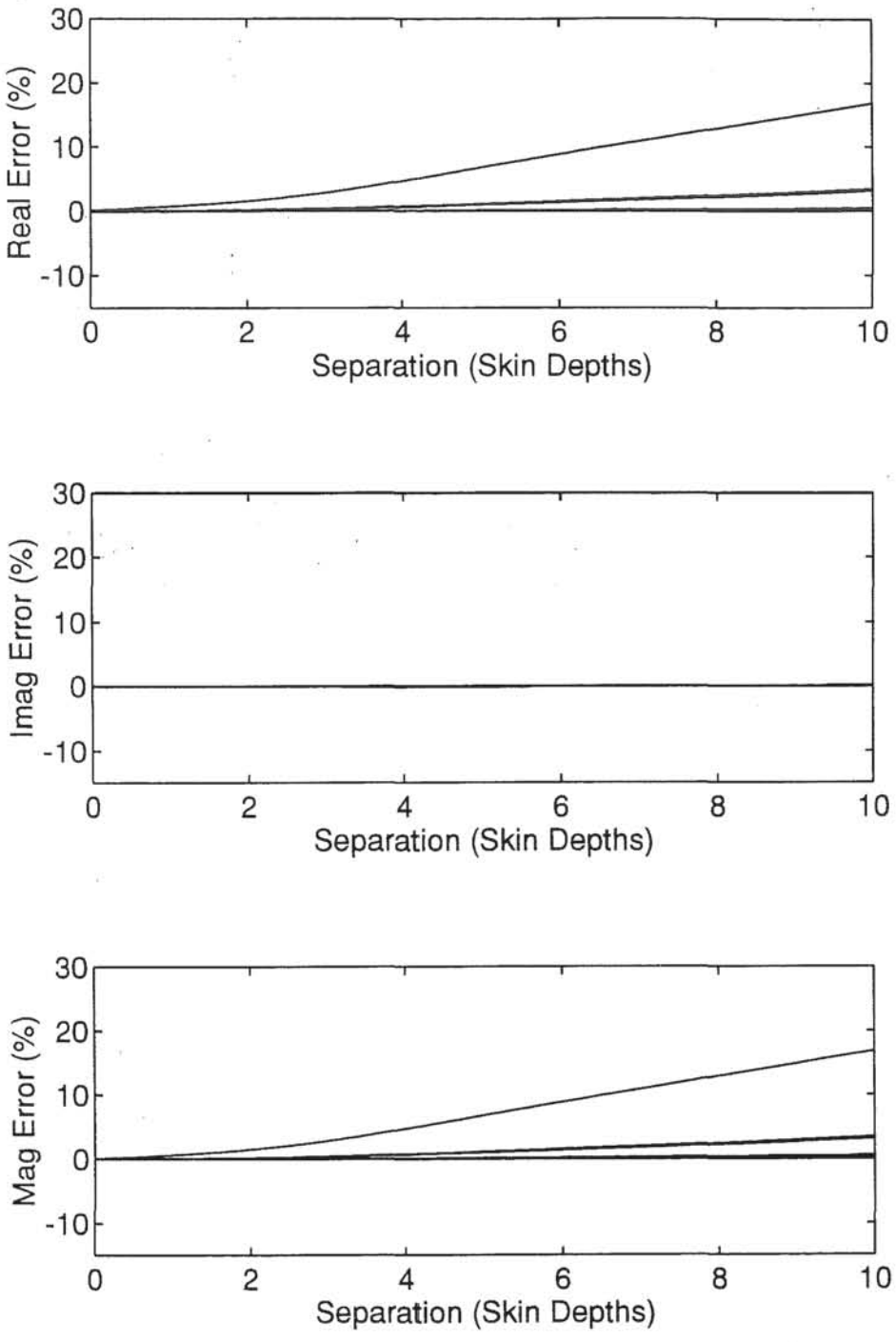

Figure 4.4. Percentage error between the Carson Integral and Exact Models for Induction from a Single Conductor Transmission Line. The upper graph is the real error ϵ_r, the middle graph the imaginary error ϵ_x, and the lower graph the magnitude error ϵ_m.

complete, small discontinuities in the mutual impedances resulted in significant discontinuities in the resultant LEF. The author minimised this effect by locking the formulas so that the same formula was used for all phase conductors, reducing the number of discontinuities to the one at which all formulas changed. Once the validity of the standard series for values of $R > 5$ had been established the author dispensed with the use of the asymptotic formula thereby avoiding this problem.

Frequency (Hz)	Earth Resistivity (Ω.m)	Extreme ε_r (%)	Extreme ε_x (%)	Extreme ε_m (%)
50	20	0.008	0.000	0.008
50	200	0.070	-0.003	0.070
50	2000	0.547	-0.013	0.547
500	20	0.059	0.002	0.059
500	200	0.501	-0.011	0.500
500	2000	3.474	-0.040	3.473
5000	20	0.363	0.023	0.358
5000	200	3.167	-0.020	3.154
5000	2000	16.849	0.142	16.847

Table 4.2. Extreme Relative Percentage Errors for the Carson Series Model

4.4.3 Acha Series

From the graphs of Figure 4.6 and the tabulated peak errors in Table 4.3, it appears that the Acha curve fitting model is a poor approximation to Z_m. On closer examination however it is apparent that the extremely high errors occur at large separations. There are two contributing factors to this phenomena: firstly the Quasi-TEM model to which the Acha curve fitting has been fitted is not accurate in this region; secondly at a separation of ten times the skin depth δ, $R = 10\sqrt{2}\,\delta$, which falls outside the defined range for this model of $0 \leq R \leq 12$. Over the range for which the Acha model is valid, $0 \leq x \leq \frac{12}{\sqrt{2}}\delta \approx 8.5\delta$, the error is comparable to that from the Carson integral and series implementations. The range of the Acha curve fitting model could be extended by the derivation of further coefficients for values of $R \geq 12$.

A high level of ripple is also apparent on the percentage error graphs in Figure 4.6. This ripple arises from poor matching of the curve fitting functions at the ends of each interval over which they are fitted. Therefore the ripple may be reduced by decreasing the size of each interval, at the expense of larger look up tables.

The presence of this ripple is a significant barrier to the application of this model to the task of predicting the inductive interference of multiconductor transmission lines carrying balanced sequence currents. The high gradient of the mutual impedance function at the ends of each subinterval may exaggerate the differences between mutual impedances that are nearly equal, resulting in invalid conclusions.

4.4.4 Complex Penetration

Of all the Quasi-TEM models considered in this section, the complex penetration model is the only one for which significant errors result at medium separations of $0.5 \leq x \leq 5\delta$. These errors result from approximations made during the derivation of this model (Section 3.5.3).

At large separations the mutual impedance and hence the error of this model tends to that of the Carson Integral and Series implementations, whilst at short separations the direct field from the conductor dominates and the error is small. The Complex

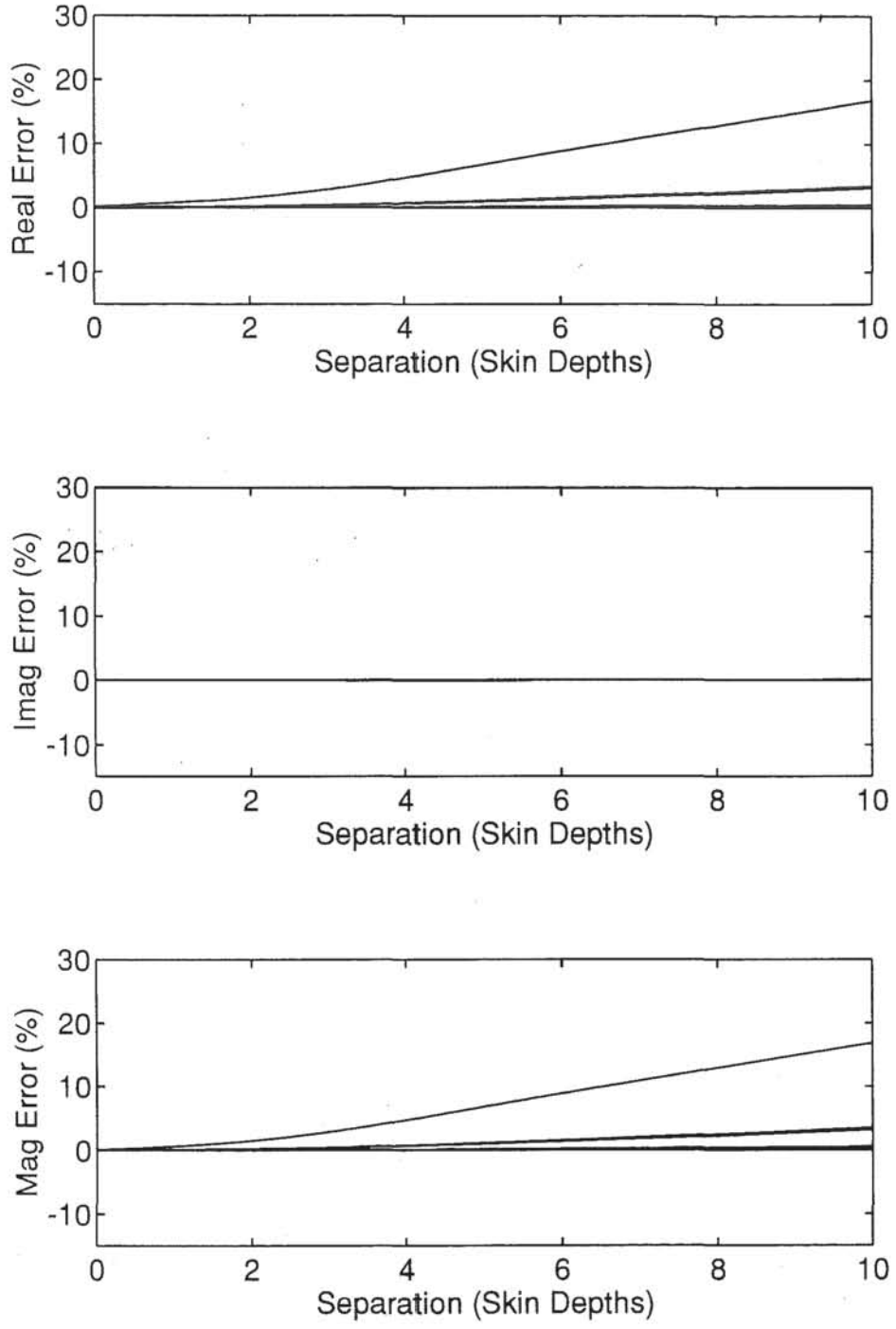

Figure 4.5. Percentage error between the Carson Infinite Series and Exact Models for Induction from a Single Conductor Transmission Line. The upper graph is the real error ε_r, the middle graph the imaginary error ε_x, and the lower graph the magnitude error ε_m.

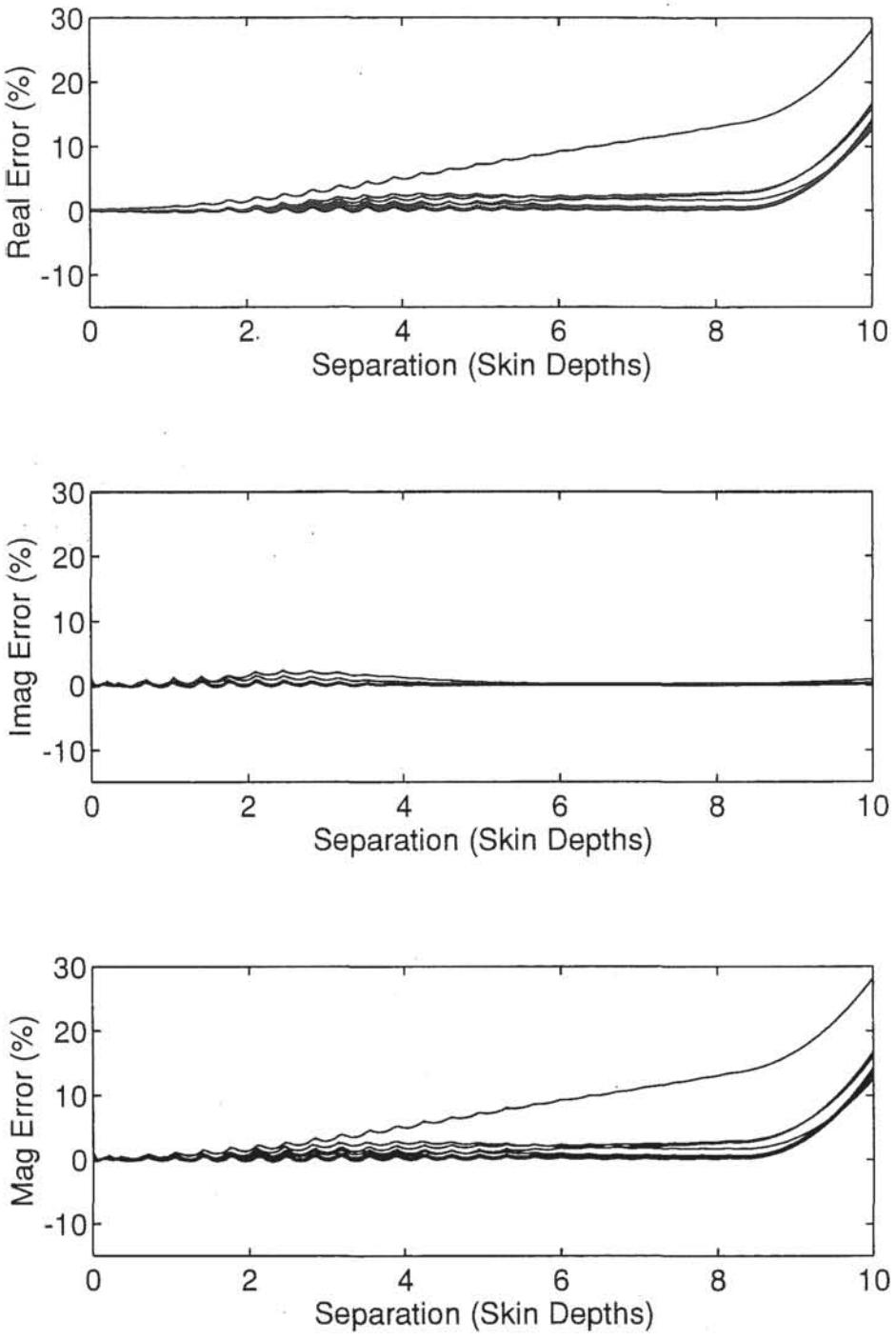

Figure 4.6. Percentage error between the Acha Curve Fitting and Exact Models for Induction from a Single Conductor Transmission Line. The upper graph is the real error ε_r, the middle graph the imaginary error ε_x, and the lower graph the magnitude error ε_m.

Frequency (Hz)	Earth Resistivity (Ω.m)	Extreme ε_r (%)	Extreme ε_x (%)	Extreme ε_m (%)
50	20	13.735	0.912	13.736
50	200	13.883	0.715	13.885
50	2000	14.324	0.978	14.324
500	20	13.467	1.533	13.451
500	200	14.160	0.912	14.160
500	2000	16.817	0.717	16.817
5000	20	12.758	2.324	12.626
5000	200	16.159	1.527	16.131
5000	2000	28.264	0.937	28.263

Table 4.3. Extreme Relative Percentage Errors for the Acha Curve Fitting Model

Penetration model may be applied to the task of predicting the LEF in the immediate vicinity of the line and at large separations. Care must be exercised at intermediate distances however as the combined effect of the magnitude error and the gradient of the mutual impedance versus separation function may lead to invalid results.

Frequency (Hz)	Earth Resistivity (Ω.m)	Extreme ε_r (%)	Extreme ε_x (%)	Extreme ε_m (%)
50	20	-11.072	-9.720	-11.124
50	200	-11.838	-10.530	-11.954
50	2000	-12.069	-10.861	-12.215
500	20	-8.974	-7.601	-8.899
500	200	-11.050	-9.719	-11.106
500	2000	-11.651	-10.515	-11.804
5000	20	-4.964	4.352	-4.688
5000	200	-8.867	-7.590	-8.773
5000	2000	16.822	-9.597	16.821

Table 4.4. Extreme Relative Percentage Errors for the Complex Penetration Model

4.4.5 Summary

The magnitude of the mutual impedance error calculated using the Quasi-TEM models discussed in this section exhibit similar error characteristics at large separations. These errors increase with frequency, earth resistivity and separation from the line. The author believes that this effect arises from the fact that the Quasi-TEM propagation assumption is not strictly valid under these conditions.

The author considers that it is valid to use either the Carson integral mutual impedance equation or infinite series equation to calculate the coupling between high voltage transmission lines and buried telecommunications cables. Over the range of parameters considered during this project the maximum error in a single mutual impedance calculation is expected to be of the order of 17%. Larger errors may result from multiconductor line calculations due to loss of significance. In cases where the Quasi-TEM propagation assumption is not strictly valid the Exact model has been used to confirm any significant phenomena.

The use of either the Carson asymptotic series, Acha curve fitting model or the complex penetration model for the task of predicting the LEF induced by multiconductor lines carrying balanced sequence currents at large separations is not recommended due to the artificial LEF variations that these models introduce.

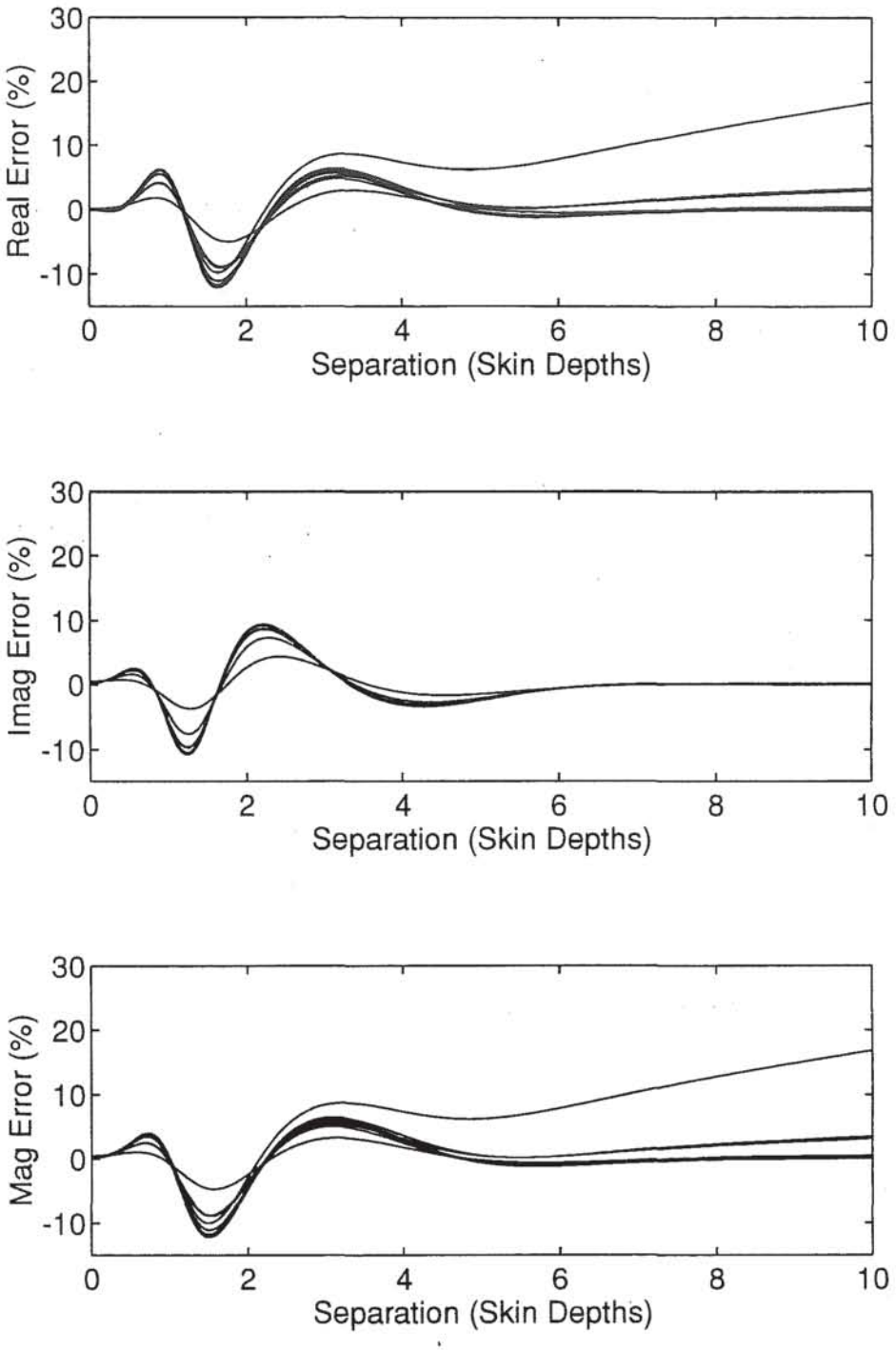

Figure 4.7. Percentage error between the Complex Penetration and Exact Models for Induction from a Single Conductor Transmission Line. The upper graph is the real error ε_r, the middle graph the imaginary error ε_x, and the lower graph the magnitude error ε_m.

As a consequence the majority of the numerical results presented in this thesis have been generated using the Carson infinite series implementation as they provide comparable accuracy to the Carson integral implementation for significantly less computational effort.

The complex penetration equation, in conjunction with the vertical inducing loop model, have been used in analytical studies of the LEF in the immediate vicinity of transmission lines and at large separations.

4.5 Inductive Influence of Single Conductor Earth Return Transmission Lines

The objective of this section is to gain an appreciation of the factors effecting the inductive influence of single conductor earth return transmission lines, and to express the gross relationships between each factor and the LEF in the form of separable functions, where possible, that are easy to understand.

Single conductor earth return transmission lines are seldom used in New Zealand, nevertheless they are a good system with which to commence the study of the inductive influence of transmission lines as they are free from the destructive interference phenomena of balanced sequence current flow in multiconductor lines, and hence are easier to understand. The results may also be applied to zero sequence current flow in multiconductor transmission lines, as at medium to large separations multiconductor lines carrying zero sequence current may be approximated by a single earth return conductor with little loss of accuracy.

In this section it is assumed that the inductive influence of a single conductor transmission line is a function of current magnitude and frequency, resistivity of the earth, conductor height and the separation between line and telecommunications cable. It is not necessary to study the dependence of the LEF on current magnitude, as the media are assumed to be linear and therefore the inductive influence is a separable, linear function of conductor current ($\mathrm{LEF} = -I_c Z_m$). The dependency of the inductive influence on the remaining variables was studied by perturbing of each of these variables from the base values defined in Figure 4.2, and evaluating the ratio of:

$$\frac{|\mathrm{PerturbedLEF}|}{|\mathrm{UnperturbedLEF}|}$$

This ratio was then plotted either as a function of separation or the perturbed variable to determine the sensitivity of the LEF to small variations about the base values, and to establish whether or not the LEF could be expressed as a separable function of the perturbed variable.

4.5.1 Frequency Dependence

Figure 4.8 is a plot of the LEF ratios for frequencies one half and twice the base frequency, as a function of separation from the line.

In the immediate vicinity of the conductor the LEF appears to be highly dependent on frequency, while at large separations it is substantially independent of frequency. Furthermore the LEF ratio tends to a constant value as the separation tends to infinity, indicating the perturbed and unperturbed fields decay at the same rate at large separations.

The frequency sensitivity is confirmed by Figure 4.9, which is a graph of the LEF ratio versus frequency at a point immediately below the line, and at a second point at a separation of 4000 m. Note that the LEF at 4000m is frequency dependent, but

notably less so than that in the immediate vicinity of the line. In both cases the LEF increases with frequency.

Given that the frequency dependence is a function of separation, it is not possible to separate these variables in general.

4.5.2 Earth Resistivity Dependence

A plot of the LEF ratios for earth resistivities of one half and twice the base resistivity is presented in Figure 4.10. In this case the LEF in the immediate vicinity of the line is only slightly dependent on earth resistivity, while in the far field the LEF is approximately directly proportional to earth resistivity, as shown in Figure 4.11. As a consequence it is not possible to separate earth resistivity dependence from separation. Once again the LEF ratios tend to a constant values as the separation tends to infinity indicating that the rate of decay of the field with separation is unaffected by earth resistivity perturbations.

4.5.3 Height Dependence

As the conductor height is increased the field intensity in the immediate vicinity of the line decreases, while that at large separations increases (Figure 4.12). The decrease near the line is a non-linear function of the perturbation, while the increase at large separations is approximately linear (Figure 4.13). In the limit as the separation tends to infinity the LEF ratio tends to a constant value. The ratio is only slightly perturbed by doubling or halving the conductor height however.

4.5.4 Separation Dependence

Figures 4.14 and 4.15 contain graphs of the real and reactive components of the mutual impedance as a function of separation. The magnitude of each component of the mutual impedance relative to the magnitude of the total impedance is displayed in Figure 4.16. It is apparent that the dominant component of the impedance in the vicinity of the line is inductive. As the separation increases the inductive component decays more rapidly than the resistive component, and crosses the axis becoming capacitive over a short interval (Figure 4.15). At large separations the resistive component of the mutual impedance dominates, although the fraction contributed by each component remains constant indicating that they are decaying at the same rate.

The effect of moving the transmission line 5 m closer and further away from the cable is depicted in Figure 4.17. Reducing the effective separation increases the mutual impedance and *vice versa* . In this case however the ratio of perturbed to unperturbed LEF tends to unity as the separation tends to infinity.

4.5.5 Summary

The LEF dependencies in the immediate vicinity of a single conductor transmission line are different from those at large separations. As a consequence it is not possible to decouple the effects of frequency, earth resistivity and conductor height from that of separation.

A partial decoupling may be achieved by considering the phenomena which occur in the immediate vicinity separately from those at large separations. The author has defined phenomena occurring near the line to be *Near Field* effects, whilst those that arise at moderate to large separations are termed *Far Field* effects. Within each region the gross field dependencies may be expressed as separable functions with the dependencies listed below.

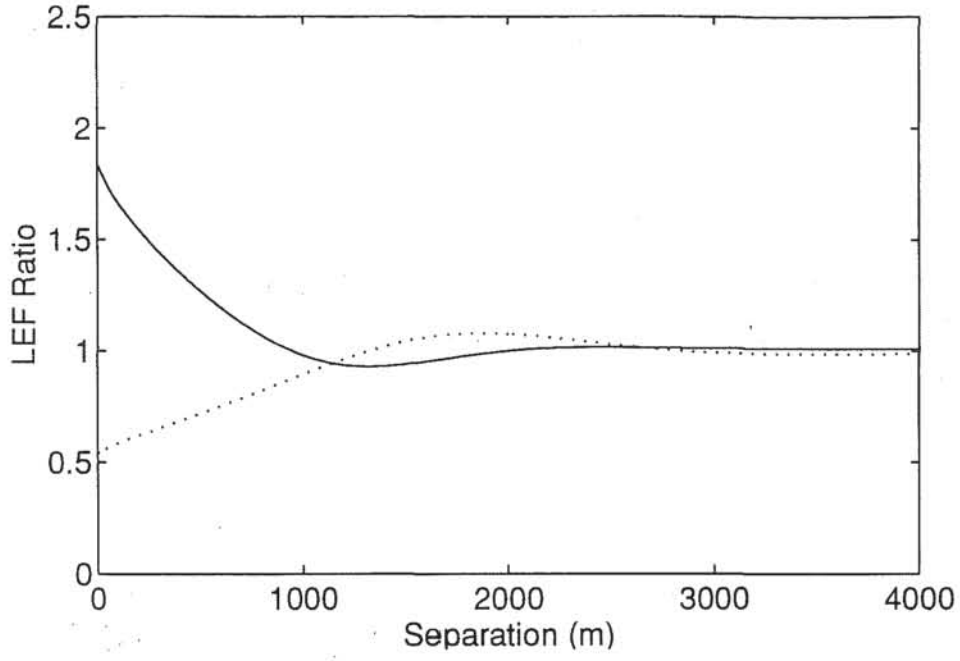

Figure 4.8. Ratio of Perturbed/Unperturbed LEF from Single Conductor Line as a function of Separation when the Frequency is Doubled (solid line) and Halved (dotted line)

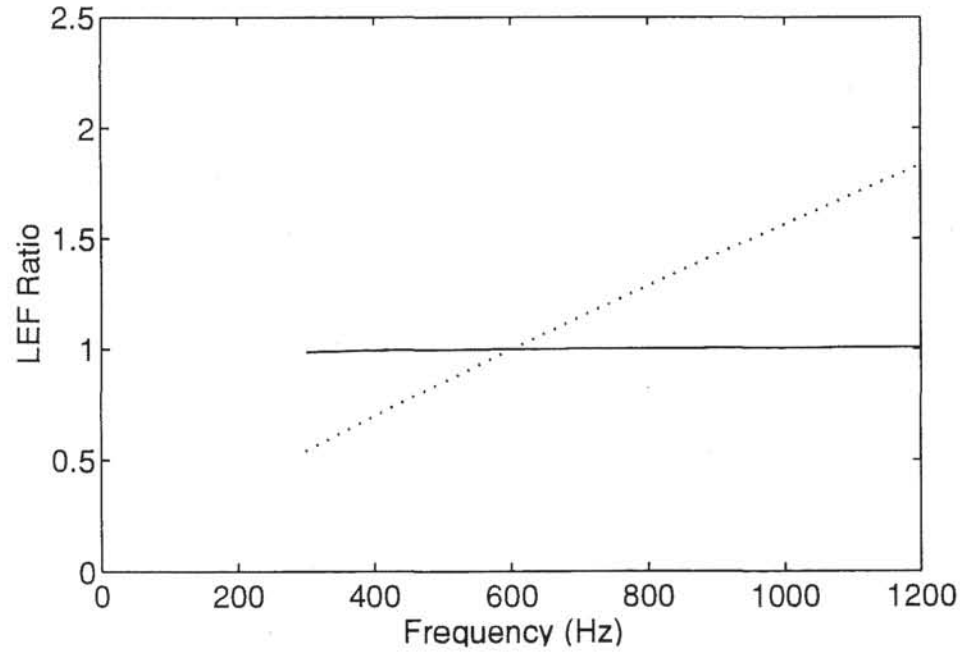

Figure 4.9. Ratio of Perturbed/Unperturbed LEF from Single Conductor Line at 0m (dotted line) and 4000m (solid line) Separations as a Function of Frequency

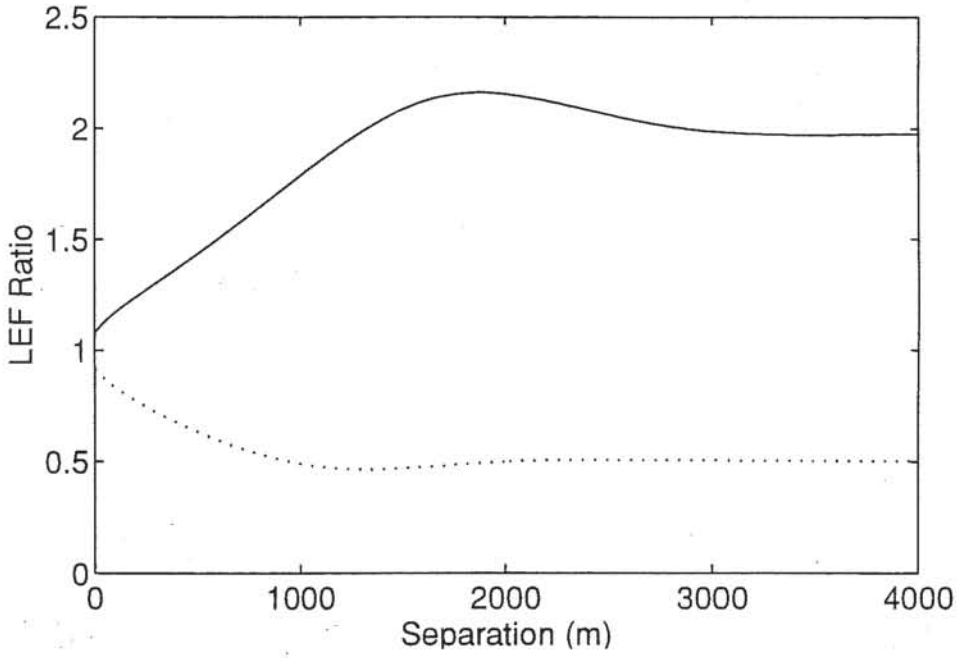

Figure 4.10. Ratio of Perturbed/Unperturbed LEF from Single Conductor Line as a function of Separation when the Resistivity of the Earth is Doubled (solid line) and Halved (dotted line)

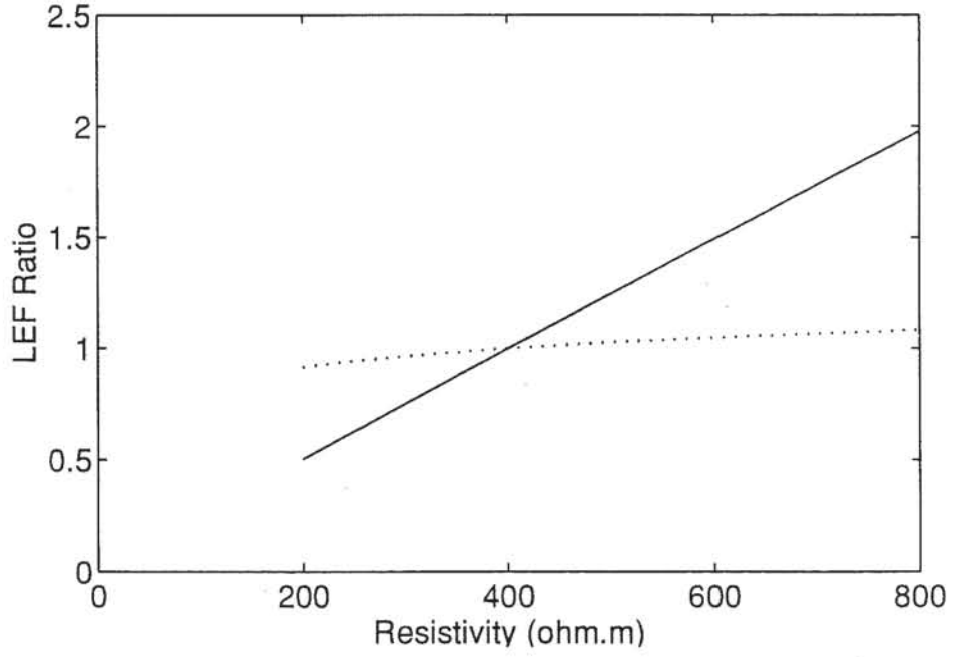

Figure 4.11. Ratio of Perturbed/Unperturbed LEF from Single Conductor Line at 0m (dotted line) and 4000m (solid line) Separations as a Function of Resistivity

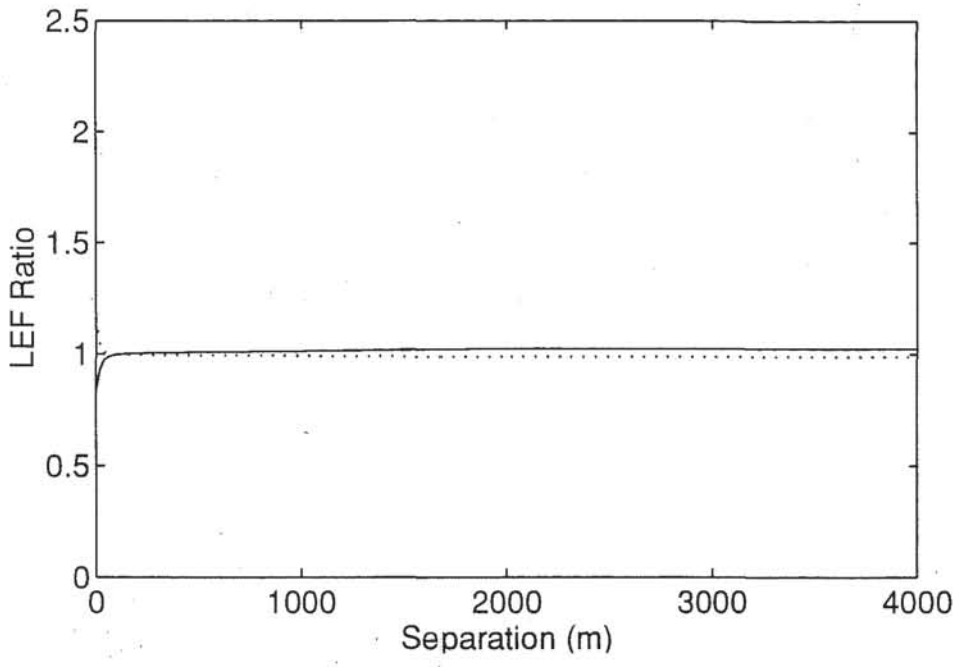

Figure 4.12. Ratio of Perturbed/Unperturbed LEF from Single Conductor Line as a function of Separation when the Height of the Conductor is Doubled (solid line) and Halved (dotted line)

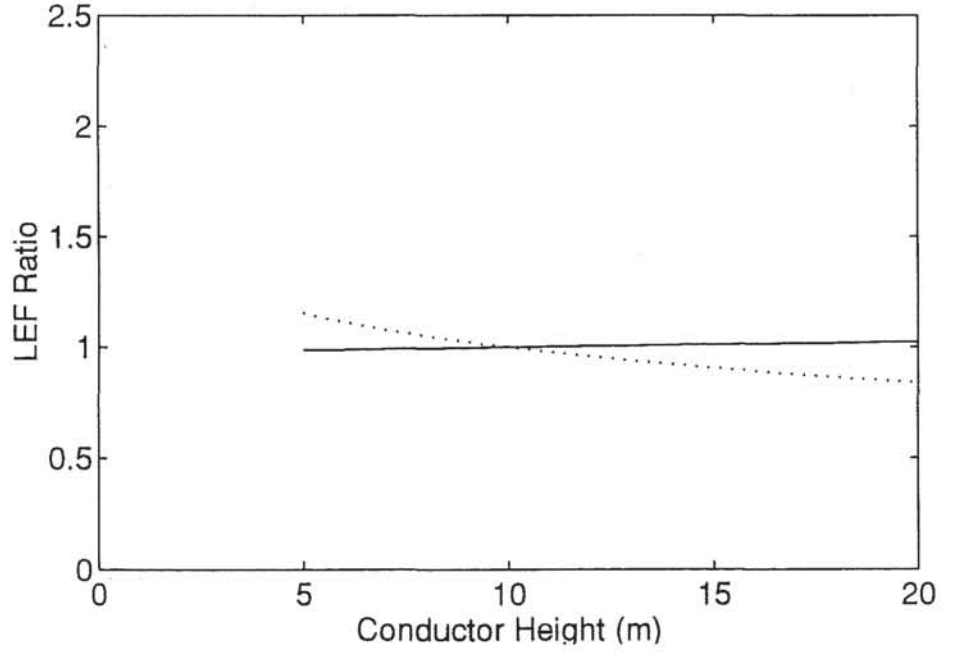

Figure 4.13. Ratio of Perturbed/Unperturbed LEF from Single Conductor Line at 0m (dotted line) and 4000m (solid line) Separations as a function of Height

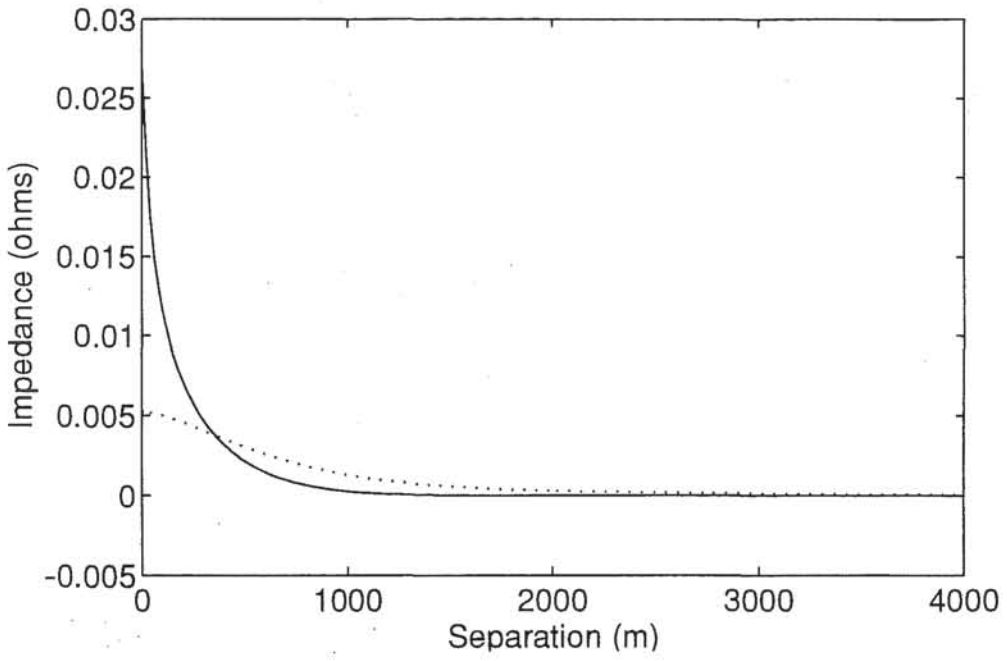

Figure 4.14. Real (dotted line) and Reactive (solid line) Components of Mutual Impedance from Single Conductor Line as a Function of Separation

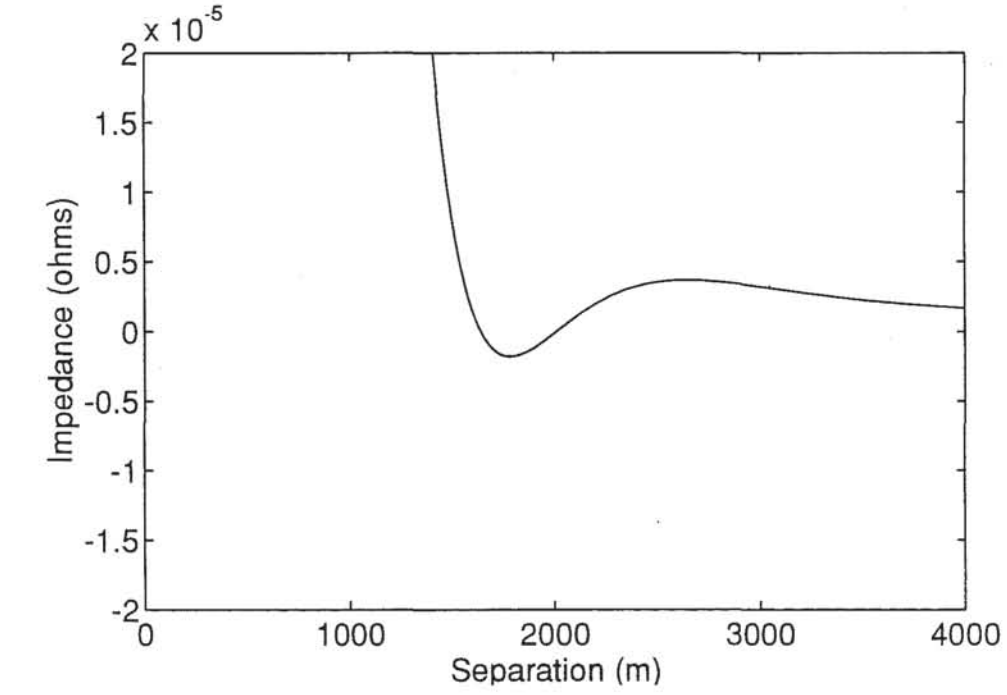

Figure 4.15. Expanded View of the Reactive Component of Mutual Impedance from Single Conductor Line as a Function of Separation

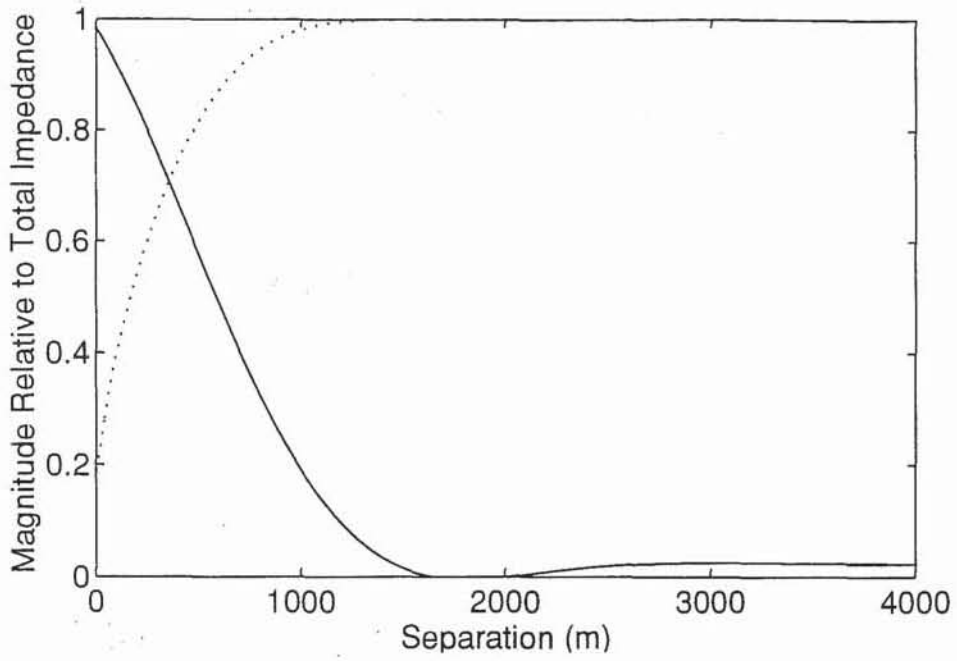

Figure 4.16. Magnitudes of the Real (dotted line) and Reactive (solid line) Components of the Mutual Impedance Relative to the Magnitude of the Mutual Impedance

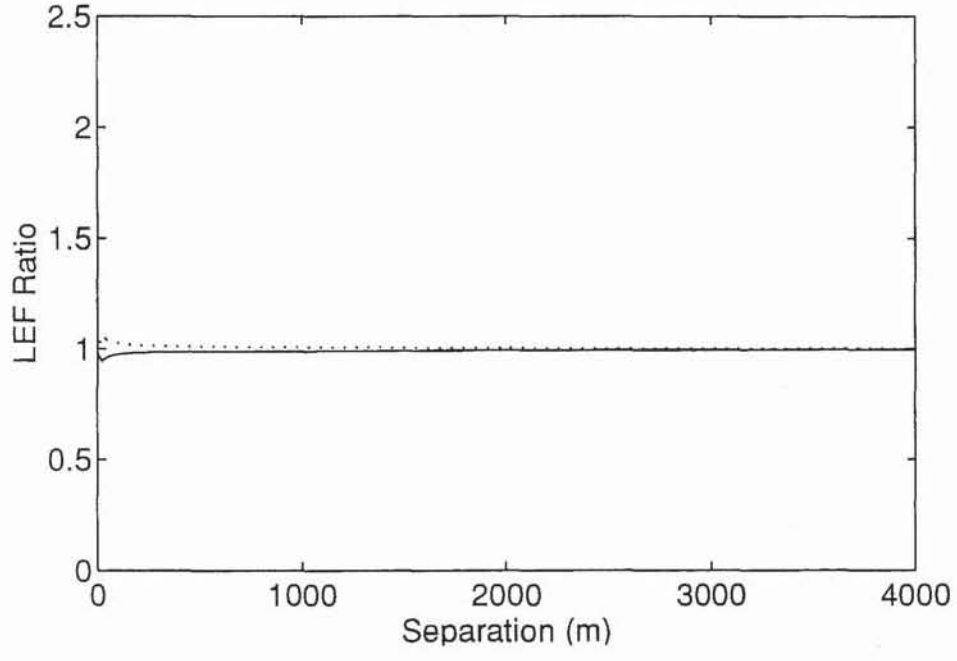

Figure 4.17. Ratio of Perturbed/Unperturbed LEF from Single Conductor Line when the Separation is Varied by Plus (solid line) or Minus (dotted line) Five Metres

Near field region : Region in the immediate vicinity of the line where the direct field from the conductor dominates. Within this region the LEF is:

- linearly proportional to conductor current,
- approximately linearly proportional to frequency,
- substantially independent of earth resistivity,
- highly sensitive to conductor geometry with respect to cable location, any perturbation which decreases the radial distance between the line and the cable will increase the LEF and *vice versa* .

Far field region In this region the direct field from the conductor and the field induced by current flow within the earth decay at the similar rates which are independent of frequency, earth resistivity and conductor geometry. Thus the ratio of perturbed to unperturbed field induced by a single conductor transmission line in the far field region tends to a constant value. The far field LEF is:

- linearly proportional to conductor current,
- substantially independent of frequency,
- approximately linearly proportional to earth resistivity,
- relatively insensitive to conductor geometry, although the LEF does increase with conductor height.

It must be noted that the *Far Field* in this context differs from that used in antenna engineering (Ramo *et al.*, 1984). In this case the dominant fields are structure attached, not radiated, and all dimensions are small in relation to the wavelength.

The transition between the Near and Far field regions is gradual, and depends upon frequency and earth resistivity. However the LEF ratios are generally within 30% of the far field values when the separation exceeds approximately twice the skin depth of the earth.

The dependencies listed above have been confirmed analytically using the Complex Penetration model, and the new Vertical Inducing Loop model (Section 4.8).

The mechanisms that give rise to these dependences are the subject of the following sections.

4.6 Physical Interpretation of Existing Earth Return Transmission Line Models

A review of the physical interpretations of existing earth return transmission line models is presented in this section. Detailed physical interpretations of these models were presented in Chapter 3.

Physical interpretations of existing mutual impedance models may be divided into three categories:

- electromagnetic wave interaction,
- skin effect,
- equivalent image.

These interpretations arise from knowledge of the physics of electromagnetic fields and from the form of the resultant mathematical models. All of these interpretations are valid ways to regard the fields around a conductor above a homogeneous earth.

In the electromagnetic wave interpretation the resultant field in the air is considered to be the sum of a direct or incident wave from the conductor and an earth wave generated by current flow within the body of the earth. The earth wave is a partial reflection of the incident wave. Energy from the incident wave is also transmitted into the earth where it dissipates in the lossy media. As the direct and earth waves waves are approximately 180 degrees out of phase with one another, they produce a destructive interference pattern in the air. This interpretation of the field in the air is shared by both the Exact and Quasi-TEM wave propagation models, and has been used to construct multi-layer versions of the Complex Penetration model (Chapter 3).

Further insight into the form of the field can be gained by dividing the earth wave into ideal and correction components. The ideal component is the reflected field that would arise if the earth were perfectly conducting, while the correction wave accounts for the distortion due to the finite conductivity of the earth. As the ideal component represents a perfect reflection, it can be represented by an image, which cancels the direct field from the conductor at the air-earth interface. The correction wave is expressed in terms of indefinite integrals for which no simple interpretations exist.

Unfortunately little physical insight can be gained into the factors effecting induction into telecommunications cables from this interpretation. At low conductor heights and at the air earth interface the correction component is dominant. Within the earth the only component of the field is the transmitted wave which has the same mathematical form as the correction term. As no simple interpretations exist for either the correction or transmitted waves, little insight can be gained.

It is possible to make a few predictions in the extreme case where the parameters of the earth approach those of an ideal conductor. In this case the correction wave and transmitted wave tend to zero, and the system can be approximated by the direct and ideal waves alone. Unfortunately this is not a reasonable assumption to make for typical earth structures at power system harmonic frequencies.

The situation of a conductor above the earth may also be regarded as a skin effect phenomena. It is more complicated than traditional skin effect problems as the earth is a semi-infinite body and is subject to extreme proximity effects. As a consequence the magnitude and phase of the current in the earth vary greatly with depth and transverse distance from the line. Furthermore circulating currents are induced to flow within the body of the earth. The current distribution is dependent on the parameters of the earth and frequency. At power system harmonic frequencies conduction currents in the earth are generally larger than displacement current, therefore traditional skin effect concepts for good conductors may be applied (Ramo *et al.*, 1984)[Chapter 3]. Unfortunately the complexity of the electromagnetic field and hence current distribution within the earth limits the insight that can be gained from this approach.

An alternative approach for solving the skin effect problem has been developed based upon approximation of the earth by a system of parallel lossy conductors (Section 3.5.4). This method trades the complexity of the detailed continuous electromagnetic field skin effect models for a quantised approximation which requires the self and mutual parameters of discrete regions of the earth. The system of equations that results may then be reduced to determine the desired parameters. Although this model reduces the complexity of the physical environment and the resultant mathematical model, it provides only limited insight into the mechanisms that give rise to these effects and introduces error into the analysis through the use of discrete approximations.

The lossy earth may also be replaced by an equivalent image conductor, as in the case of the complex penetration model. To account for both the real and reactive components of the mutual impedance, it is necessary to place this image at a complex depth. While this approach appears to offer a simple physical equivalent for the con-

ductor - earth system, it does not as complex dimensions have no physical meaning. Decomposition of the complex penetration model has demonstrated that the inductive component of the mutual impedance calculated using this model is equal to that from a three filament system in which the earth is approximated by two discrete filamentary currents (Section 3.5.3).

The author has also developed approximate models for the mutual impedance between high voltage transmission lines and telecommunications cables based upon the approximation of the continuous current distribution within the earth by a finite number of discrete filamentary currents. Details of these models are contained in the following sections.

4.7 Filamentary Current Modelling

The objective of this work was to develop efficient models for the mutual impedance between high voltage transmission lines and buried telecommunications cables which had simple physical interpretations. This work was motivated by the regular and apparently simple relationships between frequency, earth resistivity and geometry of single and multiconductor transmission lines and the resultant inductive influence (Section 4.5 and Chapter 5). Furthermore the accuracy of the complex penetration model which approximates the inductive component of the earth return current distribution by two filamentary currents suggested that such an approach may yield accurate results (Section 3.5.3).

Before deriving the models, the mechanisms which effect the current distribution within the earth are reviewed. A plausibility argument for the current distribution in the earth below a single conductor transmission line is presented (Section 4.7.1), which is confirmed using the exact model (Section 4.7.2). The theoretical basis for filamentary current modelling is discussed in Section 4.7.3 and a brief summary of the method and conclusions from this work is given in Section 4.7.5.

This section serves as background for Section 4.8 in which the Vertical Inducing Loop, the most successful filamentary current model, is discussed.

4.7.1 Plausibility Argument

Consider the case of a single conductor earth return transmission line depicted in Figure 4.2. Current flow on the line $I_c(x_c, y_c, z, t)$ induces an alternating flux which penetrates the earth. The dominant component of the electromotive force induced in the earth is $E_z^m(x_c, y_c, z, t)$ which is proportional to the rate of change of flux and lags the conductor current by ninety degrees (Figure 4.18). As the flux density induced by a cylindrical conductor decreases with radial distance (Ramo *et al.*, 1984, Chapter 2) the electromotive force is greatest in those regions of the earth closest to the conductor.

The earth is a lossy conductor and therefore its self impedance contains both resistive and reactive components. Consequently the current induced in the earth (I_e) lags the electromotive force by an angle of less than ninety degrees as shown in Figure 4.18. This current may be decomposed into *in-phase* and *quadrature* currents I_{ep} and I_{eq} defined in Figure 4.18.

Each region of the earth induces current to flow in neighbouring regions by means of the magnetic field it produces. However remote regions are screened by the intervening earth material, and as a consequence the current density in the earth decreases rapidly with increasing depth and distance from the line. The self impedance of a region of the earth and hence its screening ability and current are dependent on frequency and the electrical characteristics of the earth.

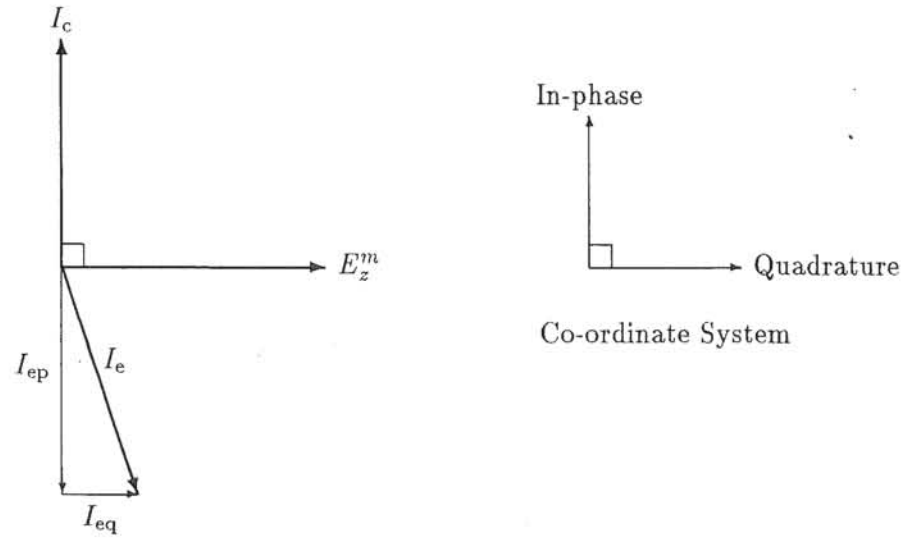

Where

I_e = longitudinal earth current (A)
I_{ep} = in-phase component of the earth current (A)
I_{eq} = quadrature component of the earth current (A)

Figure 4.18. Earth Current Phasor Diagram

The conductor current I_c, in conjunction with the in-phase earth current I_{ep}, induces flux in phase with the conductor current, resulting in a reactive mutual impedance coupling to neighbouring systems. The magnetic coupling between the quadrature current I_{eq} and other systems also results in a purely reactive mutual impedance. However from the conductor current frame of reference, this mechanism produces a purely resistive mutual impedance due to the ninety degree phase difference between the quadrature and conductor currents.

As the conductor-earth system is closed, the total current flow must be zero. The net in-phase current flow in the earth, I_{ep}, must be of equal magnitude and opposite phase to the conductor current I_c as the earth is the return path for the transmission line, while the total quadrature current I_{eq} flow within the earth must be zero. In-phase and quadrature currents will flow in both directions in different parts of the earth, as current flow in one region induces current flow in the opposite direction in neighbouring regions.

If the earth is lossless then the self impedance of the earth is purely inductive, there is no quadrature current and therefore no resistive component of the mutual impedance.

4.7.2 Ideal Distribution

The current distribution in the earth can be readily determined from the axial electric field using the relationship

$$I_e = E_z(\frac{1}{\rho_e} + j\omega\epsilon_e)$$

In practice the displacement current contribution may be ignored as it is negligible in comparison to the conduction current at power system harmonic frequencies.

Figures 4.19 and 4.20 are graphs of the real and imaginary components of the axial electric field E_z within the earth below a single conductor transmission line from which the current density may be derived. The magnitude of the resultant field is plotted in Figure 4.21. The Exact model has been used calculate the field to a depth of 800 m (five times the skin depth δ of the earth) and horizontal separation of 800 m from the line, which carries a current I_c of 1 A at 1000 Hz and is located 10 m above a homogeneous earth with a resistivity of 100 Ω.m. As the field is symmetrical about the plane $x = 0$ only that for $x \geq 0$ is shown. The imaginary component of the field gives rise to the in-phase current I_{ep}, while the real component causes the quadrature current I_{eq} to flow, as E_z lags I_c by 90 degrees.

Figures 4.22, 4.23 and 4.24 are detailed contour plots which show the fine structure of the axial electric field below ground. The greatest field intensity (and hence current magnitude) occurs at the surface of the earth immediately below the transmission line (Figure 4.21). However the peak real component of the field (and hence quadrature current I_{eq}) occurs below the surface of the earth at a depth which is frequency, earth resistivity and conductor height dependent (Figure 4.22). The imaginary component of the field and hence in-phase current I_{ep} (Figure 4.23), is generally larger than the real component of the field but has a smaller extent.

In-phase and quadrature currents are observed to flow in both directions within the earth. Integration of the current density distributions confirms that the net quadrature current flow in the earth is zero while the net in-phase current is equal to the conductor current but flows in the opposite direction.

It is also interesting to note that the contours for the magnitude of the field (Figure 4.24) are almost circular, although they are not concentric. The centres of these contours lie on the plane $x = x_c$, and increase in height with decreasing contour magnitude.

These results are in agreement with the predictions of Section 4.7.1.

4.7.3 Theoretical Basis

Filamentary current models are designed to approximate the steady state harmonic coupling between high voltage transmission lines and buried telecommunications cables. As the only coupling mechanism of consequence under normal operating conditions is that due to the alternating magnetic field, filamentary current models need only represent the magnetic component of the electromagnetic field. This is a achieved by replacing the transmission line conductor and the earth with a system of parallel filamentary currents in air. An example of one such arrangement is given in Figure 4.25.

Only axial current flow can be represented by axial filamentary currents, therefore filamentary models are only valid when the transverse currents in the earth are small, or in other words when the Quasi-TEM propagation assumption is valid.

In the limit, as the number of filaments $m_f \rightarrow \infty$, the magnetic field and hence the mutual impedance tends to Carson's result.

The mutual impedance from this system of filaments to a conductor at (x,y) may be determined using lossless propagation theory and the concept of superposition. Filamentary currents may be considered to be ideal, infinitely thin conductors. The only wave that may propagate along an electrically small, lossless system is a TEM wave (Section 3.3.1). As the media are linear, the mutual impedance may be found by superposition of Equation (3.9), giving Equation (4.9).

$$Z_m = -\frac{j\omega\mu_a}{2\pi} \sum_{n=0}^{m_f} w_f(n) \ln\left(r_f(n)\right) \tag{4.9}$$

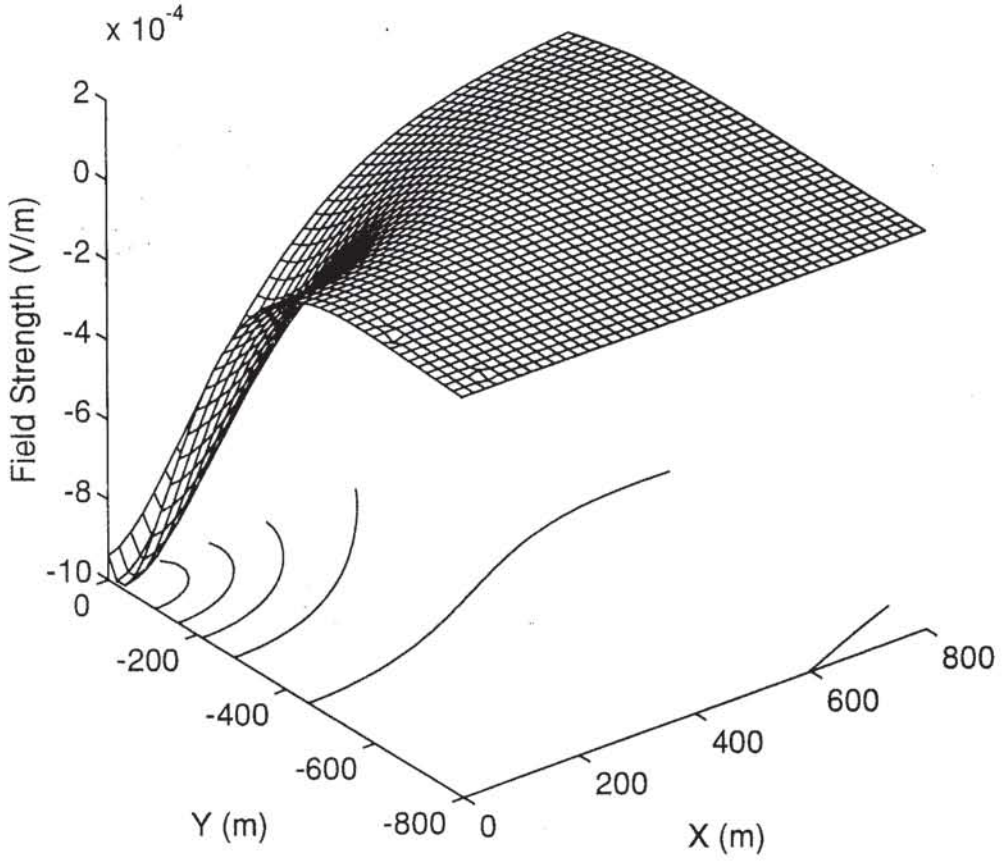

Figure 4.19. Three Dimensional Plot of the Real Component of the Axial Electric Field Below Ground

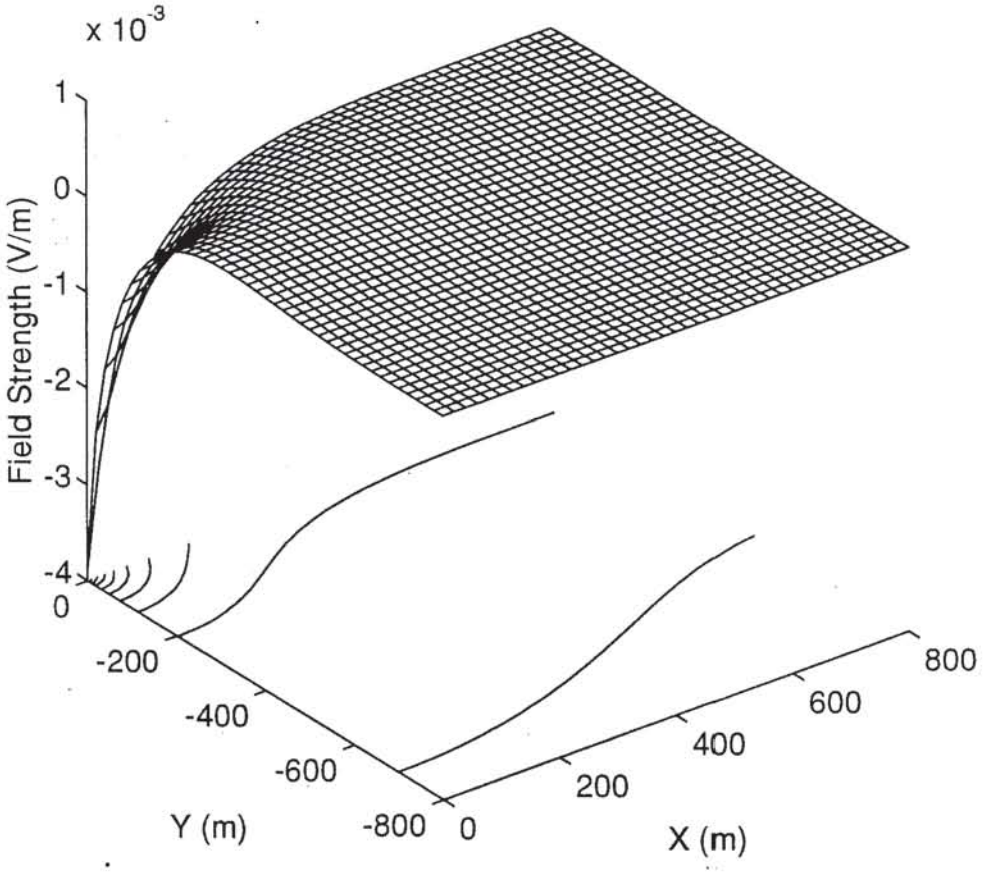

Figure 4.20. Three Dimensional Plot of the Imaginary Component of the Axial Electric Field Below Ground

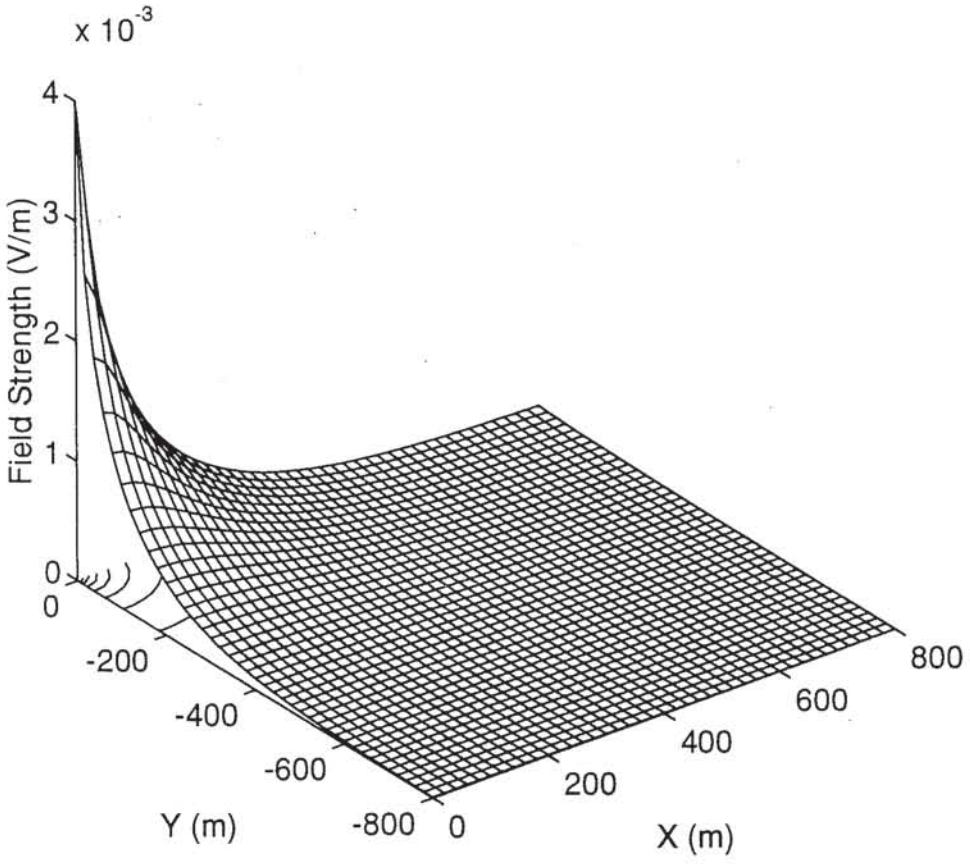

Figure 4.21. Three dimensional Plot of the Magnitude of the Axial Electric Field Below Ground

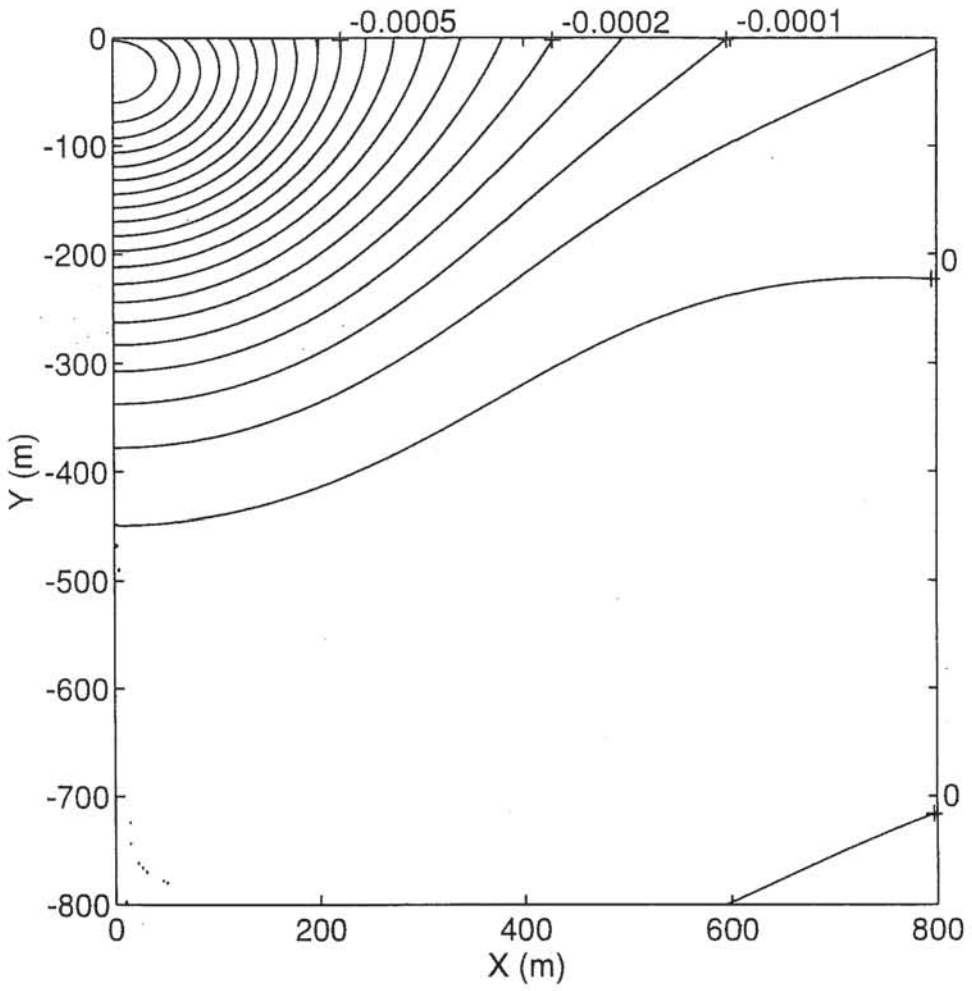

Figure 4.22. Contour Plot of the Real Component of the Axial Electric Field Below Ground

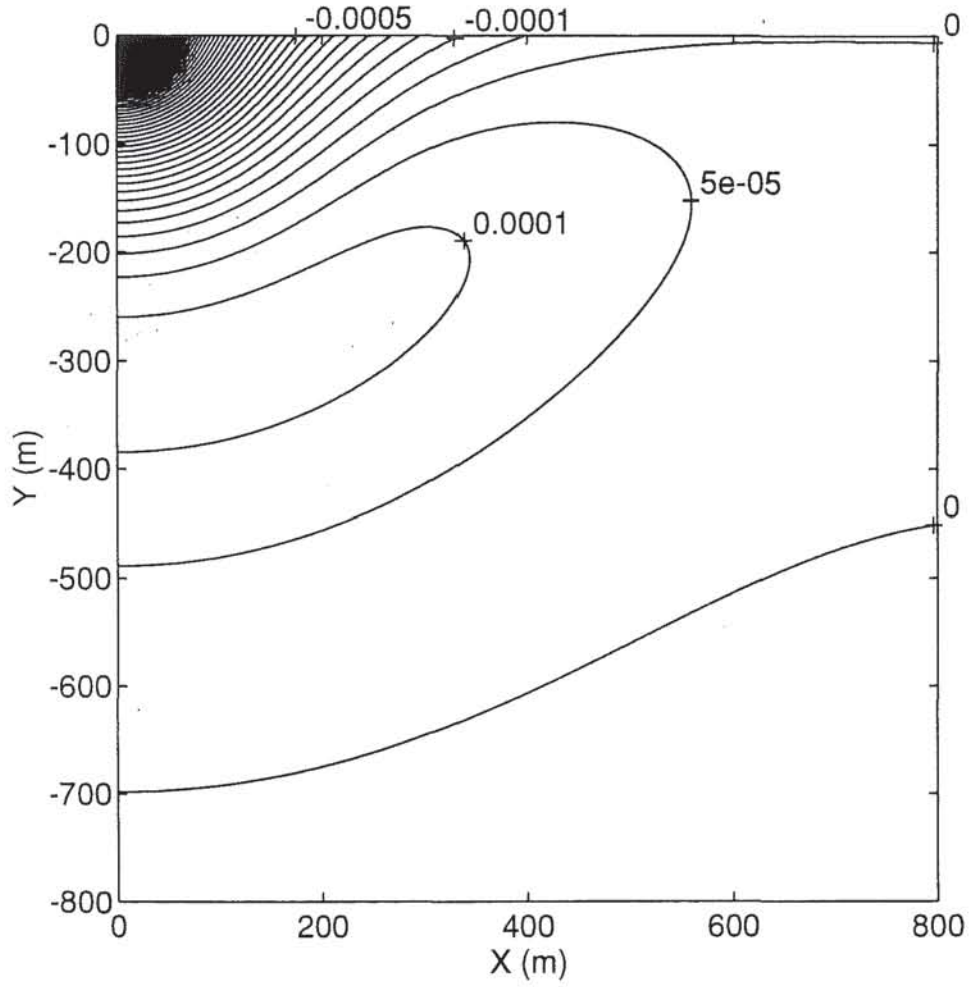

Figure 4.23. Contour Plot of the Imaginary Component of the Axial Electric Field Below Ground

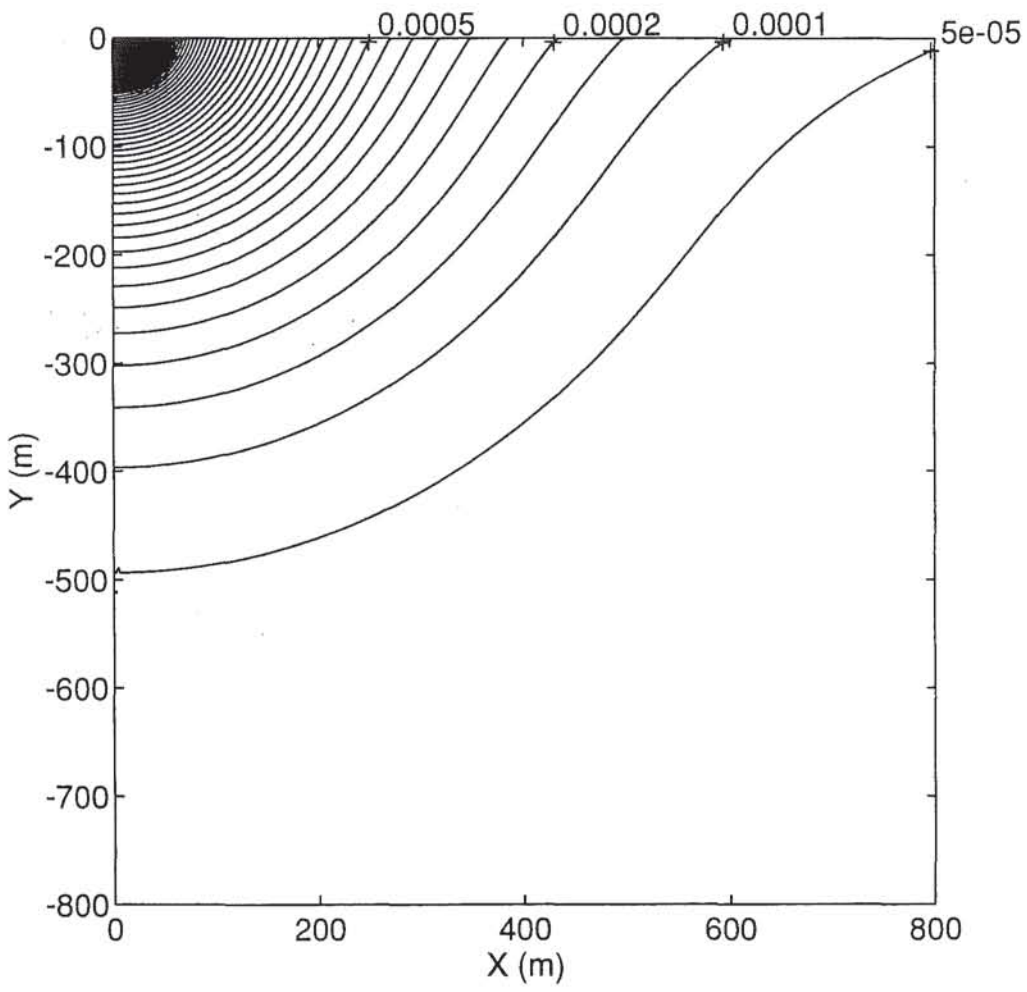

Figure 4.24. Contour Plot of the Magnitude of the Axial Electric Field Below Ground

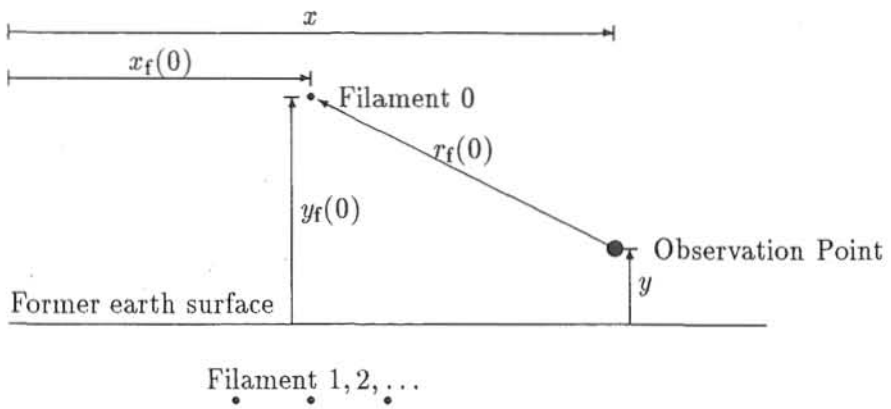

Where

$I_f(n)$ = Current in filament n (A)
For $n = 0, 1, \ldots m_f$

$x_f(n)$ = x ordinate of filament n (m)
For $n = 0, 1, \ldots m_f$

$y_f(n)$ = y ordinate of filament n (m), negative as the filaments are below the former surface of the earth
For $n = 0, 1, \ldots m_f$

$r_f(n)$ = Radial distance between filament n and the observation point (m)
$= \sqrt{(x - x_f(n))^2 + (y - y_f(n))^2}$
For $n = 0, 1, \ldots m_f$

$w_f(n)$ = Filament current weighting factor
$= \frac{I_f(n)}{I_c}$

m_f = Number of filaments approximating the continuous earth current distribution. The total number of filaments is $m_f + 1$, as one filament (number 0) is used to represent the conductor current.

Figure 4.25. Modelling of the Continuous Earth Current Distribution by a System of Filamentary Currents

Both in phase and quadrature fields must be represented to give the real and reactive components of the mutual impedance. Therefore the current weighting factors for each filament, $w_f(n)$, are complex.

There are a number of constraints, listed below, which are imposed upon filamentary models by the physics of the situation.

- Filament 0 represents the transmission line conductor. Therefore $x_f(0) = x_c$, $y_f(0) = y_c$ and $I_f(0) = I_c$.
- The magnitude of the magnetic field and hence filament positions and weighting factors must be symmetric about the vertical plane $x = x_c$.
- The sum of the weighting factors must equal zero. This is simply the requirement that the total quadrature current in the earth must be zero, while the total in phase earth current must equal that in the line but flow in the opposite direction.

4.7.4 Derivation Method

To derive a filamentary current model it is necessary to calculate the weighting factor $w_f(n)$, x ordinate $x_f(n)$ and y ordinate $y_f(n)$ for each filament. These values are functions of frequency, earth resistivity and conductor geometry. Empirical formulas may be derived which describe the relationship between these variables and the filament coefficients. The effort required to evaluate these functions increases rapidly with the number of filaments and hence coefficients that must be determined. Imposition of the constraints of Section 4.7.3, in particular the symmetry constraint, greatly reduces the number of variables however.

A multidimensional optimisation program based on the Simplex method (Nelder and Mead, 1965) was developed to determine the coefficients of the filamentary model for a given situation. Each variable was perturbed to identify the dominant dependencies with the objective of developing empirical equations to describe them. The explicit nature of the constraint equations allowed them to be used to reduce the number of variables, avoiding the need to use a constrained optimisation method. The real and reactive components of coefficients were determined separately to further reduce the number of variables being optimised at a time. Error functions were based upon the discrepancy between the filamentary model and the reference model (Carson, Complex Penetration or Exact models) over a range of separations. Either least squares, peak absolute error, normalised errors or integrals of these quantities were used to quantify the mismatch between the models.

4.7.5 Summary

From the results obtained using filamentary models with up to five filaments it soon became apparent that considerably more than five filaments would be required to obtain the desired accuracy. It was particularly difficult to match the real component of the mutual impedance, due to the wide spread of the quadrature current within the earth (Figure 4.22). Acceptable accuracy could be obtained by increasing the number of filaments, however this would have greatly increased the complexity of the model obscuring the physical interpretation, and reducing the computational efficiency. It was at this stage that the Acha Curve Fitting model was completed (Section 3.5.2). Simple filamentary models could not match the accuracy and computational efficiency of this method, and therefore work on the development of accurate filamentary models for the mutual impedance between high voltage transmission lines and buried telecommunications cables was abandoned.

4.8 Vertical Inducing Loop Model

Existing mutual impedance formulas are complicated integral functions of many variables, or logarithmic functions of complex dimensions (Section 3.5). As a consequence it is difficult to gain an understanding of the physical mechanisms affecting the inductive influence of transmission lines (Section 4.6).

The *Vertical Inducing Loop* (VIL) is a primitive filamentary model that has been developed by the author to explain the observed inductive influence phenomena of high voltage transmission lines. Two forms of the model are presented, the basic VIL model which provides an estimate of the magnitude of the mutual impedance only, and the phase corrected VIL model which provides estimates of the real and reactive components of the mutual impedance.

4.8.1 Basic Vertical Inducing Loop (VIL) Model

The basic Vertical Inducing Loop model approximates a single conductor earth return transmission system by a pair of filamentary currents located in air as shown in Figure 4.26. The upper filament represents the transmission line, and therefore is constrained to lie on the conductor axis and carry a current of I_c A. The lower filament approximates the continuous earth return current distribution and is constrained to carry a current of $-I_c$ A, and lie in the same vertical plane as the line conductor filament. These filaments form a vertical loop of circulating current which induces a LEF in parallel conductors, hence the name of the model. The effect of the lossy earth is incorporated into the model through the expression for the depth of the return filament $y_f(1)$.

Simple approximations of this form have been used in the past to estimate the mutual coupling between transmission lines and communications cables (Johansson and Ekstrom, 1989). The model proposed here employs a different expression for the depth of the return current filament, $y_f(1)$.

The VIL model is a gross approximation of the earth current distribution as it considers all of the current to be concentrated at a single point and it ignores the circulating currents that flow entirely within the earth. Furthermore only in-phase components of the current are represented, the quadrature current which produces the resistive component of the mutual impedance is not represented. The effect of the resistive component of the mutual impedance has been included in the VIL model however by fitting it to the magnitude of the mutual impedance rather than the reactive component alone.

4.8.1.1 Theoretical Development

The magnitude of the mutual impedance between a single conductor transmission line and a buried cable according to the VIL model is

$$|Z_m| = \frac{\omega\mu_a}{2\pi} \ln \frac{\sqrt{(x-x_c)^2+(y-y_f(1))^2}}{\sqrt{(x-x_c)^2+(y-y_c)^2}} \tag{4.10}$$

$$= \frac{\omega\mu_a}{2\pi} \ln \frac{r_f(1)}{r_f(0)} \tag{4.11}$$

To determine $y_f(1)$, the author imposed the additional requirement that the magnitude of the mutual impedance calculated using the VIL model should tend to that of Complex Penetration model as the separation tends to infinity. This is expressed mathematically in equation (4.12).

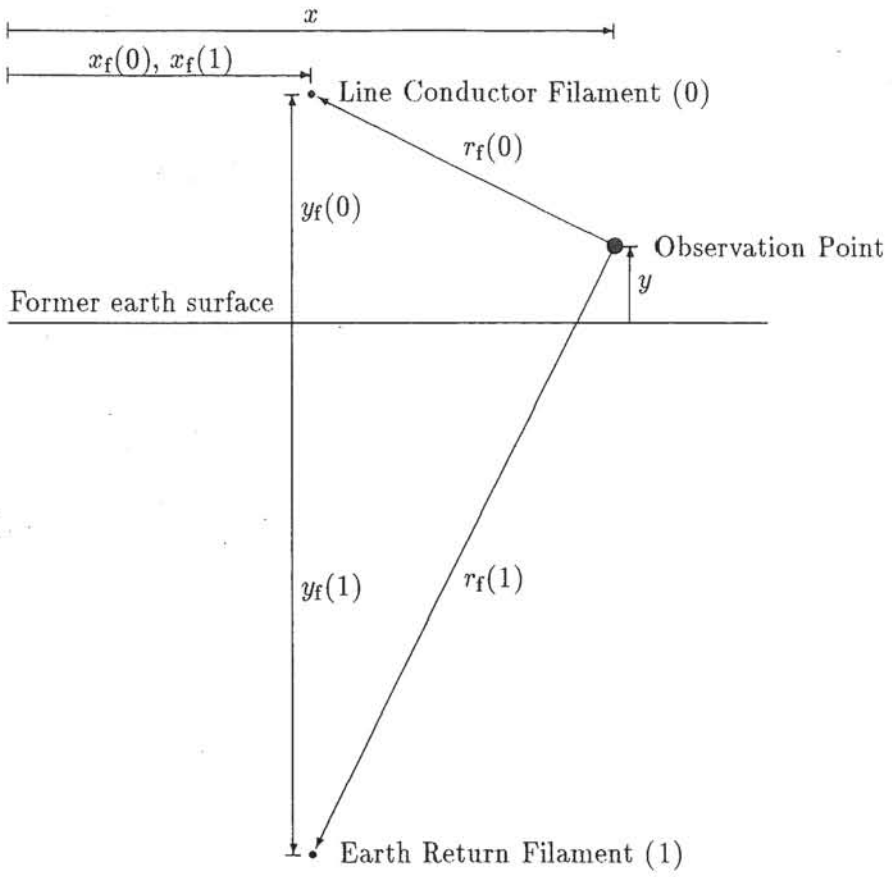

Where

$I_f(0)$ = Current in line conductor filament = I_c (A)
$I_f(1)$ = Current in earth return filament = $-I_c$ (A)
$x_f(0)$ = x ordinate of the line conductor filament = x_c (m)
$x_f(1)$ = x ordinate of the earth return filament = x_c (m)
$y_f(0)$ = y ordinate of the line conductor filament = y_c (m)
$y_f(1)$ = y ordinate of the earth return filament (m), which is negative as the filament is below the former surface of the earth
$r_f(0)$ = radial separation from line conductor filament (m)
$= \sqrt{(x - x_c)^2 + (y - y_c)^2}$
$r_f(1)$ = radial separation from earth return filament (m)
$= \sqrt{(x - x_c)^2 + (y - y_f(1))^2}$

Figure 4.26. Vertical Inducing Loop Model

$$\lim_{|x-x_c|\to\infty} \frac{|Z_m{}^{\text{VIL}}|}{|Z_m{}^{\text{Complex Penetration}}|} = 1 \tag{4.12}$$

Where

$|Z_m{}^{\text{VIL}}|$ = Magnitude of the mutual impedance calculated using the Vertical Inducing Loop model (Ω).

$|Z_m{}^{\text{Complex Penetration}}|$ = Magnitude of the mutual impedance calculated using the Complex Penetration model (Ω).

This yields the following expression for $y_f(1)$.

$$y_f(1) = -\sqrt{(y-y_c)^2 + \sqrt{4\delta^2(y+y_c+\delta)^2 + [4yy_c + 2\delta(y+y_c)]^2}} + y \tag{4.13}$$

Where

δ = Skin depth of the earth (m)
$= \sqrt{\frac{2\rho_e}{\omega\mu_e}}$

As the resistivity of the earth $\rho_e \to 0$, $y_f(1) \to -y_c$, which is the lossless earth result.

The principal disadvantage of (4.13) is that depth of the lower filament is a function of cable height y. However for the case of harmonic induction into buried telecommunication cables $\delta \gg y$ and $\delta \gg y_c$. Equation (4.13) can therefore be approximated by

$$y_f(1) \approx -\sqrt{2}\,\delta - \frac{y_c}{\sqrt{2}} - \frac{(1-\sqrt{2})y}{\sqrt{2}} \tag{4.14}$$

The term involving y may be omitted with little loss of accuracy for shallowly buried cables yielding

$$y_f(1) \approx -\sqrt{2}\,\delta - \frac{y_c}{\sqrt{2}} \tag{4.15}$$

making the geometry of the Vertical Inducing Loop independent of cable location.

4.8.1.2 Physical Interpretation

The Vertical Inducing Loop model approximates the continuous current distribution within the earth with a discrete current filament, and therefore may be regarded as simple physical approximation of reality. Alternatively it may be considered to be an adaptation of the lossless image model in which the depth of the image has been increased to account for the penetration of current flow into the lossy earth.

Each filament carries the same current, but in opposite directions, resulting in a destructive magnetic field interference pattern. The magnitude of the mutual impedance is proportional to the natural logarithm of the ratio of the radial separations, enabling accurate predictions of the LEF to be made from simple geometric concepts.

The dependencies of the inductive influence of a single conductor transmission line in the immediate vicinity of the line differ markedly from those at moderate to large separations, and have been classified as either Near or Far field effects (Section 4.5). The near field region is the region in the immediate vicinity of the line where the direct contribution from the transmission line filament dominates as $r_f(0) \ll r_f(1)$. In this region rapid field variations occur with separation ($r_f(0)$ increases rapidly with separation while $r_f(1)$ increases only slightly due to the depth of the return filament). In

the far field region the observation point is very nearly equidistant from the filaments. The fields therefore cancel almost completely, and decay at similar rates with separation. The dependencies of the fields in each of these regions, determined using the VIL model, are reported below.

4.8.1.3 Near Field Approximation

In the near field region $r_f(1)/r_f(0) \gg 1$. The logarithm of this ratio and hence the mutual coupling tends to be relatively insensitive to $r_f(1)$, but highly sensitive to $r_f(0)$. Furthermore, for small separations $r_f(1) \approx y - y_f(1)$, and therefore

$$|Z_m| \approx \frac{\omega\mu_a}{2\pi} \ln\left(\frac{y - y_f(1)}{r_f(0)}\right) \tag{4.16}$$

Inserting the linear approximation for the earth return filament depth and neglecting the term involving y in the numerator gives

$$|Z_m| \approx \frac{\omega\mu_a}{2\pi} \ln\left(\frac{\sqrt{\frac{4\rho_e}{\omega\mu_a}} + \frac{y_c}{\sqrt{2}}}{\sqrt{(x - x_c)^2 + (y - y_c)^2}}\right) \tag{4.17}$$

Consequently the inductive influence in the Near Field region is expected to be highly dependent on conductor geometry, approximately directly proportional to frequency, but substantially independent of earth resistivity variations. These predictions are in agreement with the observed behaviour for the single conductor line (Section 4.5).

4.8.1.4 Far Field Approximation

At large distances from the line $r_f(1)/r_f(0) \approx 1$, resulting in a high degree of field cancellation. As $x - x_c$ tends to ∞ Equation (4.10) reduces to

$$|Z_m| = \frac{\omega\mu_a}{4\pi} \frac{(y - y_f(1))^2 - (y - y_c)^2}{(x - x_c)^2} \tag{4.18}$$

To remove the dependence of this expression on the height of the observation point y, it may be assumed that $y \approx y_c$, giving

$$|Z_m| \approx \frac{\omega\mu_a}{4\pi} \frac{(y_c - y_f(1))^2}{(x - x_c)^2} \tag{4.19}$$

The inductive influence, according to Equation (4.19), for a cable in approximately the same plane as that in which the line filament lies is proportional to the square of the vertical distance between the filaments $(y_c - y_f(1))$ and decays as the reciprocal of the separation squared. This simple concept enables accurate predictions of the LEF induced by multiconductor transmission lines to be made without recourse to numerical evaluation (Chapter 5).

Equation (4.19) may be further simplified by the insertion of the linear approximation for the depth of the earth return filament (4.15), yielding

$$|Z_m| \approx \frac{\omega\mu_a}{4\pi} \frac{\left[(1 + \frac{1}{\sqrt{2}})y_c + \sqrt{2}\delta\right]^2}{(x - x_c)^2} \tag{4.20}$$

As the skin depth is generally much greater than the conductor height the far field approximation becomes

$$|Z_m| \approx \frac{\rho_e}{\pi(x - x_c)^2} \tag{4.21}$$

i.e. proportional to earth resistivity and substantially independent of frequency and conductor height, which agrees with the observed dependencies for the single conductor line (Section 4.5).

4.8.1.5 Accuracy

Figure 4.27 contains graphs of the relative errors ε_r, ε_x and ε_m between the VIL model (4.11) and the Exact model when applied to the task of calculating the mutual impedance between the single conductor line of Figure 4.2 and a buried cable. Error profiles for frequencies of 50, 500 and 5000 Hz, earth resistivities of 20, 200 and 2000 Ω.m, and separations from 0 to 10$\times$ the skin depth of the earth have been evaluated. Peak relative errors for each trace are listed in Table 4.5. The exact expression for the depth of the return filament (4.13) has been used.

Error profiles are included for the real and reactive components of the mutual impedance, despite the fact that the VIL model is only intended to represent the magnitude of impedance, for comparison with the Phase Corrected VIL model presented in Section 4.8.2. It has been assumed that the impedance in this case is purely resistive. The error profile graphs of Figure 4.27 indicate that this is a reasonable approximation at moderate to large separations, but is totally inappropriate in the immediate vicinity of the line.

Over the range of conditions studied the peak relative magnitude error ε_m is less than 26%. It is low in the immediate vicinity of the line and at moderate to large separations. Significant errors occur at intermediate separations of between 0.5 and 4 times the skin depth of the earth. The accuracy is good in the immediate vicinity of the line as the dominant component of the field is the direct field from the line conductor which is accurately represented by a filamentary current along the axis of the conductor. At intermediate separations the direct conductor field has decayed to the extent that the contribution from the earth current distribution becomes significant. The separation is still relatively small in relation to the extent of the current distribution within the earth, and therefore the field induced by a single filamentary current located at the centre of this distribution is only a fair approximation of the continuous earth current field. As the separation becomes large in relation to the extent of the current distribution, the field from the continuous distribution tends to that of a single current filament and hence the accuracy of the model improves.

Significant errors occur at large separations when the frequency and earth resistivity are high. Other Quasi-TEM models display similar characteristics (Section 4.4). This error is believed to be due to the Quasi-TEM propagation assumption becoming invalid under these conditions.

Figure 4.27 indicates that the Vertical Inducing Loop model using the exact expression for the depth of the return filament, is a good approximation to the magnitude of mutual coupling.

The accuracy of the VIL model has also been calculated for the case when the linear approximation, (4.15), is used to calculate the depth of the return filament. In all cases studied the relative errors were within 2% of those calculated using the exact depth expression (4.13).

4.8.1.6 Limitations of Basic VIL Model

The Vertical Inducing Loop model is a powerful tool for studying the factors effecting the steady state inductive influence of transmission lines. Difficulties can arise when using this model to predict the LEF due to balanced sequence current flow in multiconductor lines however. The far field LEF in this case is the residual of the near

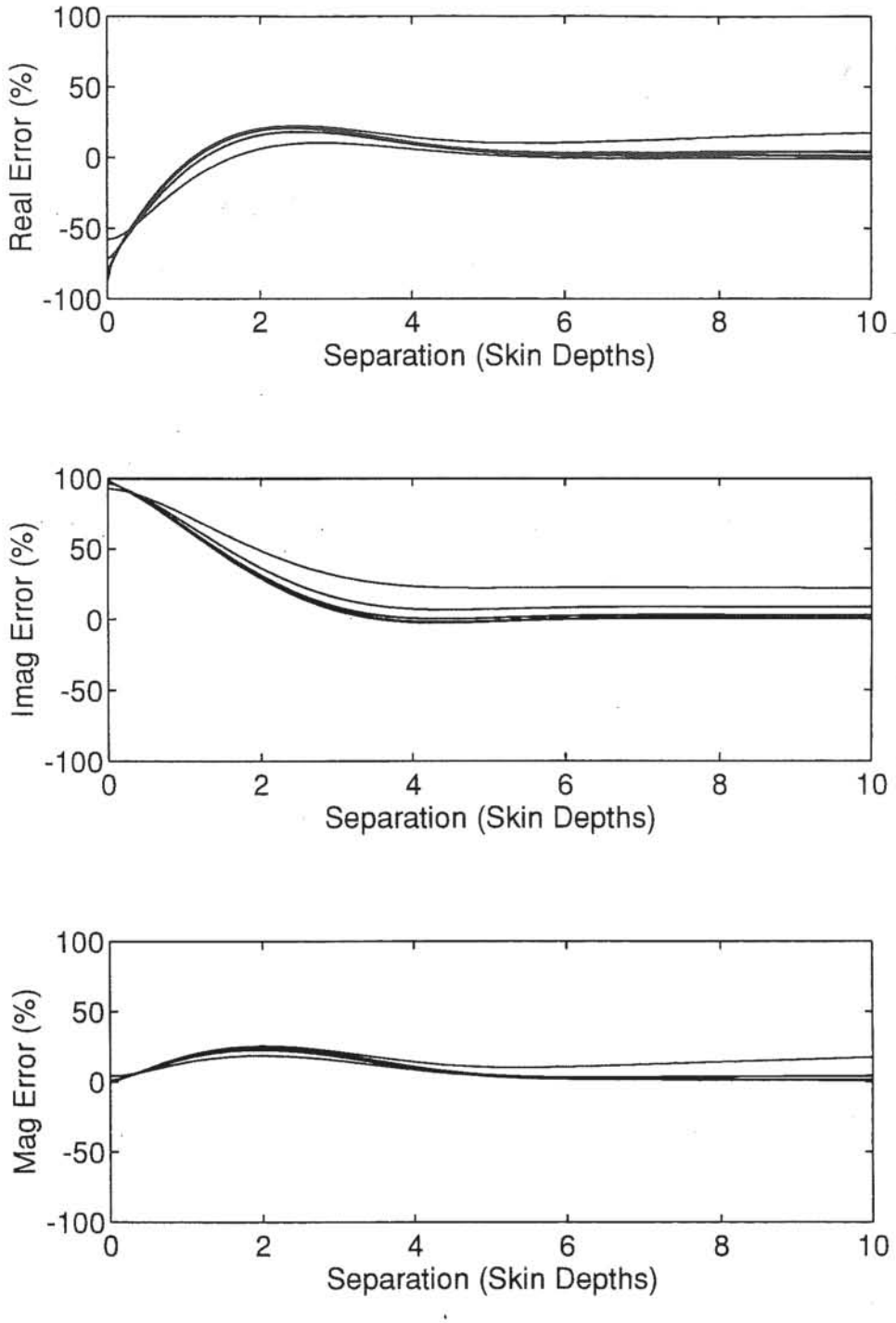

Figure 4.27. Percentage error between the Vertical Inducing Loop and Exact Models for Induction from a Single Conductor Transmission Line. The upper graph is the real error ε_r, the middle graph the imaginary error ε_x, and the lower graph the magnitude error ε_m.

Frequency (Hz)	Earth Resistivity (Ω.m)	Extreme ε_r (%)	Extreme ε_x (%)	Extreme ε_m (%)
50	20	-79.563	97.922	24.190
50	200	-84.372	98.728	24.714
50	2000	-87.446	99.154	24.899
500	20	-71.560	96.253	22.659
500	200	-79.560	97.921	24.215
500	2000	-84.354	98.725	24.867
5000	20	-58.103	92.575	18.712
5000	200	-71.529	96.246	22.796
5000	2000	-79.374	97.893	25.308

Table 4.5. Extreme Relative Percentage Errors for the Vertical Inducing Loop Model

complete cancellation of the individual conductor fields. As such it is highly sensitive to the slight differences in both magnitude and phase of the mutual impedances between each transmission line conductor and the cable. Erroneous results may be obtained when calculating the balanced sequence far field LEF induced by transmission lines in which the conductors lie in different horizontal planes using the basic Vertical Inducing Loop model, due to the inability of the model to represent the slight differences between the phase angles of the mutual impedances that result from differing conductor heights.

An extension to the basic Vertical Inducing Loop model is described in the following section which overcomes this problem.

4.8.2 Phase Corrected VIL Model

In this section a modified version of the VIL model which includes the phase of the mutual impedance is described.

4.8.2.1 Theoretical Development

The phase of the mutual impedance is a function of separation, displaying significantly different characteristics in the near field region to those in the far field. In the near field region the reactive component of the mutual impedance dominates. As the separation increases the resistive component becomes dominant. The ratio of the real to reactive components tends to a constant value as the separation tends to infinity (Section 4.5).

It was not considered appropriate to model this dependency in detail as it would have greatly increased the complexity of the model, obscuring its physical interpretation. Furthermore detailed modelling is not warranted in the author's opinion given the modest magnitude accuracy of the basic Vertical Inducing Loop model.

The principal requirement of the Phase Corrected VIL model was that it should yield accurate results in the far field region. Phase correction for the far field region has been implemented by multiplying the basic VIL result by a complex constant. The value of this constant was derived by evaluating the ratio, as the separation tends to infinity, of the real to reactive components of the mutual impedance determined using the complex penetration model. The resultant far field phase correction factor is presented in (4.22).

$$\frac{\delta(y + y_c + \delta) + \jmath(2yy_c + \delta(y + y_c))}{\sqrt{\delta^2(y + y_c + \delta)^2 + (2yy_c + \delta(y + y_c))^2}} \tag{4.22}$$

It is apparent from Figure 4.27 that the greatest relative error in the real and reactive mutual impedances calculated using the basic VIL model occurs in the immediate vicinity of the transmission line, and is of the order of 100 %. Given the good magnitude accuracy of the VIL model in this region, it was considered to be worthwhile to derive a second phase constant for use in the near field region. The near field phase factor, derived from the complex penetration model for a separation of 0 m, is given in (4.23).

$$\frac{\jmath \ln\left(\frac{y+y_c+\delta-\jmath\delta}{|y-y_c|}\right)}{\left|\ln\left(\frac{y+y_c+\delta-\jmath\delta}{|y-y_c|}\right)\right|} \tag{4.23}$$

The transition between the near and far field regions has been specified as one skin depth δ, for the purposes of switching between the near and far field phase constants, (4.22) and (4.23). The resultant phase corrected VIL model is therefore:

$$\begin{aligned} {Z_m}^{\mathrm{VIL}} & \\ &= \frac{\jmath \ln\left(\frac{y+y_c+\delta-\jmath\delta}{|y-y_c|}\right)}{\left|\ln\left(\frac{y+y_c+\delta-\jmath\delta}{|y-y_c|}\right)\right|} \frac{\omega\mu_a}{4\pi} \frac{(y-y_f(1))^2-(y-y_c)^2}{(x-x_c)^2} \\ &\quad \text{For } |x-xc| \le \delta \\ &= \frac{\delta(y+y_c+\delta)+\jmath(2yy_c+\delta(y+y_c))}{\sqrt{\delta^2(y+y_c+\delta)^2+(2yy_c+\delta(y+y_c))^2}} \frac{\omega\mu_a}{4\pi} \frac{(y-y_f(1))^2-(y-y_c)^2}{(x-x_c)^2} \\ &\quad \text{For } |x-xc| > \delta \end{aligned} \tag{4.24}$$

The addition of complex phase constants to the basic Vertical Inducing Loop model has greatly complicated the mathematical representation of the model. In the following subsections approximations which are generally valid for power telecommunication interference studies are used to simplify this model.

4.8.2.2 Near Field Approximation

If it is assumed that $\delta \gg y_c$ and $\delta \gg y$, (4.25) for the near field region reduces to

$$\begin{aligned} {Z_m}^{\mathrm{VIL}} &\approx \frac{\frac{\pi}{4}+\jmath\ln\left(\frac{\sqrt{2}\delta}{y_c}\right)}{\sqrt{\frac{\pi^2}{16}+\left(\ln\left(\frac{\sqrt{2}\delta}{y_c}\right)\right)^2}} \frac{\omega\mu_a}{2\pi} \ln\left(\frac{\sqrt{\frac{4\rho_e}{\omega\mu_a}}+\frac{y_c}{\sqrt{2}}}{\sqrt{(x-x_c)^2+(y-y_c)^2}}\right) \\ &\approx \frac{\jmath\omega\mu_a}{2\pi} \ln\left(\frac{\sqrt{\frac{4\rho_e}{\omega\mu_a}}+\frac{y_c}{\sqrt{2}}}{\sqrt{(x-x_c)^2+(y-y_c)^2}}\right) \end{aligned} \tag{4.25}$$

Which is the basic VIL result scaled by $\jmath$ indicating that the reactive component of the mutual impedance dominates in the near field region. This result is in agreement with that obtained for the single conductor transmission line in Section 4.5.

4.8.2.3 Far Field Approximation

Equation (4.26) is the phase corrected far field approximation to the mutual impedance. It was derived from (4.25) by calculating the limit of this equation as the separation tends to infinity.

$$Z_m = \frac{\omega\mu_a}{2\pi} \frac{\delta(y_c+y+\delta)+\jmath[2y_cy+\delta(y_c+y)]}{(x-x_c)^2}$$

$$\approx \frac{\rho_e}{\pi(x - x_c)^2} \tag{4.26}$$

Which agrees with the observed result for the single conductor transmission line.

4.8.2.4 Accuracy

Graphs of the percentage relative error between the Phase Corrected Vertical Inducing Loop model (4.25), and the Exact model are presented in Figure 4.28. Peak relative errors are tabulated in Table 4.6.

Comparison of Figure 4.28 with Figure 4.27 reveals that the error in both the real and reactive components of the mutual impedance in the immediate vicinity of the line has been reduced through the addition of the near field phase correction. The improvement gained is slight however as the assumption of constant phase within the near field region is not well based. The author therefore recommends that when accurate values of the mutual impedance for separations of between 0.5 and 4 times the skin depth δ are required, either the Carson integral or Carson series Quasi-TEM models should be used.

The far field impedance values calculated using the Phase Corrected Vertical Inducing Loop model are very accurate however, enabling precise predictions of the far field LEF to be obtained for all transmission line geometries and sequences of current flow.

Frequency (Hz)	Earth Resistivity (Ω.m)	Extreme ε_r (%)	Extreme ε_x (%)	Extreme ε_m (%)
50	20	58.563	61.867	24.281
50	200	61.469	64.221	24.732
50	2000	65.913	62.491	24.903
500	20	47.244	61.740	23.189
500	200	58.569	61.801	24.300
500	2000	61.519	64.174	24.865
5000	20	28.256	55.041	22.187
5000	200	47.299	61.701	23.325
5000	2000	58.962	61.465	25.391

Table 4.6. Extreme Relative Percentage Errors for the Phase Corrected Vertical Inducing Loop Model

4.9 Conclusions

In the author's opinion the magnitude of the Longitudinal Electric Field (LEF) induced by high voltage transmission lines should be used to quantify their inductive influence.

Magnetic coupling between a high voltage transmission line and a buried telecommunications cable may be estimated from the LEF at the site of the cable, but in the absence of the cable, provided that the currents induced within the cable are small.

The LEF induced within the earth varies only slightly with cable depth, and is a maximum in the direction parallel to the axis of the transmission line.

Carson's integral equation and infinite series implementations used during this project yield results which are within 17 % of the LEF determined using the Exact model over the range of conditions typically encountered in New Zealand. Acha's curve fitting model yields accurate results over the range of conditions for which it is defined, however it introduces ripple into the mutual impedance calculations which may

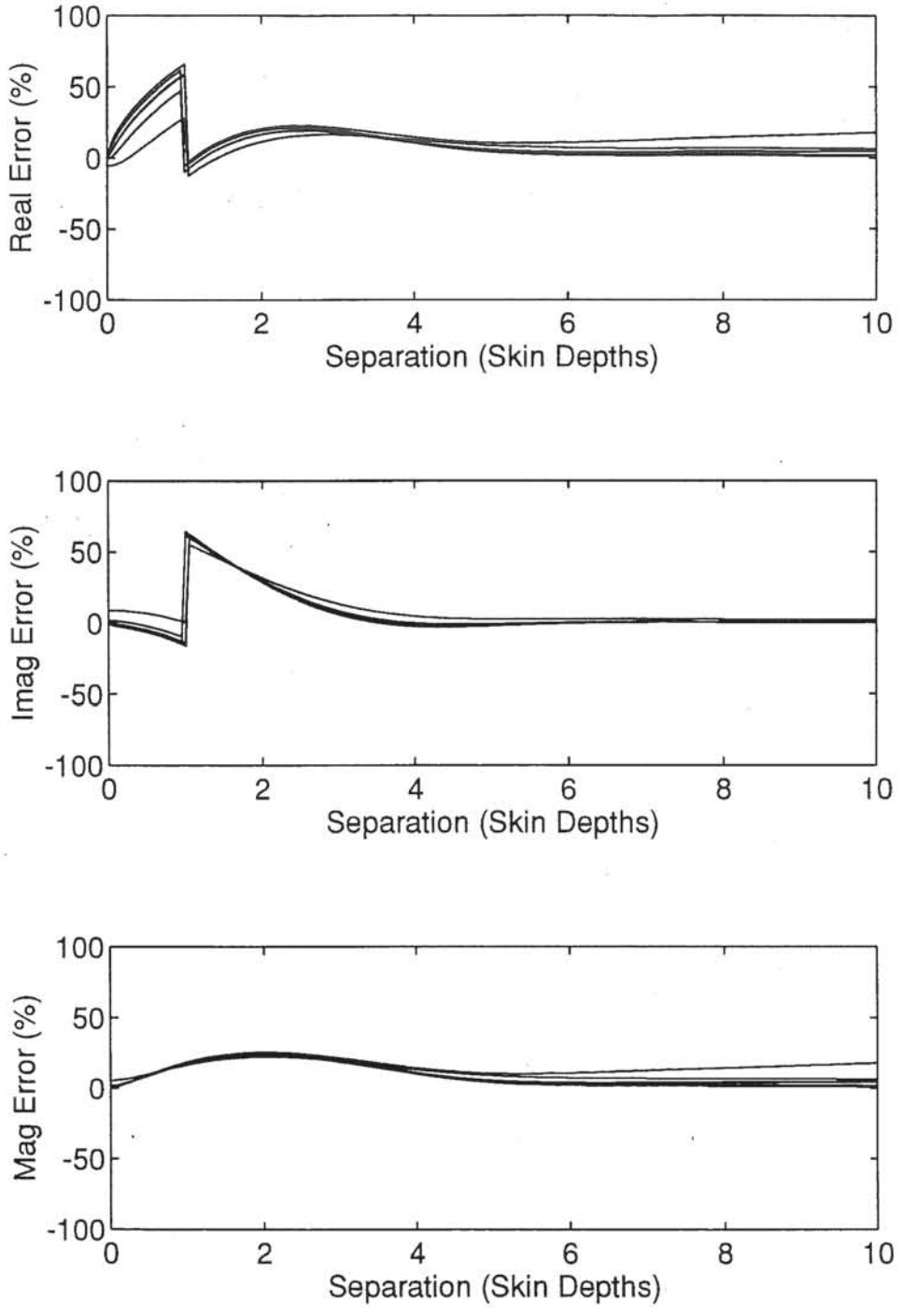

Figure 4.28. Percentage error between the Phase Corrected Vertical Inducing Loop and Exact Models for Induction from a Single Conductor Transmission Line. The upper graph is the real error ε_r, the middle graph the imaginary error ε_x, and the lower graph the magnitude error ε_m.

generate erroneous results for balanced sequence current flows in multiconductor lines. Significant errors may also result from the use of the complex penetration model for this application at separations of between 0.5 and 4 times the skin depth of the earth.

All existing Quasi-TEM models for the LEF at the site of a buried cable become inaccurate at large separations when the frequency and earth resistivity are high as the Quasi-TEM propagation is no longer strictly valid.

Single conductor earth return transmission lines exhibit significantly different inductive influence dependencies in the immediate vicinity of the line to those at moderate and large distances, and are accordingly classified as either Near Field or Far Field phenomena. In the near field region the inductive influence is linearly proportional to conductor current and frequency, highly sensitive to conductor geometry but substantially independent of earth resistivity. The inductive influence in the far field region is linearly proportional to conductor current and earth resistivity, and relatively insensitive to frequency and conductor geometry.

Transmission lines induce circulating currents within the earth both in phase and ninety degrees out of phase with the conductor current. The greatest induced current density occurs in the earth immediately below the transmission line.

The earth current distribution may be approximated by a number of filamentary currents when the Quasi-TEM propagation requirements are satisfied. It is necessary to use more than 5 filaments to accurately represent the magnetic field induced by earth return current flows for mutual impedance calculations.

A two filament model, known as the Vertical Inducing Loop model, has been developed which estimates the magnitude of the mutual impedance between a single conductor transmission line and a buried telecommunications cable to within 26 % of that obtained using the Exact model. The model has a simple mathematical form and geometric interpretation which enables the inductive influence of multiconductor lines to be estimated without recourse to numerical evaluation. A derivative of this model provides estimates of the real and reactive components of the mutual impedance in the near and far field regions.

CHAPTER 5

INDUCTIVE INFLUENCE OF MULTICONDUCTOR TRANSMISSION LINES

5.1 Introduction

The principal component of the transverse harmonic noise voltage in a telecommunications cable is generally that due to the conversion of the longitudinal voltage induced by transmission lines into a transverse voltage by an imbalance in the circuit (Section 2.5.1). To minimise interference to telecommunication services it is necessary to ensure that the circuit is well balanced and to limit the longitudinal electric field (LEF) at the site of the cable.

Historically, it has been thought that the residual currents in high voltage transmission lines are the principal cause of the induced longitudinal voltages (Ball and Poarch, 1961). Recent papers have inferred that balanced currents can induce voltages which are comparable in magnitude, if not greater than those due to residual currents (Kuussaari and Pesonen, 1976; Dabkowski, 1978; Sharaf, 1982). This may be all the more so when considering currents in the harmonic frequency range as power system impedances, and hence current resonances, may be different for balanced and zero sequences (Densem *et al.*, 1984).

The purpose of this chapter is to convey an understanding of the factors effecting the inductive influence of multiconductor transmission lines, and ways in which it may be reduced. This is achieved through discussion of the results of numerical experiments on a variety of AC transmission lines (a study on the inductive influence of a HVDC line is reported in Chapters 8 and 9). Numerical investigations were performed as it was not possible to control the environment to a sufficiently high degree to enable valid comparisons to be made between different transmission lines on the basis of measured results.

The chapter opens in Section 5.2 with a review of the Vertical Inducing Loop model concepts (Chapter 4). These concepts are used throughout this chapter to explain the observed phenomena. Rigorous mathematical proofs of the observed effects are omitted from this chapter. All observed effects have been confirmed analytically using the Complex Penetration and Vertical Inducing Loop models however. Detailed mathematical descriptions of the phenomena based upon the Vertical Inducing Loop model are contained in Chapter 7.

Section 5.3 contains details of the numerical simulation used to determine and compare the inductive influence of the multiconductor lines reported in this chapter.

A variety of transmission line geometries have been studied to gain an understanding of the factors effecting the inductive influence of multiconductor transmission lines. The inductive influence of a horizontal transmission line is reported in Section 5.4, a vertical line in Section 5.5 and a double circuit vertical transmission line in Section 5.6.

The dependencies of these lines are summarised in Section 5.7.

Methods for reducing the inductive influence of multiconductor transmission lines

are discussed in Section 5.8.

5.2 Review of Vertical Inducing Loop Concepts

A single conductor earth return transmission line may be approximated by a pair of filamentary currents located in air Sections 4.8 and 4.8.2. The upper filament represents the transmission line conductor and therefore is located at (x_c, y_c) and carries current I_c. The lower filament represents the earth return current and is constrained to lie in the plane $x = x_c$ and to carry $-I_c$, resulting in the generation of a destructive interference pattern.

The magnitude of the mutual impedance between these filaments and a parallel conductor is given by (4.11), repeated below.

$$|Z_m| = \frac{\omega \mu_a}{2\pi} \ln \frac{r_f(1)}{r_f(0)} \tag{5.1}$$

Where

$r_f(0)$ = radial separation from line conductor filament (m)
$r_f(1)$ = radial separation from earth return filament (m)

Thus the mutual impedance is proportional to the natural logarithm of the ratio of the radial separations, which can be determined from simple geometric concepts.

The depth of the return filament, $y_f(1)$, may be approximated by (4.15) given below.

$$y_f(1) \approx -\sqrt{2}\,\delta - \frac{y_c}{\sqrt{2}} \tag{5.2}$$

At large distances from this pair of filaments the magnitude of the mutual impedance may be approximated by (4.19)

$$|Z_m| \approx \frac{\omega \mu_a}{4\pi} \frac{(y_c - y_f(1))^2}{(x - x_c)^2} \tag{5.3}$$

Which states that at large distances the mutual impedance is approximately proportional to the square of the vertical distance between the filaments, and decays as the reciprocal of the square of the separation.

The Vertical Inducing Loop model may be extended to multiconductor transmission lines by applying the concept of superposition. An equivalent return path filament is introduced for each line conductor filament at a depth proportional to the height of the conductor above the ground (4.15). The resultant LEF is given by minus one times the sum over all conductors of the conductor current multiplied by the mutual impedance determined using (4.11).

5.3 Simulation Approach

The interfering ability of multiconductor lines was assessed by calculating the magnitude of the longitudinal electric field at the site of the cable, parallel to the transmission line at a depth 0.5 metres below the surface of the earth for one ampere-per-phase of positive, zero and negative sequence current in the transmission line.

As the currents within the conductors are specified and the media are assumed to be linear, the resultant LEF is the superposition of the products of the current in each conductor and the mutual impedance to the cable. An adaptive implementation of Carson's infinite series equations using double precision arithmetic was used to calculate the mutual impedances (Section 3.5.2). Double precision arithmetic was necessary to

reduce errors due to loss of significance when calculating balanced sequence longitudinal electric fields.

Magnitude ratios, defined as

$$\left|\frac{\text{Perturbed LEF}}{\text{Unperturbed LEF}}\right| \tag{5.4}$$

were calculated to as a function of separation and the perturbed variable to determine the relationships between the LEF and conductor geometry, frequency and earth resistivity over the range of values listed in Section 4.3. The base or unperturbed condition for these studies was defined to be the LEF induced by the unmodified transmission line at a frequency of 600 Hz and earth resistivity of 200 Ω.m. A base frequency of 600 Hz was chosen, despite the fact that it is unlikely that significant levels of this even harmonic will exist within a high voltage AC transmission system, as it is the average of the two characteristic harmonic frequencies of 550 and 650 Hz generated by the 12 pulse convertors used on the New Zealand HVDC link.

Sequence ratios, defined as

$$\left|\frac{\text{Balanced sequence LEF}}{\text{Zero sequence LEF}}\right| \tag{5.5}$$

were evaluated to compare the relative interfering effects of balanced and residual currents.

5.4 Horizontal Line Configuration

The first line type studied was the Invercargill to Roxburgh 220 kV circuit in the New Zealand South Island system. The structure of this line is given in Figure 5.1.

Typical variations of the longitudinal electric field magnitudes are given in Figure 5.2. As the separation of the cable from the line increases the field strength at the site of the cable generally decreases, apart from a local minimum with balanced sequence currents immediately below the line. This is caused by cancellation of the direct fields from each conductor filament, as the cable is approximately equidistant from the line conductors at this position.

The sequence ratios, given in Figure 5.3, also generally decrease with separation. A local minimum occurs immediately below the line. The maximum ratios occur within the first 100 metres on each side of the transmission line.

5.4.1 Effect of Earth Resistivity

The magnitude of the longitudinal electric field in the immediate vicinity of the transmission line is not significantly affected by an increase in earth resistivity because the dominant component of the induced LEF is that due to the direct field from the line conductors. At large separations the magnitude of the fields increases significantly however. Here the field from the current flowing in the earth is comparable in magnitude to that from the line conductors, however the fields interfere destructively. As the earth resistivity is increased the depth of the return path increases, reducing the magnitude of the earth return field, and increasing the magnitude of the resultant field.

The magnitude ratios which compare the results of Figure 5.3 with those due to a change a doubling of the earth resistivity to 400 Ω.m are shown in Figure 5.4. Only at large separations have the ratios increased by a factor of two.

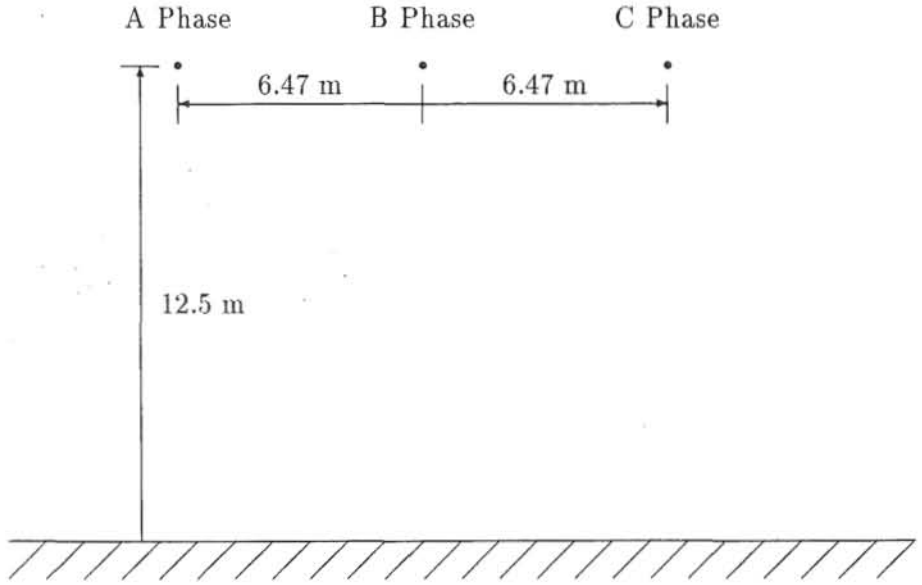

Line data

Name	:	Invercargill - Roxburgh Circuit 1 (excluding earth wires)
Nominal voltage	:	220 kV
Coordinates of A phase conductor	:	(-6.47 m, 12.5 m)
Coordinates of B phase conductor	:	(0.00 m, 12.5 m)
Coordinates of C phase conductor	:	(6.47 m, 12.5 m)
Conductor Type	:	Zebra

Figure 5.1. Horizontal Transmission Line Geometry

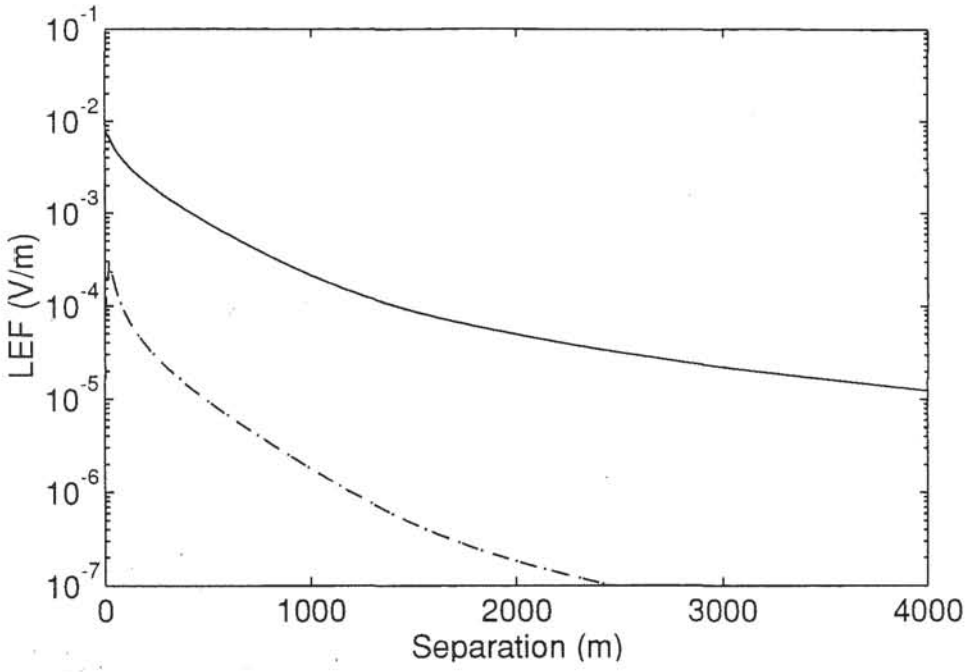

Figure 5.2. Magnitude of the LEF induced by the Positive (dotted line), Zero (solid line) and Negative (dashed line) Sequence Current Flows in the Horizontal Line Configuration for an Earth Resistivity of 200 Ω.m and Frequency of 600 Hz as a Function of Separation

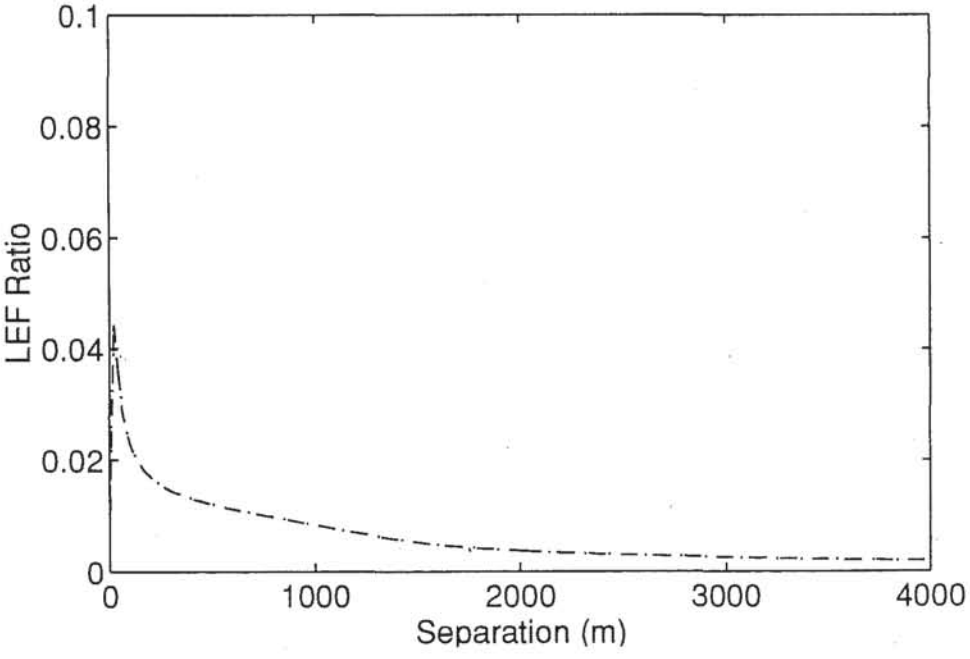

Figure 5.3. Positive/Zero (dotted line) and Negative/Zero (dashed line) LEF Sequence Ratios induced by the Horizontal Line Configuration for an Earth Resistivity of 200 Ω.m and Frequency of 600 Hz as a Function of Separation

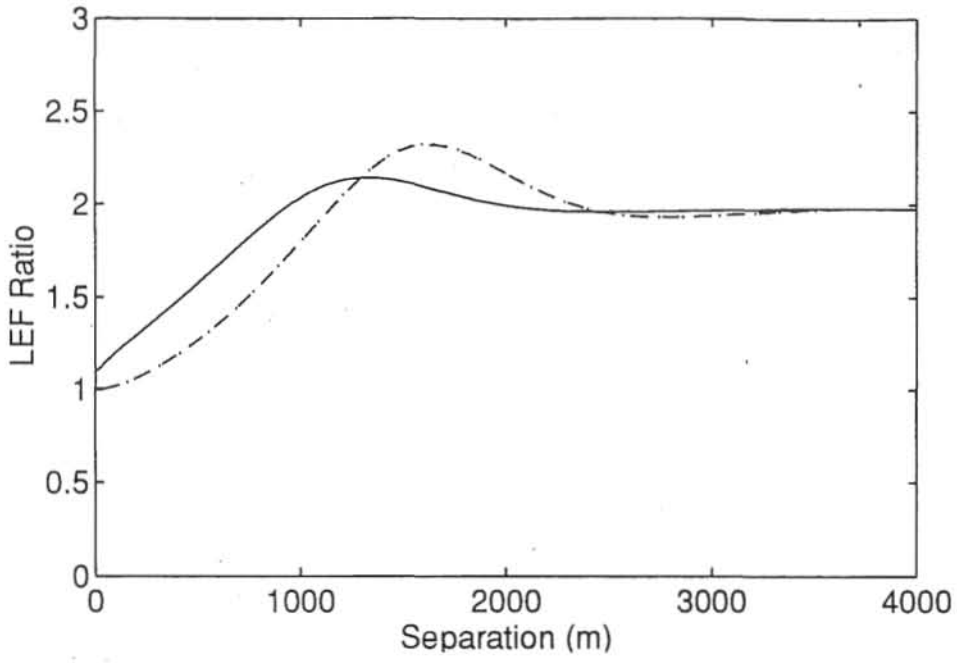

Figure 5.4. Ratio of Perturbed/Unperturbed LEF from Horizontal Line as a function of Separation when the Resistivity of the Earth is Doubled. (Positive sequence - dotted line, Zero sequence - solid line, Negative sequence - dashed line)

5.4.2 Effect of Frequency

The frequency of the line current influences the time rate of change of the magnetic flux in the vicinity of the cable, and the depth of penetration of the return current in the earth. The former implies that when the frequency is increased the magnitude of the mutual impedance will increase. This increase is approximately proportional to the ratio of frequencies, and is independent of separation. However, the depth of penetration decreases, thus reducing the depth of return. Hence the direct and earth return fields will cancel more effectively, and the resultant mutual impedance is reduced by a factor of approximately the inverse of the ratio of frequencies at large separations where the magnitude of the direct and earth return fields is similar. The two effects, when combined, imply that the mutual impedance is frequency dependant in the immediate vicinity of the line, but is relatively frequency independent at large separations.

Also the net LEF due to balanced current flow is principally due to the inter-conductor and inter-return-path spacings, as the individual conductor fields combine destructively, while that due to zero sequence current flow will increase less rapidly with frequency than that due to balanced sequence currents, as when the frequency of the line currents is increased, the depth of return reduces. These effects are shown in Figure 5.5.

5.4.3 Effect of Conductor Spacing

When the horizontal spacing of the line conductors are increased by 10 % the magnitude of induced voltage due to zero sequence currents remains relatively unaffected while the level of the longitudinal electric field due to balanced sequence currents increases

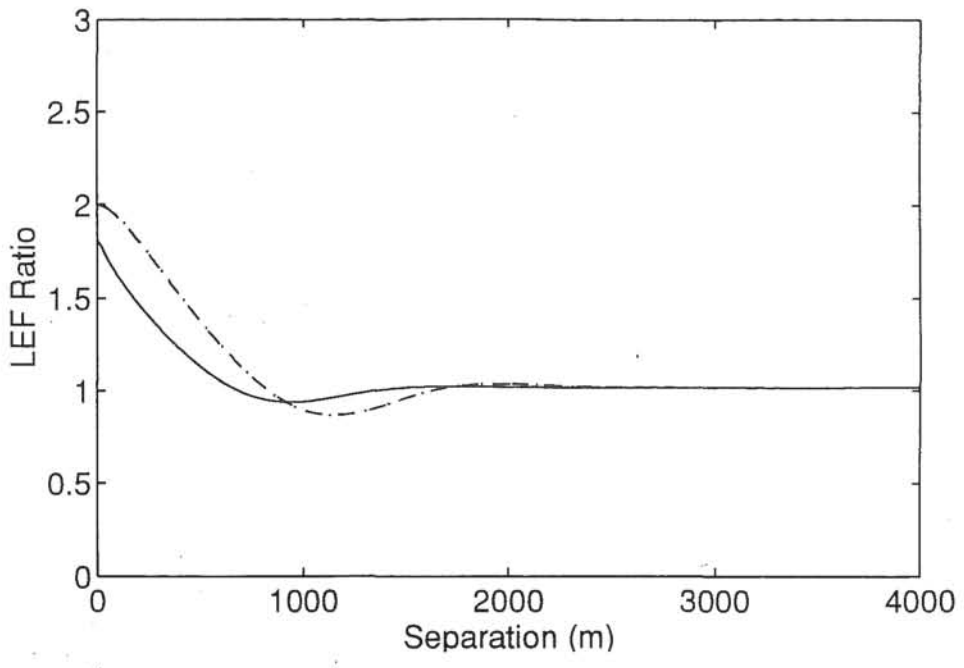

Figure 5.5. Ratio of Perturbed/Unperturbed LEF from Horizontal Line as a function of Separation when the Frequency is Doubled. (Positive sequence - dotted line, Zero sequence - solid line, Negative sequence - dashed line)

by approximately 10 %. This observation is shown in Figure 5.6 through magnitude ratios.

Increasing the height of the line conductors by 10 % would be expected to increase the level of induction due to all sequence currents at large separations. In practice this is insignificant as the height of the conductors above the earth is very small in relation to the effective depth of the return paths. A significant decrease of the induced LEF due to all sequence currents occurs when the cable is underneath the line conductors. This occurs because the 10 % increase in height of the inducing conductors is a very significant proportion of the total distance between the line conductors and cable.

5.4.4 Discussion

The most significant inducing current in the horizontal line configuration is the zero sequence current. The maximum sequence ratio of 11.7 % occurred for the frequency of 5000 Hz, and at an earth resistivity of 20 Ω.m, which were the maximum and minimum considered respectively. The depth of the return paths would thus be minimised, and hence the induced LEF due to zero sequence currents would be a minimum.

The longitudinal electric field induced by balanced sequence currents has a maximum influence on the cable (relative to the LEF due to zero sequence currents) when the cable is positioned approximately one hundred metres away from the transmission line. As the separation is increased the zero sequence LEF becomes more significant. In general for the cases studied, the sequence ratios were of the order of 1 - 2 % at a separation of 500 metres. These cases were for equal magnitude sequence currents in the transmission line. In practice the sequence currents will seldom be equal, however it is apparent that the positive or negative sequence currents will need to be of the

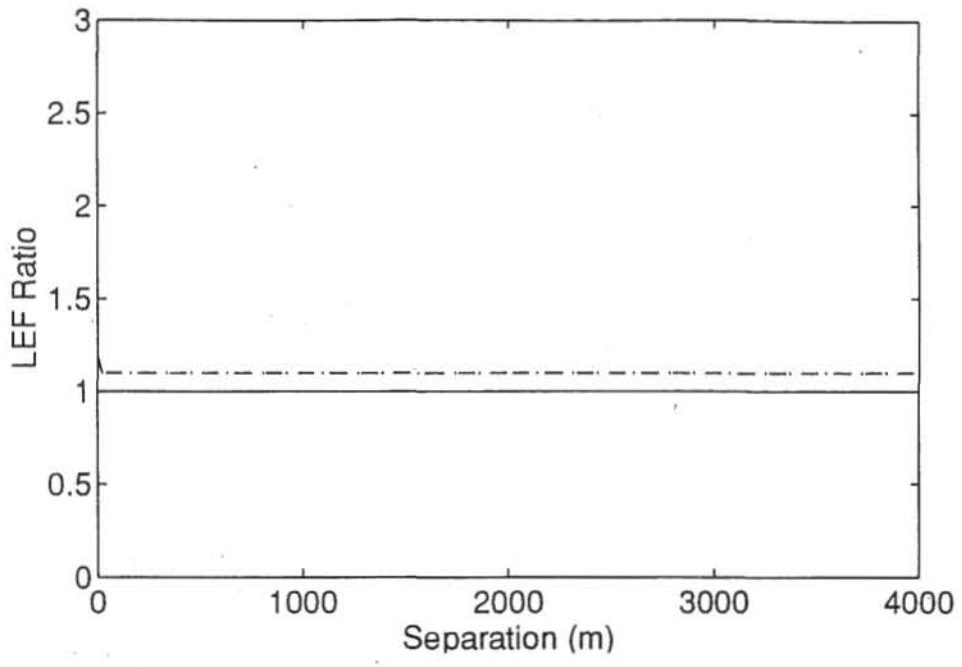

Figure 5.6. Ratio of Perturbed/Unperturbed LEF from Horizontal Line as a function of Separation when the Inter-conductor Spacings are Increased by 10% (Positive sequence - dotted line, Zero sequence - solid line, Negative sequence - dashed line)

order of 10 - 100 times greater than the zero sequence currents to produce comparable levels of interference for separations in the range of 0 - 1000 m from the transmission line.

5.5 Vertical Line Configuration

A vertical transmission circuit is shown in Figure 5.7. While this conductor arrangement is not used in practice, it is presented here to illustrate the performance of a purely vertical circuit. The vertical spacings of the conductors are identical to those of the Invercargill to Manapouri 220 kV line in the New Zealand South Island System. The variation of the longitudinal electric field magnitudes as a function of separation are shown in Figure 5.8 for the selected frequency of 600 Hz and earth resistivity of 200 Ω.m as used for the horizontal circuit.

As the separation increases, the magnitude of the induced LEF due to zero sequence current flow reduces from it's maximum value immediately below the transmission line which occurs here as the cable is closest to the line conductors. With balanced sequence current flow there is a minimum within several hundred metres of the line. This is caused by cancellation of the individual fields from the line conductors and their return paths. The location of the local minimum is frequency and earth resistivity dependant.

The sequence ratios shown in Figure 5.9 are a maximum immediately below the transmission line and reduce to a minimum at a separation the same as that shown in Figure 5.8. The ratio then increases asymptotically to a constant value. This effect can be predicted using the complex penetration formula (Gary, 1976) and the Vertical Inducing Loop model (Chapter 7).

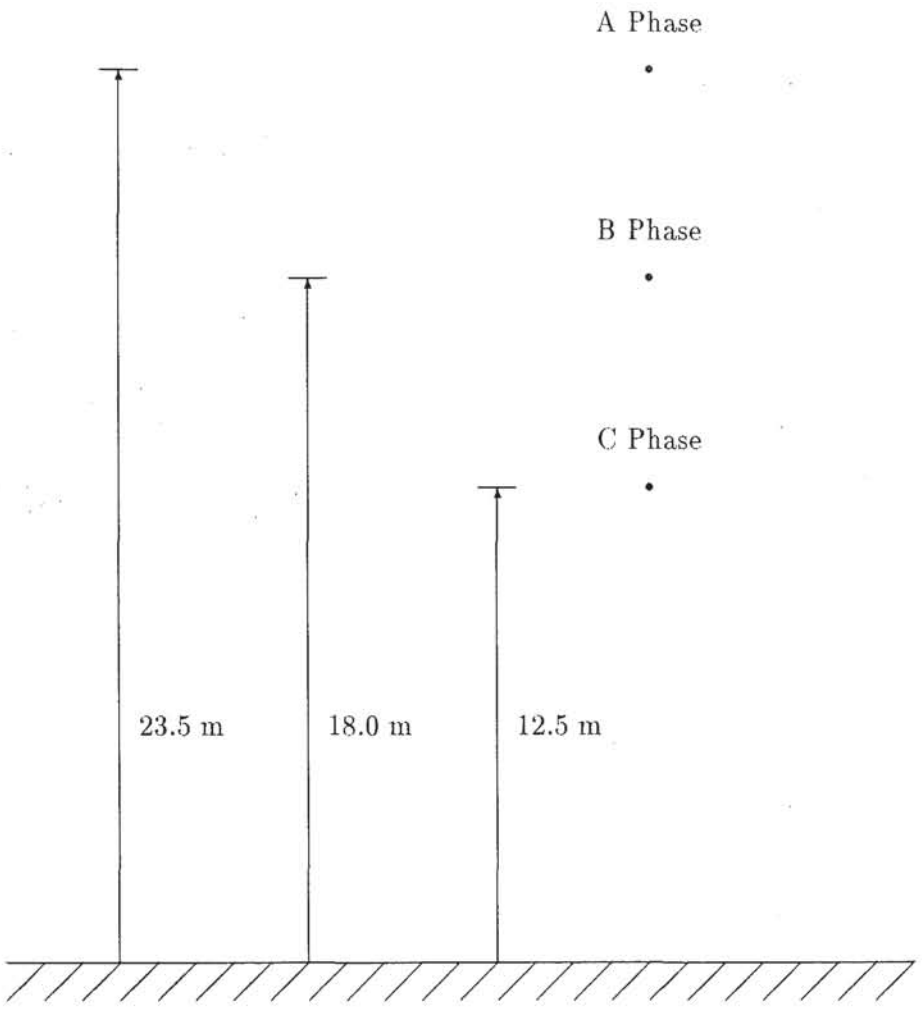

Line data

Name	:	Standard Vertical Test Circuit
Nominal voltage	:	220 kV
Coordinates of A phase conductor	:	(0.00 m, 23.5 m)
Coordinates of B phase conductor	:	(0.00 m, 18.0 m)
Coordinates of C phase conductor	:	(0.00 m, 12.5 m)
Conductor Type	:	Zebra

Figure 5.7. Standard Vertical Test Circuit Line Geometry

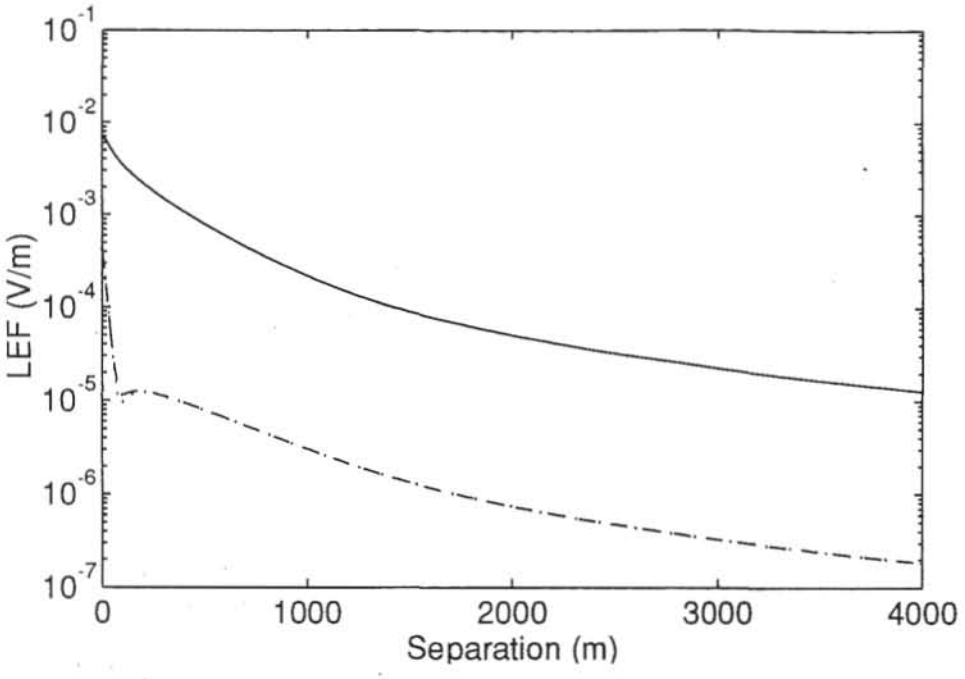

Figure 5.8. Magnitude of the LEF induced by the Positive (dotted line), Zero (solid line) and Negative (dashed line) Sequence Current Flows in the Vertical Line Configuration for an Earth Resistivity of 200 Ω.m and Frequency of 600 Hz as a Function of Separation

Equation (5.3) states that the far field induced by a vertical loop of circulating current is proportional to conductor current, the square of the vertical distance between the filaments and decays as the reciprocal of the separation squared. In the case of zero sequence current flow the fields from each loop formed by the conductors and their return paths add constructively and hence the far field will decay as $\frac{1}{(x-x_c)^2}$. Far fields induced by balanced sequence current flow cancel one another. If the line conductors lie in the same plane then the inducing loops will be the same size and extreme cancellation will occur. The far field is not zero in this case, but simply decays at a rate greater than $\frac{1}{(x-x_c)^2}$ (Chapter 7). If the line conductors lie in different horizontal planes then extreme cancellation will not occur (unless multiple conductors are used per phase such that the average conductor height per phase is the same), and the field will decay at the rate of $\frac{1}{(x-x_c)^2}$. Therefore when the phase conductors lie in the same horizontal plane the ratio of balanced to zero sequence LEF will decrease with separation. When when they lie in different horizontal planes the sequence ratios will tend to a constant with increasing separation.

The constant ratio is between 0.14 - 8.5 % for the range of frequencies and earth resistivities considered. Balanced current flow in any transmission line in which the conductors are in different horizontal planes will contribute a constant proportion of the total LEF magnitude at moderate separations, regardless of the actual separation.

5.5.1 Effect of Earth Resistivity

As the earth resistivity is increased there is a larger increase of the level of zero sequence induction when compared with that due to balanced current flow as shown in Figure 5.10. The separation at which the asymptotic ratio is reached and the separation

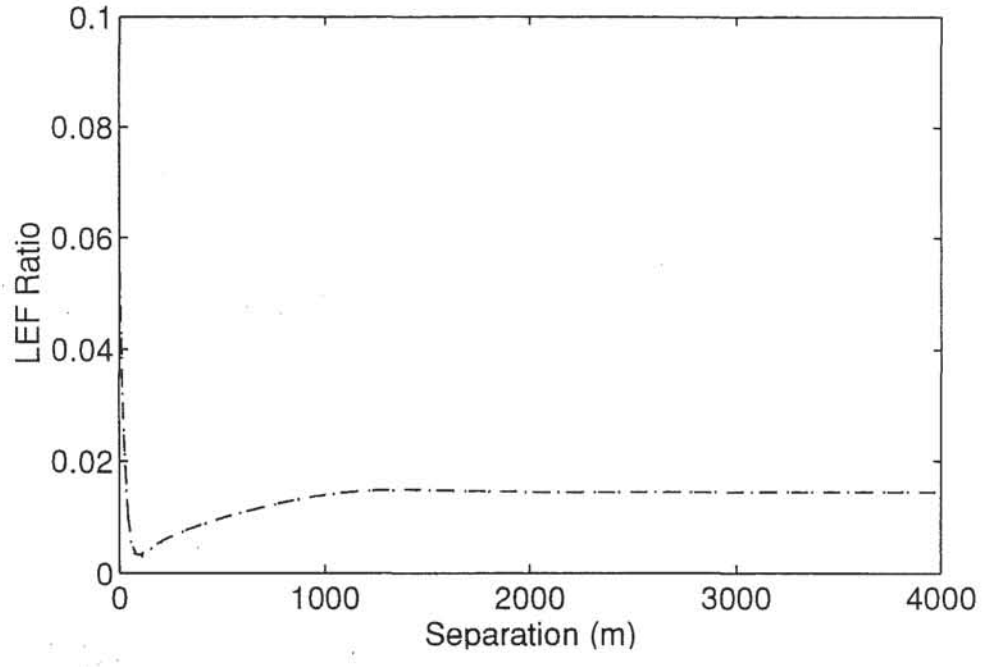

Figure 5.9. Positive/Zero (dotted line) and Negative/Zero (dashed line) LEF Sequence Ratios induced by the Vertical Line Configuration for an Earth Resistivity of 200 Ω.m and Frequency of 600 Hz as a Function of Separation

at which the minimum sequence ratio occurs, are also increased.

5.5.2 Effect of Frequency

The increase in the magnitude of the induced longitudinal electric field due to balanced sequence currents as the frequency is increased is significantly greater than that for zero sequence currents. The amount by which the magnitude of the LEF increases is dependant on the separation, generally reducing with increasing separation to a constant value. Differences are also observed between the induced voltages due to positive and negative sequence currents, particularly when the depth of return is shallow.

These trends are reflected in the magnitude ratios, shown in Figure 5.11. The separation at which the minimum sequence ratio occurs, and the separation at which the ratio reaches 98% of its asymptotic value decrease as the frequency is increased.

5.5.3 Effect of Conductor Spacings

The vertical spacings of the conductors were varied so that the mean conductor height above the ground was kept constant. The magnitude of the induced LEF due to zero sequence current flow in the transmission line remains largely unaffected by variations in conductor spacing. There are some slight differences in the immediate vicinity of the line due to the closer spacing of the lowest inducing conductor with regard to the cable. However the magnitude of the induced longitudinal electric field due to balanced current flow varies in proportion to the percentage change in spacing of the conductors, because inter-conductor spacings are the dominant factor influencing balanced current induction. When the spacing is increased, the differences between the induced fields

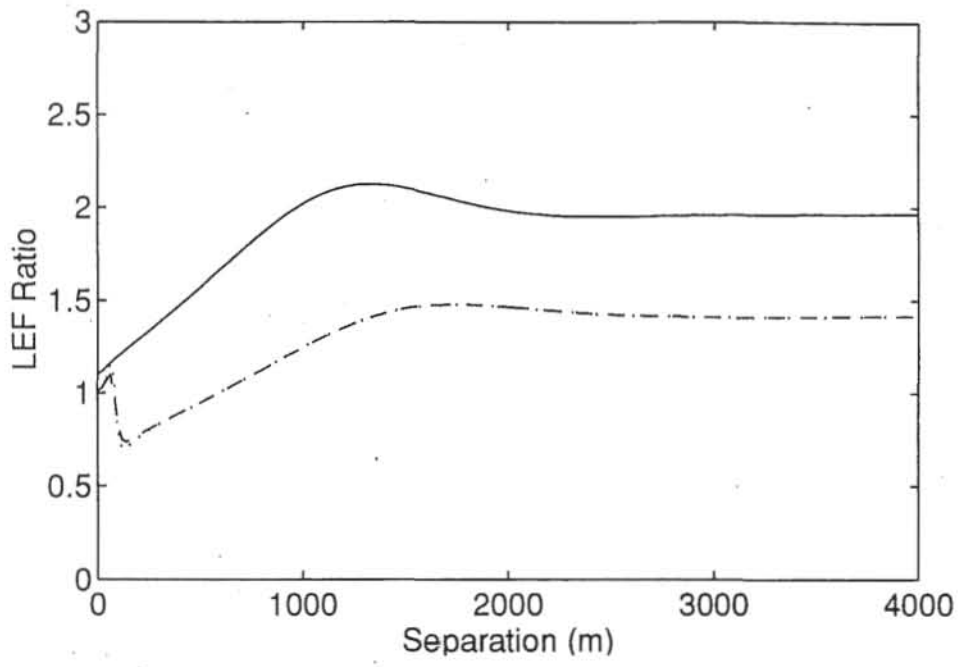

Figure 5.10. Ratio of Perturbed/Unperturbed LEF from Vertical Line as a function of Separation when the Resistivity of the Earth is Doubled. (Positive sequence - dotted line, Zero sequence - solid line, Negative sequence - dashed line)

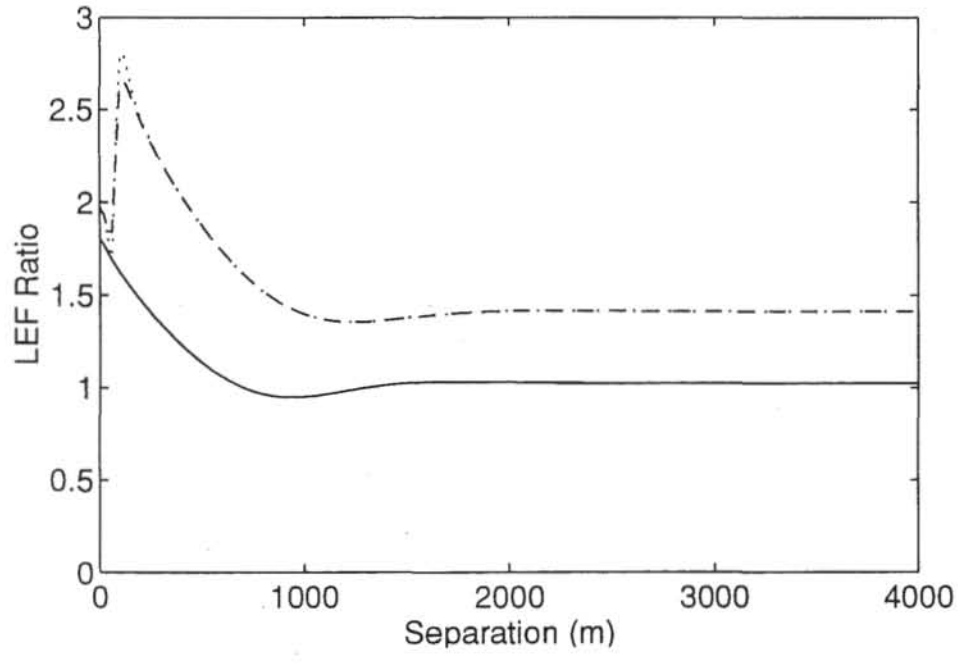

Figure 5.11. Ratio of Perturbed/Unperturbed LEF from Vertical Line as a function of Separation when the Frequency is Doubled. (Positive sequence - dotted line, Zero sequence - solid line, Negative sequence - dashed line)

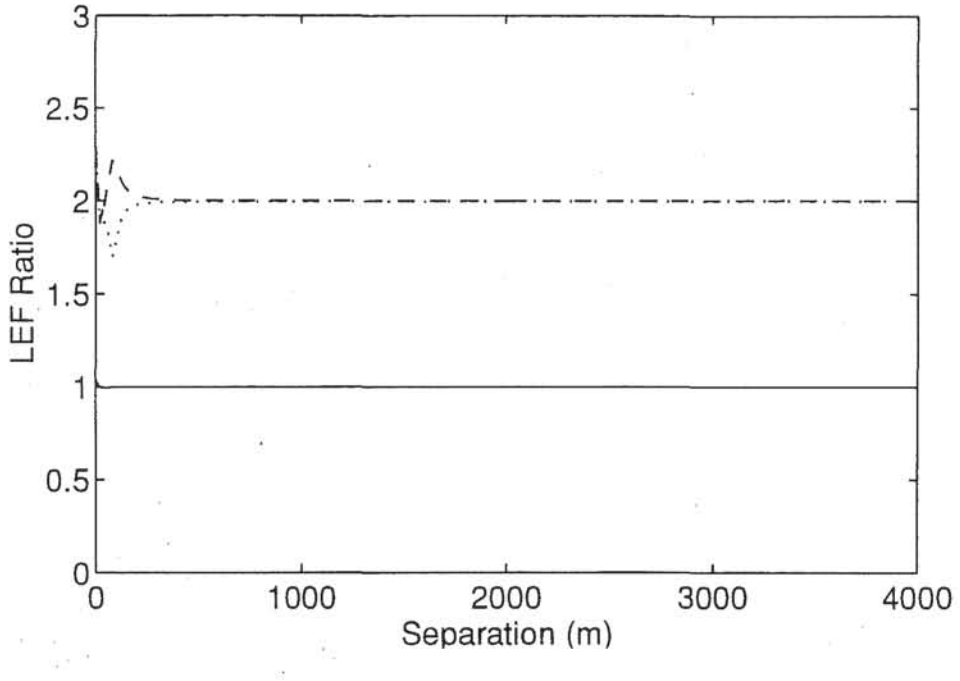

Figure 5.12. Ratio of Perturbed/Unperturbed LEF from Vertical Line as a function of Separation when the Inter-conductor Spacings are Doubled (Positive sequence - dotted line, Zero sequence - solid line, Negative sequence - dashed line)

due to positive or negative sequence currents become more obvious. This is due to the strong dependence of the mutual impedances on conductor height. Consequently the variation of the mutual impedances is greater, resulting in an increased sensitivity to the sequence of the current flow.

The resulting magnitude ratios, are shown in Figure 5.12. The separations at which the minimum occurs and the ratio reaches 98% of its asymptotic value remain constant. However the asymptotic value changes as the conductor spacings are changed.

5.5.4 Asymptotic Line Ratios

A family of curves of the asymptotic ratio as a function of frequency for a variety of earth resistivities is shown in Figure 5.13. The asymptotic ratio can be seen to increase as the frequency increases, while decreasing as the earth resistivity increases. The variation of the asymptotic ratio is large, ranging from 0.14 % to 8.5 % for the range of frequencies and earth resistivities shown. The ratio is maximised when the equivalent depth of return is minimised. Asymptotic ratios of the order of 1 % to 4 % are evident for the standard vertical test circuit above an earth plane of 200 Ω.m earth resistivity. The ratio decreases very rapidly as the earth resistivity is increased. For realistic earth resistivities the ratio is less than 7 %. When the average height of the conductors above the earth is kept constant, the asymptotic ratio is linearly proportional to the vertical distance between the conductors.

The separation at which the line ratio reaches 98% of its asymptotic value is approximately linearly proportional to the depth of the earth return current, and hence is frequency and earth resistivity dependant. Example values are shown in Table 5.1. In general the ratio reaches 98% of its asymptotic value within two kilometres of the

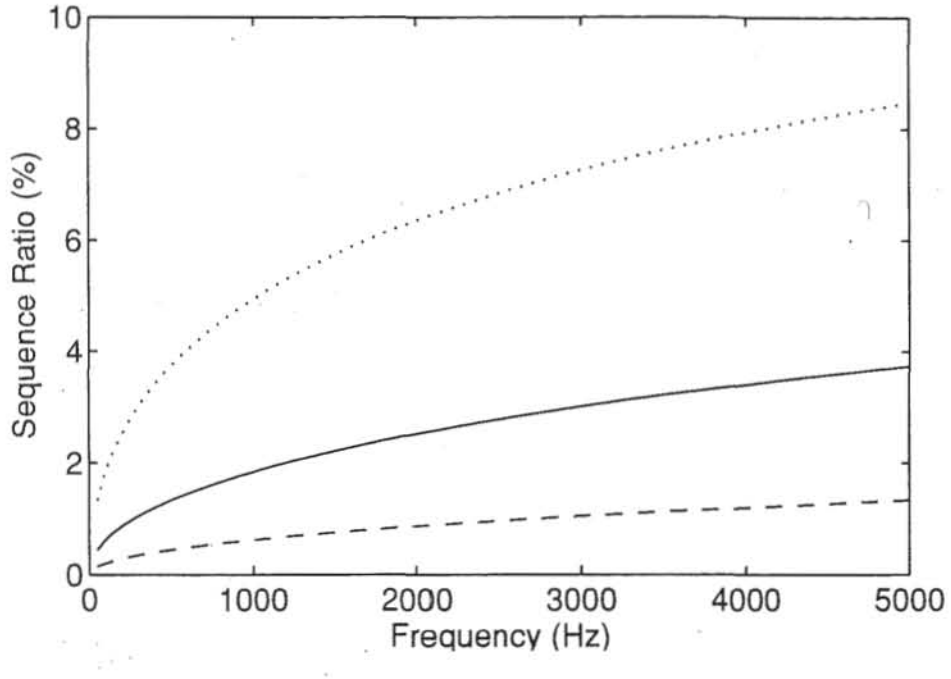

Figure 5.13. Asymptotic Positive/Zero (dotted line) and Negative/Zero (dashed line) LEF Sequence Ratios induced by the Vertical Line Configuration for Earth Resistivities of 20, 200 and 200 Ω.m as a Function of Frequency

Frequency (Hz)	Earth Resistivity (Ω.m)	Separation (m)	Skin Depth (m)
2500	10	270	58
1000	10	230	84
50	10	820	331
2500	500	820	331
1000	500	1270	516
50	500	5660	2263

Table 5.1. Cable-line Separations for which the sequence ratio reaches 98% of its asymptotic value

transmission line for harmonic currents which are likely to cause significant interference to communication cables.

5.5.5 Double Circuit Tower with One Circuit Installed

For a practical, installed line, a single vertical circuit is likely to have its conductors lying in different vertical planes. Such an arrangement is that of the Invercargill to Manapouri 220 kV transmission line as shown in Figure 5.14 with only circuit one installed.

The magnitude of the induced longitudinal electric field due to zero sequence current flow is practically identical to that of the vertical transmission line. Those induced by balanced currents are different due to the asymmetry of the line, but the average is very close to that induced by the vertical transmission line.

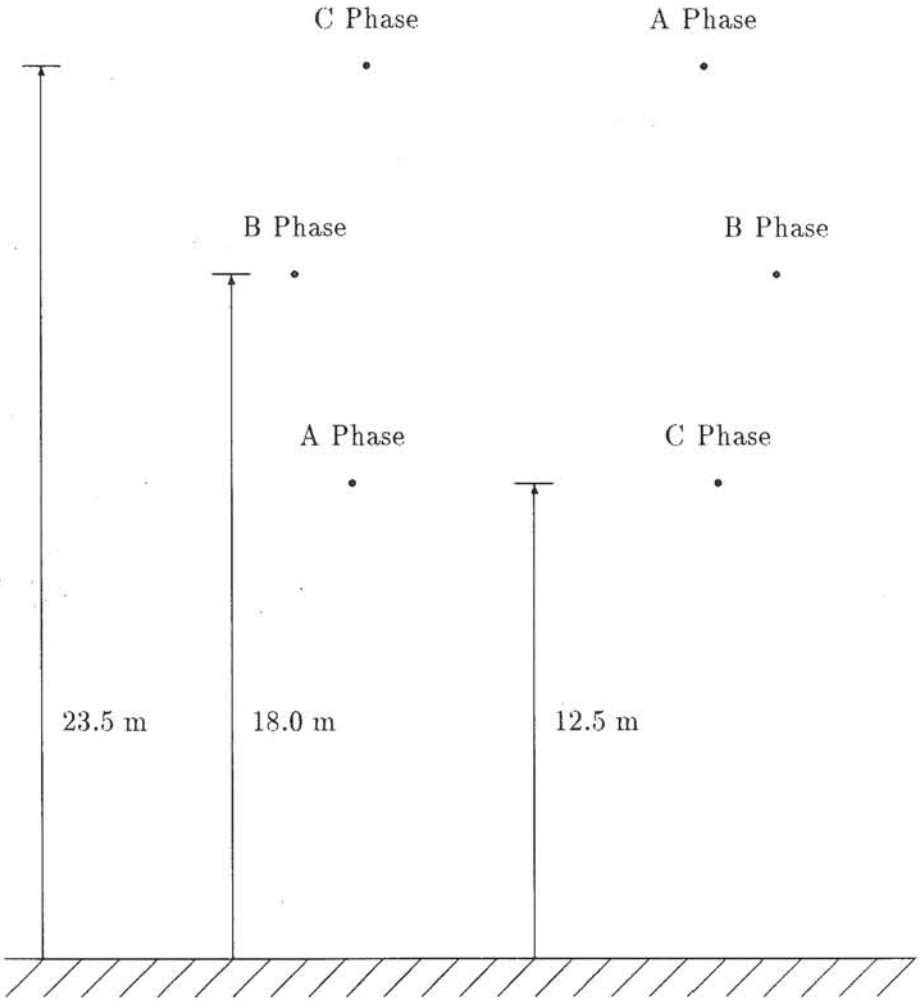

Line data

Name	:	Invercargill - Manapouri Double Circuit (excluding earth wires)
Nominal voltage	:	220 kV
Circuit 1		
Coordinates of A phase conductor	:	(4.42 m, 23.5 m)
Coordinates of B phase conductor	:	(6.33 m, 18.0 m)
Coordinates of C phase conductor	:	(4.80 m, 12.5 m)
Circuit 2		
Coordinates of A phase conductor	:	(-4.80 m, 12.5 m)
Coordinates of B phase conductor	:	(-6.33 m, 18.0 m)
Coordinates of C phase conductor	:	(-4.42 m, 23.5 m)
Conductor Type	:	Zebra

Figure 5.14. Double Circuit Transmission Line Geometry

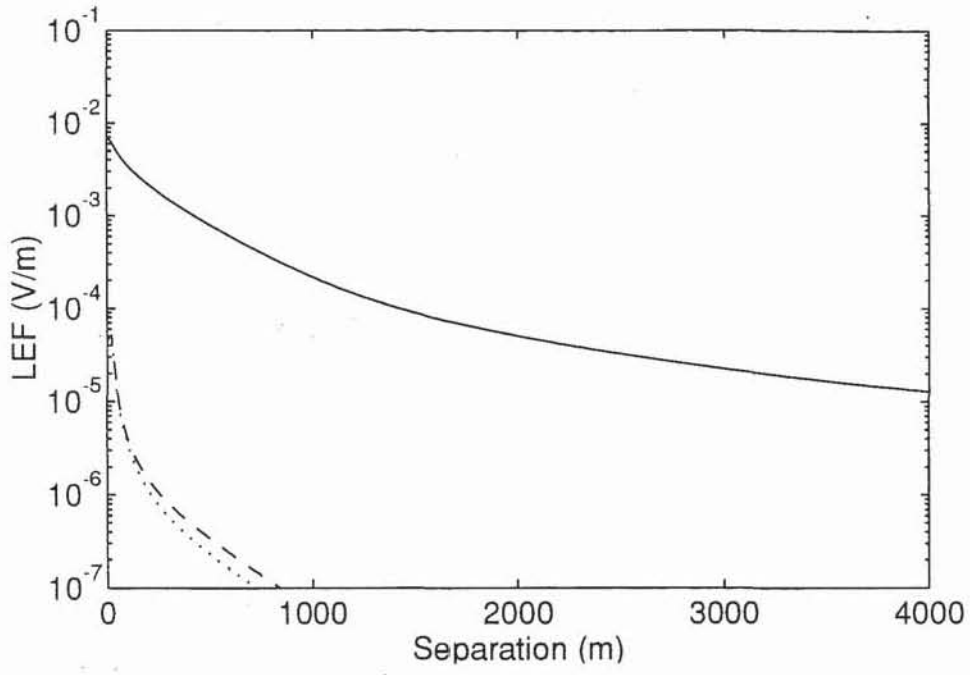

Figure 5.15. Magnitude of the LEF induced by the Positive (dotted line), Zero (solid line) and Negative (dashed line) Sequence Current Flows in the Double Circuit Line Configuration for an Earth Resistivity of 200 Ω.m and Frequency of 600 Hz as a Function of Separation

5.6 Double Circuit Line Configuration

A double circuit line with a conductor arrangement known as the centre-point-symmetric line links Invercargill and Manapouri. This is shown in Figure 5.14.

The induced longitudinal electric field shown in Figure 5.15 due to zero sequence current flow in the transmission line reaches a maximum immediately below each circuit, and reduces as the separation is increased. Those due to balanced sequence currents have a local minimum at the tower centreline, then increase to a global maximum within a short distance on either side of the line. A local minimum occurs at a larger separation when the effective depth of return is shallow. For separations greater then this, the magnitude of the LEF decreases.

In Figure 5.16 the sequence ratios are presented. These follow the same form as the magnitude graphs for the balanced sequence currents. Of particular interest is that the ratio does not tend to a constant non-zero value as the separation tends to infinity. This effect is due to the cancellation of the fields due to the phase conductor arrangement on the tower.

When the earth resistivity is increased the longitudinal electric fields induced by positive and negative sequence currents show increased differences in magnitude as compared to the vertical or single circuit line. These effects are shown in Figure 5.17. Also it is the balanced sequence line ratios, as shown in Figure 5.18, that show significant differences from the single circuit case.

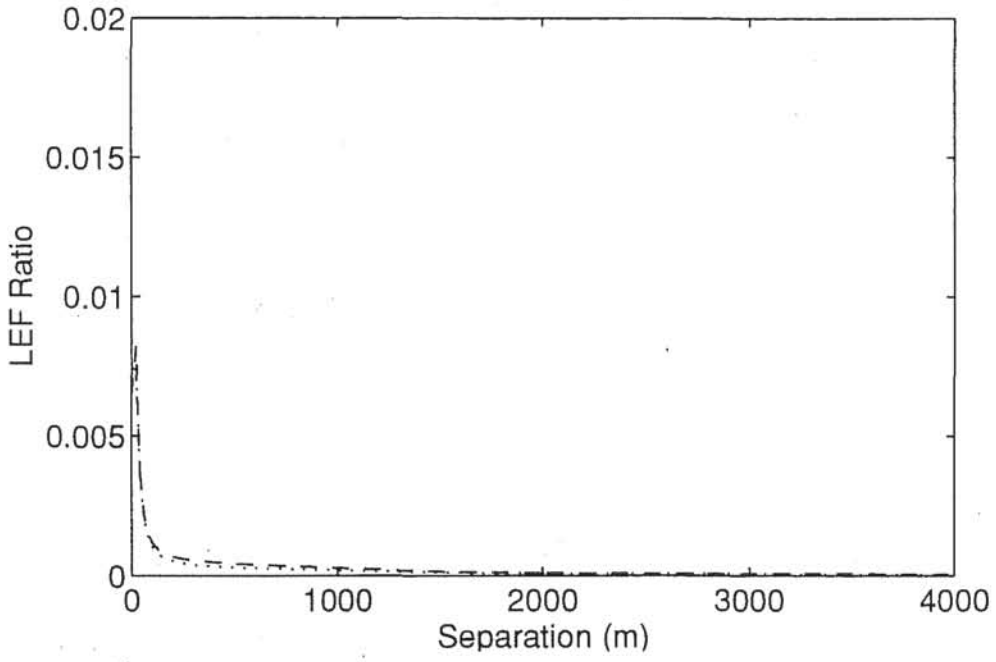

Figure 5.16. Positive/Zero (dotted line) and Negative/Zero (dashed line) LEF Sequence Ratios induced by the Double Circuit Line Configuration for an Earth Resistivity of 200 Ω.m and Frequency of 600 Hz as a Function of Separation

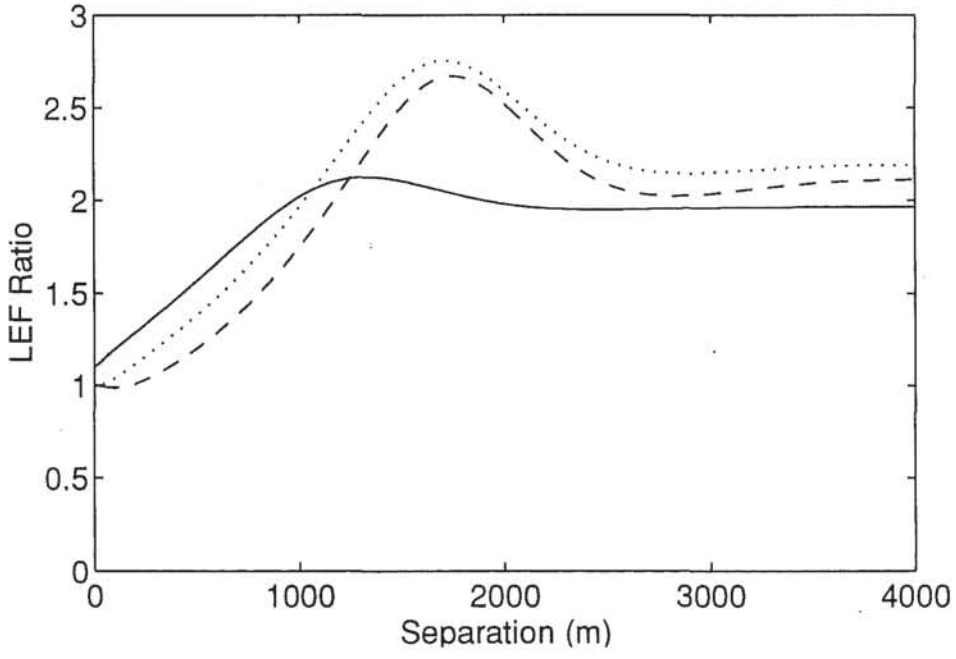

Figure 5.17. Ratio of Perturbed/Unperturbed LEF from Double Circuit Line as a function of Separation when the Resistivity of the Earth is Doubled. (Positive sequence - dotted line, Zero sequence - solid line, Negative sequence - dashed line)

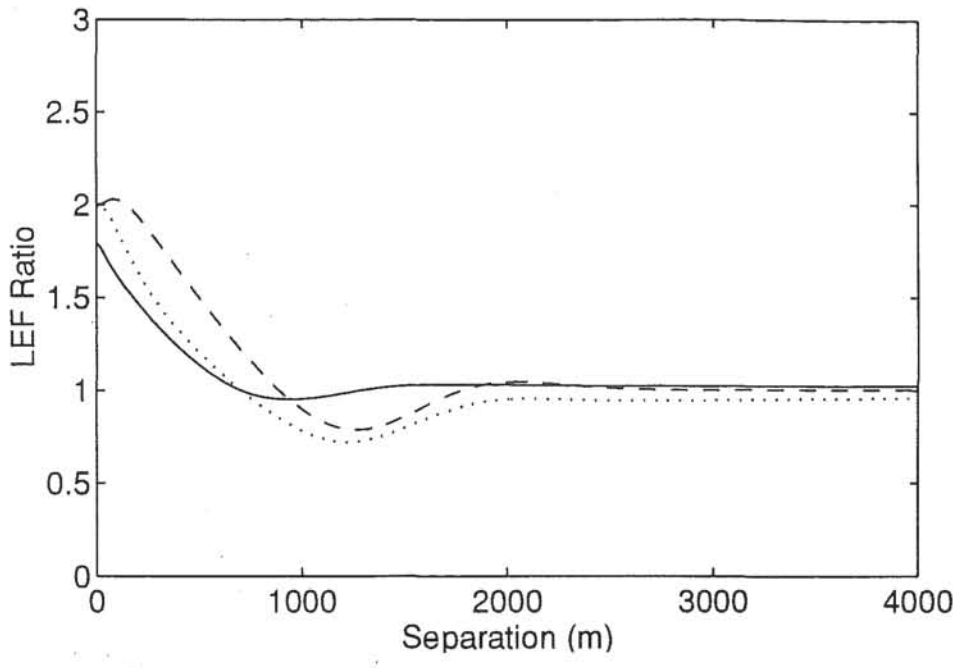

Figure 5.18. Ratio of Perturbed/Unperturbed LEF from Double Circuit Line as a function of Separation when the Frequency is Doubled. (Positive sequence - dotted line, Zero sequence - solid line, Negative sequence - dashed line)

Line Type	Current Sequence	Near Field	Far Field
Horizontal	Balanced	$\propto \omega$	independent
Horizontal	Zero	nearly $\propto \omega$	independent
Vertical	Balanced	$\propto \omega$	$\propto \sqrt{\omega}$
Vertical	Zero	nearly $\propto \omega$	independent

Table 5.2. Dependency of the LEF on Angular Frequency

5.7 Summary of the Near and Far Field Dependencies of Multiconductor Transmission Lines

Tables 5.2 to 5.5 summarise the observed relationships between the inductive influence of multiconductor transmission lines and frequency, earth resistivity, horizontal and vertical conductor spacings and current sequence.

In these tables transmission line geometries are classified as being *Horizontal* or *Vertical* depending on whether all current carrying conductors lie in the same horizontal plane or not. All transmission line geometries studied have the field dependencies described in the tables except for vertical double circuit transmission lines with centre-point symmetric phasing when carrying balanced sequence currents equally distributed between the two circuits.

A further distinction in the Tables has been made between *Near Field* and *Far Field* effects (defined in Chapter 4 as the LEF dependencies are quite different in the immediate vicinity of the line to those at moderate to large separations.

Line Type	Current Sequence	Near Field	Far Field
Horizontal	Balanced	independent	$\propto \rho_e$
Horizontal	Zero	slight increase	$\propto \rho_e$
Vertical	Balanced	independent	$\propto \sqrt{\rho_e}$
Vertical	Zero	slight increase	$\propto \rho_e$

Table 5.3. Dependency of the LEF on Earth Resistivity

Line Type	Current Sequence	Near Field	Far Field
Horizontal	Balanced	large increase	$\propto$ % increase
Horizontal	Zero	independent	independent
Vertical	Balanced	large increase	$\propto$ % increase
Vertical	Zero	independent	independent

Table 5.4. Dependency of the LEF on Increased Inter-conductor Spacings

5.8 Methods for Reducing the Inductive Influence of Multiconductor Transmission Lines

The inductive influence of a high voltage transmission line may be reduced by:

- reducing the magnitude of interfering currents on the line,
- increasing the separation between power and telecommunication systems
- rearranging the transmission line conductors,
- lowering the effective resistivity of the earth,
- adding continuously grounded earth wires to transmission lines.

This thesis is not concerned with methods for reducing harmonic current flows within power systems. Nevertheless reductions of inductive influence in direct proportion to the change in current magnitude will result from reducing the harmonic currents.

Greatest emphasis should be placed upon the removal of high order harmonics where interference is occurring to telecommunications systems in close proximity to transmission lines, as the coupling is approximately directly proportional to frequency in this region Table 5.2.

In the far field region the coupling for balanced sequence current in vertical transmission lines is approximately proportional to the $\sqrt{\omega}$ and therefore high order harmonic currents warrant greater attention than low order harmonic currents of the same

Line Type	Current Sequence	Near Field	Far Field
Horizontal	Balanced	large decrease	independent
Horizontal	Zero	slight decrease	independent
Vertical	Balanced	large decrease	independent
Vertical	Zero	slight decrease	independent

Table 5.5. Dependency of the LEF on Increased Average Conductor Height

magnitude. The far fields induced by zero sequence current, and balanced currents in horizontal lines are substantially independent of frequency however.

Zero sequence current flow will generally be the dominant component of the far field LEF induced by vertical transmission lines, unless the balanced sequence current exceeds the zero sequence current flow by an order of magnitude. In the near field region the inductive influence of balanced sequence currents can not be neglected. Detailed mathematical models of the induction between the line and telecommunication cable must be used in this case as the destructive interference of the individual conductor fields can result in rapid field variations with distance from the line.

Preferred transmission line geometries and power telephone separations can be determined by examination of Equation (5.1). The field induced by a pair of filaments is proportional to the logarithm of the ratio of the radial separations from each filament. To reduce the inductive influence of this system it is necessary to make the ratio as close as possible to one. This can be achieved by maximising the separation of the cable from the transmission line, or moving the filaments closer together.

The best way to avoid inductive coordination problems is to maximise the separation between the power and telecommunication systems. The improvement gained in the far field region is expected to be of the order of $\frac{1}{(x-x_c)^2}$. Care needs to be exercised when locating cables near transmission lines carrying balanced sequence currents as greater separation does not always result in lower LEF in the near field region.

To reduce zero sequence induction it is necessary to bring the conductor filaments and earth return filaments closer together. This may be achieved by lowering the height of the conductors or decreasing the resistivity of the earth.

The range of possible conductor heights are limited in practice by insulation and safety requirements. Furthermore the conductor height is generally low in relation to the skin depth of the earth, and therefore the improvement gained is slight.

It is not practical to create and maintain a region of low earth resistivity below a transmission line. Nevertheless consideration should be given to the siting of transmission lines to exploit areas of low resistivity where possible. The expected improvement in the far field LEF is proportional to the earth resistivity change for both balanced and zero sequence currents Table 5.3. No significant changes to the near field LEF result from reducing the resistivity.

The LEF induced by balanced sequence current flow is sensitive to inter-conductor spacings as the field induced by the line filaments interfere with one another. Reducing the interconductor spacings reduces the far field induction in proportional to the magnitude of the change Table 5.4. Insulation requirements limit the reductions that can be achieved however.

The installation of continuously grounded earth wires as a means for reducing the inductive influence of transmission lines is addressed in Chapter 6.

5.9 Conclusion

The contribution to the total longitudinal electric field induced around a transmission line due to zero sequence current flow in the line is largely independent of the geometrical and electrical arrangement of the conductors. The LEF induced by a zero sequence current flowing in a horizontal transmission line becomes the dominant contributor to the total LEF at large separations. However for transmission lines in which the conductors lie in different horizontal planes, the proportion of the total field contributed by the LEF induced by balanced and zero sequence currents is fixed in the far field region. Therefore the induced LEF due to zero sequence current flow is not necessarily the dominant interfering field at large separations. The only exception to

this statement is the case when the geometric and electrical arrangement of the conductors on the tower have been chosen so that the fields due to balanced currents cancel at large separations. This is the case with the centre point symmetric arrangement.

The most effective ways to reduce the inductive influence of a high voltage transmission line are to reduce the magnitude of harmonic currents propagating along the line (in particular the zero sequence components), and to maximise the separation between power and telecommunication systems.

CHAPTER 6

SHIELDING OF TRANSMISSION LINES

6.1 Introduction

The technique of shielding communications cables to reduce inductive interference from neighbouring transmission lines is well established (Klewe, 1958), however the installation of aerial shielding conductors on high voltage transmission lines to protect neighbouring communications circuits is less well known and accepted.

Effective shielding using aerial conductors imposes strict constraints on the shielding conductor parameters. This can be demonstrated by considering the situation in Figure 6.1.

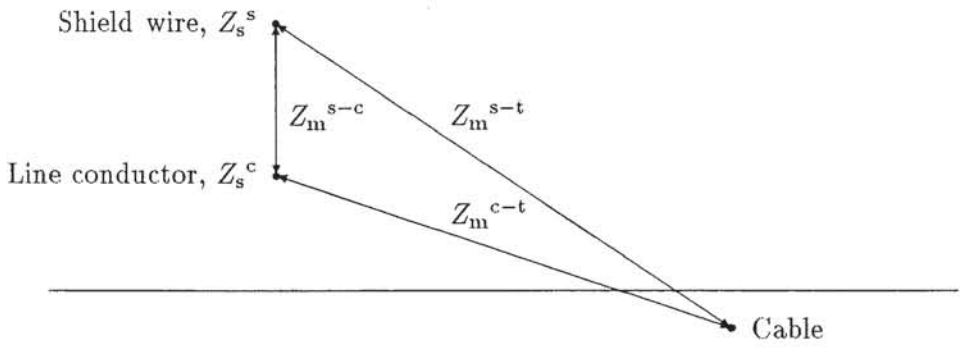

Where

Z_m^{c-t} = Mutual impedance between the line conductor and the telecommunications cable ($\Omega.m^{-1}$)

Z_m^{s-t} = Mutual impedance between the shield wire and the telecommunications cable ($\Omega.m^{-1}$)

Z_m^{s-c} = Mutual impedance between the shield wire and the line conductor ($\Omega.m^{-1}$)

Z_s^s = Self impedance of the shield wire ($\Omega.m^{-1}$)

Z_s^c = Self impedance of the line conductor ($\Omega.m^{-1}$)

Figure 6.1. Shielding of a Single Conductor Transmission Line

Conductor Type	Inside Radius (mm)	Outside Radius (mm)	Current Capacity (A)	D.C. Resistance ($\Omega.km^{-1}$)	Geometric Mean Radius (mm)
7/3.18 GEHSS		9.52		4.00000	0.000003
MINK ACSR	3.66	10.97	60	0.47290	1.49
ZEBRA ACSR	9.54	28.58	400	0.07009	11.55
CHUKAR ACSR	11.10	40.69	875	0.03134	16.34

Table 6.1. Parameters of the Shielding Conductors

In the absence of the shielding conductor, the longitudinal electric field at the cable for a current I in the line conductor is

$$\text{LEF} = -I_c {Z_m}^{c-t} \tag{6.1}$$

With the shielding conductor present and perfectly grounded at the ends, the induced electric field is

$$\text{LEF} = -I_c {Z_m}^{c-t} \left(1 - \frac{{Z_m}^{s-c} {Z_m}^{s-t}}{{Z_s}^{s} {Z_m}^{c-t}}\right) \tag{6.2}$$

If the shielding conductor is close to the line conductor, then ${Z_m}^{c-t}$ is approximately equal to ${Z_m}^{s-t}$, and the induced electric field at the cable becomes (Prevost and André, 1950);

$$\text{LEF} = -I_c {Z_m}^{c-t} \left(1 - \frac{{Z_m}^{s-c}}{{Z_s}^{s}}\right) \tag{6.3}$$

From this equation it is apparent that screening will be optimal when the mutual impedance between the line and shielding conductors (${Z_m}^{s-c}$) is equal to the self impedance of the shielding conductor (${Z_s}^{s}$). When this condition is satisfied the current in the shielding conductor is of the same magnitude as the current in the line conductor but 180 degrees out of phase.

The self impedance of a conductor is dependant on many factors, such as the conductor size, geometry, material, position, parameters of the earth, and frequency. It may also exhibit a non-linear impedance variation with current, if the conductor is made of ferrous material. The mutual impedances are only dependant on the conductor geometry, the parameters of the earth, and frequency. Therefore in practice it is very difficult to match the mutual and self impedances, due to the wide range of conditions under which shielding from harmonic currents in transmission lines must be provided.

The dependence of the shielding effectiveness on the parameters listed above implies that it is difficult to conduct a general analysis of the affects of shielding conductors on the magnetically induced electric field near transmission lines. Therefore the study was restricted to the four types of shielding conductor listed in Table 6.1, and three transmission line geometries.

The transmission lines studied are assumed to be infinitely long and uniform, therefore the grounding impedance of the shielding wire at each pylon may be neglected. For finite or non-uniform lines the ground connections will increase the impedance of the shielding circuit reducing it's effectiveness.

6.2 Horizontal Transmission Line

The Invercargill to Roxburgh 220 kV line in the New Zealand South Island system was used for this study. The arrangement of the conductors on this line is given in Figure 6.2.

6.2.1 Performance with Conventionally Placed GEHSS Shield Wires

The magnitude of the induced electric field from this transmission line varies in a similar manner with separation, to the induced electric field from the transmission line in the absence of shield wires.

Line ratio graphs are presented in Figure 6.3 which shows the ratio of the electric field induced by the line with shield wires to that induced by the line without shield wires. There is a slight reduction in the magnitude of the field due to zero sequence current flow in the transmission line over the range of separations studied. However the induced fields due to balanced currents are generally larger with shield wires, except in the immediate vicinity of the line. These increase linearly at large separations. There is also a significant difference between the line ratios due to positive and negative sequence currents in this region. This difference tends to a constant value as the separation is increased.

Although the magnitude of the constant asymptotic line ratio for zero sequence current flow and the slope of the line ratio graphs for the balanced sequence currents are frequency and earth resistivity dependant, separately changing the earth resistivity and the frequency by factors of 2 yields results very similar to those depicted in Figure 6.3.

The line ratio graphs suggest that at large separations balanced sequence currents may induce larger electric fields than zero sequence currents of the same magnitude. In Figure 6.4 the sequence ratios, which are the ratio of the field induced by a positive or negative sequence current to that induced by a zero sequence current, are presented. These ratios decay asymptotically to a constant value as the separation tends to infinity. The magnitude of this constant ratio is less than 0.6% for frequencies between 50 and 2500 Hz, and earth resistivities between 10 and 1000 Ω.m. Thus the balanced sequence currents will need to be 160 times greater than the zero sequence current in the line with shield wires to induce comparable fields at large separations.

6.2.2 Influence of Conductor Self Impedance

In Table 6.2 the mutual and self impedances for the phase conductors and the GEHSS shield wires in the transmission line are presented.

It is apparent that at 50 Hz the shielding may be improved by reducing the resistive component of the self impedance of the shield wires. At 2500 Hz the magnitude of the impedance of the shield wire is too large, although the angle is acceptable. The self impedance of the phase conductors at these frequencies is much lower than that of the shielding conductors, and at 50 Hz the impedance angle is greater than that of the shielding conductors. Thus replacing the GEHSS shield wires with low impedance ACSR conductors would be expected to improve the shielding of the line.

The line ratio graph for the horizontal transmission line with "MINK" ACSR shield wires is similar to Figure 6.3. However the zero sequence induction is reduced further, and the slope of the line ratio due to balanced sequence current flow is increased. These effects are due to larger shield wire currents. The constant sequence ratio is less than 1.6% for frequencies between 50 and 2500 Hz, and earth resistivities from 10 to 1000

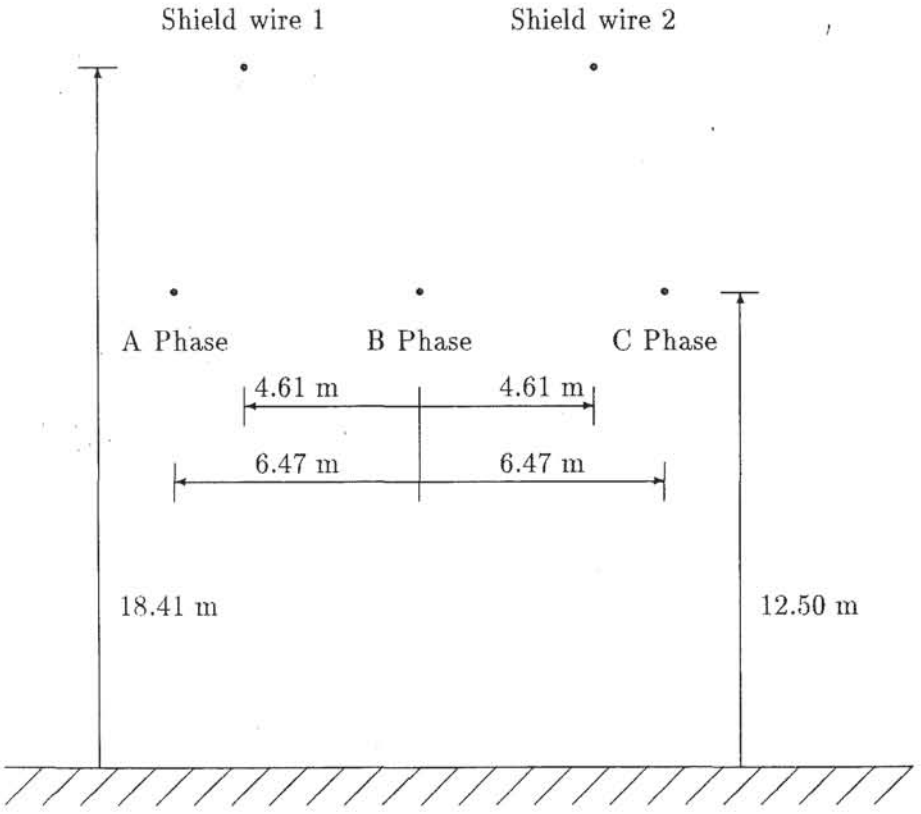

Line data

Name	:	Invercargill - Roxburgh Circuit 1
Nominal voltage	:	220 kV
Coordinates of A phase conductor	:	(-6.47 m, 12.50 m)
Coordinates of B phase conductor	:	(0.00 m, 12.50 m)
Coordinates of C phase conductor	:	(6.47 m, 12.50 m)
Coordinates of Shield Wire 1	:	(-4.61 m, 18.41 m)
Coordinates of Shield Wire 2	:	(4.61 m, 18.41 m)
Phase Conductor Type	:	Zebra
Shield Wire Type	:	GEHSS

Figure 6.2. Invercargill-Roxburgh 220 kV Line

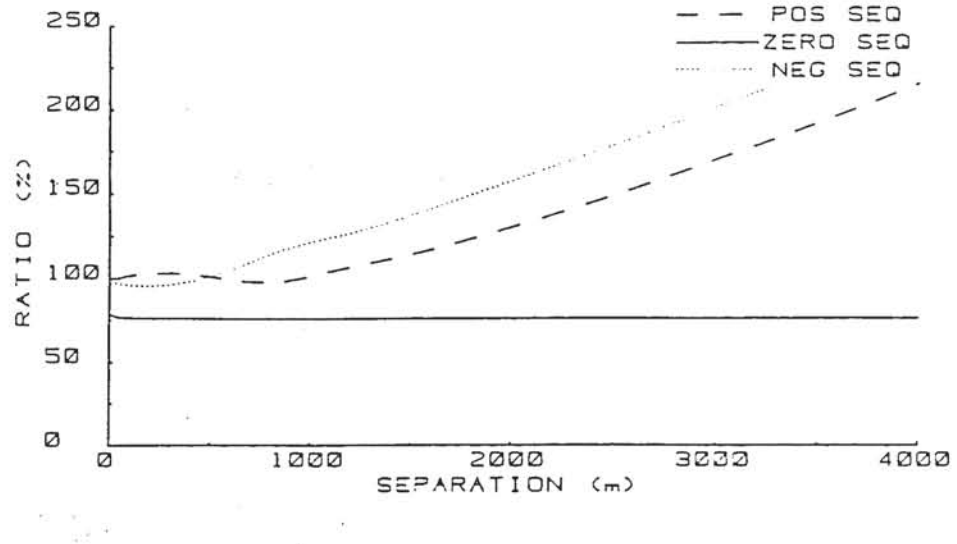

Figure 6.3. Line ratios for the horizontal line with GEHSS shield wires: earth resistivity - 100 Ω.m, frequency - 1000 Hz

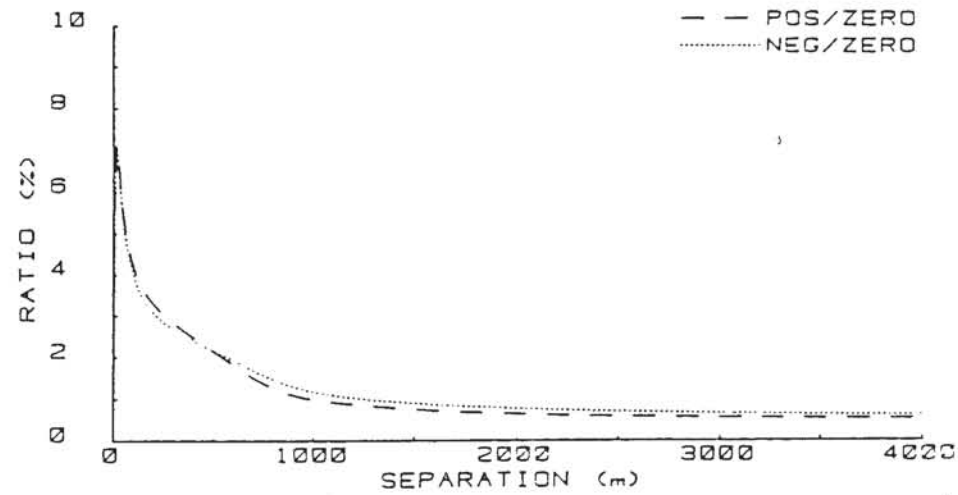

Figure 6.4. Sequence ratios for the horizontal line with GEHSS shield wires: earth resistivity - 100 Ω.m, frequency 1000 Hz

Name	50HzImpedance ($\Omega.km^{-1}$)	2500HzImpedance ($\Omega.km^{-1}$)
Phase Conductor Self Impedance	0.72 ∠ 81 lag	29.9 ∠ 86 lag
A Phase to Shield Wire One C Phase to Shield wire Two	0.32 ∠ 81 lag	10.4 ∠ 79 lag
B Phase to Shield Wire One B Phase to Shield Wire Two	0.32 ∠ 81 lag	9.8 ∠ 78 lag
C Phase to Shield Wire One A Phase to Shield Wire Two	0.28 ∠ 80 lag	8.2 ∠ 76 lag
Shield Wire Self Impedance	4.38 ∠ 22 lag	77.9 ∠ 86 lag

Table 6.2. Self and mutual impedances of the conductors in the Transmission line. 100 Ω.m earth resistivity

Shield Conductor Type	Balanced Sequence Line Current (%)	Zero Sequence Line Current (%)
GEHSS	0.33	151
MINK	1.30	230
ZEBRA	0.55	54
CHUKAR	0.28	25

Table 6.3. Total Shield Wire Losses expressed as a Percentage of the Total Phase Conductor losses at 50 Hzand 100 Ω.m

Ω.m. Thus the balanced sequence currents will need to be 60 times greater than the zero sequence currents to induce comparable electric fields at large separations.

A comparison of the reduction factors for zero sequence induction from the line with the four types of shield conductor as listed in Table 6.1, relative to the line without shield wires, is given in Figure 6.5. The reduction factors are relatively constant for the range of harmonic frequencies most likely to cause interference to communications circuits and for the range of earth resistivities most likely to occur in practice. It is possible to reduce the electric field to 40% of the value induced by the line in the absence of shield wires by installing large ACSR conductors. This is a significant advantage in regions where large steady state 50 Hz voltages are induced into neighbouring conductors. Using GEHSS shield wires this figure is 70 % to 80 % due to the high resistance of these conductors. However of the four conductor types considered in Figure 6.5, only the GEHSS and the "MINK" ACSR conductors are likely to be used in practice, as the cost of using large ACSR conductors could be prohibitive.

6.2.3 Shield Wire Losses

A common criticism of shield wires is that they introduce additional losses into the transmission network (Hedman, 1968) due to current flow in the shielding conductors. The total shield wire losses, expressed as a percentage of the total phase conductor losses are listed in Table 6.3 for balanced and zero sequence phase currents.

For a line of 100 km in length, carrying a 50 Hz balanced sequence current of 400 Amperes per phase conductor, the total shield wire losses when GEHSS shield wires are used would be 11.4 kW, which is 0.007% of the power injected. If "MINK" ACSR shield wires are used then the total shield wire losses would be 48 kW, which is 0.03% of the power injected. For "ZEBRA" and "CHUKAR" ACSR shielding conductors the figures are 31 kW, 0.02 % and 24 kw, 0.016 % respectively. The losses are greater when ACSR shield wires are used despite their lower resistance. This is due to the larger

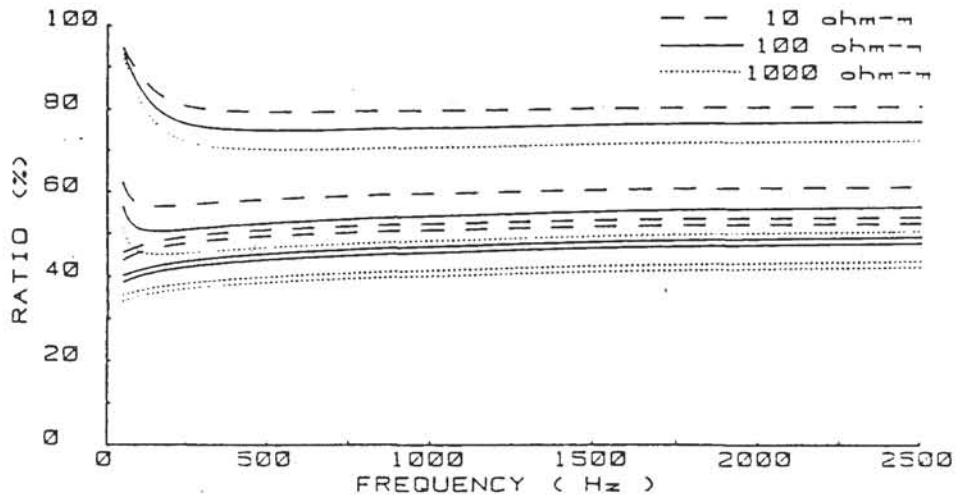

Figure 6.5. Reduction of Zero sequence induced voltage for horizontal line with 2 shield wires

currents flowing in the shield wires.

If the power is transmitted using a zero sequence mode the shield wire losses are considerably greater (Table 6.3). However the losses in the GEHSS shield wires are greater than the corresponding losses in the "ZEBRA" or "CHUKAR" ACSR shield wires.

In practice the line would carry a mixture of sequence currents and would rarely be operated at full capacity. The percentage losses then provide a realistic indication of the relative magnitude of the shield wire losses. These are significant, particularly when the line carries a zero sequence current. However they are small for this line in relation to the phase conductor losses and therefore it is unreasonable to reject the use of shield wires on this transmission line due to the increased losses which would result.

6.2.4 Relocation of the Shielding Conductors

To optimise the shielding of the transmission line, the self impedance of the shielding conductor must equal the mutual impedance between the line and shielding conductor. For the geometrical arrangement of the conductors shown in Figure 6.2, and GEHSS shielding conductors, the self impedance of the shielding conductor is greater than the mutual impedance between the line and shielding conductors (Table 6.2). By using an ACSR shielding conductor with a lower self impedance, improvements were achieved, however the self impedance of the ACSR shield conductors is still significantly greater than the mutual impedances between the phase and shielding conductors.

Consequently the behaviour of the line with repositioned shielding conductors was examined. This changes the mutual impedances between the line and shield conductors and the size of the current loop formed by the shield wires and their earth return paths. The mutual impedance variation is the most significant effect as the depth of return is very much greater than the conductor height, and therefore the size of the shield wire

current loop is not significantly changed.

The currents in the shield wires differ when balanced sequence currents flow in the transmission line due to the phase difference of the currents in the line conductors. The currents flowing in the shield wires may be divided in to the two components; a "loop" current which flows down one conductor and returns via the other (a balanced sequence current); and a common current which is of the same magnitude in both conductors (a zero sequence current). The loop current only flows when balanced sequence currents flow in the line conductors due to the symmetry of the transmission line. The loop current reduces the magnitude of the induced electric field due to balanced sequence current flow, however it increases the shield wire losses and is generally considered to be undesirable. The loop currents may be reduced by insulating and transposing the shield wires (Hedman, 1968). The zero sequence shield wire current flow acts to reduce the induction due to zero sequence current flow in the line conductors. However when the zero sequence shield wire current is induced by a balanced sequence line current, it will significantly increase the inductive influence of the line at large separations (Figure 6.3).

For balanced sequence current flow in the line conductors, the loop and common currents in the shield wires are;

$$I_{\text{s-loop}} = \frac{(Z_{\text{m}}{}^{\text{s1-ca}} - Z_{\text{m}}{}^{\text{s1-cc}})(I_{\text{c}}^{a} - I_{\text{c}}^{c})}{Z_{\text{s}}{}^{\text{s-s1}} + Z_{\text{m}}{}^{\text{s1-s2}}} \tag{6.4}$$

$$I_{\text{s-common}} = \frac{(2Z_{\text{m}}{}^{\text{s1-cb}} - Z_{\text{m}}{}^{\text{s1-ca}} - Z_{\text{m}}{}^{\text{s1-cc}})I_{\text{c}}^{b}}{2(Z_{\text{s}}{}^{\text{s-s1}} - Z_{\text{m}}{}^{\text{s1-s2}})} \tag{6.5}$$

where

$I_{\text{s-common}}$ = Common mode current in the shield wires (A)
$I_{\text{s-loop}}$ = Loop or balanced mode current flowing in the shield wires (A)
$Z_{\text{m}}{}^{\text{s1-ca}}$ = Mutual impedance between shield wire one and the A phase conductor ($\Omega.\text{m}^{-1}$)
$Z_{\text{m}}{}^{\text{s1-cb}}$ = Mutual impedance between shield wire one and the B phase conductor ($\Omega.\text{m}^{-1}$)
$Z_{\text{m}}{}^{\text{s1-cc}}$ = Mutual impedance between shield wire one and the C phase conductor ($\Omega.\text{m}^{-1}$)
I_{c}^{a} = A phase current (A)
I_{c}^{b} = B phase current (A)
I_{c}^{c} = C phase current (A)
$Z_{\text{s}}{}^{\text{s-s1}}$ = Self impedance of shield wire one ($\Omega.\text{m}^{-1}$)
$Z_{\text{m}}{}^{\text{s1-s2}}$ = Mutual impedance between shield wires one and two ($\Omega.\text{m}^{-1}$)

When zero sequence currents flow in the transmission line the loop current is zero and the common current is given by:

$$I_{\text{s-common}} = \frac{2(I_{\text{c}}^{a} + I_{\text{c}}^{b} + I_{\text{c}}^{c})(Z_{\text{m}}{}^{\text{s1-ca}} + 2Z_{\text{m}}{}^{\text{s1-cb}} + Z_{\text{m}}{}^{\text{s1-cc}})}{Z_{\text{s}}{}^{\text{s-s1}} - Z_{\text{m}}{}^{\text{s1-s2}}} \tag{6.6}$$

For optimal shielding with a balance sequence current flowing in the transmission line, the common current must be minimised. This can be achieved by minimising

$$Z_{\text{m}}{}^{\text{s1-ca}} - 2Z_{\text{m}}{}^{\text{s1-cb}} + Z_{\text{m}}{}^{\text{s1-cc}}$$

The loop current acts to reduce the induction due to balanced sequence current flow. However for the horizontal transmission line with two shield wires, the loop current has little practical value, as the common current induced in the line by balanced sequence phase currents has a far larger detrimental effect. Therefore the loop current only increases transmission line losses in practice. It may also be minimised by making Z3 equal to Z1. Combining these requirements, the most desirable situation would be when Z1 = Z2 = Z3. This cannot be achieved as the phase conductors lie in a horizontal plane above the earth.

Zero sequence induction from the transmission line is minimised when the shield wire common current is

$$-(I_c^a + I_c^b + I_c^c)$$

This implies that for minimum induction

$$\frac{Z_m{}^{s1-ca} + Z_m{}^{s1-cb} + Z_m{}^{s1-cc}}{Z_s{}^{s-s1} + Z_m{}^{s1-s2}} = \frac{3}{2}$$

From Table 6.2 it can be seen that the self impedance is greater than any of the mutual impedances between a line conductor and a shielding conductor. Therefore the shielding may be improved by increasing the mutual impedances, which can be achieved by reducing the line conductor to shield wire spacings. A study was thus made of the horizontal transmission line with two low impedance "MINK" ACSR shielding conductors in the plane of the phase conductors.

The magnitude of the induced electric field for the line with repositioned low impedance shield wires, with respect to that of the field from the line in the absence of shield wires, is similar to Figure 6.3. However there are three significant differences between the line ratio graph for this line, and the line with conventionally placed low impedance "MINK" shielding conductors.

1. The zero sequence induction is 1% to 7% smaller.

2. The slope of the balanced sequence line ratio graph is reduced by a factor of about ten.

3. The difference between the induced electric fields due to positive and negative sequence current flow, are increased when the depth of return is low.

The repositioned shield wires are not in an optimal position as the sum of the self impedance of the shield wire and the mutual impedances between the shield wires is still significantly greater than two thirds of the sum of the mutual impedances between the line conductors and the shield wires. Ideal shielding of this transmission line is impossible as the line conductors lie in the same horizontal plane, and therefore the mutual impedances cannot be made exactly equal. Also, the mutual impedances are frequency and earth resistivity dependant. Therefore an optimal position for one set of conditions is not necessarily optimal for another. However significant improvements in the shielding performance can be achieved over the conventional shielding conductor arrangements.

The asymptotic ratio of the magnitude of the induced field due to zero sequence current in the line with repositioned shield wires, relative to the line without shield wires is shown in Figure 6.6. The zero sequence induction is reduced to between 40 % - 58 % of it's previous value by the installation of "MINK" shielding conductors in the plane of the phase conductors.

Small perturbations of the impedances due to frequency or earth resistivity variations result in larger relative changes of the differences between the self and mutual

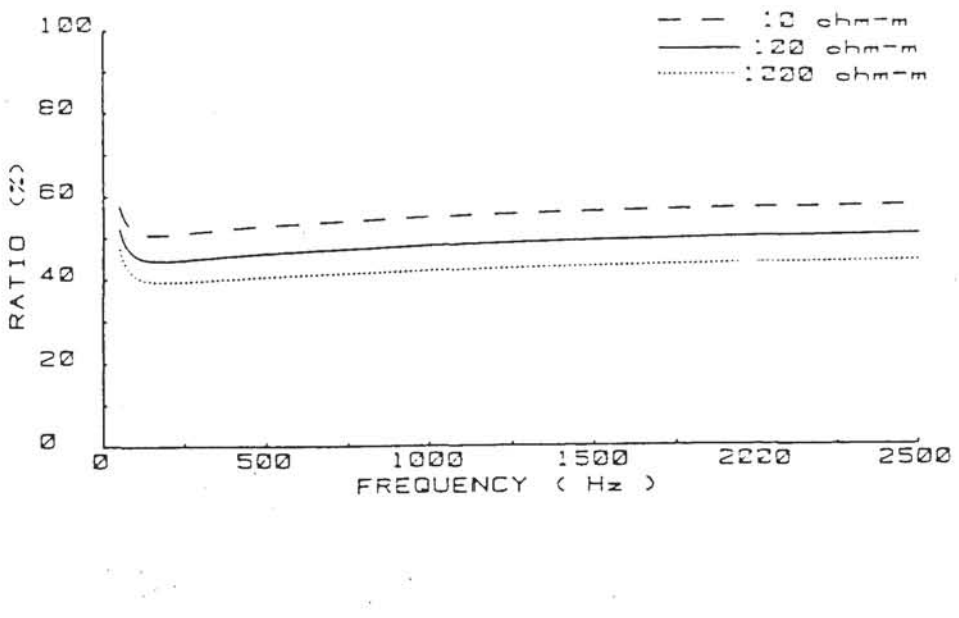

Figure 6.6. Reduction of Zero Sequence induced voltage for horizontal line with 2 repositioned MINK shield wires.

impedances, and hence larger variations of the shielding effectiveness. However as the mutual and self impedances are more similar than in the case of the conventional transmission line, the shielding is improved.

To further improve the performance of the shielding conductors it would be necessary to further reduce the inter-conductor spacings and/or reduce the self impedance of the shielding conductors. This may not be practical due to insulation requirements and conductor characteristics.

6.3 Double Circuit Line

In this section the behaviour of a double circuit line is investigated. The vertical spacings of this line are identical to those of the Invercargill to Manapouri 220 kV transmission line in the New Zealand South Island system, however the horizontal spacings have been changed so that the phase conductors lie on the circumference of a circle (Figure 6.7). A centre point symmetric phasing arrangement has been chosen to minimise the constant asymptotic sequence ratio at large separations.

6.3.1 Central Shield Wire Arrangement

By placing the shielding conductor at the centre of the circle on which the phase conductors are arranged (Figure 6.7), zero sequence currents induced in the central shield wire when balanced sequence currents flow in the phase conductors are reduced.

The line ratios of the electric fields induced by this transmission line with respect to the electric fields induced by the line in the absence of shield wires is given in Figure 6.8. These are similar in form to those obtained for the horizontal transmission line with repositioned shield wires. The zero sequence induction is reduced to 61% - 76%

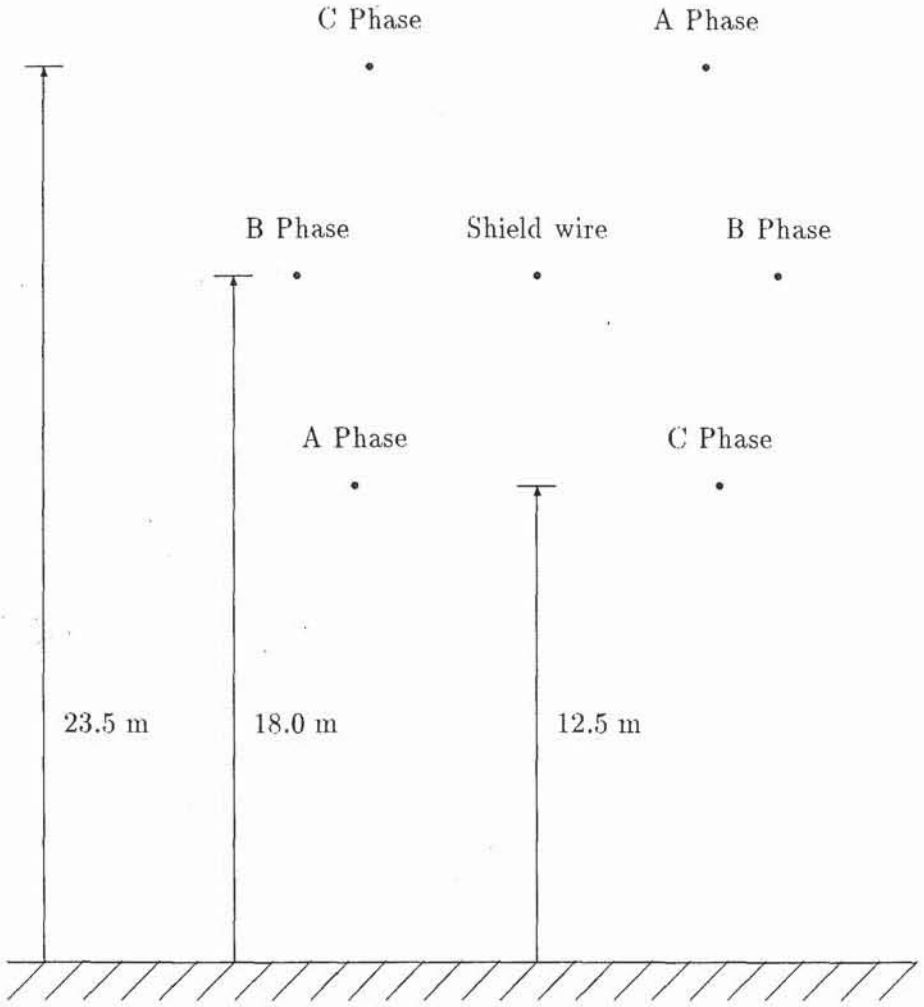

Line data

Name	:	Double Circuit Line with Central Shield Wire
Nominal voltage	:	220 kV
Circuit 1		
Coordinates of A phase conductor	:	(4.42 m, 23.5 m)
Coordinates of B phase conductor	:	(6.33 m, 18.0 m)
Coordinates of C phase conductor	:	(4.80 m, 12.5 m)
Circuit 2		
Coordinates of A phase conductor	:	(-4.80 m, 12.5 m)
Coordinates of B phase conductor	:	(-6.33 m, 18.0 m)
Coordinates of C phase conductor	:	(-4.42 m, 23.5 m)
Coordinates of shield wire	:	(0.00 m, 18.0 m)
Phase Conductor Type	:	Zebra
Shield wire type	:	Mink

Figure 6.7. Double Circuit Transmission Line Geometry with Central Shield Wire

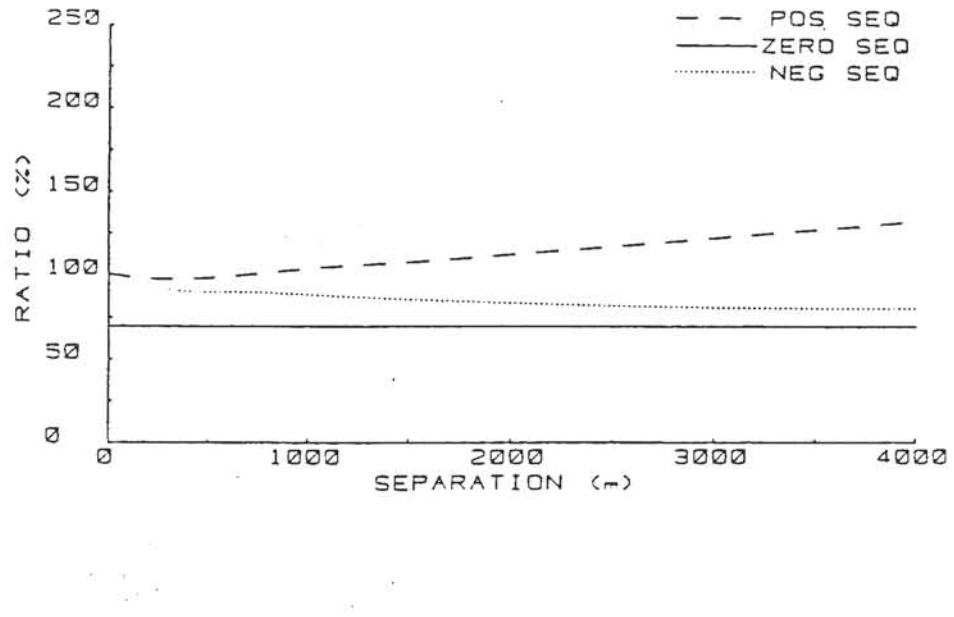

Figure 6.8. Line ratios for double circuit line with central MINK shield wire: earth resistivity - 100 Ω.m, frequency - 1000 Hz.

of that induced by the line in the absence of the "MINK" ACSR shielding conductor. The line ratios due to balanced sequence current flow in the transmission line show significant differences between the positive and negative sequence induction, and tend to a linear function of separation at large separations. The graphs are frequency and earth resistivity dependant. As the earth resistivity is increased the slope of the balanced sequence line ratio graph, and the magnitude of the zero sequence line ratio reduce, while the opposite effect occurs for an increase in frequency.

The sequence ratios of Figure 6.9 tend asymptotically to a constant value as the separation is increased, despite the centre point symmetric phasing arrangement. This is between 0.001% and 0.03%, for frequencies between 50 and 2500 Hz, and earth resistivities from 10 to 1000 Ω.m. The ratio is highly sensitive to earth resistivity and frequency. The effect occurs because the mutual impedances from each phase conductor to the shield wire are not equal. Each phase conductor is equidistant from the shield wire, however the earth distorts the fields, destroying the symmetry and creating the mutual impedance unbalance. The balanced sequence line conductor currents then induce a zero sequence current in the shield conductor. Zero sequence current flow in the phase conductors also returns via the earth, therefore the induced electric fields due to balanced and zero sequence current flow in the transmission line reduce at a similar rate with separation, and hence their ratio becomes constant. The constant ratio would be expected to be a maximum when the depth of return is minimised, as the impedance unbalance is largest for this case. The numerical results support this prediction.

The reduction factor for the induced electric field due to zero sequence current flow in the transmission line is shown in Figure 6.10. The field can be reduced to 61 % - 77 % of its previous value by installing a central "MINK" ACSR shielding conductor. Further but small improvements could be effected by using lower impedance ACSR

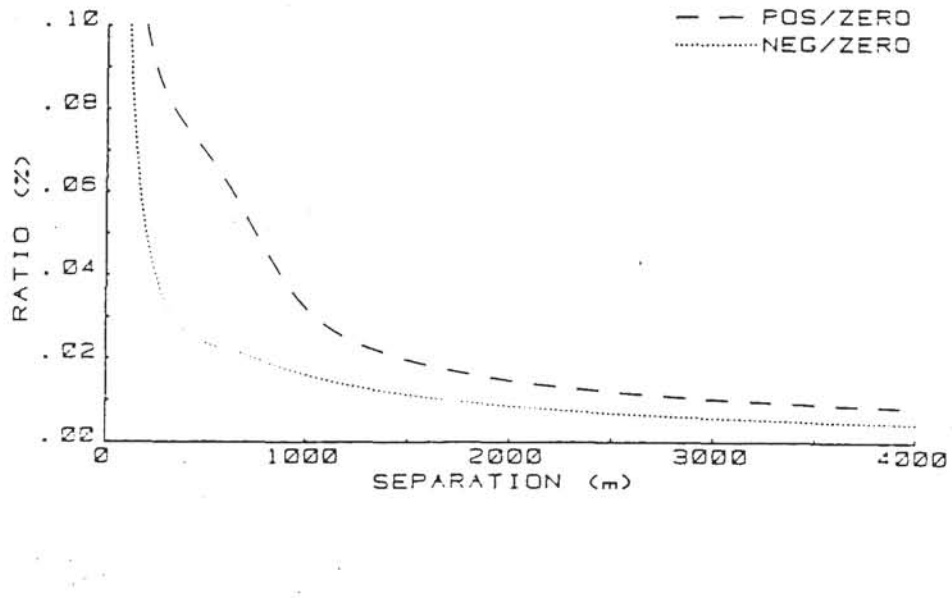

Figure 6.9. Sequence ratios for double circuit line with central MINK shield wire: earth resistivity - 100 Ω.m, frequency - 1000 Hz.

conductors, however the additional cost may not be warranted. The reduction that can be achieved is not as great as that for the horizontal transmission line. This is due mainly to the greater self impedance of the shielding circuit for this line.

6.3.2 Comparison with Conventional Shield Wire Placement

A commonly used phase conductor arrangement is shown in Figure 6.11. The low impedance MINK shield wire is located above the phase conductors to shield them from lightning discharges. Line ratio graphs for the line with a shield wire, with respect to that without any shielding conductors is similar to those of Figure 6.8. The principle differences are that the slope of the balanced sequence line ratio graph is increased, and the zero sequence reduction factor is increased. This results in larger zero sequence induction with regard to the line with a central low impedance shield conductor.

The increased slope of the balanced sequence line ratio is due to greater impedance unbalances between each phase conductor and the shield wire. This results in a larger zero sequence current flow in the shield wire due to balanced sequence current flow in the phase conductors.

A typical sequence ratio graph is shown in Figure 6.12. This indicates that the constant asymptotic ratio effect occurs for this line. For earth resistivities between 10 and 1000 Ω.m and frequencies from 50 to 2500 Hz, the asymptotic ratio is less than 1.1%. The balanced sequence current will need to be at least 90 times the zero sequence current to induce electric fields of comparable strengths at large separations.

In Figure 6.13 the ratio of the field due to zero sequence current in the line with a top shield conductor, to that from the line without a shielding conductor is shown. When compared with Figure 6.10, the top shield conductor arrangement generally results in a higher level of induced voltage due to zero sequence current, except when the earth

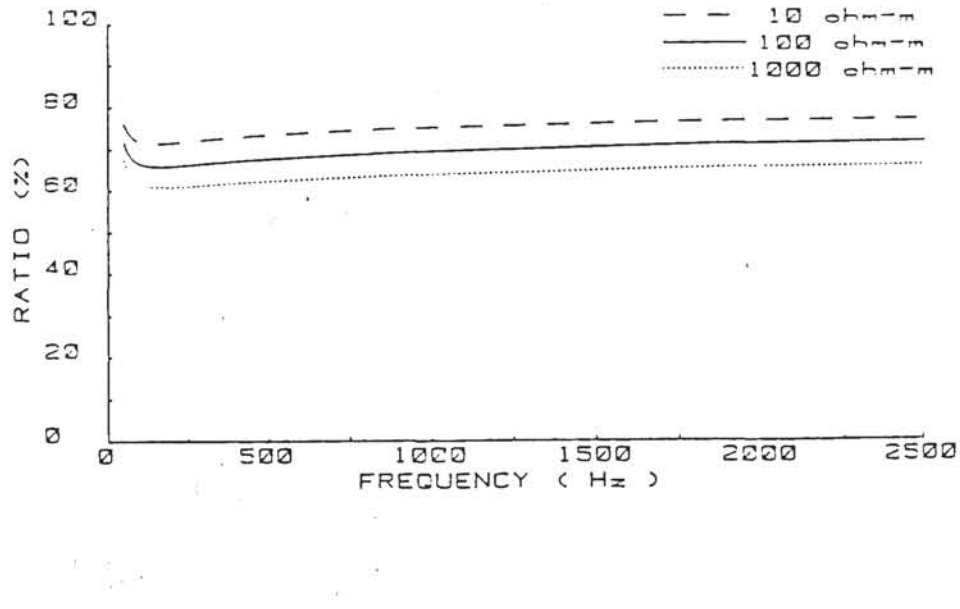

Figure 6.10. Reduction of Zero Sequence induced voltage for the double circuit line with central MINK shield wire.

resistivity is low. The magnitude is less sensitive to earth resistivity variations than with a central shield wire. The zero sequence induction can be reduced to 64 % - 78 % of its value prior to the installation of a shielding conductor by installing a "MINK" ACSR shield wire above the phase conductors.

Balanced sequence currents in the transmission line induce a zero sequence current in the shield conductor, resulting in increased losses in the latter, and increased induction. However the losses are practically insignificant regardless of whether the shield wire is located at the centre of the group of phase conductors, or above the phase conductors.

6.4 Single Circuit Line on a Double Circuit Tower

6.4.1 Central Shield Wire Arrangement

A single circuit on a double circuit tower may be viewed as an extreme case of current unbalance in a double circuit transmission line. The transmission line studied is that shown in Figure 6.7, with only the right hand circuit installed.

The induced electric fields from this line relative to the line without shield wires is shown in Figure 6.14. These are similar to those of the double circuit line with the exception that the line ratio due to balanced sequence current becomes constant at large separations, and independent of the current sequence as the phase conductors lie in different horizontal planes. However current flowing in the shielding conductor acts to reduce the influence of the phase conductors, and the line ratio is reduced to 95% - 97% of its value in the absence of shielding conductors.

The zero sequence line ratio is practically independent of separation, and is reduced to between 61% and 76% of the field from the line in the absence of the MINK ACSR

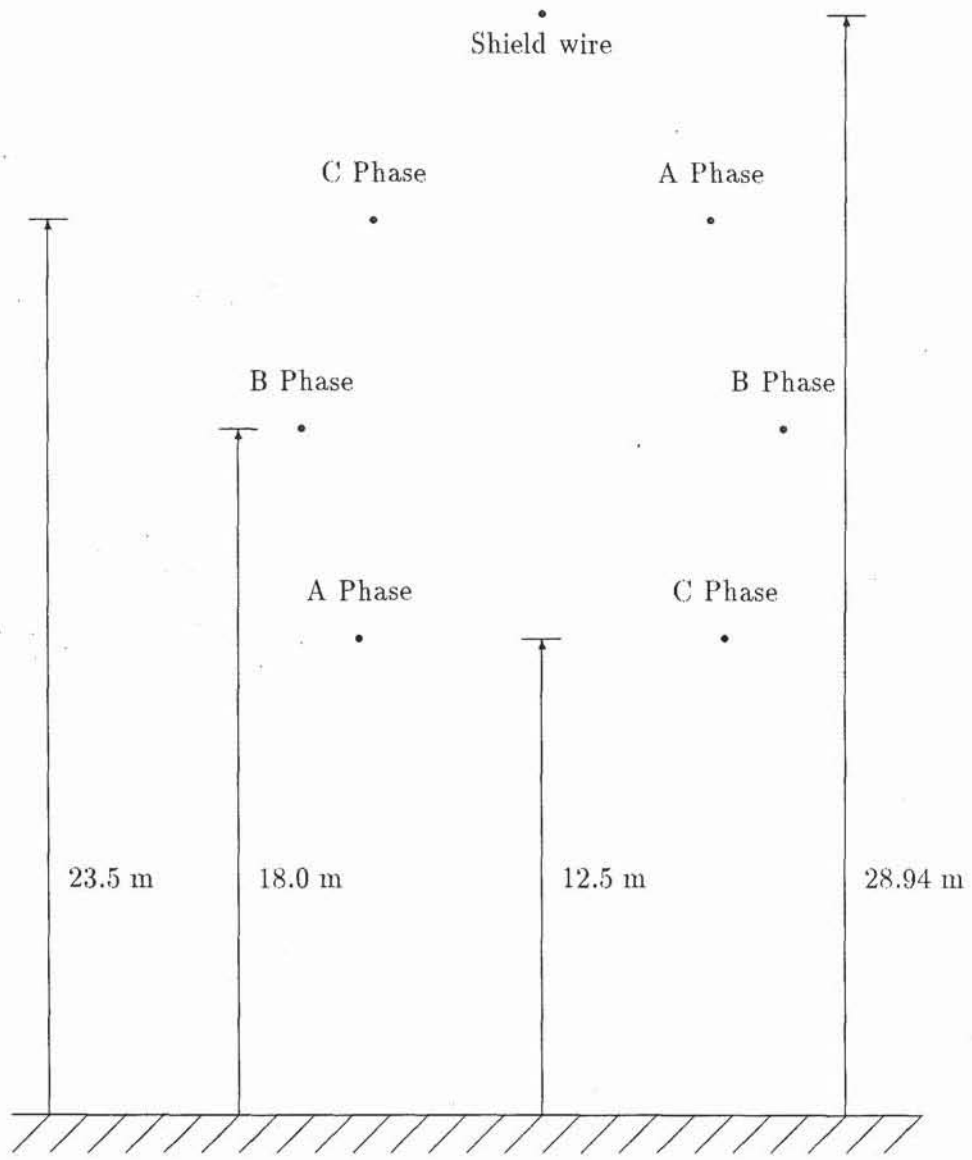

Name	:	Double Circuit Line with Top Shield
Nominal voltage	:	220 kV
Coordinates of A1 phase conductor	:	(4.42 m, 23.5 m)
Coordinates of B1 phase conductor	:	(6.33 m, 18.0 m)
Coordinates of C1 phase conductor	:	(4.80 m, 12.5 m)
Coordinates of A2 phase conductor	:	(-4.80 m, 12.5 m)
Coordinates of B2 phase conductor	:	(-6.33 m, 18.0 m)
Coordinates of C2 phase conductor	:	(-4.42 m, 23.5 m)
Coordinates of shield wire	:	(0.00 m, 28.94 m)
Phase Conductor Type	:	Zebra
Shield wire type	:	Mink

Figure 6.11. Double Circuit Transmission Line Geometry with Top Shield Wire

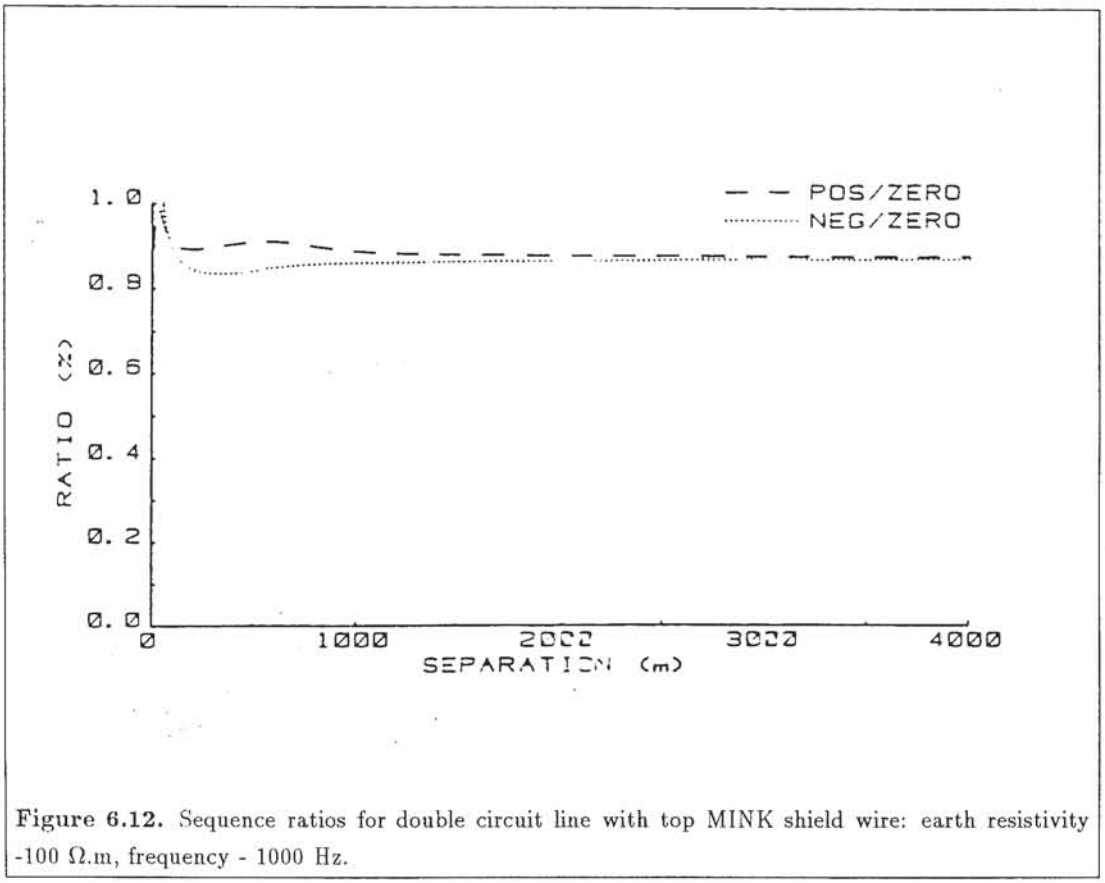

Figure 6.12. Sequence ratios for double circuit line with top MINK shield wire: earth resistivity -100 Ω.m, frequency - 1000 Hz.

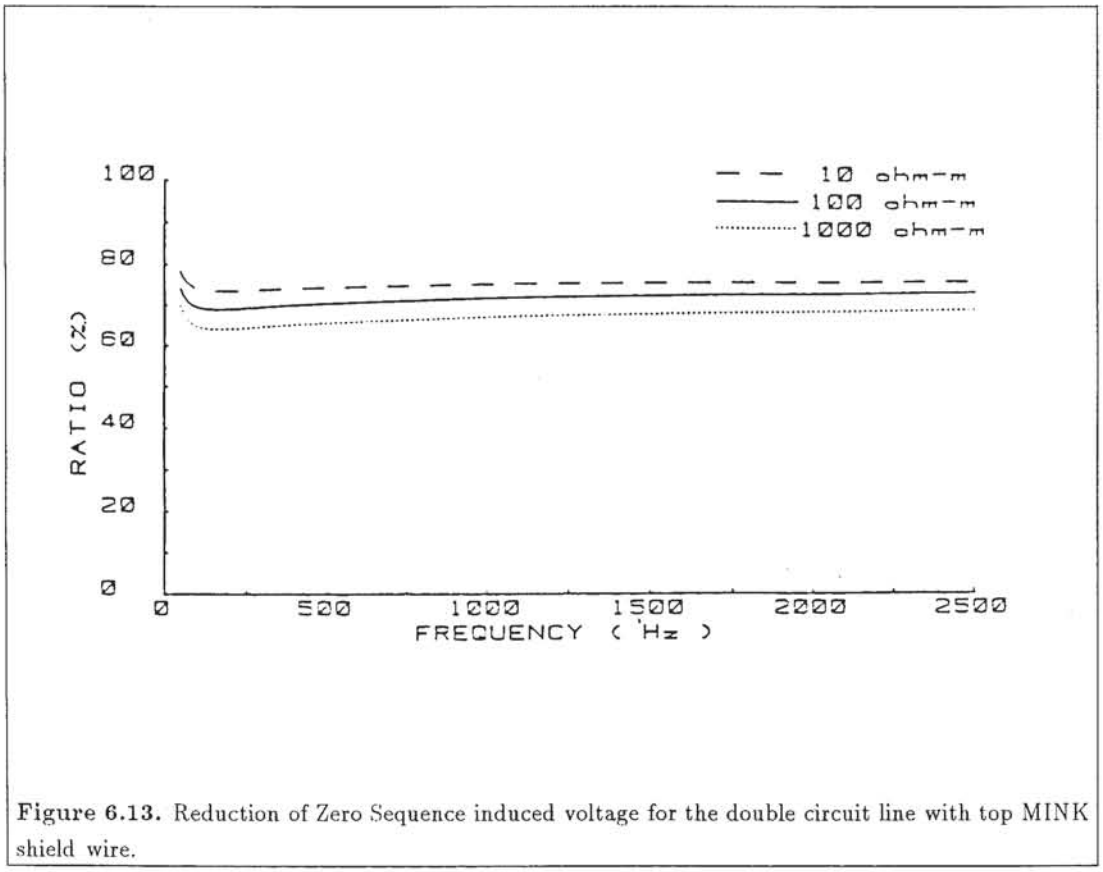

Figure 6.13. Reduction of Zero Sequence induced voltage for the double circuit line with top MINK shield wire.

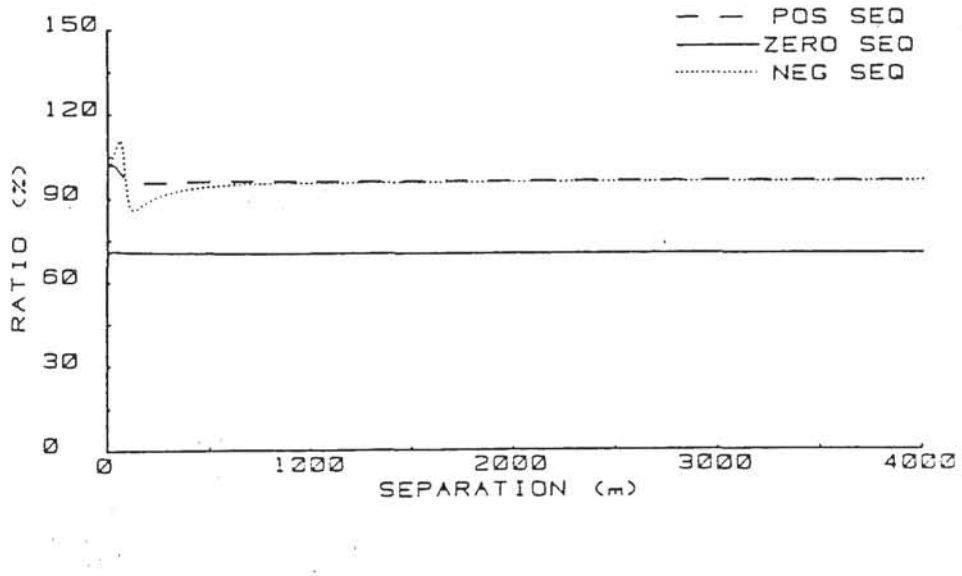

Figure 6.14. Line ratios for single circuit line with central MINK shield wire: earth resistivity - 100 Ω.m, frequency - 1000 Hz.

shielding conductor.

The constant asymptotic sequence ratio effect occurs for this line as the phase conductors lie in different horizontal planes, and do not cancel at large separations. The ratio is less than 11 % for the range of conditions studied, indicating that balanced sequence currents must be at least 9 times the zero sequence current to induce comparable fields at large separations.

The ratio of the induced electric field due to zero sequence current flow, relative to the field induced by the line in the absence of a shielding conductor is trivially different from the corresponding graph for the double circuit line with a central shield wire (Figure 6.7).

6.4.2 Top Shield Wire Arrangement

Figure 6.15 is the line ratio graph for the single circuit line with a single low impedance shield wire mounted above the pylon, as shown in Figure 6.11.

The balanced sequence line ratios increase to a peak near the transmission line (135% to 2700%) which is highly sensitive to frequency and earth resistivity. The peak line ratio is maximized when the depth of return is maximized. The field due to balanced sequence current is less than 15% of that due to zero sequence current. Consequently the latter will only be the dominant interfering current when the balanced sequence current is less than 6 times the magnitude. This condition will not be satisfied by the 50 Hz current under normal power system operating conditions.

Significant differences occur between the line ratios due to positive and negative sequence currents. The ratios tend to a constant value as the separation is increased and lie between 23% and 800% for the range of frequencies and earth resistivities studied. In general when the depth of return is moderate or small, the balanced sequence induction

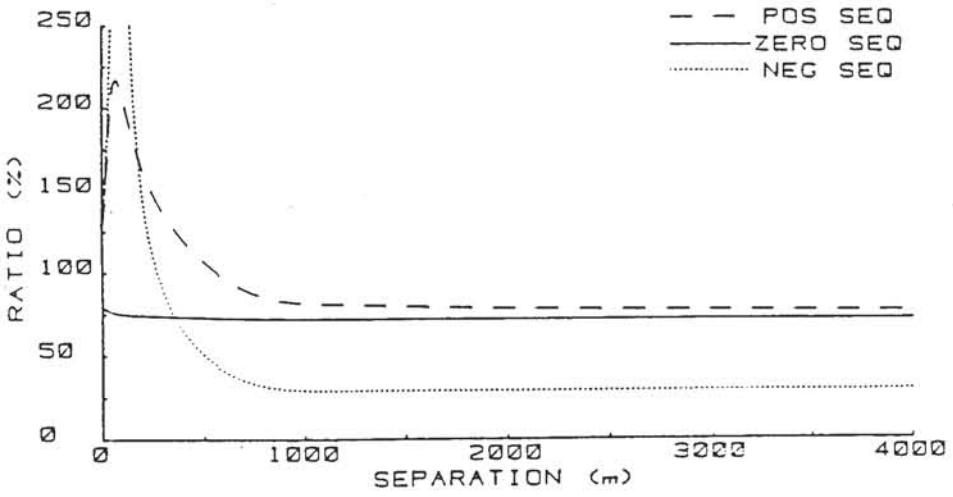

Figure 6.15. Line ratios for single circuit line with top MINK shield wire: earth resistivity - 100 Ω.m, frequency - 1000 Hz.

is reduced significantly by the top shield wire. However when the depth of return is large, it is increased by the top shield wire.

The electric field at large separations from a transmission line carrying balanced currents is determined mainly by the phase and position of the highest conductor on the pylon. Thus the induction from a line in which the phase conductors lie in different horizontal planes may be improved by reducing the influence of the highest phase conductors in relation to the lower ones. This can be achieved by placing the shield wire closer to the upper phase conductors than the lower ones. This technique can be very effective, as demonstrated by the performance of the line with a top shield wire. The main problem with this technique is that when the depth of return is large the upper phase conductors do not require very much additional shielding as the mutual impedances between each phase conductor and the cable are more similar in magnitude than when the depth of return is shallow. Therefore the use of a top shield wire can increase the mutual impedance unbalance, increasing the induction.

The zero sequence induction can be reduced to between 64 % and 78 % by installing the top mounted shield conductor.

The sequence ratios are given in Figure 6.16. The constant asymptotic sequence ratio effect occurs as the phase conductors are in different horizontal planes, and lie between 0.55% and 7.1% for the range of conditions studied. The ratios differ for positive and negative sequence currents as the transmission line is asymmetric.

6.4.3 Comparison of Shield Wire Losses

The shield wire losses when 400 amperes per phase of positive sequence, 50 Hertz current flows in the 100 km line are listed in Table 6.4.

The losses are significantly greater when the top shield wire arrangement is used.

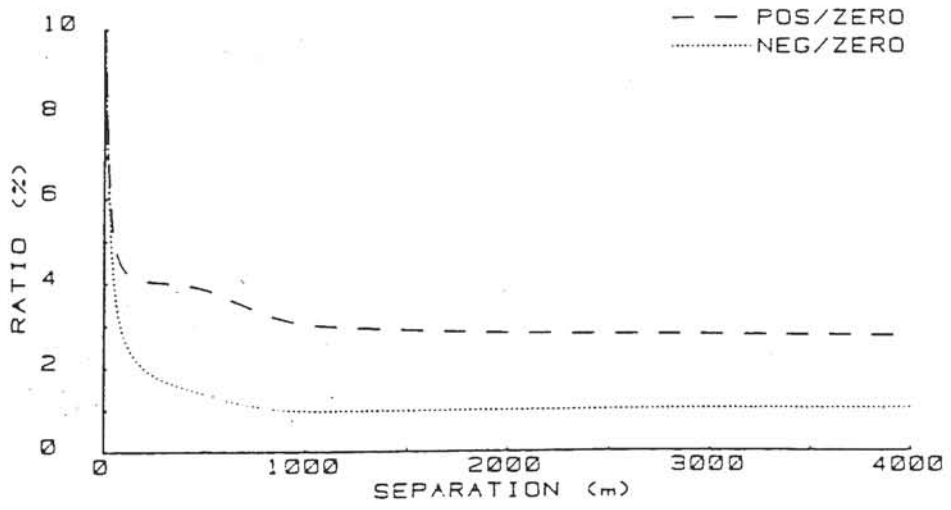

Figure 6.16. Sequence ratios for single circuit line with top MINK shield wire: earth resistivity -100 Ω.m

Shield wire position	Total Losses (w)	% of Phase Conductor Losses	Percentage of Injected Power
Central	45	0.0008 %	0.00003 %
Top	260000	4.6 %	0.17 %

Table 6.4. Shield Wire Losses for the Single Circuit Line at 50 Hz and 100 Ω.m

However in all cases the losses are sufficiently small to be of no practical concern.

6.5 Conclusion

Shield wires on high voltage transmission lines can be used to reduce interference from zero sequence currents flowing in the transmission line. The level of induction can be reduced to less than 50% of the field magnitude induced by the line in the absence of shield wires, however for common transmission line geometries and conductor types, it is only practical to reduce the induced electric field to 70% of its previous value.

Shield wires tend to increase the induction due to balanced sequence current flow and careful consideration should be given to this effect for fundamental frequency currents. At harmonic frequencies the balanced sequence current must be many times greater than the zero sequence current to induce comparable electric fields at large separations. This may occur at power system resonant frequencies which are different for the balanced and zero sequence components.

The shielding effectiveness is dependant on the impedance of the shielding conductor. The GEHSS conductors currently used are considerably less effective than lower impedance ACSR conductors. It is recommended that ACSR shielding be used particularly when high 50 Hertz induction problems are expected, as GEHSS conductors are largely ineffective at low frequencies. The shielding can be improved significantly by reducing the shield wire - line conductor spacings. However in practice consideration must be given to the insulation requirements of the phase conductors.

The effectiveness of the shielding from zero sequence induction is largely independent of conductor location, provided that the "average" phase conductor to shield wire separation is kept constant. However the shield wire losses and the influence of the shield wire on the balanced sequence induction are highly dependant on shield wire position. In general, to minimise shield wire losses, and the influence of the shield wire on balanced sequence induction, the shield wire should be positioned so that it is equidistant from all phase conductors.

Shield wire losses can be significant. However for the transmission lines studied, it has been found that the losses are small in relation to the phase conductor losses. Also by installing the shield wires only in areas of high interference, little regard for this factor is necessary.

CHAPTER 7

INDUCTIVE INFLUENCE MEASURES

7.1 Introduction

Accurate measures of the inductive influence of transmission lines are required for the inductive coordination of power and telecommunication systems. These measures should quantify the resultant disturbing ability from the telecommunication users perspective. Failure to select an appropriate measure may result in the definition of interference limits that are either excessively stringent to guarrantee protection for telecommunications users, or lenient to avoid imposing overly restrictive requirements on power authorities.

In the author's opinion, limits for the inductive influence of high voltage transmission lines should be based upon the intensity of the Longitudinal Electric field (Section 4.2). This quantity accurately represents the ability of the line to induce voltages in buried telecommunication cables.

There are a number of disadvantages with the use of the LEF as an inductive influence measure however:

- The calculation of the Longitudinal Electric Field from conductor current information is computationally intensive. The mutual impedance between each current carrying conductor and the telecommunications cable must be evaluated for all harmonic orders, be scaled by the current and combined to give the resultant LEF for the line.

- Detailed transmission line geometry data, current magnitude and phase information for all conductors and harmonic orders, and the parameters of the earth are required to calculate the LEF. It is difficult to perform accurate measurements of harmonic current flows within the power system due to the lack of suitable transducers. As a consequence LEF calculations are seldom performed in practice. It is possible to estimate conductor currents from magnetic field measurements (Chapter 9), however this is not necessary in practice as the LEF can be determined directly from the voltage induced in a loop aerial. A simple analog computer, consisting of an appropriate frequency weighting network and rms voltmeter, can be used to transform the harmonic voltages induced in the loop into a direct reading of the equivalent LEF.

- The LEF is a function of separation which often has localised extrema in the near field region. Therefore it is necessary to calculate and/or measure the LEF at a number of points, and combine them into a single "equivalent" figure to ensure that the results do not happen to fall on local minimum or maximum which could lead to erroneous conclusions.

Detailed LEF studies are generally only performed when a potential problem has been identified that requires investigation. Other measures of the inductive influence

such as the Equivalent Disturbing Current or 1 km Test Line method are used to specify the performance objective of transmission systems. These measures are discussed in Section 7.3.

The regular nature of the far field dependencies of multiconductor transmission lines, coupled with the success of the Basic and Phase Corrected Vertical Inducing Loop models, prompted the author to study simplified expressions for the LEF based upon the far field VIL approximations for the mutual impedance. The resultant measures are reported in Sections 7.3.3 and 7.3.4. They exhibit the same frequency, earth resistivity and conductor geometry dependencies as LEF calculations using accurate mutual impedance models. The Phase Corrected inductive influence measure also displays the correct far field current sequence dependencies for all transmission line geometries.

The chapter opens in Section 7.2 with the derivation of the Basic and Phase Corrected equations for the mutual impedance between a multiconductor line and a buried cable. Comparisons are made between the gross far field dependencies predicted using these models and the observed behaviour of the LEF calculated using Carson's equation Chapter 5, to establish the validity of the approximations.

Existing measures of inductive influence are reviewed in Section 7.3. The new measures are then presented, compared with existing measures and recommnedations made as to when they should be used.

7.2 Application of the Vertical Inducing Loop model to Multiconductor Transmission Lines

In this section far field approximations for the longitudinal electric field induced by the multiconductor transmission lines based upon the Basic and Phase Corrected Vertical Inducing Loop Models.

7.2.1 Net Vertical Inducing Loop Concept for Far Field Effects

The Net VIL concept is based upon (4.19) which states that the far field inductive influence of a conductor is proportional to both frequency and the size of the loop squared, and decays as the reciprocal of square of the separation. Superimposing the individual conductor fields yields

$$\mathrm{LEF} \approx \sum_{i=1}^{n} I_i \frac{\omega \mu_a}{4\pi} \frac{(y_i - y_f(i))^2}{(x - x_i)^2} \tag{7.1}$$

Where

I_i = current in conductor i (A)
$y_f(i)$ = depth of the i'th conductor's return path (m)
y_i = y ordinate of the i'th conductor (m)
n = total number of current carrying conductors
x_i = x ordinate of the i'th conductor (m)

Since the horizontal component of the inter-conductor spacing is very small in relation to the cable-line separation, differences in the mutual impedances due to differing conductor-cable spacings may be ignored as a first approximation, giving

$$\mathrm{LEF} \approx \frac{\omega \mu_a}{4\pi} \frac{1}{(x - x_{\mathrm{ref}})^2} \sum_{i=1}^{n} I_i (y - y_f(i))^2 \tag{7.2}$$

where

x_{ref} = average x ordinate of the conductors (m)

The summation term may be considered to be the square of the size of a single *Equivalent Vertical Inducing Loop* (EVIL) that has the same inductive influence as the multiconductor line. An EVIL factor has been defined to be

$$\begin{aligned} \text{EVIL} &= \omega \sum_{i=1}^{n} I_i (y - y_{\text{f}}(i))^2 \\ &\approx \omega \sum_{i=1}^{n} I_i \left[(1 + \frac{1}{\sqrt{2}}) y_i + \sqrt{2}\delta \right]^2 \\ &\approx \omega \sum_{i=1}^{n} I_i \left[(1 + \frac{1}{\sqrt{2}})^2 {y_i}^2 + 2(1 + \sqrt{2}) y_i \delta + 2\delta^2 \right] \end{aligned} \tag{7.3}$$

Any system of conductors that forms a net vertical loop of current (non-zero EVIL factor) induces a far field that decays as the reciprocal of the separation squared.

All transmission lines carrying a zero sequence current have a non-zero EVIL factor. As the conductor fields add constructively the EVIL factor is dominated by the δ^2 term, therefore the far field is directly proportional to earth resistivity and independent of frequency (Tables 5.2 and 5.3). Increasing the inter-conductor spacings does not increase the EVIL factor for a line carrying zero sequence current, however raising the average conductor height does regardless of the line geometry (Tables 5.4 and 5.5).

Vertical transmission lines carrying balanced sequence currents may also have a non-zero EVIL factor. This effect arises because the conductor heights, and therefore the size of the Vertical Inducing Loops, differ. Consequently the loops to not cancel exactly unless special precautions are taken as in the case of a double circuit line with centre point symmetric phasing. The balanced and zero sequence far fields decay at a rate equal to the reciprocal of the cable-line separation squared, resulting in a constant sequence ratio. As the conductor fields induced by a vertical line carrying balanced sequence currents interfere destructively, the dominant term of the EVIL factor is $2\sqrt{2}(1 + \frac{1}{\sqrt{2}}) y_i \delta$. The far field is therefore proportional to the square root of both frequency and earth resistivity, and increases with inter-conductor spacing and average conductor height (Tables 5.2, 5.3, 5.4 and 5.5).

Horizontal transmission lines carrying balanced sequence currents have a zero EVIL factor. The far field is not zero in this case, but decays at a rate greater than one upon the separation squared. The constant sequence ratio effect does not occur for horizontal transmission lines.

7.2.2 Phase Corrected Far Field Effects

With respect to Figure 7.1, the far field LEF induced by single conductor line based upon the Phase Corrected VILmodel ((4.26)) is

$$\text{LEF} \approx I_{\text{c}} \frac{\omega \mu_{\text{a}}}{2\pi} \frac{\delta(y + y_{\text{ref}} + \Delta y_i + \delta) + \jmath[2(y_{\text{ref}} + \Delta y_i) y + \delta(y_{\text{ref}} + \Delta y_i + y)]}{[x - (x_{\text{ref}} + \Delta x_i)]^2} \tag{7.4}$$

The denominator may be expanded using the binomial series as

$$\frac{1}{[x - (x_{\text{ref}} + \Delta x_i)]^2} = \frac{1}{(x - x_{\text{ref}})^2} \left[1 + \frac{2\Delta x_i}{(x - x_{\text{ref}})} - \frac{3{\Delta x_i}^2}{(x - x_{\text{ref}})^2} + \cdots \right] \tag{7.5}$$

which on substitution into (7.4) yields

$$\text{LEF} \approx Ici \frac{\omega \mu_{\text{a}}}{2\pi} \frac{\alpha + \beta \Delta y_i}{(x - x_{\text{ref}})^2} \left[1 + \frac{2\Delta x_i}{(x - x_{\text{ref}})} - \frac{3{\Delta x_i}^2}{(x - x_{\text{ref}})^2} + \cdots \right] \tag{7.6}$$

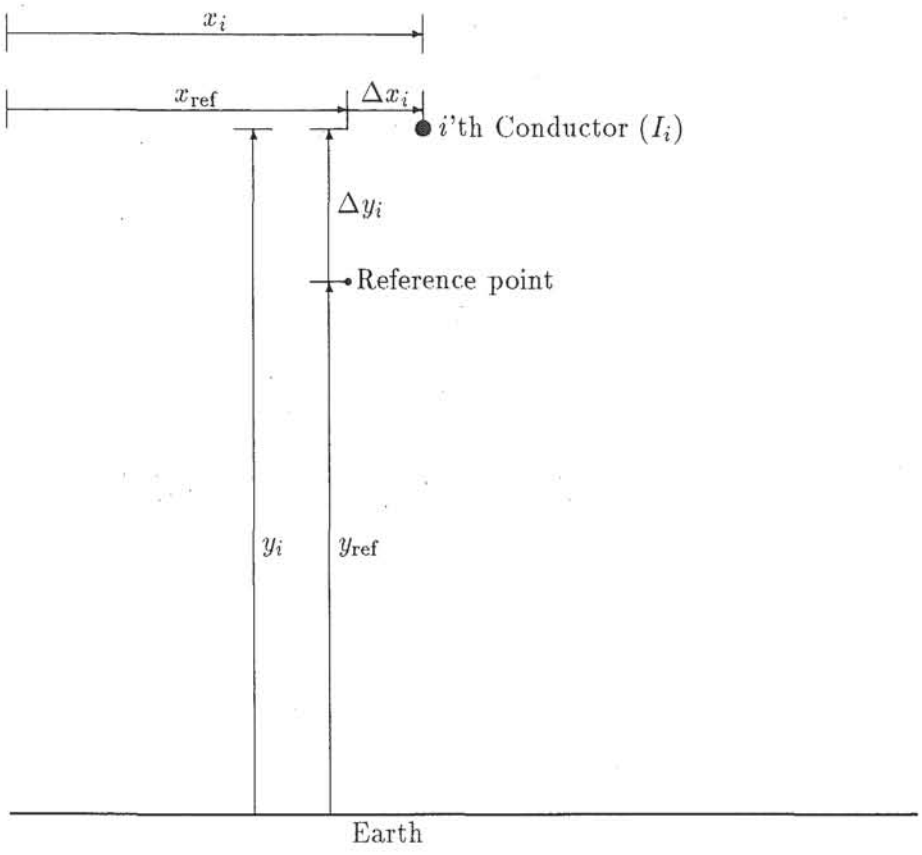

where

y_i = height of the i'th conductor (m)
y_{ref} = height of the reference point (m)
Δy_i = height difference between the i'th conductor and the reference point (m)
$= y_i - y_{\text{ref}}$
I_i = current in the i'th conductor (A)
x_i = x ordinate of the i'th conductor (m)
x_{ref} = x ordinate of the reference point (m)
Δx_i = horizontal distance between the i'th conductor and the reference point (m)
$= x_i - x_{\text{ref}}$

Figure 7.1. Example Transmission Line

where

$$\alpha = \delta(y + y_{\text{ref}} + \delta) + \jmath\,[2y_{\text{ref}}y + \delta(y_{\text{ref}} + y)] \tag{7.7}$$

$$\beta = \delta + \jmath(2y + \delta) \tag{7.8}$$

Applying the concept of superposition, the far field from an arbitrary system of n parallel conductors can be shown to be

$$\text{LEF} \approx \frac{\omega\mu_{\text{a}}}{2\pi}\left[\frac{\alpha\sum_{i=1}^{n} I_i}{(x - x_{\text{ref}})^2} + \frac{\beta\sum_{i=1}^{n} I_i\Delta y_i}{(x - x_{\text{ref}})^2} + \frac{2\alpha\sum_{i=1}^{n} I_i\Delta x_i}{(x - x_{\text{ref}})^3} + \frac{2\beta\sum_{i=1}^{n} I_i\Delta x_i\Delta y_i}{(x - x_{\text{ref}})^3} + \cdots\right] \tag{7.9}$$

The first term of this equation is dependent on the zero sequence current only. If the reference position $(x_{\text{ref}}, y_{\text{ref}})$ is set equal to the average conductor position then this term provides a good estimate of the LEF due to zero sequence current flow. The next term accounts for the effect of different conductor heights which result in balanced sequence currents inducing a field which decays at the same rate as the zero sequence field. Subsequent terms are functions of differences in the horizontal conductor spacings alone or the product of spacing and height differences.

(7.9) yields the same gross frequency, earth resistivity and geometry dependencies as the Net Vertical Inducing Loop model for cases in which the EVIL factor is not zero.

An example of a situation for which the EVIL factor is zero is a horizontal transmission line carrying balanced sequence current. In this case $\Delta y_i = 0$ for all i and $\sum_{i=1}^{n} I_i = 0$. (7.9) then reduces to

$$\text{LEF} \approx \frac{\omega\mu_{\text{a}}}{2\pi}\frac{2\delta(y + y_{\text{ref}} + \delta) + 2\jmath\,[2y_{\text{ref}}y + \delta(y_{\text{ref}} + y)]}{(x - x_{\text{ref}})^3}\sum_{i=1}^{n} I_i\Delta x_i + \cdots \tag{7.10}$$

In the far field region the horizontal inter-conductor spacings are very much smaller than the cable-line separation, therefore the additional terms in (7.10) which are of the order of

$$\frac{\Delta x_i{}^2}{(x - x_{\text{ref}})^4}$$

or higher and may be ignored with little loss of accuracy. As $\delta \gg y_{\text{ref}}$ and y, the balanced sequence far field is approximately directly proportional to $\omega\delta^2$ and hence earth resistivity, but is independent of frequency (Tables 5.2 and 5.3). It is also directly proportional to inter-conductor spacings Δx_i and increases with average conductor height y_{ref} (Tables 5.4 and 5.5).

7.3 Inductive Influence Measures

The total interfering ability of a spectrum of harmonic currents on a multiconductor line is calculated using

$$\text{Inductive Influence Measure} = \sqrt{\sum_{k=1}^{u}\left|P_k\sum_{i=1}^{n} I_{ik}\ \text{Kernel}\right|^2} \tag{7.11}$$

Where

Ici_k = k'th harmonic current in conductor i (A)
Kernel = a function describing the ability of the conductor to cause interference
P_k = psophometric, C message or other appropriate frequency weighting factor describing the frequency dependence of the sensitivity of the induced system (cable) to interference at the k'th harmonic
u = number of harmonics

In this section four measures for quantifying the interfering ability of transmission lines are discussed.

7.3.1 Longitudinal Electric Field Measure

The most obvious kernel function to use in Equation (7.11) is the mutual impedance between each conductor and the cable, yielding a direct estimate of the LEF. Unfortunately the LEF is expensive to evaluate due to the complexity of rigorous models (Carson, 1926; Wait, 1972; Wedepohl and Efthymiadis, 1978; Gary, 1976) and is highly dependent on the cable-line separation. Nevertheless it is the most accurate measure for investigating existing situations.

7.3.2 Equivalent Disturbing Current

The most commonly used interference assessment measure is the *Equivalent Disturbing Current.* This is the 800 Hz current that causes the same disturbance as the full spectrum of currents that exist on the line. It is calculated by using a linear function of frequency for the Kernel

H_k = frequency dependent coupling factor for the k'th harmonic of 50 Hz ($= k/16$)

Equation (7.11) may be simplified to

$$\text{Equivalent Disturbing Current} = \sqrt{\sum_{k=1}^{u} \left| P_k H_k \sum_{i=1}^{n} I_{ik} \right|^2} \tag{7.12}$$

The equivalent disturbing current is a measure of the interfering ability of the current spectrum on the transmission line rather than of the line itself as it is not dependent on the line or earth parameters. As earth return effects are not included, this measure is incapable of representing the true frequency, earth resistivity and separation dependencies of the inductive influence, or the constant sequence ratio effect. The only concession to modelling these dependencies is a linear approximation to the frequency dependence of the coupling, which is valid only in the near field region (Table 5.2).

7.3.3 Net Vertical Inducing Loop Inductive Influence Measure

A measure based upon the Net VIL concept is now proposed. The Kernel function in this measure is the size of the VIL formed by each conductor.

$$\omega(y_i - y_f(i))^2 \approx \omega[(1 + \frac{1}{\sqrt{2}})y_i + \sqrt{2}\delta]^2 \tag{7.13}$$

The complete measure is therefore

$$\text{Net VILMeasure} = \sqrt{\sum_{k=1}^{u} \left| P_k \sum_{i=1}^{n} I_{ik} \omega[(1 + \frac{1}{\sqrt{2}})y_i + \sqrt{2}\delta]^2 \right|^2} \tag{7.14}$$

The inner summation of Equation (7.14) is the EVIL factor defined in Equation (7.3), which is proportional to the far field LEF induced by a multiconductor line. It includes the frequency, earth resistivity and geometry dependence due to differing conductor heights, yet is independent of the cable location although it is assumed that the cable is in the far field region. The measure always provides an accurate estimate of the far field due to zero sequence current flow. However it fails to provide a reasonable estimate of the interfering ability of horizontal transmission lines or vertical double circuit transmission lines with centre point symmetric phasing carrying balanced sequence currents evenly distributed between the circuits, as the EVIL factor is zero for these cases.

7.3.4 Phase Corrected Far Field Inductive Influence Measure

It has been shown in Equation (7.9) that the resultant field from a multiconductor line is the sum of a sequence that proceeds as

$$\text{LEF} = \frac{E_s}{(x - x_{\text{ref}})^2} + \frac{E_c}{(x - x_{\text{ref}})^3} + \cdots$$

Where

E_s = coefficient of separation squared term
E_c = coefficient of separation cubed term

These coefficients can be used as a measure of the inductive influence of multiconductor transmission lines. Two measures are proposed: one with E_s as the kernel function, the other with E_c. The first measure is essentially the Net VIL model with phase correction and the cable height (y_i) retained explicitly in the mutual impedance approximation. The second measure, which is only required when the first measure is zero, accounts for the horizontal spacing between the conductors and overcomes the deficiences of the Net VIL Model at the expense of added complexity.

The measures may be expressed as

$$\text{Square Measure} = \sqrt{\sum_{k=1}^{u} \left| P_k \frac{\omega \mu_a}{2\pi} \left(\alpha \sum_{i=1}^{n} I_i + \beta \sum_{i=1}^{n} I_i \Delta y_i \right) \right|^2} \tag{7.15}$$

$$\text{Cubic Measure} = \sqrt{\sum_{k=1}^{u} \left| P_k \frac{\omega \mu_a}{2\pi} \left(2\alpha \sum_{i=1}^{n} I_i \Delta x_i + 2\beta \sum_{i=1}^{n} I_i \Delta x_i \Delta y_i \right) \right|^2} \tag{7.16}$$

Other higher order measures may be derived, however it has been found that Equation (7.15) and (7.16) are sufficient to accurately quantify the inductive influence of all multiconductor lines studied. These measures differ only in the addends of the inner summations and therefore can be evaluated simultaneously with high efficiency. If the Square measure is not zero then it is generally not necessary to evaluate the Cubic measure as the field associated with the Square term decays at a slower rate and therefore will be dominant in the far field region.

7.3.5 Discussion

Although the Net VIL and Phase Corrected Far Field Inductive Influence measures appear complicated, they are in fact easier to evaluate than the Longitudinal Electric Field measure. Complex addition, multiplication and real arithmetic and square root operations are required, which may be implemented on programmable calculators or measuring instruments with real arithmetic.

A disadvantage of the new models is the volume of data required. Conductor currents at all frequencies, the geometry of the line and the earth resistivity are needed. However as all conductor currents are required for the existing measures the additional data needs are small.

The new measures presented in this paper are superior to existing methods due to their inclusion of line geometry and earth resistivity effects, and their simple form. The Net VIL model may be adequate in practice as almost all transmission lines carry zero sequence currents which will normally be dominant. However it can lead to errors for lines carrying balanced sequence currents. In this case the Square measure should be used, although this is not sufficient for horizontal and double circuit centre point symmetric lines carrying balanced sequence currents.

Only the Longitudinal Electric Field measure or the combined Square and Cubic measures provide a reliable measure for all line types studied, but are unfortunately more expensive to implement.

7.4 Conclusions

New measures of the interfering ability of multiconductor transmission lines have been derived which are superior to existing methods as they include the effect of transmission line geometry, earth resistivity, frequency and all current flows on the interfering ability. They are easier to evaluate than Longitudinal Electric Field measures based upon existing mutual impedance formulas.

CHAPTER 8

INDUCTIVE INFLUENCE OF THE NZ HVDC LINK: COMPUTER STUDIES

8.1 Introduction

Knowledge of the inductive influence of a transmission system is required for the co-ordination of the system with communication services. The inductive influence of a system may be determined by direct measurement or by simulation. However it is impractical to determine the inductive influence of a large system by measurement due to the need to perform measurements at many sites to ensure that no resonant effects are missed, and the requirement that measurements be made over a complete range of operating conditions to establish the severity of the problem.

An accurate model of the transmission system is required for the calculation of the inductive influence. Unfortunately the interfering ability of a line is highly dependent on earth resistivity which may vary greatly along the line. Previous models assume that the resistivity is uniform thereby enabling the current at any point to be calculated from the terminal conditions and modal propagation constants (Meyer and Dommel, 1969). Realistic modelling requires the use of non-homogeneous line models which also allows discontinuities such as line transpositions, static VAR compensation devices and filters to be included.

This chapter describes a general algorithm for the determination of the probability distribution of the inductive influence of a transmission system. The algorithm was developed for the study of the Benmore-Haywards HVDC transmission system between the North and South Islands of New Zealand, but may be applied to multiconductor transmission lines of practically any configuration. Realistic tranmission lines can be represented using models for the analysis of harmonic propagation (Arrillaga *et al.*, 1983; Dommel, 1984). Harmonic voltage and current injections can be represented and provision is made to derive harmonic information at any point along the line.

Clearly, the use of rigorous analytical techniques will normally demand a considerable amount of computer time and storage, and will require careful management of the data and results. Moreover, determination of the probability distribution of the residual current and inductive fields requires many repetitive studies. It is therefore important to pursue ways of reducing time scales without degrading accuracy.

Several novel features are added to the transmission line parameter program which make the present approach considerably more efficient than the basic method (Arrillaga *et al.*, 1983), while the interference algorithm uses superposition to reduce the computation burden of repetitive studies.

8.2 The Algorithm

The aim of the algorithm is to provide a qualitative measure of the interfering ability of a transmission system. This is assessed through the use of the Equivalent Disturbing

1. Select observation points and prepare the system data.
2. Calculate the electrical characteristics of the elements.
3. Calculate the distribution of the residual current or inductive field of the system at each observation point for unit injections into each phase from the sending and receiving terminals
4. For each set of harmonic injection spectra, calculate the total inductive influence of the system
5. Form the probability distribution of the equivalent disturbing current or inductive field at each observation point

Figure 8.1. Overview of the Algorithm

Current or Longitudinal Electric Field measures discussed in Chapter 7. The algorithm can calculate either of these quantities.

The algorithm utilizes the principle of superposition to determine the inductive influence of the system from a set of precalculated results. The base set of results is selected to span the space containing all inductive influence profiles for the system. In this algorithm the set of Equivalent Disturbing Current or Longitudinal Electric Field profiles resulting from unit injections into each phase from each end of the system have been used. Consequently a study of u harmonics in an n phase phase system requires the evaluation of $2.n.u$ profiles before calculation of the total inductive influence begins. Obviously this method is less efficient for single case studies than a direct solution, however for repetitive studies it significantly reduces the computational requirements as the currents in all conductors are not calculated for each injection.

To maximize computer efficiency the system components are represented by ABCD parameter matrices. This limits the application of the algorithm to systems in which the phase conductors are continuously connected. Interconnected systems may be solved using nodal analysis to determine the terminal conditions of the continuous sub-systems.

An overview of the algorithm is presented in Figure 8.1.

The input data to step 1 of the algorithm contains details of each element in the system; an element in this context being a homogeneous transmission line section, a cable, a series impedance or a shunt admittance. Component connections are inferred from the order of presentation. Element type data and those parameters necessary for the determination of the elements' electrical characteristics are entered, such as the conductor type, arrangement and earth resistivity in the case of a transmission line element.

The user is prompted for the location of observation points at which the inductive influence is to be calculated. If standing waves are to be observed then observation points should be inserted at intervals of less than one tenth of a wavelength at the highest frequency. The elements' data is then partitioned so that the observation points fall at the junction of two elements.

Output from this step consists of an unformatted file of element data which has been checked for validity.

Step 2 calculates the reduced equivalent phase ABCD matrix for each element at all frequencies of interest. A frequency dependent transformation matrix from equivalent phase currents, to currents within all conductors of the line (including earth wires and optionally, sub-conductors in a bundle) is calculated for aerial line sections. The output from this step is an unformatted file of ABCD matrices for all elements, with data on the physical arrangement of the conductors and equivalent phase to conductor current

transformation matrix for aerial line sections. Details of the method of calculation and the features used to improve computational efficiency are contained in sections 8.3 and 8.4.

Once the electrical parameters of each element have been determined, it is necessary to calculate the response of the system to unit injections on each phase, from both ends, for all harmonics (step 3). Each harmonic, and indeed each injection, is considered independently of all others. Details of the process are given in section 8.5.

Output from step 3 is a set of $2.u.u$ complex numbers for each observation point. This represents a significant reduction in data volume over that input. As a consequence it is practical to retain the output in the computer memory, whereas this is frequently impractical with the output of step 2.

Having calculated the set of base Equivalent Disturbing Current or LEF profiles, the inductive influence for each harmonic is calculated by scaling and superimposing the base results for injections of the same frequency. The total inductive influence over all harmonics is then formed.

The equivalent disturbing currents or Longitudinal Electric Fields for each injected spectrum are then combined to form cumulative probability distributions in step 5.

The data generation and presentation steps of the algorithm have been separated to enable customizing of the presentation format to suit the user's requirements.

8.3 Transmission Line Parameters

Transmission line parameters can be evaluated very efficiently by exploiting the symmetry of the matrices, the linear variation of some quantities with frequency, curve fitting approximations to complicated functions, and approximations to the diagonalization matrices when calculating long line parameters. However to maximize these efficiencies it is necessary to calculate the parameters of the line for all frequencies of interest at the same time.

8.3.1 Evaluation of Lumped Parameters

The lumped series impedance matrix Z of a multiconductor transmission line consists of three components, while the shunt admittance matrix Y contains one (Galloway *et al.*, 1964).

$$Z = Z_e + Z_g + Z_c$$

$$Y = Y_g$$

Where

Z_c = is the internal impedance of the conductors ($\Omega.\mathrm{km}^{-1}$),
Z_g = is the impedance due to the physical geometry of the conductor's arrangement ($\Omega.\mathrm{km}^{-1}$),
Z_e = is the earth return path impedance ($\Omega.\mathrm{km}^{-1}$), and
Y_g = is the admittance due to the physical geometry of the conductor ($\Omega^{-1}.\mathrm{km}^{-1}$).

All primitive matrices are symmetric, and therefore the functions defining the elements need only be evaluated for elements on or above the leading diagonal.

8.3.1.1 Earth Impedance Matrix Z_e

The impedance due to the earth path varies with frequency in a non-linear fashion. The solution of this problem, under idealized conditions, has been discussed in Chapter 3.

A variety of earth return models were included in the algorithm. Nagakawa's multi-layer integral equation model (Nakagawa and Iwamoto, 1976) was used for its ability to represent stratified earth structures at the sites where measurements were performed. The Infinite series form of Carson's equation (Carson, 1926) and the complex penetration model (Deri and Tevan, 1981) were implemented to enable accuracy and computational efficiency comparisons to be made between them and the Acha Curve Fitting model (Daza, 1988). These studies indicated that the accuracy of the Acha model is adequate (Section 4.4, and that the use of this model resulted in a 98implementation, and 69penetration model.

8.3.1.2 Geometrical Impedance Matrix Z_g and Admittance Matrix Y_g

If the conductors and the earth are assumed to be equipotential surfaces, the geometrical impedance can be formulated in terms of potential coefficients theory.

The self potential coefficient ψ_{ii} for the i'th conductor and the mutual potential coefficient ψ_{ij} between the i'th and j'th conductors are defined as follows,

$$\psi_{ii} = \ln \frac{2y_i}{a_i}$$

$$\psi_{ij} = \ln \frac{\sqrt{(x_i - x_j)^2 + (y_i + y_j)^2}}{\sqrt{(x_i - x_j)^2 + (y_i - y_j)^2}}$$

where a_i is the radius of the i'th conductor (m) while the other variables are as defined earlier.

Potential coefficients depend entirely on the physical arrangement of the conductors and need only be evaluated once.

For practical purposes the air is assumed to have zero conductance, and

$$Z_g = 1000\jmath\frac{\omega\mu_a}{2\pi}[\Psi]$$

where $[\Psi]$ is a matrix of potential coefficients.

The lumped shunt admittance parameters Y are completely defined by the inverse relation of the potential coefficients matrix (Galloway *et al.*, 1964), *i.e.*

$$Y_g = 1000\jmath\omega 2\pi\epsilon_a[\Psi]^{-1}$$

where ϵ_a = permittivity of free space = 8.854×10^{-12} (F.m^{-1}).

As Z_g and Y_g are linear functions of frequency, they need only be evaluated once and scaled for other frequencies.

8.3.1.3 Conductor Impedance Matrix Z_c

This term accounts for the internal impedance of the conductors. Both resistance and inductance have a non-linear frequency dependence, and need to be computed at each harmonic frequency. An accurate answer for a homogeneous non-ferrous conductor of annular cross-section involves the evaluation of long equations based on the solution of Bessel functions, as shown in (8.1).

$$z_c = \frac{\jmath\omega\mu_a}{2\pi}\frac{1}{x_e}\frac{J_0(x_e)N_0'(xii) - N_0(x_e)J_0'(xii)}{J_0'(x_e)N_0'(xii) - N_0'(x_e)J_0'(xii)} \tag{8.1}$$

Where

$x_e = \jmath\sqrt{\frac{\jmath\omega\mu_a}{\rho_c}}\, a_e$
$xii = \jmath\sqrt{\frac{\jmath\omega\mu_a}{\rho_c}}\, a_i$
a_e = external radius of the conductor (m)
a_i = internal radius of the conductor (m)
J_0 = Bessel function of the first kind and zero order
J_0' = derivative of the Bessel function of the first kind and zero order
N_0 = Bessel function of the second kind and zero order
N_0' = derivative of the Bessel function of the second kind and zero order
ρ_c = resistivity of the conductor material at the average conductor temperature (Ω.m)

The Bessel functions and their derivatives are solved, within a specified accuracy, by means of their associated infinite series. Unfortunately convergence problems are frequently encountered at high frequencies and low ratios of conductor thickness to external radius *i.e.* $(r_e - r_i)/r_e$, necessitating the use of asymptotic expansions.

A new closed form solution has been proposed based on the concept of complex penetration (Semlyen and Deri, 1985); unfortunately errors of up to 6.6 per cent occur at low frequencies making the method unsuitable for harmonic studies.

To overcome the difficulties of slow convergence of the Bessel function approach and the inaccuracy of the complex penetration method, an alternative approach based upon curve fitting to the Bessel function formula has been developed by Daza, 1988. Equation (8.2) is used to approximate the internal impedance.

$$z_c = (s_c + t_c c)R_{dc} + \jmath(u_c + v_c c)R_{dc} \tag{8.2}$$

Where

$z_c \in Z_c$
$c = \sqrt{\frac{f}{R_{dc}}}$
R_{dc} = direct current resistance of the conductor ($\Omega.km^{-1}$)
s_c, t_c, u_c, v_c = curve fitting coefficients

A maximum value of $c = 300$ and thickness to radius ratios of between 1.0 and 0.4 were considered. Coefficients for thickness ratios not provided for in Table A2 are calculated using linear interpolation.

An assessment of the errors introduced by the curve fitting approach shows, a maximum error of 2 per cent for the real and reactive components of the internal impedance for a thickness ratio of 0.5.

The matrix Z_c is diagonal, and normally computations for one phase conductor and one earth-wire are sufficient.

A comparison of the computational requirements of the Acha Curve Fitting, Semlyen and Bessel Function models for conductor impedance calculations indicate that 70% and 90% reductions of CPU time are achieved through the use of the Acha curve fitting model for conductor impedance.

8.3.1.4 Reduced Equivalent Matrices Z_p and Y_p

Although transmission lines contain a large number of conductors, *i.e.* earth-wires and several bundle conductors per phase, it is more efficient to solve the system in terms of reduced equivalent phase parameters.

Reduction of bundle conductors can be achieved in two ways. One of them, the Geometric Mean Radius (GMR) concept (Anderson, 1973), although frequency independent, provides an efficient computational solution. This method can only be used when information on the distribution of currents within a bundle is not required. However such detailed information is only required when calculating the inductive field at very small distances from the line. It is not required for the calculation of equivalent disturbing currents.

The second method uses matrix reduction techniques. It includes frequency dependence for the series impedance but requires considerable computation, with the following three steps carried out for each frequency (except for ψ_m since this matrix is frequency independent).

1. Setting up of Z and ψ_m with an order equal to the total number of conductors plus earth-wires.

2. By assuming that the voltage from the line to ground is exactly the same for all the conductors in the bundle, and that of an earth wire is zero, two transformation matrices B_m and B_{mt} are built up, so that modified matrices Z_{pp} and ψ_{mpp} are obtained, *i.e.*

$$Z_{pp} = B_{mt} Z B_m$$

$$\psi_{mpp} = B_{mt} \psi_m B_m$$

   By way of example, for a system of 3 conductors, A1, A2 and E, where A1 and A2 are bundled together while the E is continuously earthed. Matrix B_m will then be

$$B_m = \begin{array}{c|ccc} & \text{A1} & \text{A2} & \text{E} \\ \text{A1} & +1 & -1 & 0 \\ \text{A2} & 0 & +1 & 0 \\ \text{E} & 0 & 0 & +1 \end{array}$$

3. Next a partial inversion (Shipley and Coleman, 1959) is applied to the matrices Z_{pp} and ψ_{mpp}. All but those phase conductor rows that have not been modified are inverted. Thus, final reduced equivalent matrices Z_p and ψ_{mp} are arrived at, whose order equals the number of phases but implicitly accounts for the original configuration.

8.3.1.5 Transformation Matrix from Equivalent Phase Currents to Conductor Currents

Information on all conductor currents is required for a thorough interference assessment near the line. A transformation matrix from equivalent phase to conductor

currents is calculated during the reduction of the series impedance matrix. After the partial inversion, the following partitioned matrix equation is obtained.

$$\begin{vmatrix} V_{sp} \\ I_{be} \end{vmatrix} = \begin{vmatrix} Z_{\mathrm{p}} & K_a \\ T_{be} & K_b \end{vmatrix} \times \begin{vmatrix} I_{\mathrm{ep}} \\ 0 \end{vmatrix}$$

Where

V_{sp} = vector of series voltage drops in the equivalent phase conductors (V)
I_{be} = subconductor and earth wire current vector (A)
T_{be} = matrix relating subconductor currents to equivalent phase currents
I_{ep} = vector of equivalent phase currents (A)

The currents in the bundle subconductors and earth wires can be calculated using (8.3).

$$I_{be} = T_{be} I_{\mathrm{ep}} \tag{8.3}$$

This equation determines the currents in those conductors that have been eliminated. To determine the current in the principal conductor of each bundle the relationship that the equivalent phase current is the sum of the subconductor currents is used. Matrix T_{be} is augmented with these equations to yield the complete transformation matrix.

8.3.2 Evaluation of Distributed Parameters

As the electrical distance increases with frequency, long-line effects must be taken into account in harmonic propagation analysis.

To date only equivalent π circuits have been used for harmonic distortion applications (Arrillaga *et al.*, 1983; Dommel, 1984). However, the transfer function approach seems to be a more efficient alternative (Semlyen and Abdel-Rahman, 1982).

8.3.2.1 Modal Analysis at Harmonic Frequencies

The inclusion of long-line effects in multiconductor transmission line models is not as simple as for single phase lines, because it involves matrix rather than scalar operations.

Operations such as square roots, logarithms, circular and hyperbolic functions *etc.* are not directly defined in matrix theory. In the solution adopted by Dommel (Dommel, 1984), Galloway (Galloway *et al.*, 1964) and Semlyen (Semlyen and Abdel-Rahman, 1982) the matrices are diagonalized, *i.e.* decoupled, through modal analysis and then normal scalar operations are carried out for the decoupled matrices.

In transmission line theory two transformation matrices are needed. One defines the modal voltages and the other the modal currents, *i.e.*

$$V_p = T_v V_m$$

$$I_p = T_i I_{mo}$$

Where

V_p = vector of phase voltages,
I_p = vector of phase currents,
V_m = vector of modal voltages,
I_{mo} = vector of modal currents,
T_v = eigensolution of the product ZY, and
T_i = eigensolution of the product YZ.

The matrices Z and Y are the lumped parameter matrices derived earlier.
Also, as an extension,

$$Z_{\mathrm{m}} = T_v^{-1} Z T_i$$

$$Y_{\mathrm{m}} = T_i^{-1} Y T_v$$

At this stage, both Z_{m} and Y_{m} are fully diagonal and scalar operations are permitted. For instance,

$$\gamma_{\mathrm{m}} = \sqrt{z_{\mathrm{m}} y_{\mathrm{m}}}$$

$$z_{\mathrm{om}} = \sqrt{\frac{z_{\mathrm{m}}}{y_{\mathrm{m}}}}$$

where $z_{\mathrm{m}} \in Z_{\mathrm{m}}$ and $y_{\mathrm{m}} \in Y_{\mathrm{m}}$.

The same is true for all the hyperbolic and transfer functions discussed below.
Also a transformation from modal to phase domain is possible,

$$Z = T_v Z_{\mathrm{m}} T_i^{-1}$$

$$Y = T_i Y_{\mathrm{m}} T_v^{-1}$$

For an efficient numerical solution, the proposed algorithm uses the following simplifications:

1. Theoretically, transformation matrices T_v and T_i must be obtained at each harmonic frequency, as modal transformations are unique and frequency dependent. However it has been observed that they do not vary much for a wide range of frequencies (Semlyen and Deri, 1985). Our investigation has found that a single eigenanalysis, carried out at the fundamental frequency, is sufficiently accurate for use at harmonic frequencies.

2. The transformation matrices T_v and T_i are non-singular and the following relationships exist between them (Dommel, 1984),

$$[\mathbf{T_i}]^{\mathrm{T}} = T_v^{-1}$$

$$[\mathbf{T_v}]^{\mathrm{T}} = T_i^{-1}$$

Thus, only one eigensolution is needed rather than two.

8.3.2.2 ABCD Parameters

The ABCD parameters matrix equation for a transmission line section, is

$$\begin{vmatrix} V_s \\ I_s \end{vmatrix} = \begin{vmatrix} [\boldsymbol{A}_m] & B_m \\ [\boldsymbol{C}_m] & [\boldsymbol{D}_m] \end{vmatrix} \times \begin{vmatrix} V_r \\ -I_r \end{vmatrix}$$

Where

$$\begin{aligned} [\boldsymbol{A}_m] &= T_v \times \mathrm{Diag}(\cosh \gamma_\mathrm{m} \ell) \times T_v^{-1} \\ B_m &= T_v \times \mathrm{Diag}(z_\mathrm{om} \times \sinh \gamma_\mathrm{m} \ell) \times T_i^{-1} \\ [\boldsymbol{C}_m] &= T_i \times \mathrm{Diag}(\tfrac{1}{z_\mathrm{om}} \sinh \gamma_\mathrm{m} \ell) \times T_v^{-1} \\ [\boldsymbol{D}_m] &= [\boldsymbol{A}_m]^\mathrm{T} \end{aligned}$$

8.4 Auxiliary Plant Models

For a lumped series element, the ABCD parameter matrix equation is,

$$\begin{vmatrix} V_s \\ I_s \end{vmatrix} = \begin{vmatrix} [\mathbf{U}] & [\mathbf{Z}_\mathrm{se}] \\ & [\mathbf{U}] \end{vmatrix} \times \begin{vmatrix} V_r \\ -I_r \end{vmatrix}$$

Where

$[\mathbf{Z}_\mathrm{se}]$ = Diag (series impedance of each phase)
$[\mathbf{U}]$ = identity matrix

While for a shunt element,

$$\begin{vmatrix} V_s \\ I_s \end{vmatrix} = \begin{vmatrix} [\mathbf{U}] & \\ [\mathbf{Y}_\mathrm{sh}] & [\mathbf{U}] \end{vmatrix} \times \begin{vmatrix} V_r \\ -I_r \end{vmatrix}$$

Where

$[\mathbf{Y}_\mathrm{sh}]$ = Diag(shunt admittance of each phase)

8.5 Calculation of the Inductive Influence Profiles

The procedure for the determination of the base set of inductive influence profiles is given in Figure 8.2.

As the system is linear, the inductive profile can be solved for each frequency independently of all others.

The first step towards the solution of the base inductive influence profiles for a given harmonic on the system is the entry of the ABCD matrices. At this stage the entire system of w elements can be represented by the equation

$$\begin{vmatrix} V_s \\ I_s \end{vmatrix} = \begin{vmatrix} A_{n1} & B_{n1} \\ C_{n1} & D_{n1} \end{vmatrix} \times \cdots \times \begin{vmatrix} A_{nw} & B_{nw} \\ C_{nw} & D_{nw} \end{vmatrix} \times \begin{vmatrix} V_r \\ -I_r \end{vmatrix}$$

```
Do for all frequencies
    Read in the ABCD matrices for all elements
    Cascade ABCD matrices so that the system between observation points is repre-
    sented by a single matrix
    Cascade ABCD matrices to give the system ABCD matrix
    Transform system ABCD matrix into an admittance matrix
    Do for the sending and receiving ends of the system
        Do for each phase
            Form the terminal voltage injection vector
            Solve for the terminal currents
            Assemble the receiving end vector
            Solve for the equivalent phase currents at each observation point
            Calculate all conductor currents at each observation point
            Calculate the residual current or the inductive field
            Store the residual current or inductive field profile
        End do
    End do
End do
```

Figure 8.2. Solution of the Base Set of System Responses

This equation frequently contains more information than required, so to reduce the volume of data ABCD matrices are cascaded so that the system between neighbouring observation points is represented by a single matrix. These matrices are retained for later use, and cascaded to yield a single matrix for the entire system *i.e.*

$$\begin{vmatrix} V_s \\ I_s \end{vmatrix} = \begin{vmatrix} [\boldsymbol{A}_m] & B_m \\ [\boldsymbol{C}_m] & [\boldsymbol{D}_m] \end{vmatrix} \times \begin{vmatrix} V_r \\ -I_r \end{vmatrix}$$

In general $[\boldsymbol{A}_m] \neq [\boldsymbol{D}_m]^{\mathrm{T}}$ for non-homogeneous systems.

However, an equivalent matrix equation in the form of ABCD parameters may not be the most desirable answer as it will depend on the source to be injected and the response to be observed, *i.e.* voltages or currents. Thus a systematic way of transforming a particular transfer function into another is proposed next. The partial inversion algorithm (Shipley and Coleman, 1959) is central to the present approach.

For instance, for converting (8.5) into a nodal admittance matrix equation the following steps are needed,

1. Interchange block rows.

$$\begin{vmatrix} I_s \\ V_s \end{vmatrix} = \begin{vmatrix} [\boldsymbol{C}_m] & [\boldsymbol{D}_m] \\ [\boldsymbol{A}_m] & B_m \end{vmatrix} \times \begin{vmatrix} V_r \\ -I_r \end{vmatrix}$$

2. Move the negative sign inside the matrix.

$$\begin{vmatrix} I_s \\ V_s \end{vmatrix} = \begin{vmatrix} [\boldsymbol{C}_m] & -[\boldsymbol{D}_m] \\ [\boldsymbol{A}_m] & -B_m \end{vmatrix} \times \begin{vmatrix} V_r \\ I_r \end{vmatrix}$$

3. Partially invert the last block equation.

$$\begin{vmatrix} I_s \\ I_r \end{vmatrix} = \begin{vmatrix} Y_{n2} & Y_{n1} \\ Y_{n4} & Y_{n3} \end{vmatrix} \times \begin{vmatrix} V_r \\ V_s \end{vmatrix}$$

4. Change the order of the block columns.

$$\begin{vmatrix} I_s \\ I_r \end{vmatrix} = \begin{vmatrix} Y_{n1} & Y_{n2} \\ Y_{n3} & Y_{n4} \end{vmatrix} \times \begin{vmatrix} V_s \\ V_r \end{vmatrix}$$

With the formation of these matrices we now proceed with the solution of the system for a unit voltage injection into each phase, from each end of the link, with all other injections set to zero.

If a single profile was to be determined then the actual terminal conditions are inserted into the injection vector instead of each of the 2.k unit injection vectors, otherwise the method is unchanged.

A direct solution for the sending and receiving end currents I_s and I_r is found by multiplying the system admittance matrix and the injection vector.

The vector of receiving end conditions

$$\begin{vmatrix} V_r \\ I_r \end{vmatrix}$$

is then assembled and the equivalent phase currents and voltages calculated by multiplying by each of the ABCD matrices from the receiving to the sending end.

All conductor currents are calculated using the method described in section 8.3.1.5, from which the residual current I_n or inductive field E_n can be determined. The profiles of these quantities are retained for later use, while the conductor currents, ABCD and transformation matrices are discarded.

8.6 Calculation of the Total Inductive Field

To determine the total inductive field it is necessary to solve for the total inductive influence for each harmonic using scaling and superposition of the base results from section 8.5, and then to combine the effect of all harmonics. The algorithm is shown in Figure 8.3. Implementation is simple and will not be expanded upon here.

8.7 Efficient Calculation of the Cumulative Probability Distribution

Cumulative probability distributions are a particularly useful means to present the interfering ability of a transmission system as the mean and spread of the interference can be assessed at a glance, and confidence limits on the interference can be read directly from the graph.

As the output from section 8.6 is raw data, it may be processed by the user into any form using commonly available statistical analysis packages or custom software.

```
Do for each injected spectra
    Zero the vector of inductive influences at each observation point
    Do for each harmonic
        Zero the vector of single harmonic contributions at each observation point
        Do for the sending and receiving ends of the system
            Do for each phase
                Scale the base profile by the actual injection
                Add the resultant quantity to the harmonic contribution for each ob-
                servation point
            End do
        End do
        Scale the single harmonic contribution by the frequency weighting factor if
        appropriate, square the result, and add to the inductive influence at each
        observation point
    End do
    Take the square root of the inductive influence at each observation point
    Output the total inductive influence profile for the injected spectra
End do
```

Figure 8.3. Calculation of the Total Inductive Influence

8.8 Application to HVDC Link

The algorithm was originally derived for the determination of the inductive influence of the New Zealand HVDC transmission system from long term measurements of the harmonic voltage spectra at the terminals. The link consists of 569.7 km of aerial transmission line, 39.1 km of submarine cable, harmonic filters, surge capacitors, smoothing reactors and earth return electrodes. Due to the use of five different line geometries, the wide variation in the earth resistivity below the line and the need to observe standing waves at frequencies up to the 50'th harmonic, the line had to be partitioned into 113 sections. The parameters for the aerial line alone occupied 8 megabytes.

Harmonic voltages of all orders up to the 50'th were measured at 3 minute intervals for a period of 12.5 days at the terminals and were used in the program to determine the cumulative probability distributions of the inductive influence, and the profile of the inductive influence along the link.

The profile of the average equivalent disturbing current profile along the link is given in Figure 8.4. Figure 8.5 contains the cumulative probability distribution of the equivalent disturbing current at the Benmore terminal of the link.

To confirm the validity of the computer model simultaneous measurements of the injected voltage at Benmore and the resultant pole currents were conducted at two sites at distances of 123 and 390 km from Benmore. In all cases the calculated 600 Hz pole currents (dominant harmonic on the link) were within 5% of those measured. Details of the experimental procedure and results are contained in Chapter 9.

Given the success of the simple models discussed in this paper the authors believe that the use of more rigorous models is not warranted. All existing models employ simplifying assumptions about the structure of the line, earth and electrical characteristics of the materials as the actual case of a finite length line above an inhomogeneous

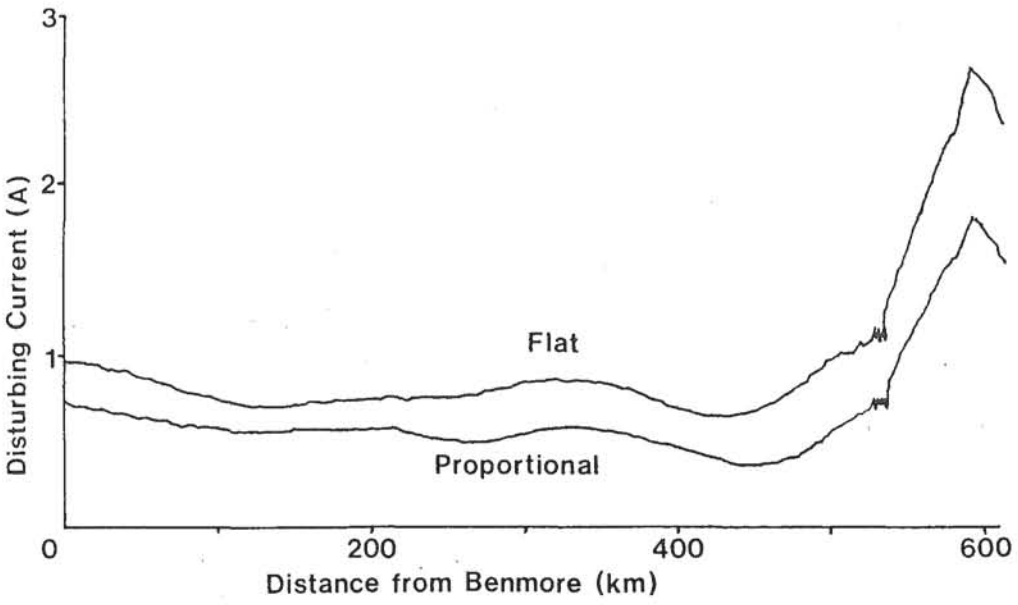

Figure 8.4. Equivalent Disturbing Current Profile on the NZ HVDC Link

earth is impossible to model in detail. Therefore there is no guarantee that existing rigorous models are more accurate than the approximate models as they share the same fundamental modelling assumptions.

8.9 Conclusions

An efficient algorithm for the assessment of the inductive influence of a transmission system has been presented. Superposition is employed to greatly reduce the computation effort required for repetitive studies, while the use of residual currents and induced fields for intermediate results reduces storage requirements.

A transmission line model of general applicability in harmonic penetration and interference studies is employed in the algorithm. In common with existing algorithms the proposed model includes long line effects and frequency dependence representation. The main feature distinguishing this algorithm is the incorporation of line discontinuities such as phase transpositions, line geometry or earth resistivity variations, and filters or static VAR compensation devices.

It has also been shown that the computing requirements can be substantially reduced, without loss of accuracy, by several novel simplifications of the rigorous formulation of transmission line parameters, particularly in the case of earth and conductor impedance calculation. As a result the proposed algorithm is extremely efficient and can be used economically in repetitive studies.

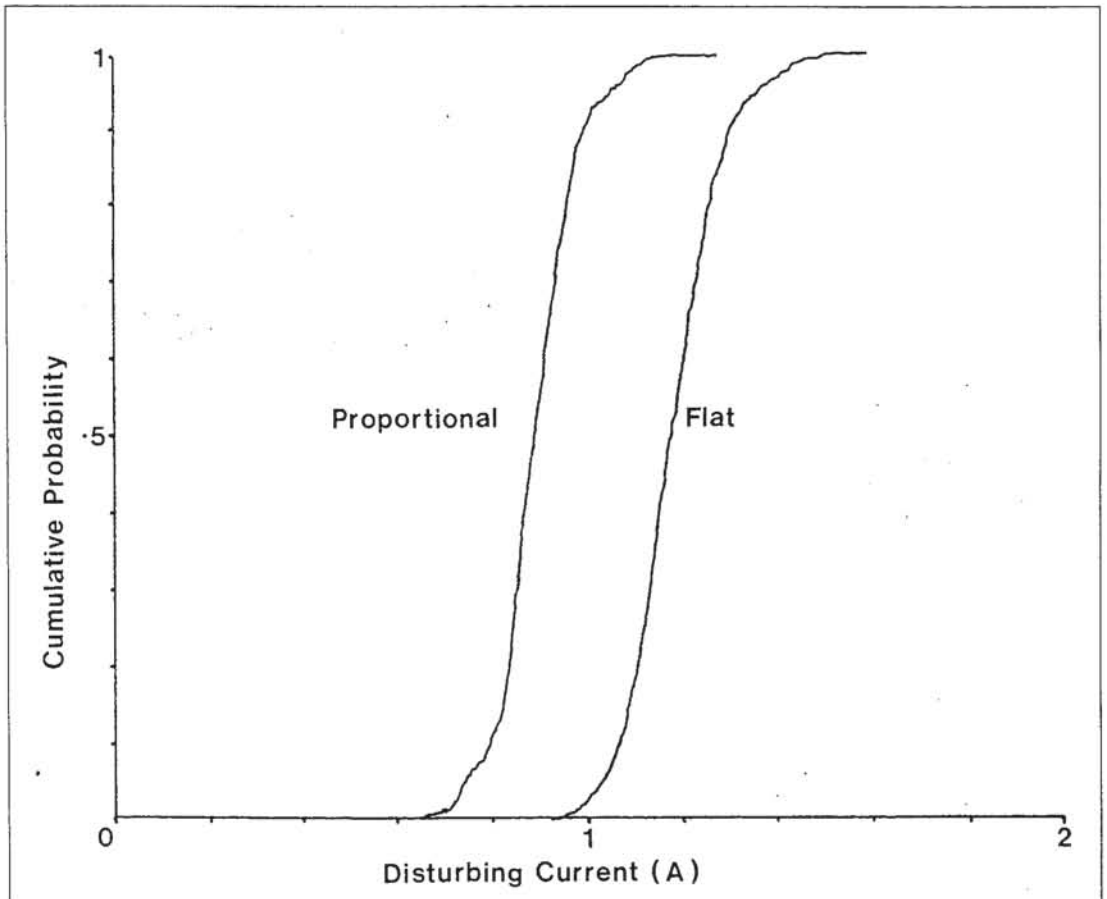

Figure 8.5. Cumulative Probability Distribution of the Equivalent Disturbing Current at the Benmore Terminal of the NZ HVDC Link

CHAPTER 9

INDUCTIVE INFLUENCE OF THE NZ HVDC LINK: EXPERIMENTAL STUDIES AND RESULTS

9.1 Introduction

The proposal by Electricorp to increase the capacity of the HVDC transmission system from 600 to 992 mega-watts would have resulted in increased telephone interference from the DC transmission line unless additional protection measures are taken. However before the design of such protective devices could be undertaken, an acceptable level of interference from the upgraded link had to be established.

The philosophy of Electricorp when specifying the performance of the upgraded link was that the interference should be no greater than that from the existing system. Interference to communication services from the existing link was considered to be acceptable, although problems did exist in some rural areas.

Unfortunately the interfering ability of the existing system was unknown. Therefore a study was undertaken by the University of Canterbury to determine the performance of the existing link.

The principal aims of this work were:

- To provide a profile of the equivalent disturbing current along the line to identify regions of high interference.
- To calculate the probability distribution of the disturbing current injected into the line to determine a maximum acceptable disturbing current.

Two approaches to this problem were possible. Either measure the disturbing currents along the line over a long period of time, or predict the current using a computer model. The first option was impractical for a transmission system of this length as many observation sites would be required to observe the standing waves at harmonic frequencies. Therefore a program of computer simulations was devised, complemented by a series of experiments to establish the validity of the models used.

This report describes the experimental and computational methods used to determine the interfering ability of the existing link, and presents the results of these studies in a form suitable for specifying the performance of DC filters.

9.2 Field Experiments: Design and Implementation

The aim of the experiments was to confirm the validity of the computer models, and to provide data for use in the models. Two experiments were devised for confirming the validity of the computer models, while two other experiments were conducted to provide data for the models.

The first experiment, known as the *Line Tuning* experiment, was designed to confirm the accuracy of the model for the entire transmission system by comparing calculated

conductor currents in the transmission line with measured values. Any differences between the computed and measured values were reduced by scaling the earth resistivities under the transmission lines in the model.

The *Test Line* experiment was intended to confirm the accuracy of the power-telephone coupling models. This involved the comparison of calculated and measured voltages induced in a length of cable laid parallel to the transmission line.

Measurements of the earth resistivity were conducted in the *Earth Parameter* experiments for use in the power-telephone coupling models.

The last experiment comprised the measurement of the DC side harmonics of a convertor for a period in excess of one week. The purpose of this *Long Term Harmonic Voltage* experiment was to provide a data base of typical harmonic spectra, to be used in the computer model for determining the average disturbing current profile on the link.

9.2.1 Experimental Procedures

The next four sub-sections describe experimental procedures for each of the four experiments.

9.2.1.1 Line Tuning Experiment

To determine the harmonic currents on a DC transmission line it is necessary to know the harmonic injections at both ends of the link. Unfortunately the harmonic injections vary significantly with time, therefore it is necessary to measure the injections at the same time as the line currents.

In the case of the New Zealand HVDC system, this problem is simplified by the presence of the Cook Strait cable. The high shunt admittance of the cable at harmonic frequencies may be considered to effectively decouple the north and south island sections of the link. As a consequence it is only necessary to consider, as a first approximation, current flow due to an injection from the convertor on the same side of Cook Strait as the observation point.

As the transmission system is longer than one wavelength for high order harmonics, standing waves of current will occur on the link. To confirm the existence of these waves it was decided to measure the line currents at two points on the transmission line. Due to equipment limitations the line currents at the two sites could not be measured simultaneously. Therefore on one day simultaneous measurements of the Benmore convertor voltage and the line currents were taken at the first site, with the procedure repeated for the second site at a latter date.

The line current measurement sites were located hundreds of kilometres from the convertor. Due to the mountainous nature of the terrain between the convertor and the field sites it was not possible to establish direct communication between the measuring instruments. Synchronising of the instruments was achieved by prearranging the sampling time, with the clocks in the instruments synchronised to the time signals broadcast by Radio New Zealand. The harmonic analyzers were controlled by IBM personal computers, programmed to sample each harmonic fifteen times, starting at zero seconds. Fifteen samples was the maximum number of samples that the instruments could measure in fifty seconds. By averaging the samples, errors due to poor synchronisation are reduced. All harmonic orders from one to fifty inclusive were sampled with the results stored on machine readable media for analysis. Further details of the experimental apparatus are contained in Section 9.2.3.

The first line tuning experiment was conducted at the Peel Forest field site in conjunction with Benmore on the 22nd of February 1988. Two further experiments

were undertaken at the Isolated Flat field site in conjunction with Benmore at 11:30 and 19:30 on the 24th of February 1988.

9.2.1.2 Test Line Experiment

To confirm the validity of the power-telephone coupling models it was necessary to simultaneously measure the currents in the transmission line and the resultant induced voltage in a neighbouring cable. As the electric field induced by the line currents was small, care must be taken to ensure that external influences do not significantly effect the results. Consequently great care must be taken when selecting the experiment site. Details of the these requirements and the sites used are contained in Section 9.2.2.

The test cable was laid on the surface of the earth, parallel to the transmission line, at separations of between ten and one thousand metres. Measurements of the line currents and the induced cable voltage were taken at each selected harmonic. The harmonic orders measured were determined by the dynamic range of the analyzer. Many harmonics were so small that they were not worth measuring. Each harmonic was sampled for a period of thirty seconds, and the results averaged to reduce errors due to poor synchronisation. A UHF radio was used to communicate between the measuring sites, with the initiation of a measurement started on a verbal command. Further details of the equipment used are contained in Section 9.2.3.2 and Section 9.2.3.3.

Test line experiments were conducted at the field sites on the 22nd and 24th of February respectively.

9.2.1.3 Long Term Harmonic Voltage Monitoring

The long term harmonic voltage monitoring experiment was conducted at Benmore for a period of twelve and one half days starting on the 25th of February 1988.

Single measurements of the voltage on both poles of the convertor for each harmonic order from one to fifty inclusive were recorded. A measurement cycle of a single sample of each harmonic took approximately two and a half minutes, with the next cycle started at the following zero second time. The harmonic analyzer was controlled by an IBM personal computer, which recorded the data with a time stamp on machine readable media.

A copy of the Benmore station log for the duration of the experiment was also obtained so that measurements taken during periods of atypical convertor operation could be excluded.

Details of the harmonic voltage measuring equipment are contained in Section 9.2.3.1.

9.2.1.4 Earth Resistivity Experiment

Details of the earth resistivity were required at the field sites for use in the computer programs that calculate the line currents, and the induced voltages in neighbouring cables.

The earth resistivity was measured at two locations at the Peel Forest and Isolated Flat sites. One set of readings was obtained at a distance of fifty metres from the line, while a second was obtained for a separation of five hundred metres. A profile of the apparent earth resistivities to depths of one hundred metres was calculated.

9.2.2 Selection of Experiment Sites

The computer models used to represent transmission lines include many simplifying assumptions that limit the accuracy with which the computer model can match reality. Transmission line models assume that the transmission line is perfectly straight, that the conductors are parallel to the earth, and that the earth can be represented by an infinite plane surface comprising several horizontal layers of homogeneous earth. In addition to these assumptions the electromagnetic induction program ignores the effect of other structures and external sources which would disrupt the fields around the test line. For these reasons care must be taken to select an experimental site which fits as closely as possible to the mathematical model to determine the accuracy of the models.

The requirements for the field experiment site may be summarized as follows.

1. The transmission line should be straight and uniform.
2. The terrain should be flat for the test line experiments.
3. There should be no other interfering sources in the vicinity.
4. Periodically grounded structures such as metal post fences, and irrigation channels which could shield the test line should be avoided.
5. The two sites selected should be sufficiently far apart to observe standing waves of current on the line.
6. Communication to the Benmore was required.

The two sites which satisfied these requirements were Peel Forest, and Isolated Flat. These sites are discussed in greater detail below.

In addition to the field sites, a site at one of the convertor stations was required for the harmonic voltage measurements. The selection of Benmore as the site for these measurements is discussed below.

9.2.2.1 Benmore Convertor

The Benmore convertor was selected as the site for the harmonic voltage measurements as the transmission line to which it is connected is electrically long, and therefore standing waves would occur. Selection of the convertor station as a test site also enabled the use of existing services such as power supplies, voltage transducers, and station personnel for the experiment.

9.2.2.2 Peel Forest

The Peel Forest test site was located midspan, between towers 361 and 362. There are 123 kilometres of transmission line between this site and Benmore.

The experiment site was located in a paddock, on a semi-intensive sheep farm. In this region the transmission line is approximately three kilometres from the foothills, and two kilometres from the Rangitata river. The terrain in this area is flat, being part of a river plain, and is very rocky and prone to drought in summer. Many fences crossed the experiment area which extended from the mid-span position in a south-easterly direction for one kilometre. Most of these fences were of wooden post construction, and would not therefore influence the test line or earth resistivity experiments. However care was taken to avoid the fences as much as possible. A eleven kilo-volt distribution line was located located half a kilometre from the HVDC transmission line, on the opposite side to that used for the test line experiments. Preliminary tests at the one

kilometre test line site indicated that the HVDC transmission line was the dominant noise source.

9.2.2.3 Isolated Flat

The Isolated Flat test site was approximately 390 kilometres from Benmore, between towers 1135 and 1136.

The experiment site was located on Molesworth station, an extensive beef farm. Isolated flat is part of a long river valley, composed of out-wash from the surrounding hills. Near the hills the ground was practically devoid of soil, resulting in extremely high surface resistivities. However the main experiment site under the line was near a spring. There were no fences or other transmission lines near the experiment site, and therefore it was electrically very quiet.

9.2.3 Equipment Requirements

To perform the four experiments, four sets of equipment were required.

A DC voltage measurement system was required at Benmore for the Line Tuning and Long Term Harmonic Voltage Monitoring experiments.

Line current measuring equipment was needed for the Line Tuning, and the Test Line experiments at the field sites.

Also required for the test line experiment was an induced cable voltage measuring system at the field sites.

A resistivity set was necessary to determine the conductivity of the earth.

Each of these items, and additional support equipment are discussed in the following sub-sections.

9.2.3.1 DC Voltage Harmonic Measurement

The DC harmonic voltage measuring equipment was required to simultaneously measure the magnitude of the harmonics on outer poles of groups 1 and 4, and the phase angle between the voltages.

Transducers

Existing resistive voltage dividers A62-79 on groups 1 and 4 were used to measure the harmonic voltages. These dividers are located between the wall bushings and the smoothing reactor, and measure the pole voltage with respect to the station ground. Capacitive voltage dividers in the wall bushings are normally connected in parallel with the resistive dividers, but were disconnected for the harmonic measurements.

An additional adjustable resistive divider was connected to the output of the primary dividers. This device removed the DC component and reduced the signal to a level compatible with a fibre optic transmission system used to convey the signals from the DC switchyard to the spectrum analyzer. The secondary dividers were adjusted so that signal into the analyzer was reaching one hundred percent of the rated input, to minimise the effect of the limited dynamic range of the analyzer. On completion of the experiments, the secondary dividers, fibre optic transmission system, and harmonic analyzers were calibrated. It was not possible to calibrate the primary resistive dividers, therefore manufacturers data was used to predict the response of these dividers when loaded.

Instrumentation

A two channel spectrum analyzer was required to measure the voltage harmonics. As described previously the harmonic voltage measurements were taken in synchronisation with line current measurements during the Line Tuning experiment, and continuously during the Long Term Harmonic Voltage Measuring Experiment. To achieve these goals a fully automated system was required. This was implemented by using an IBM personal computer to control and store the measurements taken by a Wandel and Goltermann NOWA-1 harmonic analyzer.

The principal limitations of this measurement system were the slow data acquisition rate, and the poor resolution of the NOWA-1. When measuring voltage magnitudes and phase of a single harmonic on both channels, the sampling rate was only one sample every three seconds. Resolution of the samples was limited to one milli-volt for a maximum permissible input of one volt, while the phase angle resolution was one degree. The error limits for the NOWA-1 are 1.5frequencies below 1 kilo-hertz with an additional error of 3 degrees for higher frequencies. A further phase error may occur when the magnitude of the input signals is small.

Control of the NOWA-1 was affected by an IBM personal computer. Data acquisition was controlled by the computers clock. An operator was required to set the starting time, and to transfer data from the hard disk. However no other assistance was required. The sampling strategies used for the Line Tuning and Long Term Harmonic monitoring experiments were discussed in Section 9.2.1.1 and Section 9.2.1.3 respectively.

The instruments were located in the convertor control room. A fundamental frequency reference was required for the harmonic analyzer, this was obtained from a 400 volt signal derived from the convertor supply in one of the controller cabinets.

Direct communications to the field sites was not possible. However indirect communications was established by telephone and VHF radio.

9.2.3.2 Line Current Measurement

Line current measurements were required for the Line Tuning and Test Line experiments.

A non-contact method was desired for measuring the currents as it could be installed quickly, and without having to shut down the link. As there were no systems of this type available locally, a custom system was designed and built by the University of Canterbury. The design and testing of the line current measuring equipment is discussed in the following sections.

Transducers

It is possible to solve explicitly for all currents in a multiconductor transmission line if the equivalent phase currents and the primitive series impedance matrix are known (see Section 9.3.1). Therefore if the series impedance matrix is known, then it is only necessary to take sufficient measurements to uniquely determine the equivalent phase currents to determine all conductor currents in the system. For an N phase system, N independent readings are required to solve for the N equivalent phase currents. Thus in the case of the HVDC transmission only two independent readings are required to uniquely determine all conductor currents.

Sensing of the harmonic currents on each of the poles was achieved by using air cored loop antenna to measure the magnetic field. The loop antennae were located at the apex of an right angled triangle .In this way the null of the loop reduced the unwanted signal due to the other pole.

The loop antenna consisted of one hundred turns of wire wound on a square wooden former with sides one metre long. A conducting sheath was wound around the coils to provide electrostatic shielding. Each coil was centre-tapped, with the centre tap connected to ground. The ends of the coil were connected to a high common mode rejection ratio, low noise preamplifier.

The preamplifier provided calibrated gain settings from ten to one thousand. An attenuator was used after the preamplifier to provide gain control when the amplifier was in use. Theoretically the loop antenna and preamplifiers were capable of detecting one milli-amp of fifty hertz current flow on a pole conductor.

Accurate positioning of the loop antenna was very important as the sensitivity of the antenna is dependant on position. The loop antenna and preamplifiers were mounted on a telescopic mast. The mast was located on the tower centre-line, at the mid-span position. This position was used as the conductors are low and horizontal at this point. A theodolite was used to measure the height of the conductors, and the mast was then raised so that the centre of the loop antenna formed a right angled triangle with the bundle centres of the pole conductors. Adjustments were made during the course of the day as the temperature, and therefore the height of the conductors varied.

Calibration tests on the loop antennae were conducted in the laboratory before and after the field experiments. A reference loop antenna was used in the calibration tests to generate a known field. The output voltage of the preamplifiers was measured using an Hewlett Packard 3561A signal analyzer instead of NOWA-1, in all other respects the system tested was identical to that used in the field. Unfortunately the tests revealed that one of the antennae had become faulty between the two calibration tests, possibly during the field experiments. It was also discovered that the NOWA-1 analyzers have a high input capacitance which would load the output of the attenuator. The effect of this additional loading has been predicted using the known circuit for the devices. All measurements taken using the antennae have been processed assuming that the antenna were faulty and working.

Instrumentation

A NOWA-1 harmonic analyzer under control of an IBM personal computer was used to measure the harmonic voltages.

A fifty hertz signal was required by the harmonic analyzer for determining the sampling rate. However preliminary studies indicated that the fifty hertz current on the pole conductors varied significantly with time, and was unsuitable for use as a triggering source. This observation is not surprising as fifty hertz is an uncharacteristic harmonic, and therefore its magnitude will vary significantly with time as the factors which produce it change. The most stable harmonic current on the transmission line is the twelfth, as it is the fundamental for the convertor. Therefore a phase-locked loop was designed to track the twelfth harmonic. The output of the filter was divided by twelve to produce a stable fifty hertz trigger signal.

9.2.3.3 Induced Cable Voltage Measurement

The major method used for telephone reticulation in rural New Zealand is buried plastic unshielded cable. The purpose of the test line experiment was to confirm the accuracy of the models used to predict coupling to buried cables.

Transducer

A one hundred metre length of URM67 coaxial cable was used to detect the induced voltages for the Test Line experiments. The cable was laid on the surface of the earth parallel to the transmission line. Both the inner and outer conductor were grounded at one end of the cable, with a preamplifier connected between the inner conductor and ground at the other. The outer conductor was earthed at only one point so that it would act as an electrostatic shield, simulating the conditions for a shallowly buried cable. Earth connections were made using fifteen centimetre steel stakes driven into the ground.

The test line cable sites were surveyed at separations of ten, twenty, fifty, one hundred, two hundred, five hundred and one thousand metres from the line. All cable sites were located on a line perpendicular to the transmission line, which passed through the line current measuring site. The line current measuring equipment would therefore be measuring the currents at those parts of the conductors closest to the test line.

Instrumentation

A preamplifier and single channel spectrum analyzer were required for measuring the induced voltages in the cable.

A YEW type 3131 DC amplifier was used to amplify the cable voltages. This device can provide calibrated gains of between one and ten thousand. The main advantage of this instrument is its very high input impedance of ten mega-ohms. A high input impedance device reduces the effect of poor ground connections on the measured voltage, although it does make the results more susceptible to error due to coupling by means of the electric field.

A Hewlett Packard 3561A dynamic signal analyzer was used to measure the output voltage from the preamplifier. This instrument has built in averaging functions, therefore it was not necessary to store the raw data on computer for latter processing. The analyzer was set up to sample the input continuously for a period of thirty seconds, and to calculate either the time or RMS average of the samples for the selected harmonic. The NOWA-1 analyzer at the line current test site was set up to take ten samples during the same thirty second period. Synchronisation of the two analyzers was achieved by verbal command over a UHF radio link.

An external signal was required for triggering the analyzer when time averaging the samples. This signal was derived from the twelfth harmonic signal from the output of the preamplifier using the phase-locked loop system described in Section 9.2.3.2 .

9.2.3.4 Earth Resistivity Measurement

Earth resistivity data to a depth of one hundred metres was required to form a three layer model for computer model of the test line experiment, and for determining all conductor currents from the loop antenna voltages.

Instrumentation

An expanding Wenner method was used to measure the earth resistivity. Care was take when performing these tests to avoid long earthed structures, such as fences and the pylons, which would effect the results.

9.2.3.5 Power Supplies

Power for the instruments at the field sites was generated by a portable alternator. The output of the alternator was fed to an invertor operating at fifty five hertz. This technique was used to reduce interference from the local supplies. To further reduce this problem the alternator and invertor were located fifty metres from the experiment sites, with the connecting cable run at right angles to those used for the Test Line experiments. Preliminary tests at the one kilometre test line site indicated that the noise due to the instrument supply was well below that due to the DC transmission line. The bandwidth of the analyzer was sufficient to distinguish the fifty hertz DC line current from the fifty five hertz supply current.

Instruments at the Benmore convertor station were powered from the station supply.

9.3 Computer Simulations: Algorithms and Models

Computer programs were required to perform the following tasks :

1. Calculate the conductor currents in the transmission line.
2. Predict the voltage induced in the Test Line.
3. Determine the disturbing current profile along the entire link.

Several computer programs were written to achieve these goals. Details of the algorithms and models used in these programs are given below.

9.3.1 Determination of the Line Currents from Field Measurements

The loop antennae used to sense the line currents do not output a voltage dependant solely on the pole that they are directed at. Current flow in the other pole, the earth wire, and the earth itself all influence the measured voltage. If the geometry of the transmission line, loop antennae, and the earth resistivity are known, then an equation can be formed for each loop output voltage in terms of the conductor currents and mutual impedances. However the currents in the conductors cannot be uniquely determined from this system of equations as the number of unknown quantities (the conductor currents) exceeds the number of known quantities (the loop antenna voltages).

Current flow in a transmission line is constrained by the mutual and self impedances of the conductors. If these constraints and interrelationships are known, then it is possible to solve for all currents in the transmission line given the equivalent phase currents. (The equivalent phase current is the vector sum of all currents in the subconductors connected to that phase.) This is achieved in practice by manipulating the primitive series impedance matrix, which expresses the voltage drop per unit length due to current flow in the conductors. Using the assumptions that the series voltage drop in bundled conductors is identical, and that the series voltage drop in an earth wire is zero, a system of equations can be formed which expresses all conductors currents in terms of the equivalent phase currents. The assumptions made are those used in transmission line parameter programs when reducing matrices to equivalent phase parameters. These assumptions are valid at frequencies of interest for telephone interference studies.

The problem of determining the conductor currents from the loop antenna voltages may now be solved by combining the system of equations relating the loop antenna

voltages to the conductor currents, with the equations expressing the conductor currents in terms of the equivalent phase currents. The resultant system relating the loop voltages to the equivalent phase currents may be solved directly. Finally all conductor currents can be found from the equivalent phase currents.

The accuracy of this method is dependant on the accuracy of the primitive series impedance matrix. This matrix is formed by a transmission line parameter program, and is discussed in greater detail in Section 9.3.4.1. To form this matrix details of the line geometry, conductor type, and earth resistivity are required. The line geometry and earth resistivity were measured at the experiment sites to reduce errors. A three layer earth model was used when calculating earth return impedances.

Measured transducer characteristics were used in the program to correct for differences between the ideal and actual responses.

The major modelling error in this method is the representation of the earth wire. The earth wire is assumed to be perfectly grounded at each pylon. In a discussion with G Campbell (technician, Addington Test Room, Electricorp) it was stated that during tests on two towers of the DC transmission line it was discovered that the earth wire was effectively insulated from the pylon at low voltages due to corrosion. The computer model also ignores the footing resistance of the towers. Ideally the effect of these discrepancies will be small as very little current flows through the pylons on a long, uniform line. However further tests should be conducted to confirm the validity of this model.

9.3.2 Predicting the Test Line Voltages

Predictions of the test line voltages were made by forming the sum over all conductors, of the products of the conductor current and the mutual impedance between the test line and the conductor. The conductor currents were determined using the method described in section 3.1 . Mutual impedance calculations being made using measured earth resistivity data in a three layer earth model.

The result of these calculations is the electric field at the site of the test line, assuming that the inducing line is infinitely long. This result must be corrected to account for the finite length of the test cable, the resistance of the ground connections, and the loading effect of the preamplifier. The cable was modelled by a uniform transmission line with a distributed source emf representing the field induced by the harmonic currents. Electrical parameters of the test line were calculated using Foster's mutual impedance formula for finite line conductors on the surface of the earth. The resistance of the earth return path was represented in two ways. In the "lumped" model the resistance between the earth stakes was halved, and the cable modelled as a transmission line connected to ground at the ends via this "lumped" resistance. A "distributed" model was also formed, in which the earth resistance was assumed to be uniformly distributed along the line, with ideal ground connections at the ends. This results in a higher attenuation term in the propagation factor for the test line. In reality the cable should be modelled using a non-uniform model incorporating concepts from both the distributed and lumped models.

Both the distributed and lumped models were used to predict the input voltage to the preamplifier as a function of earth resistivity. The earth connections will only effect the test line output voltage for earth resistivities above one thousand ohm-metres. Measured surface resistivities at the test sites ranged from five hundred to forty thousand ohm-metres. Therefore the ground connections could be expected to reduce the measured voltage.

9.3.3 Predicting the Disturbing Ability of the Link

The algorithm for the calculation of the disturbing ability of the HVDC link has been described in Chapter 8.

9.3.4 Computer Models

The accuracy of the model used is dependant mainly on the models used to represent the elements of the transmission system. Details of the models used are contained in the following sections.

9.3.4.1 Transmission Lines

The major factor influencing the accuracy of the transmission line models is the electrical characteristics of the earth, as the characteristics of the conductors are known. Four models of the earth are available within the transmission line parameter program. Two of the models are based on Carson's equation, the third uses Dubanton's complex penetration model, and the fourth is a three layer model that includes the permeability and permittivity of each layer in addition to the resistivity.

Resistivity data provided by the DSIR has been used in the earth return models. Where a range of earth resistivities was provided, a value has been calculated from the extreme values by interpolation. A scale factor was used in this interpolation process to specify the weightings applied to each extreme value. In this way the transmission system model could be optimised to fit measured data by adjusting a single parameter.

For the majority of the computer simulations a single layer earth model has been used, as it was discovered that the results were relatively insensitive to earth resistivity variations, and the three layer model is computationally expensive. The three layer model has been used for calculating the parameters of the line at the test sites where the structure of the earth was measured. Carson's equation was used to calculate the earth return parameters for a single layer earth, with the earth resistivity of the bottom layer provided by the DSIR used in the model.

The skin effect, bundling of sub-conductors, and earth wires are all modelled within the program using established techniques. Long line effects are included in the model. The program has been verified by comparison with the University of British Columbia Line Constants program.

Earth resistivity data was provided along the entire length of the line. The line has been broken into sections no greater than ten kilometres long to observe the standing waves. Most of the section breaks occur at points were the earth resistivity changes.

9.3.4.2 Smoothing Reactors

The smoothing reactors were modelled as a 0.8 henry inductor in series with a 0.32 ohm resistor representing the copper losses. A 3.0 nano-farad capacitor is connected in parallel with the reactor to account for inter-turn capacitance. This capacitance is a typical figure for other convertor installations, and may not be accurate for the New Zealand system. The capacitance was included as the smoothing reactor is the major item of plant limiting harmonic current flow on the link. Therefore a small shunt conductance across the reactor could increase current flow in the link due to the high voltage drop across the reactor. Tests indicated that the capacitance has little effect however.

9.3.4.3 Surge Capacitors

Surge capacitors of 0.9 micro-farads are installed on each pole at Benmore. Capacitors of 25.0 micro-farads at Benmore, and 100.0 micro-farads at Haywards, are connected between neutral and station ground. All of these components are modelled as ideal capacitors. The impedance of the station grounds was not known, and has not been modelled. This should not introduce a significant error as impedance of the ground connection is low in relation to other elements.

9.3.4.4 Line Traps

Line traps are installed in the DC switchyard, at the carrier injection points, and at fighting bay. They are modelled as 1.05 milli-henry inductors.

9.3.4.5 Ground Electrodes

A 0.22 ohm resistor is used to represent the Benmore land electrode, while the sea electrode is modelled by a 0.265 ohm resistor. The parameters of the electrode lines were calculated using the transmission line parameter program. It is assumed that the link is operating in bipolar mode, and therefore the sea electrode is disconnected. However as the electrode line is located on the same towers as the pole conductors, there is coupling between the pole conductors and the electrode line, and therefore it must be modelled.

9.3.4.6 High Frequency Capacitor and Damping Filter

A high frequency capacitor of 0.1 micro-farads is installed at Benmore. At Haywards this capacitor is split into a hanging part of 1.1 micro farads and a standing part of 5.0 micro-farads. The standing capacitor is tuned by a 14.0 milli-henry inductor to form a 600 hertz blocking filter. A resistor is included in the model of the blocking filter to dampen the response.

9.3.4.7 Cook Strait Cables

The parameters of the Cook Strait cables were calculated using a program developed by the University of British Columbia.

9.3.4.8 Convertors

The convertors are represented by ideal voltage sources. An additional constraint on the convertor model is that the sum of the currents into the convertor must be zero. This constraint is necessary to solve the system as the neutral voltage is unknown.

9.4 Results

The results of the experimental measurements and computer simulations are presented and compared in the following sections.

9.4.1 Earth Resistivity Experiments

Earth resistivity measurements were conducted at the Peel Forest and Isolated Flat test sites. Measurements were taken near the line, and approximately half a kilometre from the line. From these measurements a profile of the effective earth resistivity to a depth of one hundred metres was obtained. The effective earth resistivity profile was

decomposed into a three layer earth model for the computer studies. Details of these models are given below.

Location : Peel Forest, below the transmission line.
Top layer: 12500 ohm-metre 4.0 metres thick
Middle layer : 6500 ohm-metre 10.0 metres thick
Bottom layer : 380 ohm-metre

Location : Peel Forest, 700 metres from the transmission line.
Top layer: 12100 ohm-metre 4.5 metres thick
Middle layer : 2800 ohm-metre 13.5 metres thick
Bottom layer : 460 ohm-metre

Location : Isolated Flat, below the transmission line.
Top layer: 500 ohm-metre 6.5 metres thick
Middle layer : 240 ohm-metre 53.5 metres thick
Bottom layer : 300 ohm-metre

Location : Isolated Flat, 500 metres from the transmission line.
Top layer: 40600 ohm-metre 4.0 metres thick
Middle layer : 360 ohm-metre 10.0 metres thick
Bottom layer : 940 ohm-metre

The results for the Peel Forest test site are reasonably consistent between the two locations. However this is not the case for the Isolated Flat tests. Ground conditions varied significantly at the Isolated Flat test site. The moisture content of the soil was high under the line due to a spring, but at distances greater than one hundred metres from the line there was practically no moisture at the surface, and very little soil. Difficulties were encountered performing the experiments at Peel Forest and Isolated Flat due to the high surface resistivities. The measurements taken at Isolated Flat varied significantly, and often in an inconsistent manner, therefore the accuracy of the results at large depths is poor.

9.4.1.1 Line Tuning Experiments

The aim of the experiments was to tune the computer model by comparing the line currents measured with the loop antennae, to those predicted using a model of the link and measured voltage injections. Tuning of the computer model by adjustment of the earth resistivity would then be performed to minimize the error.

The raw data from each experiment consisted of fifteen measurements of the phase and magnitude of the convertor and loop antennae output voltages for each harmonic.

To calculate the line currents from the convertor voltage spectra, the measurements were scaled by the inverse transfer function of measuring system and injected at Benmore. The system was then solved for the equivalent phase currents at the test site. This procedure was repeated for each injection, and the results averaged. Voltage spectra measured at the Benmore convertor were injected at the Haywards end of the model to estimate the effect of a north island injection on current flow in the south island.

Equivalent phase currents were determined from the loop antennae voltages by scaling the measurements by the inverse of the transducer characteristics and applying the method described in Section 9.3.1.

Three experiments were performed, one at Peel Forest and two at Isolated Flat. Average twelfth harmonic equivalent phase currents for each of these tests are listed below.

Peel Forest
Measured phase currents
Pole 1 : 9.304 Amps
Pole 4 : 9.674 Amps
Phase angle between poles : 3.729 radians
Calculated phase currents for an injection at Benmore
Pole 1 : 8.984 Amps
Pole 4 : 9.100 Amps
Phase angle between poles : 3.087 radians
Calculated phase currents for an injection at Haywards
Pole 1 : 1.739 Amps
Pole 4 : 1.728 Amps
Phase angle between poles : 3.139 radians
Total calculated current
Pole 1 : 9.151 Amps 98% of measured value
Pole 4 : 9.263 Amps 96% of measured value

First Isolated Flat experiment
Measured phase currents
Pole 1 : 4.914 Amps
Pole 4 : 4.798 Amps
Phase angle between poles : 3.431 radians
Calculated phase currents for an injection at Benmore
Pole 1 : 4.496 Amps
Pole 4 : 4.920 Amps
Phase angle between poles : 2.996 radians
Calculated phase currents for an injection at Haywards
Pole 1 : 1.180 Amps
Pole 4 : 1.094 Amps
Phase angle between poles : 3.210 radians
Total calculated current
Pole 1 : 4.648 Amps 95% of measured value
Pole 4 : 5.040 Amps 103% of measured value

Second Isolated Flat experiment
Measured phase currents
Pole 1 : 4.850 Amps
Pole 4 : 4.979 Amps
Phase angle between poles : 3.199 radians
Calculated phase currents for an injection at Benmore
Pole 1 : 4.745 Amps
Pole 4 : 5.005 Amps
Phase angle between poles : 3.107 radians
Calculated phase currents for an injection at Haywards
Pole 1 : 1.204 Amps
Pole 4 : 1.153 Amps
Phase angle between poles : 3.165 radians
Total calculated current
Pole 1 : 4.895 Amps 101% of measured value
Pole 4 : 5.136 Amps 103% of measured value

Only the twelfth harmonic current has been considered here, as all other harmonic

voltages measured by the loop antenna were less than five percent of the twelfth. Therefore the accuracy of measurements at other frequencies was be poor due to the low resolution of the NOWA-1 harmonic analyzer.

A single layer earth model was used in the computer model for the transmission line. The earth resistivities used in this model were half way between the extremes estimated for the bottom earth layer by the DSIR. Measured earth resistivities were used in a three layer model at the experiment sites.

The total calculated current was formed by taking the square root of the sum of the squared currents due to each injection. This averaging method is used as the north and south island power systems are not frequency locked. Consequently the phase of the harmonics will vary continuously with time. Measurements were made over a period of forty five seconds, therefore the phase between the currents should have varied sufficiently to consider it to be randomly distributed.

The results indicate that an injection at Haywards can cause significant current flow in the south island. However as the harmonic voltages were not measured at Haywards, the magnitude of these currents could differ significantly from those calculated above. Consequently tuning of the computer model was abandoned as small variations in the calculated currents with earth resistivity are swamped by the uncertainty in the current flow due to the injection at Haywards. Preliminary tests indicated that the current flow on the link was relatively insensitive to earth resistivity.

In general the agreement between the magnitudes of the measured and computed phase currents is good. All calculated currents are within six percent of the measured values. However there is a larger difference between the phase angles. The measured phase angles are often larger than those calculated, suggesting that there is a larger component of zero sequence current flowing in the line than the model predicts. This difference is discussed in the following section.

9.4.2 Test Line Experiments

The test line experiment was designed to confirm the validity of the power-telephone coupling models. However it also serves as a further check on the validity of the entire transmission line model by measuring the residual current on the transmission line.

Test line experiments were conducted at the Peel Forest and Isolated Flat sites.

The raw data from the experiment consisted of ten measurements of the output voltage from the loop antennae, and the average voltage on the test line. Samples were measured continuously on the test cable for a period of thirty seconds, and averaged internally by the instrument. However the signals from the loop antennae were just sampled as often as possible and stored for later processing.

The method for determining the conductor currents from the loop antenna voltages was discussed in Section 9.3.1 and Section 9.3.2 . An additional step of correcting for the imperfect transducer characteristics was performed prior to using these algorithms. The electric field at the site of the cable was calculated for each set of transducer measurements, and averaged to estimate the cable emf.

A specific model of a finite length cable was discussed in Section 9.3.2 . However this model is not included in the electric field calculation, as it is highly dependant on cable type, and more importantly, the grounding electrodes at the ends of the test cable, and load on the cable. The electric field at the cable site is a better indication of the interfering ability of the line than the EMF induced in the cable. Also the surface resistivity at the test sites was high, and highly variable. Consequently the calculated cable voltage could vary significantly.

When faulty, gain and phase response of one of the loop antenna changed. The characteristics of the faulty antenna were determined by measurement in the laboratory

after the field tests. It is possible however that the antenna was in an indeterminate state, between working and faulty, during the field tests.

The results show that the calculated electric fields do not fit the measured data. However a sensitivity analysis revealed that the calculated field was highly dependant on the phase angle between the measured loop antenna voltages.

To determine where the cause of the discrepancy lay, the equivalent phase currents calculated by the program from measured voltage injection data were used to predict the electric fields at the cable position. Measured injection data for a eleven hour period on the 26th of February was used to determine the average fields at the cable. Voltage injections from both ends of the link were used to determine the currents at the experiment sites.

In summary, the fit of the electric field predicted using loop antenna voltages to the measured data is poor. However the electric fields predicted using harmonic voltage injection data measured at Benmore is considerably better. The line currents calculated from the loop antenna voltages are similar in magnitude to those predicted using voltage injections at the ends of the link (see Section 9.4.1.1), however there is a significant difference in the phase angles. Therefore it is likely that there was a phase error in the line current measuring system. Furthermore the agreement between the measured test line voltage, and the electric field predicted using the full model of the link is good. Consequently the conductor currents predicted using this model will be a reasonable estimate of the actual currents.

9.4.3 Predicted Disturbing Current Profile

Predictions of the disturbing current profile on the entire link were made using the tuned computer model and measured injection data. The injection data contained measurements of all harmonics from the first to the fiftieth. Each set of single measurements of all harmonics was injected into the link, and the equivalent disturbing current profile calculated. Proportionally and flat weighted disturbing currents were calculated. The RMS average of these disturbing current profiles is shown in figure 3.

This graph differs from those previously presented, in that the disturbing current profile for the south island is reduced. This is due to changes made in the modelling of the earth wire. Reductions would also be expected in the north island profile, however this is not the case, and will be investigated further.

9.5 Conclusion

A non invasive system consisting of a pair of crossed loop antenna has been developed for the measurement of harmonic currents in high voltage transmission lines. An inversion algorithm derived by the author enables all conductor and earth wire currents to be determined using this system.

Despite the apparent failure of a transducer during the experiments, the agreement between experimental and computed results is good indicating that the harmonic propagation model is valid.

Therefore predictions of the disturbing current made using this model for the south island should be close to the actual current flow. The calculated results for the north island show some unusual trends. As the calculated results for the north island are high, and unusual, it is recommended that measurements be performed on the north island system to determine the accuracy of the model.

CHAPTER 10

CONCLUSIONS

The electromagnetic field induced by harmonic current flows in high voltage transmission lines couples energy into neighbouring telecommunications cables which may impair the operation of communication systems. Problems of this type can be avoided by the inductive coordination of the power and telecommunication systems. Such an approach requires an understanding of: harmonic current sources within the power system and the ways in which they can be mitigated; the ability of a transmission line to induce voltages into communication cables and the manner in which this can be reduced; and the susceptibility of telecommunications equipment and methods for reducing this susceptibility.

This research project has been concerned with the ability of high voltage transmission lines to induce voltages into communications cables under steady state conditions, and techniques for reducing this inductive influence. This thesis has contributed to this topic by:

- Reviewing the procedure for the determination of the state of power and telecommunication systems coupled via an electromagnetic field.

  It has been shown that if the coupling between power and telecommunication systems is weak, then the power system, electromagnetic field determination and telecommunication system studies may be partially decoupled. Such an approach is valid for coupling to buried cables under steady state conditions.

- Summarizing existing wave propagation and mutual impedance models for a conductor above a lossy earth.

  Propagation along a transmission line may be considered to be Lossless (TEM), Quasi-TEM or Exact. The conditions under which these models are valid have been stated. Mutual impedance models have been reviewed with emphasis being placed on the assumptions made during the derivation of the models, how they may be implemented and their physical interpretation.

- Establishing the accuracy of existing models.

  Existing models have been applied to the task of predicting the coupling between a single conductor transmission line and a buried cable over the range of conditions typically encountered in New Zealand. The maximum error expected in any single mutual impedance calculation relative to that obtained using the Exact model is 17% for Carson's equation (both integral and series forms), and occurs when both the earth resistivity and frequency are high. Under these conditions Quasi-TEM models are not strictly valid.

- Determining the factors affecting the inductive influence of the single conductor lines.

It has been demonstrated that the LEF dependencies in the immediate vicinity of the line differ significantly from those at large separations. In the immediate vicinity of the line the LEF is highly sensitive to geometry and frequency variations but substantially independent of earth resistivity. At moderate to large separations these sensitivities are reversed.

- Developing a new family of simple Quasi-TEM models.

  New models for the mutual impedance of conductors in the presence of the earth have been derived. They are based upon the approximation of the continuous current distribution in the ground by an ensemble of filamentary currents. The Vertical Inducing Loop model, the simplest member of the family, has a clear physical interpretation which enables accurate predictions of the LEF induced by multiconductor lines to be made without recourse to numerical evaluation.

- Determining the factors affecting the inductive inflence of multiconductor transmission lines.

  The LEF induced by multiconductor lines has been studied as a function of separation, frequency, earth resistivity, geometry and current sequence. The dependencies in the immediate vicinity of the transmission line differ from those at large separations. Fields induced by zero sequence current display similar dependencies to those of the single conductor line. Balanced sequence current flows have significantly different frequency and earth resistivity dependencies that are also highly sensitive to transmission line geometry. The field at large distances from multiconductor lines is dominated by the zero sequence component, unless the conductors and earth wires lie in two or more different horizontal planes. In this case the balanced sequence field decays at the same rate as the zero sequence field, but is an order of magnitude smaller for the same current magnitude. It is not valid therefore to consider only zero sequence current flows when assessing the interfering ability of transmission lines. The inductive influence of a transmission line may be reduced by choosing phasing arrangements that are symmetric with respect to the earth, and by minimising conductor height and interconductor spacings.

- Studying the effect of continuously grounded earth wires on the inductive influence of multiconductor lines.

  The installation of a continuous grounded earth wire can reduce the LEF induced by zero sequence current flows by up to 50%, although it may worsen the induction due to balanced sequence components. ACSR earth wires offer significantly better shielding than GEHSS conductors at low frequencies due to their lower resistance. Shield wire losses are significant, but are small in relation to phase conductor losses.

- Deriving new measures for quantifying inductive influence.

  New measures for quantifying the ability of high voltage transmission lines have been proposed, based upon the Vertical Inducing Loop model. They are superior to existing measures as they include the effect of transmission line geometry, earth resistivity, frequency and all sequences of current flow on the inductive influence.

- Designing an efficient algorithm for calculating the LEF along transmission lines.

  An efficient algorithm for the calculation of inductive influence along transmission lines from terminal busbar conditions has been developed and applied to the New Zealand inter-island HVDC link. Comparison of the simulation results with

currents along the line measured using a non-invasive loop antenna system has confirmed the validity of the transmission line model.

- Development of a non-invasive system for the measurement of harmonic currents.

  A transducer consisting of a pair of crossed loop antennae was used to measure the alternating magnetic field below the DC transmission line of the New Zealand HVDC link. An inversion algorithm was developed which determined both the pole and earth wire currents from the magnitude and phase of the loop voltages, measured values of the earth resistivity and transmission line geometry. The principal advantage of this system is that it enabled measurements to performed safely anywhere along the transmission line without having to physically alter or come into contact with the transmission line conductors.

- Verification of mutual impedance formulas.

  The accuracy of the mutual impedance formulas for the coupling between transmission lines and buried cables have been established by comparison of the voltage induced in a cable parallel to the HVDC link with that calculated from the pole currents sensed using the loop antenna. The results suggest that the models are valid, but they also emphasised the need for very accurate transducers and instrumentation when attempting to determine balanced sequence transmission line currents from electromagnetic field measurements.

APPENDIX A

ACHA'S EARTH IMPEDANCE COEFFICIENTS

The following tables contain the coefficients for the piecewise curve fitting approximation to Carson's equation described in Section 3.5.2.

r		θ						
		0°	15°	30°	45°	60°	75°	90°
0.2	s_{acha}	.3910	.3911	.3915	.3922	.3929	.3937	.3944
	t_{acha}	.1892	.1854	.1739	.1545	.1268	.09050	.04560
	u_{acha}	.3795	.3773	.3710	.3606	.3467	.32990	.31120
	v_{acha}	.4817	.4822	.48380	.48640	.49000	.49420	.49910
0.5	s_{acha}	.3796	.3804	.3829	.3869	.3922	.3983	.4044
	t_{acha}	.1426	.1418	.1391	.1338	.1248	.1100	.08700
	u_{acha}	.4652	.4613	.4496	.4302	.4032	.36890	.32810
	v_{acha}	.4248	.4264	.43140	.43980	.45180	.46750	.48690
1.0	s_{acha}	.3591	.3606	.3654	.3734	.3847	.3993	.4167
	t_{acha}	.1042	.1047	.1064	.1087	.1112	.1127	.1107
	u_{acha}	.5018	.4978	.4856	.4650	.4356	.39710	.34930
	v_{acha}	.3680	.3699	.37550	.38550	.40070	.42240	.45220
1.5	s_{acha}	.3293	.3313	.3373	.3480	.3643	.3876	.4195
	t_{acha}	.07400	.07500	.07800	.08320	.09090	.1014	.1143
	u_{acha}	.5033	.4992	.4870	.4663	.4367	.39790	.34950
	v_{acha}	.3073	.3085	.31260	.32000	.33220	.35150	.38190
2.0	s_{acha}	.3019	.3037	.3095	.3201	.3371	.3631	.4025
	t_{acha}	.05560	.05650	.05940	.06460	.07280	.08510	.10320
	u_{acha}	.4855	.4812	.4679	.4454	.4132	.37060	.31730
	v_{acha}	.2623	.2628	.26440	.26750	.27310	.28310	.30180
2.5	s_{acha}	.2774	.2790	.2838	.2927	.3074	.3310	.3695
	t_{acha}	.04330	.04410	.04650	.05080	.05790	.06910	.08680
	u_{acha}	.4618	.4569	.4421	.4167	.3796	.32930	.26400
	v_{acha}	.2278	.2276	.22690	.22570	.22420	.22310	.22440
3.0	s_{acha}	.2559	.2570	.2605	.2670	.2779	.2959	.3268
	t_{acha}	.03470	.03530	.03710	.04050	.04610	.05500	.06970
	u_{acha}	.4370	.4316	.4150	.3864	.3438	.28410	.20270
	v_{acha}	.2006	.1998	.19720	.19240	.18490	.17360	.15740
3.5	s_{acha}	.2371	.2377	.2398	.2437	.2502	.2611	.2803
	t_{acha}	.02840	.02890	.03020	.03280	.03690	.04340	.05420
	u_{acha}	.4130	.4071	.3890	.3574	.3097	.24130	.14390
	v_{acha}	.1788	.1775	.17340	.16600	.15390	.13460	.10370
4.0	s_{acha}	.2205	.2207	.2216	.2230	.2252	.2287	.2348
	t_{acha}	.02370	.02400	.02500	.02680	.02970	.03410	.04120
	u_{acha}	.3906	.3843	.3649	.3309	.2792	.20400	.09390
	v_{acha}	.1608	.1592	.15420	.14490	.12950	.10470	.06370

Table A.1. Acha's Coefficients for the calculation of earth return impedances.

r		θ						
		0°	15°	30°	45°	60°	75°	90°
4.5	s_{acha}	.2058	.2057	.2054	.2046	.2029	.1997	.1932
	t_{acha}	.02000	.02024	.02096	.02222	.02413	.02688	.03081
	u_{acha}	.3699	.3633	.3430	.3073	.2528	.17300	.05524
	v_{acha}	.1459	.1441	.13840	.12780	.11040	.08229	.03572
5.0	s_{acha}	.1929	.1924	.1912	.1886	.1838	.1741	.1573
	t_{acha}	.01712	.01726	.01781	.01866	.01987	.02120	.02282
	u_{acha}	.3505	.3445	.3238	.2855	.2299	.14830	.02789
	v_{acha}	.1330	.1316	.12560	.11330	.09516	.06582	.01749
5.5	s_{acha}	.1809	.1812	.1781	.1727	.1646	.1551	.1274
	t_{acha}	.01473	.01501	.01519	.01552	.01609	.01734	.01684
	u_{acha}	.3375	.3255	.3026	.2730	.2127	.12860	.010340
	v_{acha}	.1247	.1199	.11260	.10520	.08436	.05360	.006572
6.0	s_{acha}	.1709	.1703	.1669	.1611	.1508	.1358	.1034
	t_{acha}	.01291	.01304	.01316	.01340	.01359	.01384	.01247
	u_{acha}	.3202	.3105	.2882	.2547	.1957	.11390	.0002289
	v_{acha}	.1146	.1110	.10410	.09442	.07436	.04499	.0006278
6.5	s_{acha}	.1617	.1608	.1570	.1504	.1386	.1202	.08458
	t_{acha}	.01137	.01144	.01150	.01161	.01155	.01122	.009331
	u_{acha}	.3051	.2965	.2746	.2392	.1816	.10250	-.004619
	v_{acha}	.1062	.1033	.09649	.08578	.06650	.03860	-.002085
7.0	s_{acha}	.1534	.1522	.1481	.1407	.1278	.1072	.07006
	t_{acha}	.01009	.01012	.01013	.01013	.009886	.009229	.007094
	u_{acha}	.2916	.2837	.2620	.2258	.1697	.09355	-.006136
	v_{acha}	.09895	.09640	.08975	.07866	.06016	.03382	-.002899
7.5	s_{acha}	.1460	.1444	.1398	.1322	.1184	.09621	.05893
	t_{acha}	.009039	.009005	.008957	.008912	.008548	.007662	.005504
	u_{acha}	.2790	.2720	.2508	.2139	.1594	.08693	-.005799
	v_{acha}	.09248	.09040	.08399	.07252	.05485	.03040	-.002728
8.0	s_{acha}	.1390	.1374	.1326	.1244	.1101	.08729	.05041
	t_{acha}	.008108	.008074	.008000	.007869	.007433	.006472	.004367
	u_{acha}	.2681	.2611	.2401	.2037	.1507	.08109	-.004632
	v_{acha}	.08705	.08499	.07867	.06746	.05044	.02751	-.002149
8.5	s_{acha}	.1327	.1310	.1261	.1174	.1027	.07973	.04383
	t_{acha}	.007314	.007278	.007182	.006994	.006513	.005528	.003544
	u_{acha}	.2580	.2511	.2303	.1946	.1431	.07633	-.003265
	v_{acha}	.08219	.08018	.07397	.06307	.04689	.02521	-.001492
9.0	s_{acha}	.1269	.1252	.1201	.1111	.09621	.07329	.03866
	t_{acha}	.006632	.006593	.006481	.006254	.005748	.004769	.002935
	u_{acha}	.2486	.2419	.2213	.1863	.1364	.07233	-.002039
	v_{acha}	.07784	.07586	.06979	.05922	.04375	.02335	-.0009185
9.5	s_{acha}	.1216	.1199	.1147	.1054	.09044	.06774	.03451
	t_{acha}	.006040	.006000	.005875	.005623	.005107	.004153	.002473
	u_{acha}	.2400	.2333	.2131	.1789	.1304	.06890	-.001093
	v_{acha}	.07391	.07197	.06605	.05583	.04103	.02179	-.0004877
10.0	s_{acha}	.1167	.1149	.1097	.1003	.08529	.06293	.03109
	t_{acha}	.005524	.005482	.005349	.005082	.004565	.003646	.002113
	u_{acha}	.2320	.2254	.2056	.1721	.1250	.06590	-.0004458
	v_{acha}	.07034	.06845	.06269	.05280	.03864	.02045	-.0002001
10.5	s_{acha}	.1121	.1104	.1051	.09560	.08067	.05872	.02821
	t_{acha}	.005072	.005028	.004889	.004614	.004103	.003226	.001825
	u_{acha}	.2245	.2180	.1986	.1658	.1202	.06323	-.00005569
	v_{acha}	.06710	.06525	.05965	.05010	.03652	.01929	-.00003059

Table A.1. Acha's Coefficients for the calculation of earth return impedances continued.

r		θ						
		0°	15°	30°	45°	60°	75°	90°
11.0	s_{acha}	.1079	.1062	.1009	.09133	.07650	.05501	.02573
	t_{acha}	.004672	.004628	.004486	.004207	.003706	.002872	.001589
	u_{acha}	.2175	.2112	.1921	.1601	.1157	.06082	.0001423
	v_{acha}	.06413	.06233	.05689	.04766	.03464	.01827	.0000537
11.5	s_{acha}	.1040	.1023	.09693	.08742	.07274	.05172	.02357
	t_{acha}	.004318	.004273	.004129	.003851	.003364	.002573	.001393
	u_{acha}	.2110	.2048	.1860	.1548	.1117	.05862	.0002129
	v_{acha}	.06141	.05966	.05437	.04545	.03295	.01735	.0000832
12.0	s_{acha}	.1004	.09867	.09330	.08382	.06931	.04878	.02166
	t_{acha}	.004002	.003957	.003813	.003538	.003066	.002317	.001227
	u_{acha}	.2049	.1988	.1804	.1499	.1079	.05661	.0002097
	v_{acha}	.05891	.05720	.05206	.04343	.03142	.01653	.00008188

Table A.1. Acha's Coefficients for the calculation of earth return impedances continued.

REFERENCES

[Alvarado and Betancourt 1983]
Alvarado, F.L. and Betancourt, R. "An accurate closed-form approximation for ground return impedance calculations," *Proceedings of the IEEE*, Vol. 71, No. 2, February, pp. 279–280.

[Ametani and Aoki 1989]
Ametani, A. and Aoki, M. "Line parameters and transients of a non-parallel conductors system," *IEEE Transactions on Power Delivery*, Vol. PWRD-4, No. 2, April, pp. 1117–1126.

[Anderson 1973]
Anderson, P.M. *Analysis of faulted power systems*, Iowa State University Press, 1st ed.

[Arrillaga and Callaghan 1989]
Arrillaga, J. and Callaghan, C.D. "A Double-Iterative Algorithm for the analysis of Power and Harmonic Flows at AC/DC Convertor Terminals," *Proceedings of the Institutionof Electrical Engineers, Part C*, Vol. 136, No. 6, November, pp. 319–324.

[Arrillaga *et al.* 1983]
Arrillaga, J., Densem, T.J. and Harker, B.J. "Zero sequence harmonic current generation in transmission lines connected to large convertor plant," *IEEE Transactions on Power Apparatus and Systems*, Vol. PAS-102, No. 7, July, pp. 2357–2363.

[Arrillaga *et al.* 1985]
Arrillaga, J., Bradley, D.A. and Bodger, P.S. *Power System Harmonics*, John Wiley & Sons, Chichester, 1st ed.

[Arrillaga *et al.* 1987]
Arrillaga, J., Watson, N.R., Eggleston, J.F. and Callaghan, C.D. "Comparison of steady-state and dynamic models for the calculation of AC/DC system harmonics," *Proceedings of the Institutionof Electrical Engineers Proceedings, Part C*, Vol. 134, No. 1, January, pp. 31–37.

[Ball and Poarch 1961]
Ball, W.C. and Poarch, C.K. "Telephone Influence Factor (TIF) and its Measurement," *AIEE Transactions, Part I*, Vol. 79, January, pp. 659–664.

[Bannister 1968]
Bannister, P.R. "Electric and magnetic fields near a long horizontal line source above the ground," *Radio Science*, Vol. 3, No. 2, February, pp. 203–204.

[Bannister 1970]
Bannister, P.R. "Utilization of image theory techniques in determining the mutual coupling between elevated long horizontal line sources," *Radio Science*, Vol. 5, No. 11, November, pp. 1375–1381.

[Bannister 1986]
Bannister, P.R. "Applications of complex image theory," *Radio Science*, Vol. 21, No. 4, July-August, pp. 605–616.

[Bridges and Shafai 1989]
Bridges, G. and Shafai, L. "Plane Wave Coupling to Multiple Conductor Transmission Lines above a Lossy Earth," *IEEE Transactions on Electromagnetic Compatability*, Vol. EMC-31, No. 1, February, pp. 21–33.

[Bridges *et al.* 1988]
Bridges, G., Aboul-Atta, O. and Shafai, L. "Solution of Discrete Modes for Wave Propagation along Multiple Conductor Structures above a Dissipative Earth," *Canadian Journal of Physics*, Vol. 66, pp. 428–438.

[Cameron *et al.* 1989]
Cameron, G., Arrillaga, J., Gleadow, J. and McKenzie, N. "Estimation of Equivalent Disturbing Currents in the Cook Strait HVDC Transmission System,", In *Symposium of Specialists in Electric Operational and Expansion Planning*, Sao Paulo - Brazil, August.

[Cameron *et al.* 1990]
Cameron, G.R., Acha, E. and Arrillaga, J. "An Efficient Algorithm for the Calculation of Harmonic Interference from Long Transmission Lines," *Journal of Electrical and Electronics Engineering, Australia*, Vol. 10, No. 2, June, pp. 73–82.

[Campbell 1923]
Campbell, G.A. "Mutual Impedances of Grounded Circuits," *Bell System Technical Journal*, Vol. 2, No. 4, October, pp. 1–30.

[Carson 1926]
Carson, J.R. "Wave Propagation in Overhead Wires with Ground Return," *Bell System Technical Journal*, Vol. 5, pp. 539–554.

[Carter 1947]
Carter, R.O. "The Mutual Impedance between Short Earth-Return Circuits," *The Journal of the Institution of Electrical Engineers, Part I*, Vol. 94, No. 78, June, pp. 275–277.

[CCITT 1989a]
CCITT *Directives concerning the Protection of Telecommunication Lines against Harmful Effects from Electric Power and Electrified Railway Lines, Volume I, Design, Construction and Operational Principles of Telecommunication, Power and Electrified Railway Facilities*, International Telecommunications Union, Geneva.

[CCITT 1989b]
CCITT *Directives concerning the Protection of Telecommunication Lines against Harmful Effects from Electric Power and Electrified Railway Lines, Volume VI, Danger and Disturbance*, International Telecommunications Union, Geneva.

[Chang and Olsen 1975]
Chang, D.C. and Olsen, R.G. "Excitation of an Infinite Antenna above a Dissipative Earth," *Radio Science*, Vol. 10, No. 8-9, August-September, pp. 823–831.

[Dabkowski 1978]
Dabkowski, J. "AC Voltage Induction on Buried Pipelines,", In *IEEE International Symposium on Electromagnetic Compatability*, pp. 243–246.

[Daza 1988]
Daza, E.A. *Modelling of Power System Transformers in the Complex Conjugate Harmonic Space*, PhD thesis, Electrical and Electronic Engineering Department, University of Canterbury, Christchurch, New Zealand.

[de Boor 1971]
de Boor, C. "CADRE: An algorithm for numerical quadrature,", In Rice, J.R. (Editor.), *Mathematical Software*, Academic Press, New York, ch. 7, pp. 417–449.

[Degauque *et al.* 1983]
Degauque, P., Courbet, G. and Heddebaut, M. "Propagation Along a Line Parallel to the Ground Surface: Comparison between the Exact Solution and the Quasi-TEM Approximation," *IEEE Transactions on Electromagnetic Compatability*, Vol. EMC-25, No. 4, November, pp. 422–427.

[Densem 1983]
Densem, T.J. *Three Phase Power System Harmonic Penetration*, PhD thesis, Electrical and Electronic Engineering Department, University of Canterbury, Christchurch, New Zealand.

[Densem *et al.* 1984]
Densem, T.J., Bodger, P.S. and Arrillaga, J. "Three Phase Transmission System Modelling for Harmonic Penetration Studies," *IEEE Transactions on Power Apparatus and Systems*, Vol. PAS-103, No. 2, February, pp. 310–317.

[Deri and Tevan 1981]
Deri, A. and Tevan, G. "Mathematical verification of Dubanton's simplified calculation of overhead transmission line parameters and its physical interpretation," *Archiv für Elektrotechnik*, Vol. 63, pp. 191–198.

[Deri *et al.* 1981]
Deri, A., Tevan, G., Semlyen, A. and Castanheira, A. "The complex ground return plane, a simplified model for homogeneous and multi-layer earth return," *IEEE Transactions on Power Apparatus and Systems*, Vol. PAS-100, No. 8, August, pp. 3686–3693.

[Dickens 1965]
Dickens, T.A.J. "A direct current transmission line. The design and construction of the 600 MW, 500 kV D.C. line between Benmore and Haywards," *New Zealand Engineering*, Vol. 20, No. 4, April 15, pp. 121–129.

[Dommel 1974]
Dommel, H.W. "Discussion on *Electromagnetic effects of overhead transmission lines Practical problems, safeguards, and methods of calculation* ," *IEEE Transactions on Power Apparatus and Systems*, Vol. PAS-93, May, pp. 900–901.

[Dommel 1984]
Dommel, H.W. "Transmission line models for harmonic studies,", In *International Conference on Harmonics in Power Systems*, Worcester, Massachusetts, October, pp. 127–131.

[Dommel 1985]
Dommel, H.W. "Overhead Line Parameters from Handbook Formulas and Computer Programs," *IEEE Transactions on Power Apparatus and Systems*, Vol. PAS-104, No. 2, February, pp. 366–372.

[Dudley and Casey 1989]
Dudley, D.G. and Casey, K.F. "Pulse propagation on a horizontal wire above ground: Far-zone radiated fields," *Radio Science*, Vol. 24, No. 2, March-April, pp. 224–234.

[Dwight 1918]
Dwight, H.B. "Skin Effect in Tubular and Flat Conductors," *Transactions of the AIEE*, Vol. 37, Part 2, July to December, pp. 1379–1403.

[Efthymiadis and Wedepohl 1978]
Efthymiadis, A.E. and Wedepohl, L.M. "Propagation Characteristics of Infinitely – long Single – conductor Lines by the Complete Field Solution Method," *Proceedings of the Institutionof Electrical Engineers*, Vol. 125, No. 6, June, pp. 511–517.

[Eggleston 1985]
Eggleston, J.F. *Harmonic Modelling of Transmission Systems Containing Synchronous Machines and Static Convertors*, PhD thesis, Electrical and Electronic Engineering Department, University of Canterbury, Christchurch, New Zealand.

[Evans 1930]
Evans, H.P. "A Two Dimensional Boundary Value Problem for the Transmission of Alternating Currents through a Semi-infinite Heterogeneous Conducting Medium," *Physical Review*, Vol. 36, No. 10, November 15, pp. 1579–1588.

[Faure *et al.* 1979]
Faure, J.L., Fontaine, J.M. and Kouteynikoff, P. "Numerical method of Near-field Evaluation, in Electromagnetic Interference Problems in Presence of the Earth,", In *Third Symposium and Technical Exhibition on Electromagnetic Compatability*, Rotterdam, May 1-3, pp. 101–106.

[Foster 1931]
Foster, R.M. "Mutual Impedance of Grounded Wires Lying On the Surface of the Earth," *Bell System Technical Journal*, Vol. 10, July, pp. 408–419.

[Foster 1933]
Foster, R.M. "Mutual Impedance of Grounded Wires Lying On or Above the Surface of the Earth," *Bell System Technical Journal*, Vol. 12, July, pp. 264–287.

[Galloway *et al.* 1964]
Galloway, R.H., Shorrocks, W.N. and Wedepohl, L.M. "Calculation of electrical parameters for short and long polyphase transmission lines," *Proceedings of Institutionof Electrical Engineers*, Vol. 111, No. 12, December, pp. 2051–2059.

[Garbow *et al.* 1977]
Garbow, B.S., Boyle, J.M., Dongarra, J.J. and Moler, C.B. *Matrix Eigensystem*

Routines - EISPACK Guide Extension, Lecture Notes in Computer Science 51, Springer - Verlag, Berlin, 1st ed.

[Gary 1976]
Gary, C. "Approche complète de la propagation multifilaire en haute fréquence par utilisation des matrices complexes," *E.D.F. Bulletin de la Direction des Etudes et Recherches, Serie B*, Vol. 3 4, pp. 5–20.

[Gill and MacDonald 1967]
Gill, P.J. and MacDonald, W.J.P. "Large Scale Earth Resistivity Experiment in New Zealand," *Nature*, Vol. 216, No. 5121, December 23, pp. 1195–1197.

[Hartenstein *et al.* 1972]
Hartenstein, R., Koglin, H.J. and Rees, V. "Equivalent circuit of HVDC lines for symmetric and unsymmetric operation in a frequency region 0 to 100 kHz," *ETZ-A (in German)*, Vol. 93, No. 3, pp. 148–152.

[Hedman 1968]
Hedman, D.E. "345–kV Line 60–Hz Ground Wire Losses," *IEEE Transactions on Power Apparatus and Systems*, Vol. PAS-87, No. 2, February, pp. 420–427.

[IEEE 1984]
IEEE *IEEE Standard Dictionary of Electrical and Electronic Terms*, IEEE Press, New York, 3rd ed.

[IEEE 1985]
IEEE *ANSI/IEEE Standard 455-1985, IEEE Standard Test Procedure for Measuring Longitudinal Balance of Telephone Equipment Operating in the Voice Band*, IEEE Press, New York, 25 July.

[Johansson and Ekstrom 1989]
Johansson, A.V. and Ekstrom, A. "Telephone Interference Criteria for HVDC Transmission Lines," *IEEE Transactions on Power Delivery*, Vol. 4, No. 2, April, pp. 1408–1421.

[Judkins and Nordell 1974]
Judkins, R.E. and Nordell, D.E. "Discussion on *Electromagnetic effects of overhead transmission lines Practical problems, safeguards, and methods of calculation* ," *IEEE Transactions on Power Apparatus and Systems*, Vol. PAS-93, May, pp. 901–902.

[Klewe 1958]
Klewe, H.R.J. *Interference between Power Systems and Telecommunication Lines*, Edward Arnold Ltd., London, 1st ed.

[Krakowski 1967]
Krakowski, M. "Mutual Impedance of Crossing Earth-return Circuits," *Proceedings of the Institution of Electrical Engineers*, Vol. 114, No. 2, February, pp. 253–257.

[Kuester *et al.* 1978]
Kuester, E.F., Chang, D.C. and Olsen, R.G. "Modal Theory of Long Horizontal Structures above the Earth, 1, Excitation," *Radio Science*, Vol. 13, No. 4, July–August, pp. 605–613.

[Kuester *et al.* 1981]
Kuester, E.F., Chang, D.C. and Plate, S.W. "Electromagnetic Wave Propagation along Horizontal Wire Systems in or near a Layered Earth," *Electromagnetics*, Vol. 1, No. 3, July–September, pp. 243–265.

[Kuussaari and Pesonen 1976]
Kuussaari, M. and Pesonen, A.J. "Measured Power-line Harmonic Currents and Induced Telephone Interference with Special Reference to Statistical Approach,", CIGRE, Volume 2, session paper 36–05, August 25 – September 2.

[Lacey 1952]
Lacey, L.J. "The Mutual Impedance of Earth-Return Circuits," *The Proceedings of the Institution of Electrical Engineers, Part IV*, Vol. 99, No. 28, pp. 156–167.

[Lewis and Tuttle 1958]
Lewis, W.A. and Tuttle, P.D. "The Resistance and Reactance of Aluminium Conductors, Steel Reinforced," *AIEE Transactions, Part III*, Vol. 77, No. 2, pp. 1189–1214.

[Lindell and Alanen 1984a]
Lindell, I.V. and Alanen, E. "Exact image theory for the Sommerfeld half space problem, Part I: Vertical Magnetic Dipole," *IEEE Transactions on Antennas and Propagation*, Vol. AP-32, No. 2, February, pp. 126–133.

[Lindell and Alanen 1984b]
Lindell, I.V. and Alanen, E. "Exact image theory for the Sommerfeld half space problem, Part II: Vertical Electric Dipole," *IEEE Transactions on Antennas and Propagation*, Vol. AP-32, No. 8, August, pp. 841–847.

[Lindell and Alanen 1984c]
Lindell, I.V. and Alanen, E. "Exact image theory for the Sommerfeld half space problem, Part III: General Formulation," *IEEE Transactions on Antennas and Propagation*, Vol. AP-32, No. 10, October, pp. 1027–1033.

[Lindell *et al.* 1986]
Lindell, I.V., Alanen, E. and von Bagh, H. "Exact image theory for the calculation of fields transmitted through a planar interface of two media," *IEEE Transactions on Antennas and Propagation*, Vol. AP-34, No. 2, February, pp. 129–137.

[Lo and Goh 1986]
Lo, K.L. and Goh, K.M. "Harmonic Analysis for Power Networks," *Electric Power Systems Research*, Vol. 10, pp. 189–203.

[MacDonald 1988]
MacDonald, W.J.P. *An Estimate of the Near Surface Resistivity Structure of the Ground below the Haywards-Benmore HVDC Transmission Line*, Technical Report 45, Geophysics Division, Department of Scientific and Industrial Research, PO Box 1320, Wellington, New Zealand, February.

[Mahmoud and Mohsen 1985]
Mahmoud, S.F. and Mohsen, A.A. "Assessment of image theory for field evaluation over a multilayer earth," *IEEE Transactions on Antennas and Propagation*, Vol. AP-33, No. 10, October, pp. 1054–1058.

[Metwally and Mahmoud 1982]
Metwally, A.D. and Mahmoud, S.F. "Error analysis of image representations for sources near to a dissipative earth," *IEEE Transactions on Antennas and Propagation*, Vol. AP-30, No. 5, September, pp. 1005–1008.

[Meyer and Dommel 1969]
Meyer, W.S. and Dommel, H.W. "Telephone-Interference Calculation for Multiconductor Power Lines," *IEEE transactions on Power Appartatus and Systems*, Vol. PAS-88, No. 1, January, pp. 35–41.

[Miller *et al.* 1972a]
Miller, E.K., Poggio, A.J., Burke, G.J. and Selden, E.S. "Analysis of Wire Antennas in the Presence of a Conducting Half-Space. Part 1. The Vertical Antenna in Free Space.," *Canadian Journal of Physics*, Vol. 50, pp. 879–888.

[Miller *et al.* 1972b]
Miller, E.K., Poggio, A.J., Burke, G.J. and Selden, E.S. "Analysis of Wire Antennas in the Presence of a Conducting Half-Space. Part 2. The Horizontal Antenna in Free Space.," *Canadian Journal of Physics*, Vol. 50, pp. 2614–2627.

[Mizuma *et al.* 1985]
Mizuma, T., Sagisaka, Y., Neri, K. and Sekine, Y. "Harmonic Analysis of Synchronous Machine with AC/DC Convertor, Part 1. Harmonic Characteristics of AC/DC Convertor.," *Electrical Engineering in Japan*, Vol. 105, No. 3, May–June, pp. 71–79.

[Mullineux and Reed 1965]
Mullineux, N. and Reed, J.R. "Calculation of Electrical Parameters for Short and Long Polyphase Transmission Lines," *Proceedings of the Institutionof Electrical Engineers*, Vol. 112, No. 4, April, pp. 741–742.

[Nakagawa and Iwamoto 1976]
Nakagawa, M. and Iwamoto, K. "Earth-return Impedance for the Multi-layer Case," *IEEE Transactions on Power Apparatus and Systems*, Vol. PAS-95, No. 2, March/April, pp. 671–676.

[Nakagawa *et al.* 1973]
Nakagawa, M., Ametani, A. and Iwamoto, K. "Further studies on wave propagation in overhead lines with earth return: Impedance of stratified earth," *Proceedings of the Institutionof Electrical Engineers*, Vol. 120, No. 12, December, pp. 1521–1528.

[Nelder and Mead 1965]
Nelder, J.A. and Mead, R. "A Simplex Method for Function Minimisation," *Computer Journal*, Vol. 7, pp. 308–313.

[NZECP 36 1993]
NZECP 36:1993 New Zealand Electrical Code of Practice for Harmonic Levels, Issued by the Office of the Chief Electrical Inspector, Energy and Resources Division, Ministry of Commerce.

[Olsen and Jaffa 1984]
Olsen, R.G. and Jaffa, K.C. "Electromagnetic Coupling from Power Lines and Magnetic Field Safety Analysis," *IEEE Transactions on Power Apparatus and Systems*, Vol. PAS-103, No. 12, December, pp. 3595–3607.

[Olsen and Pankaskie 1983]
Olsen, R.G. and Pankaskie, T.A. "On the Exact, Carson and Image Theories for Wires at or above the Earth's Interface," *IEEE Transactions on Power Apparatus and Systems*, Vol. PAS-102, No. 4, April, pp. 769–778.

[Olsen and Wong 1992]
Olsen, R.G. and Wong, P.S. "Characteristics of Low Frequency Electric and Magnetic Fields in the Vicinity of Electric Power Lines," *IEEE Transactions on Power Delivery*, Vol. PWRD-7, No. 4, October, pp. 2046–2053.

[Olsen *et al.* 1978]
Olsen, R.G., Kuester, E.F. and Chang, D.C. "Modal Theory of Long Horizontal Wire Structures above the Earth, 2, Properties of Discrete Modes," *Radio Science*, Vol. 13, No. 4, July-August, pp. 615–623.

[Orr *et al.* 1983]
Orr, J.A., Emanuel, A.E., Pileggi, D.J. and Levitsky, F.J. "Determination of Harmonic Interference Voltages in Paired-Cable Communications Circuits by Harmonic Currents in Adjacent Power Lines," *IEEE transactions on Power Apparatus and Systems*, Vol. PAS-102, No. 7, July, pp. 2278–2283.

[Ovick and Kusic 1984]
Ovick, N.L. and Kusic, G.L. "Including Corona Effects for Travelling Waves on Transmission Lines," *IEEE transactions on Power Apparatus and Systems*, Vol. PAS-103, No. 12, December, pp. 3643–3650.

[Parker, Jr. 1978]
Parker, Jr., J. "Analytical Foundation for Low Frequency Power-telephone Interference," *Bell System Technical Journal*, Vol. 57, No. 5, May–June, pp. 1663–1697.

[Perz and Raghuveer 1974a]
Perz, M.C. and Raghuveer, M.R. "Generalised Derivation of Fields, and Impedance Correction Factors of Lossy Transmission Lines. Part 1 Lossy Conductors above Lossless Ground.," *IEEE Transactions on Power Apparatus and Systems*, Vol. PAS-93, No. 6, November–December, pp. 1827–1831.

[Perz and Raghuveer 1974b]
Perz, M.C. and Raghuveer, M.R. "Generalised Derivation of Fields, and Impedance Correction Factors of Lossy Transmission Lines. Part 2 Lossy Conductors above Lossy Ground.," *IEEE Transactions on Power Apparatus and Systems*, Vol. PAS-93, No. 6, November–December, pp. 1832–1841.

[Piessens *et al.* 1983]
Piessens, R., de Doncker-Kapenga, E., Uberhuber, C.W. and Kahaner, D.K. *QUADPACK: A Subroutine Package for Automatic Integration*, Springer-Verlag, Berlin.

[Pogorzelski and Chang 1977]
Pogorzelski, R.J. and Chang, D.C. "On the validity of the thin wire approximation in analysis of wave propagation along a wire over a ground," *Radio Science*, Vol. 12, No. 5, September–October, pp. 699–707.

[Pollaczek 1926]
Pollaczek, F. "Ueber das Feld einer Unendlich langen Wechselstromdurchflossenen

Einfachleitung," *Elektrische Nachrichlen-Technik*, Vol. 3, September, pp. 339–359. French translation by POMEY, J. B. (1931), 'Sur le champ produit par un conducteur simple infiniment long parcouru par un courant alternatif', *Revue Generale de L'Electricite*, Vol. 29, No. 22, 30th May, Pp. 851–867.

[Prevost and André 1950]
Prevost and André "The Effect of Soil Conductivity Upon Induced Voltages from Power Lines into Telecommunication Circuits. Results of Experiments,", CIGRE 13th meeting, Volume 3, session paper 343.

[Ramo *et al.* 1984]
Ramo, S., Whinnery, J.R. and van Duzer, T. *Fields and Waves in Communication Electronics*, John Wiley & Sons, New York, 2nd ed.

[Riordan and Sunde 1933]
Riordan, J. and Sunde, E.D. "Mutual Impedance of Grounded Wires for Horizontally Stratified Two-Layer Earth," *The Bell System Technical Journal*, Vol. 12, No. 2, April, pp. 162–177.

[Robinson 1966]
Robinson, G.H. "Harmonic Phenomena associated with the Benmore-Haywards HVDC Scheme," *New Zealand Engineering*, Vol. 22, No. 1, January, pp. 16–29.

[Rodgers and White 1989]
Rodgers, E.J. and White, J.F. "Mutual Coupling between Finite Lengths of Parallel or Angled Horizontal Earth Return Conductors," *IEEE Transactions on Power Delivery*, Vol. PWRD-4, No. 1, January, pp. 103–113.

[Sarmiento *et al.* 1988]
Sarmiento, H.G., Mukhedkar, D. and Ramachandran, V. "An Extension to the Study of Earth-Return Mutual Coupling Effects in Ground Impedance Field Measurements," *IEEE Transactions on Power Delivery*, Vol. PWRD-3, No. 1, January, pp. 96–101.

[Semlyen 1981]
Semlyen, A. "Approximation to Carson's loss formulae," *Canadian Electrical Engineering Journal*, Vol. 6, No. 2, April, pp. 30–31.

[Semlyen and Abdel-Rahman 1982]
Semlyen, A. and Abdel-Rahman, M.H. "Transmission line modelling by rational transfer functions," *IEEE Transactions on Power Apparatus and Systems*, Vol. PAS-101, No. 9, September, pp. 3576–3584.

[Semlyen and Deri 1985]
Semlyen, A. and Deri, A. "Time domain modelling of frequency dependent three-phase transmission line impedance," *IEEE Transactions on Power Apparatus and Systems*, Vol. PAS-104, No. 6, June, pp. 1549–1555.

[Semlyen and Shirmohammadi 1982]
Semlyen, A. and Shirmohammadi, D. "Calculation of Induction and Magnetic Field Effects of Three Phase Overhead Lines above Homogeneous Earth," *IEEE Transactions on Power Apparatus and Systems*, Vol. PAS-101, No. 8, August, pp. 2747–2754.

[Semlyen *et al.* 1985]
Semlyen, A., Eggleston, J.F. and Arrillaga, J. "Admittance Matrix Model of a Synchronous Machine for Harmonic Analysis,", IEEE Summer Power Meeting, Mexico City, paper SM 350-3(86).

[Semlyen *et al.* 1987]
Semlyen, A., Acha, E. and Arrillaga, J. "Harmonic Norton Equivalent for the Magnetizing Branch of a Transformer," *Proceedings of the Institution of Electrical Engineers, Part C*, Vol. 134, No. 2, March, pp. 162–169.

[Sharaf 1982]
Sharaf, A.M. "Harmonic Interference from Distribution Systems," *IEEE Transactions on Power Apparatus and Systems*, Vol. PAS-101, No. 8, August, pp. 2975–2981.

[Shipley and Coleman 1959]
Shipley, R.B. and Coleman, D. "A new direct matrix inversion method," *AIEE Transactions, Part 1*, Vol. 78, November, pp. 568–572.

[Smith *et al.* 1974]
Smith, B.T., Boyle, J.M., Garbow, B.S., Ikebe, Y., Klema, V.C. and Moler, C.B. *Matrix Eigensystem Routines - EISPACK Guide*, Lecture Notes in Computer Science 6, Springer - Verlag, Berlin, 1st ed.

[Sommerfeld 1909]
Sommerfeld, A. "Über die Ausbreitung der Wellen in der drahtlosen Telegraphie," *Annalen der Physik*, Vol. 28, No. 4, pp. 665–736.

[Sunde 1949]
Sunde, E.D. *Earth Conduction Effects in Transmission Systems*, D. van Nostrand Company, Inc., New York, 1st ed.

[Syman and Hore 1981]
Syman, G.L. and Hore, G.N. *Induced Noise on Telecom Lines in the Rolleston Area*, Engineering Paper 92, New Zealand Post Office, Christchurch, July.

[Tamby and John 1988]
Tamby, J.P. and John, V.I. "Q'HARM – A Harmonic Powerflow Program for Small Power Systems," *IEEE Transactions on Power Systems*, Vol. 3, No. 3, August, pp. 949–955.

[Tevan and Deri 1984]
Tevan, G. and Deri, A. "Some remarks about the accurate evaluation of the Carson integral for mutual impedances of lines with earth return," *Archiv für Elektrotechnik*, Vol. 67, pp. 83–90.

[Vance 1978]
Vance, E.F. *Coupling to Shielded Cables*, Wiley Interscience, New York, 1st ed.

[Velazquez *et al.* 1983]
Velazquez, R., Reynolds, P.H. and Mukhedkar, D. "Earth-Return Mutual Coupling Effects in Ground Resistance Measurements of Extended Grids," *IEEE Transactions on Power Apparatus and Systems*, Vol. PAS-102, No. 6, June, pp. 1850–1857.

[Wait 1972]
Wait, J.R. "Theory of wave propagation along a thin wire parallel to an interface," *Radio Science*, Vol. 7, No. 6, June, pp. 675–679.

[Wait and Spies 1969]
Wait, J.R. and Spies, K.P. "On the image representation of the quasi-static fields of a line current source above the ground," *Canadian Journal of Physics*, Vol. 47, No. 23, pp. 2731–2733.

[Watson and Arrillaga 1987]
Watson, N.R. and Arrillaga, J. "Frequency - Dependent AC System Equivalents for Harmonic Studies and Transient Convertor Simulation,", IEEE/PES Winter Meeting, New Orleans, Louisiana, paper 87 WM 171-2.

[Wedepohl and Efthymiadis 1978]
Wedepohl, L.M. and Efthymiadis, A.E. "Wave Propagation in Transmission Lines over Lossy Ground: A New, Complete Field Solution," *Proceedings of the Institution of Electrical Engineers*, Vol. 125, No. 6, June, pp. 505–510.

[Wedepohl and Wasley 1965]
Wedepohl, L.M. and Wasley, R.G. "Wave propagation in polyphase transmission systems, Resonance effects due to discretely bonded earth wires.," *Proceedings of the Institution of Electrical Engineers*, Vol. 112, No. 11, November, pp. 2113–2119.

[Wedepohl and Wasley 1966]
Wedepohl, L.M. and Wasley, R.G. "Wave Propagation in Multiconductor Overhead Lines: Calculation of Series Impedance for Multilayer Earth," *Proceedings of the Institution of Electrical Engineers*, Vol. 113, No. 4, April, pp. 627–632.

[Whitehouse 1988]
Whitehouse, A.C.D. "EMC Regulations within Europe,", In *Sixth International Conference on Electromagnetic Compatibility, Publication No. 81*, The Institution of Electronic and Radio Engineers, York, England, September, pp. 369–373.

[Wise 1931]
Wise, W.H. "Effect of Ground Permeability on Ground Return Circuits," *Bell System Technical Journal*, Vol. 10, No. 3, July, pp. 472–484.

[Wise 1934]
Wise, W.H. "Propagation of High Frequency Currents in Ground Return Circuits," *Proceedings of the Institute of Radio Engineers*, Vol. 22, No. 4, April, pp. 522–527.

[Wise 1948]
Wise, W.H. "Potential Coefficients for Ground Return Circuits," *Bell System Technical Journal*, Vol. 27, No. 2, April, pp. 365–371.

[Xia and Heydt 1982]
Xia, D. and Heydt, G.T. "Harmonic Power Flow Studies: Part 1 – Formulation and Solution," *IEEE Transactions on Power Apparatus and Systems*, Vol. PAS-101, No. 6, June, pp. 1257–1270.

[Yang and Matsuura 1988]
Yang, C. and Matsuura, K. "Effect of Conductor Height and Terrain on the Steady-State Induced Voltage and Transient Current through a Linesman's Body

on a De-energized Line," *Electric Power Systems Research*, Vol. 15, No. 3, December, pp. 219–227.